

**The role of thiol-redox protein modifications in ROS-
dependent metabolic reprogramming during germination
suppression in wheat seeds**

by

© A. V. Pabasari Sachinthana

A thesis submitted to the

School of Graduate Studies

in partial fulfillment of the requirements for the degree of

MASTER OF SCIENCE IN BIOLOGY

DEPARTMENT OF BIOLOGY

Memorial University of Newfoundland

St. John's, Newfoundland and Labrador

Date: December 2023

Abstract

Pre-harvest sprouting (PHS) is a recurring problem for wheat growers worldwide. However, the molecular mechanisms underlying PHS remain elusive. Redox changes in seed tissues and reactive oxygen species-based triggers are essential for seed germination, with plant NADPH oxidases (NOXs) playing an important role. This study demonstrated the link between ROS production, cellular oxidative metabolism, and sensitivity to external ABA in white-seeded spring wheat. In this study, pharmacological treatments using Diphenylene iodonium (DPI), an inhibitor of NOXs, abscisic acid (ABA) phytohormone, and their combination were used to inhibit germination in freshly harvested (FH) and after-ripened (AR) wheat seeds from doubled haploid (DH) lines with non-dormant genotype. Changes to embryo and aleurone thiol-redoxomes during germination suppression were identified and quantified using iodoTMT labeling, nano-liquid chromatography tandem mass spectrometry (nanoLC-MS/MS) analysis in conjunction with IWGSC RefSeq and EST wheat databases. The thiol-redoxomes were studied using two different approaches, analyzing changes in reversibly modified proteins (RMPs) (approach I) and in Cys-containing differentially abundant proteins (CysDAPs) (approach II). FH wheat seeds showed higher germination resistance (GR) response to ABA treatment in the presence of DPI as compared to AR seeds. In FH tissues, all RMPs were up-regulated in the reduction level, and most CysDAPs increased in abundance during ABA-mediated germination inhibition under oxidative stress. Most thiol-responsive proteins in FH embryos were involved in cellular respiration, protein biosynthesis and lipid metabolism. High number of storage- and pathogen-responsive proteins were identified in FH aleurones. In contrast to FH tissues, AR tissues contained a minimal amount of RMPs and CysDAPs.

Keywords- Pre-harvest sprouting, ROS, NADPH oxidases, post-translational thiol modifications, thiol-redoxome, germination suppression, *Triticum aestivum* L.

Acknowledgement

The study presented here would not have been a success without the collaboration and utmost support of many people, and hereby, I wish to extend my heartiest gratitude to them. First and foremost, my deepest appreciation and gratitude are offered to my supervisor, Dr. Natalia Bykova, Agriculture and Agri-Food Canada, and co-supervisor, Dr. Abir U. Igamberdiev, Department of Biology, Memorial University of Newfoundland, for providing me with the opportunity to work under their guidance, providing financial assistance and devoting their valuable time for excellent supervision, encouragement, motivation, useful suggestions and untiring guidance throughout the study. I would like to express my gratitude to the supervisory committee members, Dr. Christof Rampitsch, Agriculture and Agri-Food Canada and Dr. Brian Staveley, Department of Biology, Memorial University of Newfoundland, for their valuable input and guidance throughout my study program.

Further, I am profoundly grateful to Ms. Natasa Radovanovic, Ms. Michelle Ramptisch and Dr. Mei Huang for their exceptional guidance, supervision, instructions and technical support during the research project at Morden Research and Development Centre, Agriculture and Agri-Food Canada (AAFC). Their expertise, feedback and assistance in day-to-day situations have been instrumental in enhancing the quality of my research. I am genuinely grateful for their valuable contributions to my project. Further, I extend my heartiest thanks to Dr. Avanthi Wijesinghe, Dr. Ursula Fernando, Dr. Dinushika Thambugala, Ms. Slavica Djuric, Dr. Mitali Banik, Dr. Brent McCallum, Dr. Taye Zegeye-Gebrehiwot, all the staff at Morden Research and Development Centre, Agriculture and Agri-Food Canada and Department of Biology at Memorial University of Newfoundland for their valuable support and facilities provided with relevant guidance. I appreciate not only their help with my research but also their guidance in adapting to the new environment and advice in various aspects of life.

I would like to express my deepest appreciation and gratitude to my husband, Mr. A. V Ujith Imantha, for his constant support and understanding. His belief in me has been a

driving force behind my success, and I am truly grateful for his presence in my life. To my mother, Mrs. K. S Chandrika, and my brother, Mr. M. K Madusha Sachintha, I express my heartfelt thanks for their unwavering support and encouragement throughout my scientific career. Their love and guidance have been invaluable and significantly shaped my personal and professional growth. I would like to thank my daughter, A. V Akyana Yusheily, for bringing immense joy and meaning to my life. Her presence has been a constant reminder of why I pursue my scientific career with passion and dedication. She is a source of inspiration and motivation, and I am grateful for the love and happiness she brings to our world. I want to thank my in-laws for their constant attention, love, care, encouragement, and positive influence throughout my journey. Their kind words and gestures have provided me with motivation and inspiration to pursue my goals and dreams. I am truly blessed to have such a wonderful family.

I would like to express my heartfelt gratitude to my colleague, Ms. Jayamini Jayawardhene and her husband, Dr. L. Mihiran Muditha Upeksha, for their invaluable support and assistance. Their guidance, encouragement, and willingness to help have made a significant impact on my academic life. I am truly indebted to them for their contributions, as without their assistance, this achievement would have remained a distant dream. Finally, I sincerely thank from the bottom of my heart to all my well-wishers and helpers, who were important to the successful realization of this research.

Table of contents

Abstract.....	i
Acknowledgement.....	ii
Table of contents	iv
List of tables	xiv
List of Figures.....	xv
List of abbreviations	xxii
1 Introduction.....	1
1.1 Wheat kernel morphology and developmental phases	2
1.2 Seed dormancy and germination	3
1.3 Pre-harvest sprouting.....	5
1.3.1 Pre-harvest sprouting in wheat.....	5
1.3.2 The economic impact of pre-harvest sprouting.....	6
1.3.2.1 Effects of PHS on wheat grain quality.....	6
1.3.2.2 Effect of PHS on the quality of wheat-based products	7
1.3.3 Factors affecting pre-harvest sprouting in wheat.....	9
1.3.3.1 The influence of environmental conditions on PHS in wheat	9
1.3.3.2 Genes controlling seed dormancy and germination potential	10
1.3.3.3 The role of phytohormones.....	14
1.3.3.4 The role of α -amylase.....	21
1.4 Role of reactive oxygen species and reactive nitrogen species in plants and the regulation of seed germination and dormancy	23

1.4.1	Reactive oxygen and nitrogen species	23
1.4.2	ROS and RNS production sites in plants	24
1.4.2.1	NADPH oxidases in the plasma membrane.....	24
1.4.2.2	Other intracellular locations of RONS generation.....	26
1.4.3	Enzymatic and non-enzymatic antioxidant mechanisms of ROS/RNS scavenging in plants.....	29
1.4.3.1	Enzymatic antioxidant mechanisms of ROS/RNS scavenging in plants.....	29
1.4.3.2	Non-enzymatic antioxidant mechanisms of ROS/RNS scavenging in plants.....	32
1.4.4	ROS-mediated reversible and irreversible protein modifications.....	34
1.4.5	Evidence for the redox regulation of seed dormancy and germination .	39
1.5	Proteomic approaches to study seed dormancy, germination and redox control	45
1.5.1	Two-dimensional gel electrophoresis-based proteomics	47
1.5.2	Quantitative shotgun-based proteomics technique	48
1.5.3	Quantitative redox proteomics	49
1.6	Objectives of the project.....	51
2	Materials and Methods	54
2.1	Plant material and seed sampling procedure	54

2.2 Germination resistance tests	56
2.2.1 Germination assay for freshly-harvested seeds.....	56
2.2.2 Germination resistance tests of non-dormant FH and AR seeds treated with DPI, ABA, and DPI in the presence of ABA and water as a control	57
2.2.3 Germination resistance tests to control the effect of different solvent concentrations used in pharmacological treatments of non-dormant wheat kernels	59
2.2.4 Statistical analysis for GR tests with DPI, ABA, DPI combined with ABA and water treatments of FH and AR wheat seeds from non-dormant DH lines	60
2.3 Experimental design for identification and quantitation of Cys Thiol Redox Modified Proteins (RMPs) and Cys-containing Differentially Abundant Proteins (CysDAPs) by iodoacetyl Tandem Mass Tags (iodoTMT)-based labeling approach	62
2.3.1 Treatments for non-dormant white-seeded spring wheat DH Lines	62
2.3.2 Dissection of embryo and aleurone tissues and extraction of proteins from FH and AR pharmacologically treated seeds.....	63
2.3.3 Bradford assay to determine the protein concentration of extracts from FH and AR, embryos and aleurones	66

2.3.4 Preparation of the FH and AR, embryo and aleurone protein extractions for iodoTMT labeling	67
2.3.5 IodoTMT labeling procedure	69
2.3.6 Digestion of iodoTMT labeled proteins	71
2.3.7 C18 clean-up of the peptide digests	72
2.3.8 Enrichment of iodoTMT reagent-labeled peptide digests.....	73
2.3.9 Preparation of eluates after anti-TMT resin incubation	74
2.3.10 C18 clean-up and NanoLiquid Chromatography Tandem Mass Spectrometry (nanoLC-MS/MS) analysis of enriched embryo and aleurone peptide digests	76
2.3.11 Database searching, and comparative quantitative and statistical analysis	77
2.3.12 The data analysis strategy, further data curation and organization of quantitative peptide reports.....	79
2.3.13 The database search of protein sequences and functional annotation of the identified proteins	80
3 Results.....	82
3.1 Germination resistance of non-dormant seeds treated with an inhibitor of cell redox metabolism and ABA phytohormone	82

3.1.1 Changes in germination resistance of seeds with non-dormant genotypes under DPI, ABA, and DPI combined with ABA treatment conditions.....	82
3.1.1.1 Physiological changes in germination resistance of freshly harvested seeds under different DPI, ABA and DPI combined with ABA treatments.....	83
3.1.1.2 Physiological changes in germination resistance of after-ripened seeds under different DPI, ABA, and DPI combined with ABA treatment conditions.....	85
3.1.2 Comparison of physiological changes in GR between FH and AR seeds from non-dormant wheat DH lines in response to DPI and ABA treatments.....	87
3.1.3 Comparison of the effect of different concentrations of DPI, ABA and DPI combined with ABA on physiological changes for GR in FH and AR seeds	90
3.1.4 Effect of solvents on germination resistance of seeds from non-dormant DH lines and AC Karma parent	92
3.2 Identification and quantitation of Cys Thiol Redox Modified Proteins (RMPs) and Cys-containing Differentially Abundant Proteins (CysDAPs) by Iodoacetyl Tandem Mass Tags (iodoTMT)-based labeling approach	98

3.2.1 Unique significant RMPs found in embryo and aleurone tissues of DPI-treated seeds after the differential blocking of redox-active protein thiols with IAA (DPI-IAA).....	102
3.2.1.1 Unique significant RMPs found in freshly harvested embryos in the DPI-IAA category.....	102
3.2.1.2 Unique significant RMPs found in after-ripened embryos in the DPI-IAA category.....	106
3.2.1.3 Unique significant RMPs found in FH aleurones in the DPI-IAA category.....	106
3.2.1.4 Unique significant RMPs found in AR aleurones in the DPI-IAA category.....	106
3.2.2 Unique significant RMPs found in embryo and aleurone tissues of seeds treated with DPI in the presence of ABA after the differential blocking of redox-active protein thiols with IAA (DPI+ABA)-IAA category.....	107
3.2.2.1 Unique significant RMPs found in FH embryos in (DPI+ABA)- IAA category.....	107
3.2.2.2 Unique significant RMPs found in AR embryos in (DPI+ABA)- IAA category.....	110
3.2.2.3 Unique significant RMPs found in FH aleurones in (DPI+ABA)- IAA category.....	111

3.2.2.4 Unique significant RMPs found in AR aleurones in (DPI+ABA)- IAA category.....	114
3.2.3 Common RMPs found in embryo and aleurone tissues of seeds treated with DPI and DPI in the presence of ABA after the differential blocking of redox-active protein thiols with IAA in both DPI-IAA and (DPI+ABA)-IAA categories (Common-IAA)	115
3.2.3.1 Common RMPs found in FH embryos in both DPI-IAA and (DPI+ABA)-IAA categories.....	115
3.2.3.2 Common RMPs found in AR embryos in both DPI-IAA and (DPI+ABA)-IAA categories.....	119
3.2.3.3 Common RMPs found in FH aleurones in both DPI-IAA and (DPI+ABA)-IAA categories.....	119
3.2.3.4 Common RMPs found in AR aleurones in both DPI-IAA and (DPI+ABA)-IAA categories.....	121
3.2.4 Unique significant CysDAPs found in embryo and aleurone tissues of seeds treated with DPI after the reduction of all redox-active protein thiols with DTT, (DPI- DTT) category.....	121
3.2.4.1 Unique significant CysDAPs found in FH embryos in the DPI-DTT category.....	121
3.2.4.2 Unique significant CysDAPs found in AR embryos in DPI- DTT category.....	123

3.2.4.3 Unique significant CysDAPs found in FH aleurones in DPI- DTT category.....	124
3.2.4.4 Unique significant CysDAPs found in AR aleurones in DPI- DTT category.....	125
3.2.5 Unique significant CysDAPs found in embryo and aleurone tissues of seeds treated with DPI in the presence of ABA after the reduction of all redox-active protein thiols with DTT, (DPI+ABA)-DTT category.....	126
3.2.5.1 Unique significant CysDAPs found in FH embryos in the (DPI+ABA)-DTT category.....	126
3.2.5.2 Unique significant CysDAPs found in AR embryos in the (DPI+ABA)-DTT category.....	129
3.2.5.3 Unique significant CysDAPs found in FH aleurones in the (DPI+ABA)-DTT category.....	131
3.2.5.4 Unique significant CysDAPs found in AR aleurones in the (DPI+ABA)-DTT category.....	132
3.2.6 Common CysDAPs found in embryo and aleurone tissues of seeds treated with DPI or DPI in the presence of ABA after the reduction of all redox-active protein thiols with DTT, both DPI-DTT and (DPI+ABA)-DTT categories (Common-DTT).....	133

3.2.6.1	Common CysDAPs found in FH embryos in both DPI-DTT and (DPI+ABA)-DTT categories	133
3.2.6.2	Common CysDAPs found in AR embryos in both DPI-DTT and (DPI+ABA)-DTT categories	137
3.2.6.3	Common CysDAPs found in FH aleurones in both DPI-DTT and (DPI+ABA)-DTT categories	137
3.2.6.4	Common CysDAPs found in AR aleurones in both DPI-DTT and (DPI+ABA)-DTT categories	137
3.3	Comparison of the thiol-containing proteins identified in FH and AR wheat kernels in each approach.....	138
3.3.1	Comparison of the RMPs in FH and AR wheat kernels identified using the approach I that quantifies oxidative changes in reversible Cys PTMs (IAA and iodoTMT differential alkylation).....	138
3.3.2	Comparison of the CysDAPs in FH and AR wheat seeds in approach II that quantifies differential protein abundance changes (DTT reduction and iodoTMT labeling).....	145
3.4	Comparison of the thiol-containing proteins identified from the approach I and II in FH and AR wheat kernels	153
3.4.1	Comparison of the thiol-containing proteins identified from approaches I and II in FH and AR embryos.....	153

3.4.1.1 Comparison of the thiol-containing proteins identified from approaches I and II in FH embryos.....	153
3.4.1.2 Comparison of the thiol-containing proteins identified from approaches I and II in AR embryos	158
3.4.2 Comparison of the thiol-containing proteins identified from approaches I and II in FH and AR aleurones	162
3.4.2.1 Comparison of the thiol-containing proteins identified from approaches I and II in FH aleurones	162
3.4.2.2 Comparison of the thiol-containing proteins identified from approaches I and II in AR aleurones.....	165
4 Discussion.....	169
5 Conclusion.....	198
6 References.....	202
7 Appendices.....	255

List of tables

Table 1: Properties and antioxidant scavengers of major ROS.....	34
Table 2: Treatments, solvent controls and percentage of DMSO and methanol concentrations of solvents used in treatment and control experiments.....	60
Table 3: IodoTMT labeling matrix showing the allocation of biological replicate experiments with FH and AR, embryo and aleurone protein extracts to labeling tags. ...	70
Table 4: Number of the unique up- and down-regulated (in the level of the reduced fraction), and common RMPs in FH and AR wheat kernels identified using the approach I (IAA and iodoTMT differential alkylation).....	141
Table 5: Number of unique up- and down-regulated (in the level of the reduced fraction), and common CysDAPs in FH and AR wheat kernels identified using the approach II (complete DTT reduction and iodoTMT labeling).....	148
Table 6: Number of thiol-containing proteins identified in approaches I and II that changed in the redox level only, protein abundance only and in both redox and abundance levels in FH and AR embryos	160
Table 7: Number of the thiol-containing proteins identified in approaches I and II that changed in the redox level only, protein abundance only and in both redox and abundance levels in FH and AR aleurones	167

List of Figures

Figure 1: Cultivation of Spring wheat (<i>Triticum aestivum</i> L.) DH lines in the climate-controlled growth chambers at Agriculture and Agri-Food Canada based in Morden Research and Development Centre.....	55
Figure 2: Treated wheat kernels from DH lines after 48h incubation at 15°C in a representative replicate experiment.	63
Figure 3: Workflow diagram of the procedures for protein extraction from embryo and aleurone tissues of wheat seeds using DH lines with marginally non-dormant phenotype.	64
Figure 4: Workflow diagram of the iodoTMT labeling procedure of protein extracts from seed tissues of DH wheat lines.....	69
Figure 5: Data processing workflow of the raw data obtained from the nanoLC-MS/MS analysis for identification and quantitation of thiol-containing proteins in embryo and aleurone tissues of FH and AR seeds from DH wheat lines.	78
Figure 6A: Comparison of germination resistance in freshly harvested (stored at -20°C) wheat (<i>Triticum aestivum</i> L.) kernels treated with different concentrations of ABA, DPI and DPI in the presence of ABA.....	82
Figure 6B: Comparison of germination resistance in after-ripened wheat (<i>Triticum aestivum</i> L.) kernels treated with different concentrations of ABA, DPI and DPI in the presence of ABA.....	84

- Figure 7A:** Comparison of germination resistance in freshly harvested (stored at -20°C) wheat (*Triticum aestivum* L.) kernels after each experimental treatment..... 88
- Figure 7B:** Comparison of germination resistance in AR wheat (*Triticum aestivum* L.) kernels after each experimental treatment.....89
- Figure 8:** Effect of treatments with DPI, ABA and DPI in the presence of ABA on germination resistance in FH and AR wheat (*Triticum aestivum* L.) kernels..... 91
- Figure 9A:** Effect of DMSO combined with methanol solvent on germination resistance in FH (stored at -20°C) (*Triticum aestivum* L.) kernels at concentrations of 1.5% and 0.17%, respectively, used during the treatment with DPI in the presence of ABA.....93
- Figure 9B:** Effect of DMSO combined with methanol solvent on germination resistance response in AR (*Triticum aestivum* L.) kernels at concentrations of 1.5% and 0.17%, respectively, used during the treatment with DPI in the presence of ABA.....95
- Figure 9C:** Effects of DMSO or methanol individual solvents on germination resistance response in kernels (*Triticum aestivum* L.) subjected to slow after-ripening process under -20 °C low-temperature conditions at different concentrations used during the treatment with either DPI or ABA, respectively.....97
- Figure 10:** Strategy for comparative analysis in the iodoTMT labeling experiment. The quantitative redox strategy was comprised of two approaches: (i) Approach I - analysis of the reversibly oxidized or reduced thiol fraction in FH and AR embryos and aleurones during the germination inhibition by the DPI and DPI combined with ABA treatment; (ii)

Approach II – evaluation of the total thiol content that irreversibly oxidized/ changed in abundance in FH and AR embryos and aleurones during the germination inhibition by the DPI and DPI combined with ABA treatment	101
Figure 11A: Functional annotation of unique significant redox-modified proteins (RMPs) ($FC \leq -1.5$, $p < 0.05$) found in FH embryos from DPI-treated seeds and after the differential blocking of free thiol-containing redox proteins with IAA in the DPI-IAA category....	104
Figure 11B: Mapman visualization of the unique significant redox-modified proteins (RMPs) and their functional groups found in FH embryos from DPI-treated seeds and after the differential blocking of free thiol-containing redox proteins with IAA in the DPI-IAA category.....	105
Figure 12A: Functional annotation of the unique significant RMPs ($FC \leq -1.5$, $p < 0.05$) found in FH embryos from seeds treated with DPI in the presence of ABA and after the differential blocking of thiol-redox proteins with IAA, in the (DPI+ABA)-IAA category.	108
Figure 12B: Mapman visualization of the unique significant RMPs and their functional groups found in FH embryos from seeds treated with DPI in the presence of ABA and after the differential blocking of thiol-redox proteins with IAA, in the (DPI+ABA)-IAA category.....	109
Figure 13: Unique significant RMPs found in AR embryos from seeds treated with DPI in the presence of ABA, and after the differential blocking of thiol-redox proteins with IAA, in the (DPI+ABA)-IAA category.....	110

Figure 14A: Functional annotation of unique significant RMPs ($FC \leq -1.5$, $p < 0.05$) found in FH aleurones from seeds treated with DPI in the presence of ABA, and after the differential blocking of thiol-redox proteins with IAA, in the (DPI+ABA)-IAA category.	112
Figure 14B: Mapman visualization of the unique significant RMPs and their functional groups found in FH aleurones from seeds treated with DPI in the presence of ABA, and after the differential blocking of thiol-redox proteins with IAA, in the (DPI+ABA)-IAA category.....	113
Figure 15: Unique significant RMPs found in AR aleurones from seeds treated with DPI in the presence of ABA, and after the differential blocking of thiol-redox proteins with IAA, in the (DPI+ABA)-IAA category	115
Figure 16A: Functional annotation of common significant RMPs ($FC \leq -1.5$, $p < 0.05$) found in FH embryos from seeds treated with either DPI or DPI in the presence of ABA, and after the differential blocking of thiol-redox proteins with IAA, common in DPI-IAA and (DPI+ABA)-IAA categories	117
Figure 16B: Mapman visualization of the common significant RMPs and their functional groups found in FH embryos from seeds treated with either DPI or DPI in the presence of ABA, and after the differential blocking of thiol-redox proteins with IAA, common in DPI-IAA and (DPI+ABA)-IAA categories	117

Figure 17: Common significant RMPs found in FH aleurones from seeds treated with either DPI or DPI in the presence of ABA, and after the differential blocking of thiol-redox proteins with IAA, common in DPI-IAA and (DPI+ABA)-IAA categories.	120
Figure 18A: Functional annotation of unique significant CysDAPs ($-1.5 \geq FC \geq +1.5$, $p < 0.05$) found in FH embryos from seeds treated with DPI, and after the complete reduction of thiol-redox proteins with DTT, in the DPI-DTT category	122
Figure 18B: Mapman visualization of the unique significant CysDAPs and their functional groups found in FH embryos from seeds treated with DPI, and after the complete reduction of thiol-redox proteins with DTT, in the DPI-DTT category	123
Figure 19: Unique significant CysDAPs found in FH aleurones from seeds treated with DPI, and after the complete reduction of thiol-redox proteins with DTT, in the DPI-DTT category.....	125
Figure 20: Unique significant CysDAPs found in AR aleurones from seeds treated with DPI, and after the complete reduction of thiol-redox proteins with DTT, in the DPI-DTT category.....	126
Figure 21A: Functional annotation of unique significant CysDAPs ($-1.5 \geq FC \geq +1.5$, $p < 0.05$) found in FH embryos from seeds treated with DPI in the presence of ABA, and after the complete reduction of thiol-redox proteins with DTT, in (DPI+ABA)-DTT category.	128

Figure 21B: Mapman visualization of the unique significant CysDAPs and their functional groups found in FH embryos from seeds treated with DPI in the presence of ABA, and after the complete reduction of thiol-redox proteins with DTT, in (DPI+ABA)-DTT category..... 128

Figure 22: Unique significant CysDAPs found in AR embryos from seeds treated with DPI in the presence of ABA, and after the complete reduction of thiol-redox proteins with DTT, in (DPI+ABA)-DTT category..... 130

Figure 23: Unique significant CysDAPs found in FH aleurones from seeds treated with DPI in the presence of ABA, and after the complete reduction of thiol-redox proteins with DTT, in (DPI+ABA)-DTT category 132

Figure 24: Unique significant CysDAPs found in AR aleurones from seeds treated with DPI in the presence of ABA, and after the complete reduction of thiol-redox proteins with DTT, in (DPI+ABA)-DTT category 133

Figure 25A: Functional annotation of common significant CysDAPs ($FC \geq 1.5$, $p < 0.05$) found in FH embryos from seeds treated with either DPI or DPI in the presence of ABA, and after the complete reduction of thiol-redox proteins with DTT, in both DPI-DTT and (DPI+ABA)-DTT categories 135

Figure 25B: Mapman visualization of the common significant CysDAPs and their functional groups found in FH embryos from seeds treated with either DPI or DPI in the presence of ABA, and after the complete reduction of thiol-redox proteins with DTT, in both DPI-DTT and (DPI+ABA)-DTT categories.....136

Figure 26: (A) Comparison of the total number of RMPs found in FH and AR embryos in the approach I (IAA category) (B) Comparison of the total number of RMPs found in FH and AR aleurones in the approach I (IAA category).	139
Figure 27: (A) Comparison of the total number of CysDAPs found in FH and AR embryos in approach II (DTT category) (B) Comparison of the total number of CysDAPs found in FH and AR aleurones in approach II (DTT category).	146
Figure 28A: Comparison of the thiol-containing proteins identified from the approach I (IAA category) and II (DTT category) in FH embryos	155
Figure 28B: Comparison of the thiol-containing proteins identified from the approach I (IAA category) and II (DTT category) in AR embryos.....	159
Figure 29A: Comparison of the thiol-containing proteins identified from the approach I (IAA category) and II (DTT category) in FH aleurones	163
Figure 29B: Comparison of the thiol-containing proteins identified from the approach I (IAA category) and II (DTT category) in AR aleurones	166
Figure 30: Functional distribution of embryo and aleurone thiol-redoxomes during ABA-mediated germination suppression in the presence of DPI in DH lines of non-dormant FH white-seeded spring wheat	175

List of abbreviations

$\cdot\text{OH}$	Hydroxyl
$^1\text{O}_2$	Singlet oxygen
2D-PAGE	Two-dimensional polyacrylamide gel electrophoresis
2ODDs	2-Oxoglutarate-Dependent Dioxygenases
A	Alanine
ABA	Abscisic acid
ABA 8'OH	ABA 8'-hydroxylase enzyme
ABC	ATP-Binding Cassette
ABI5	Abscisic acid-insensitive 5 protein
ACN	Acetonitrile
AN	AB015AN
Approach I	First approach
Approach II	Second approach
APX	Ascorbate peroxidase
AR	AA016AR
AR	After-ripened
Arg	Arginine
AsA	Ascorbate
AsA-GSH	Ascorbate-Glutathione cycle
Asn	Asparagine

ATIs	α -Amylase/trypsin-inhibitors
AX	Arabinoxylans
<i>AXR/IAA</i>	<i>Auxin inducible gene</i>
BioReps	Biological Replicates
BQ	AA016BQ
BR	Brassinosteroid
BSA	Bovine Serum Albumin
C	Cysteine
C	Modified cysteine
Ca ²⁺	Calcium
CAT	Catalase
CCT	Chaperonin containing T-complex polypeptide
CDPKs	Ca ²⁺ -dependent protein kinases
CHI	Chalcone flavanone isomerase
CHS	Chalcone synthase
CK	Cytokinin
CM-types	Chloroform/methanol
cPGM	cytosolic Phosphoglucomutase
CYP	Cyclophilin
Cys	Cysteine
CysDAPs	Cys-containing Differentially Abundant Proteins
Cys-S ⁻	Thiolate anions

Cys-S(O)S-Cys	Thiosulfinate
Cys-S [•]	Thiyl radicals
Cys-SH	Cys thiol
Cys-S-N	Sulfenylamide
Cys-SO ₂ H	Sulfinic acid
Cys-SO ₃ H	Sulfonic acid
Cys-SOH	Sulfenic acid (S-sulfenation)
Cys-S-S-Cys	S-cysteinylation
Cys-S-S-GSH	S-glutathionylation
Cys-SSH	Persulfidation
Cys-S-SH	S-sulfhydration
D	Aspartic acid
DFR	DihydroFlavonol-4-reductase
DH	Doubled Haploid
DHAR	Dehydroascorbate reductase
DIR	Dirigent
DMSO	Dimethylsulfoxide
<i>DOG1</i>	<i>Delay of germination 1</i>
DPI	Diphenylene iodonium
DTT	Dithiothreitol
E	Glutamic acid
eEF2	mRNA-translocation factor

ER	Endoplasmic reticulum
EST	in-house customized and annotated wheat EST
ET	Ethylene
ExpReps	Experimental Replicates
F	Phenylalanine
F3H	Flavanone 3-hydroxylase
FA	Formic acid
FAH	Fumarylacetoacetate hydrolase
FC	Fold change
FH	Freshly harvested
G	Glycine
GA	Gibberellin
GA20ox	GA 20-oxidase
GA3ox	GA 3-oxidase
GGDP	Geranylgeranyl diphosphate
GHPR	Glyoxylate/hydroxypyruvate reductase
GOPX	Guaiacol peroxidase
GPI	Glycosylphosphatidylinositol
GPX	Glutathione peroxidase
GR	Germination Resistance
GSH	Reduced glutathione
GSNO	S-nitrosoglutathione

GSSH	Glutathione disulfide
GST	Glutathione S-transferase
H	Histidine
H ₂ O ₂	Hydrogen peroxide
HCl	Hydrochloric acid
His	Histidine
HMW-GS	High Molecular Weight Glutenin Subunits
HOCl	Hypochlorous acid
HPLC	High-performance liquid chromatography
I	Isoleucine
IAA	Iodoacetamide
ICAT	Isotope-Coded Affinity Tags
ICPL	Isotope-Coded Protein Labeling
iodoTMT	Cys-specific Iodoacetyl Isobaric Tandem mass tags
iTRAQ	Isobaric Tags for Relative and Absolute Quantification
IWGSC	International Wheat Genome Sequencing Consortium
JA-Ile	Jasmonyl Isoleucine
JAs	Jasmonates
<i>JIN4</i>	<i>Jasmonate insensitive4</i>
K	Lysine
L	Leucine
LEA	Late Embryogenesis Abundant protein

LMW-GS	Low Molecular Weight Glutenin Subunits
LSU	Large ribosomal subunit
Lys	Lysine
M	Methionine
m	Modified methionine
MDHAR	Monodehydroascorbate reductase
MeJA	Methyl Jasmonate
<i>MFT</i>	<i>Mother of flowering time</i>
MKK3-A	Mitogen-activated protein kinase kinase3
mMDH	NAD-dependent malate dehydrogenase
MRDC	Morden Research and Development Centre
mtETC	Mitochondrial electron transport chain
N	Asparagine
n	Modified Asparagine
NaCl	Sodium chloride
NADH	Nicotinamide adenine dinucleotide reduced form
NADPH	Nicotinamide adenine dinucleotide phosphate reduced form
NanoLC-MS/MS	nanoLiquid Chromatography Tandem Mass Spectrometry
NCED	9-cis-epoxycarotenoid dioxygenase
ND	Non-dormant
NO [•]	Nitric oxide
NO ₂ [•]	Nitrogen dioxide

NOSs	Nitric oxide synthases
NOXs	NADPH oxidases
NPQ	Non-photochemical quenching
nsLTPs	Non-specific Lipid Transfer Proteins
$O_2^{\bullet -}$	Superoxide
O_3	Ozone
ONOO•	Peroxynitrite
P	Proline
P450	Cytochrome P450 monooxygenase
PDCB	beta 1,3-glucan hydrolases
PGDH1	3-phosphoglycerate dehydrogenase 1
PHS	Pre-harvest sprouting
pI	Isoelectric point
PIC	Pre-Initiation Complex
PMPs	Peroxisomal membrane polypeptides
PPIs	Plant protease inhibitors
PR	Pathogenesis-related proteins
Pro	Proline
PSI	Photosystem I
PSII	Photosystem II
PTM	Post-translational modification
Q	Glutamine

q	Modified glutamine
QTLs	Quantitative trait loci
R	Arginine
RBOHs	Respiratory burst oxidase homologs
RMPs	Cys Thiol Redox Modified Proteins
RNS	Reactive Nitrogen Species
RO•	Alkoxy
RO ₂ •	Peroxy
RONS	Reactive Oxygen and Nitrogen Species
ROS	Reactive Oxygen Species
RT	Room temperature
S	Serine
SA	Salicylic Acid
<i>Sdr4</i>	<i>Seed dormancy 4</i>
SDS	Sodium dodecyl sulfate
SEM	Scanning electron microscopy
Ser	Serine
SILAC	Stable Isotope Labeling by Amino acids in Cell culture
SODs	Superoxide Dismutases
<i>sscd1</i>	<i>Short-day sensitive cell death1</i>
SSU	Small ribosomal subunit
T	Threonine

<i>TaABA8'OH1</i>	ABA 8'-hydroxylase gene
TBS	Tert-butyldimethylsilyl
TCA	Tricarboxylic acid cycle
TechReps	Technical Replicates
Thr	Threonine
TMT	Tandem Mass Tags
TPSs	Terpene synthases
Trp	Tryptophan
Trx	Thioredoxin
Tyr	Tyrosine
V	Valine
VDAC	Voltage-gated Anion Channel
<i>Vp-1</i>	<i>Viviparous-1</i>
W	Tryptophan
WASI	Wheat amylase subtilisin inhibitor
WDAI	Wheat dimeric amylase inhibitor
Y	Tyrosine
ZEP	Zeaxanthin epoxidase

1 Introduction

The introductory section offers a comprehensive exploration of wheat kernels' morphology and developmental phases, emphasizing the seed maturation process and highlighting the significant influence of hormones, particularly abscisic acid (ABA), on seed dormancy and germination. The intricate role of reactive oxygen species (ROS) and reactive nitrogen species (RNS) in plants is elucidated, shedding light on their diverse sources, production sites, the complex network of enzymatic and non-enzymatic mechanisms employed by plants to regulate ROS/RNS levels. The section underscores the multifaceted function that ROS plays in seed germination and dormancy. Diverse production sites of ROS in plants are outlined, with the plasma membrane being a significant contributor through the action of NADPH oxidases. The subsequent portion of the introduction addresses pre-harvest sprouting (PHS) in wheat, elucidating its causes, potential economic implications and emphasizing the pivotal role of dormancy in conferring resistance to PHS. PHS has a significant financial impact on wheat grain quality, wheat-based products, and the overall profitability of farmers and production companies. The economic implications of PHS highlight the importance of adopting proactive measures to address this issue. The significance of breeding PHS-resistant wheat varieties is underscored to mitigate losses and ensure stability in crop yield. The utilization of proteomic approaches is emphasized for enhancing our understanding of the molecular mechanisms underlying critical stages in plant development, including seed dormancy and germination, with potential implications for advancing agriculture and crop management practices, providing valuable resources for

creating wheat varieties that are more productive and resilient which can withstand the challenges posed by PHS.

1.1 Wheat kernel morphology and developmental phases

Wheat (*Triticum aestivum* L.) belongs to the family Poaceae (Gramineae), which contains major crop plants such as rice (*Oryza sativa* L.), oat (*Avena sativa* L.), maize (*Zea mays* L.) and barley (*Hordeum vulgare* L.). The wheat kernel is known as a caryopsis, which is a one-seeded fruit. Generally, wheat kernels are oval-shaped, but some have diverse shapes ranging from spherical to long, narrow, and flattened. The wheat kernel has a crease extending to the kernel's center (Evers & Millar, 2002). The wheat grain primarily comprises three major parts: i) the seed coat, ii) the endosperm, and iii) the embryo. The seed coat, also known as testa, is the seed's outer layer and is made up of dead cells, which serve as a barrier between the outer environment and the embryo. It permits water inside the wheat embryo (Bewley & Black, 1994). The endosperm is comprised of an aleurone and a starchy endosperm. Aleurone is a one-cell layer comprised of thick-walled cells filled with nutritional components and functional proteins, and it encloses the starchy endosperm, which reserves both carbohydrates and proteins. Large cells in the endosperm store starch granules, and these granules are surrounded by a thin layer of adherent proteins. The embryo contains the genetic information that controls germination, giving rise to a new plant (Evers & Millar, 2002). Therefore, the embryo and aleurone layer of the wheat grain are crucial components to study to gain insights into the molecular and biochemical processes involved in wheat germination.

During wheat seed development, seed structure is formed due to cell division, expansion, and differentiation. There is a considerable increase in seed size, while seed moisture content remains constantly high during this period. The seed maturation period starts after seed formation, including reserve accumulation, embryo growth arrest, tolerance to desiccation, and dormancy induction. At the end of the maturation period, a significant decrease in seed moisture content occurs (Gutierrez et al., 2007). Hormones are the major controlling factors of seed maturation, particularly abscisic acid (ABA) and gibberellins (GAs). ABA substantially impacts the synthesis and accumulation of seed storage proteins, promoting desiccation tolerance during seed maturation and initiation of dormancy (Bewley & Nonogaki, 2017). Physiological maturity is typically considered as the harvesting stage of the wheat. Seeds are considered physiologically mature upon gaining maximum dry weight, germinability, and vigour (Calderini & Reynolds, 2000). The seeds are fully matured, have sufficient reserves, and are ready for harvesting and further storage or planting at this point.

1.2 Seed dormancy and germination

Cessation of seed development, also called dormancy, is crucial for surviving intact viable seeds under various environmental conditions, where the seeds remain quiescent until conditions become favourable for germination (Bewley, 1997). Many genes and environmental factors influence this complex adaptive trait (Gubler, Millar, & Jacobsen, 2005). The cell metabolism is active at this stage, but growth processes are repressed (Bewley, 1997). Dormancy can be caused by a variety of factors arising from both embryonic tissues (embryo-based dormancy) and maternal tissues (coat-based dormancy)

(Gubler, Millar, & Jacobsen, 2005). The release of dormancy is governed by intricate interactions between genetic and environmental factors. It is well established that ABA and GA regulate seed dormancy and germination antagonistically. Accumulation of ABA enhances dormancy (Kermode, 2005), while the accumulation of GA promotes seed germination (Finch-Savage & Leubner-Metzger, 2006). Thus, ABA and GA are two key hormones that play crucial roles in regulating seed dormancy and germination.

The break of dormancy is commenced by imbibition under natural, defined environmental conditions such as chilling at low temperature, cold stratification or by gradual dormancy decay through a period of dry storage of seeds, which is called after-ripening (AR) (Bewley & Black, 1994; Gubler, Millar, & Jacobsen, 2005; Koornneef et al., 2002). AR of seeds is a time- and environment-sensitive process in which seeds undergo a consecutive reduction of dormancy until the complete loss of it (Bewley & Black, 1994; Carrera et al., 2008). At the early stages of AR, favourable environmental conditions for germination will not prompt germination. However, after an appropriate period of AR, the same environmental conditions may trigger germination (Carrera et al., 2008). Thus, once imbibed, the seed's AR status determines whether to remain dormant or complete germination. AR represents a key characteristic in determining the germination potential in seeds, which is defined as the seed's ability to finish germination following imbibition (Finch-Savage and Leubner-Metzger, 2006). Oxidation by reactive oxygen species (ROS) mainly causes AR during dry seed storage (Buijs et al., 2018). However, a high accumulation of ROS due to prolonged storage can progressively cause the depletion of the seed quality and viability, leading to seed aging and deterioration of the seeds (Bailly, El-Maarouf-Bouteau, & Corbineau, 2008). Therefore, understanding the dynamics of AR and the role of ROS in this process

is crucial for managing seed dormancy, optimizing germination rates and establishing optimal seed storage and handling practices.

Upon cellular rehydration by imbibition, viable seeds initiate the germinative program. During wheat seed germination, embryo and endosperm play different roles. Germination is a physiological process that initiates with water uptake by the seed and finishes with the emergence of the embryonic axis (Bewley & Black, 1994). Water absorption increases hormonal activity. Upon the accumulation of GA, the α -amylase enzyme is released due to the expression of specific genes in aleurone cells, producing mRNA transcript, which is transported to the cytoplasm, where ribosomes initiate the process of α -amylase synthesis. Upon secretion of α -amylase, the enzymatic cleavage of starch into sugar molecules begins, and sugar is transported to the embryo (De Laethauwer et al., 2013; Gao et al., 2013), which acts as a fuel for the embryo growth and results in the emergence of the radical.

1.3 Pre-harvest sprouting

1.3.1 Pre-harvest sprouting in wheat

Precocious grain germination within the wheat spike before harvest is referred to as pre-harvest sprouting (PHS), which occurs due to the lack of harvest dormancy (Derera, Bhatt, & McMaster, 1977). PHS is a major and modern issue that arose due to the domestication of wheat, aiming to achieve rapid and uniform crop germination (Harlan, De Wet, & Price, 1973). Visible indications of PHS include swelling of the kernel, germ discoloration, splitting of the seed coat, and the emergence of the radical and shoot (Thomason et al., 2019). The sprouting process damages the grain by producing α -amylase, which leads to

endosperm starch degradation (Ross & Bettge, 2009). This phenomenon severely affects the yield and downgrades the bread-making quality of wheat (Imtiaz et al., 2008; Moot & Every, 1990). Many wheat-growing regions worldwide, including Canada, are affected by PHS, which causes direct average annual losses of up to \$1 billion worldwide (Ellis, 2007). The average annual loss in Canada is estimated at more than \$100 million (DePauw et al., 2012). The development of PHS-resistant cultivars with an intermediate level of dormancy is essential to bring down these losses.

1.3.2 The economic impact of pre-harvest sprouting

1.3.2.1 Effects of PHS on wheat grain quality

Absorption of moisture from the air initiates the germination process, resulting in a series of major anatomical and physicochemical changes in the seed during germination (Derera, Bhatt, & McMaster, 1977). Hormonal activity causes the production of enzymes such as amylases, lipases, and proteases that break down starch, oil, and protein, respectively (Simsek et al., 2013), to produce the required energy and nutrients for germination.

Approximately 70 – 80 % of the total dry weight of wheat grain is built up by starch (Simsek et al. 2014). α -Amylase acts on the carbohydrate reserves and hydrolyzes starch to sugar (Derera, Bhatt, & McMaster, 1977). Scanning electron microscopy (SEM) studies conducted by Naguleswaran et al. (2012) showed the stages of enzymatic hydrolysis of starch granules. Hydrolysis starts from the surface of the granule by generating pits, progressively enlarging pore size and penetrating an interior granule, producing a honeycomb-like structure which reduces paste viscosity (the density of the paste) (Naguleswaran et al., 2012), thus leading to lower grain quality.

Proteins account for 10 % -18 % of the total dry matter in wheat grain (Kraic & Herdu, 2009). Chemically, wheat proteins can be divided into two groups: low molecular weight soluble proteins consisting of albumins, globulins, and peptides, and high molecular weight insoluble gluten representing 80-85% of wheat storage proteins (Shewry et al., 2002; Simsek et al., 2013). Increasing production of proteolytic enzymes in sprouted wheat affects wheat's rheological properties (Shafqat, 2013), causing inferior grain quality. Understanding wheat grain composition and its changes during germination is critical for determining wheat quality and suitability for various food applications.

1.3.2.2 Effect of PHS on the quality of wheat-based products

According to the studies, PHS has negatively impacted the quality parameters of different wheat-based products. The types of products and the processing methods are directly affected by wheat quality (Mansour, 1993). Starch degradation decreases the water-holding capacity, leading to a sticky dough (Fu, Hatcher, & Schlichting, 2014), thus causing handling problems.

The bread flour quality mainly depends on the quantity and quality of wheat proteins. The composition of gluten proteins is highly correlated with dough strength and baking quality (Simsek et al., 2013). Gluten proteins can form a cohesive viscoelastic dough that can hold gas, produced during oven rise and fermentation (Veraverbeke & Delcour, 2002). Flour milled from the sprouted wheat produces porous, sticky, and low-loaf volume bread products (Mansour, 1993), and the bread loaves often end up grayish in colour with a compact interior (Fu, Hatcher, & Schlichting, 2014). Moreover, the extreme stickiness of

the dough requires special handling when processing (Paulsen & Auld, 2004), which can disrupt bakery operations.

The study of Simsek et al. (2013) has shown that the action of proteolytic enzymes breaks high molecular weight proteins, resulting in an increased amount of free asparagine (Asn) in the sprouted wheat kernels. Asn is a precursor of acrylamide, formed during bread baking, which has potential risks of carcinogenic activity in humans. The degradation of AX affects wheat grain and wholemeal flour functionality during the bread-making process, decreases dough handling properties and loaf volume (Shafqat, 2013), and impacts wheat products' nutritional value.

The quality and processing of different types of noodles and pasta are affected by sprout damage. Pasta made using sprouted wheat flour can easily be soft or mushy due to overcooking. In noodle production, high levels of sprout damage cause strand stretching, uneven extrusion, irregular drying, and strand cracking during storage (Donnelly, 1980). The studies of Hatcher and Symons (2000) have shown that flour from severely sprouted wheat can increase the discolorations (spots) on the noodles up to five times due to the alkaline activity created by sprouting, thus making the product unattractive for the customers.

In conclusion, PHS directly impacts the farmer's profitability because of the yield loss and reduced weight. It is revealed that more than 4% of the damage to the wheat kernel is classified as unsuitable for human consumption. The price of the damaged wheat could be reduced by 20%–50%, and usually, these are fed to animals (Simsek et al., 2014).

Furthermore, the depletion of the end-product quality causes substantial financial losses for milling and wheat-based production companies.

1.3.3 Factors affecting pre-harvest sprouting in wheat

PHS is a phenomenon that is influenced by the interaction of specific environmental conditions with the plant's intrinsic factors, such as plant genotype, seed dormancy level, endogenous hormone levels, α -amylase activity in seeds, functional proteins, and plant morphology (Gao et al., 2013). PHS resistance in wheat is a complex, quantitatively inherited trait controlled by environmental conditions, genotype and plant morphological factors (Rasul et al., 2009; Singh et al., 2014). Genetic studies have revealed that several genetic regions or quantitative trait loci (QTLs) control the PHS resistance trait (Ogbonnaya et al., 2008; Rasul et al., 2009; Knox et al., 2012). Efforts to reduce PHS involve breeding for PHS-resistant wheat varieties, which can help mitigate the impact of unfavourable environmental conditions and preserve grain quality for better crop yields and end-use applications.

1.3.3.1 The influence of environmental conditions on PHS in wheat

Environmental conditions such as temperature, rainfall, and extended periods of high relative humidity during the grain filling and maturation period significantly affect PHS in wheat (Biddulph et al., 2005). Mares (1993) discovered that seeds exposed to significant rainfall and humidity during the grain ripening stage are more sensitive to sprouting damage due to the kernel's ability to absorb moisture from the air. Specifically, precipitation occurring 20 days prior to harvest contributed to nearly 85% of the variability in sprouting tolerance, primarily due to the impact on diminished grain drying rates.

Furthermore, temperature is a salient factor influencing seed dormancy. However, the impact of temperature on PHS mainly depends on the grain development stage and the genotype. In general, cool conditions (12-18°C) during the grain filling stage are favourable to promote seed dormancy, making it less susceptible to sprouting damage. However, when the grain reaches maturity, low temperatures, along with rainfall or high moisture content, increase the vulnerability to the PHS of wheat (Nyachiro et al., 2002). Monitoring weather patterns and selecting wheat varieties with appropriate PHS resistance characteristics are key strategies for mitigating the adverse effects of PHS.

1.3.3.2 Genes controlling seed dormancy and germination potential

In wheat, seed dormancy is considered the most crucial factor for resistance against PHS. Most sprouting-resistant wheat varieties require an AR period after harvest to germinate, but in susceptible varieties, AR usually occurs on the ear prior to harvest (Thomason et al., 2019). Dormancy is classified as primary or secondary based on the timing of development. The primary dormancy of seed commences during the seed and embryo development stage and depends on genetic and environmental factors. Secondary dormancy develops in mature seeds that have already lost their primary dormancy either due to prolonged inhibition of germination under external factors such as unfavourable environmental conditions (anoxia and high temperature) (Gubler et al., 2005) or internal factors such as endogenous ABA and secondary metabolites (Hilhorst, 2007). Genetic dormancy is the most reliable method to reduce the PHS in wheat due to the ability to resist sprouting even under favourable environmental conditions. A variety of factors can cause dormancy, arising from both embryonic tissues (embryo-based dormancy) and maternal tissues (coat-

based dormancy) (Gubler et al., 2005). Generally, the seed coat determines the seed's resistance toward PHS. Loosely arranged epidermic cells in the seed coat provide higher permeability for the exchange of water and gases, consequently favouring PHS, while tightly arranged epidermic cells ensure resistance to PHS (Gao et al., 2013). Thus, seed coat characteristics can assist in identifying seed susceptibility to sprouting, offering significant insights for crop management practices and variety selection to reduce PHS risk.

Maternally inherited seed coat colour is another regulatory factor linked to grain dormancy and is potentially active in wheat. Generally, white-grained wheat is observed to be almost always less dormant than red-grained wheat (Gao et al., 2013). The seed coat's colour is controlled by the R genes, *R-A1*, *R-B1*, and *R-D1*, which are located on chromosomes 3A, 3B, and 3D, respectively (Metzger et al., 1970) and can be passed on to offspring (Gao et al., 2013). Dominant alleles of R genes promote the production of phlobaphenes, which are reddish, water-insoluble flavonoid pigments that accumulate in the testa in mature seeds and cause the red colour in red-grained wheat (Metzger et al., 1970). Furthermore, the *R1* gene encodes the Myb-type transcription factors (Himi & Noda, 2005) and increases seed dormancy by increasing embryo sensitivity towards ABA (Himi et al., 2002). A study by Kadariya et al. (2011) revealed that these genes' additive and dominant effects are responsible for PHS resistance.

Proanthocyanidins are another well-known flavonoid compound that acts as precursors to reddish-brown pigments, which are converted into insoluble compounds as the seeds mature (Kohyama et al., 2017). These pigments are synthesized in the flavonoid

biosynthesis pathway, which is regulated by several enzymes such as dihydroflavonol-4-reductase (DFR), flavanone-3-hydroxylase (F3H), chalcone flavanone isomerase (CHI), and chalcone synthase (CHS). Himi & Noda (2005) reported that these enzymes were almost completely repressed in white wheat grains and expressed only in immature red grains. These flavonoid compounds stored in the seed coat have been shown to increase mechanical strength and testa thickness (Bewley & Black, 1994; Debeaujon et al., 2007); thus, reinforce seed-coat imposed dormancy and act as a germination inhibitor.

Delay of germination 1 (DOG1), *Viviparous-1 (Vp-1)*, *Seed dormancy 4 (Sdr4)*, *Mother of flowering time (MFT)*, and mitogen-activated protein kinase kinase3 (MKK3-A) have been identified as the genes driving seed dormancy/ PHS resistance using map-based or homology-based cloning techniques (Wei et al., 2019). The *vp-1* gene has been identified as the major gene that regulates seed germination and dormancy and is used as a model to improve PHS resistance in wheat. After flowering, the *Vp-1* gene is expressed in the cytoplasm, promotes seed maturation and represses the expression of germination-related genes, thus regulating the seed dormancy at the transcriptional level (Gao et al., 2013; McCarty et al., 1991). In wheat, three *Vp-1* orthologous loci have been identified on the long arms of 3A, 3B and 3D chromosomes and named *Vp-1A*, *Vp-1B*, and *Vp-1D*, respectively (Bailey et al., 1999; Chang et al., 2011). Six allelic variations of the *Vp-1A* regulator gene, termed *Vp-1Aa*, *Vp-1Ab*, *Vp-1Ac*, *Vp-1Ad*, *Vp-1Ae*, and *Vp-1Af* have been identified among 81 wheat cultivars and advanced lines by a study conducted by Chang et al. (2011). The study revealed that the allelic variations *Vp-1Ab* and *Vp-1Ad* were distributed in the genotypes with higher seed dormancy and stronger PHS resistance.

Another study by Chang et al. (2010) discovered six allelic variations of the regulator gene *Vp-1B*, designated as *Vp-1Ba*, *Vp-1Bb*, *Vp-1Bc*, *Vp-1Bd*, *Vp-1Be* and *Vp-1Bf* among 276 Chinese wheat varieties. Among these allelic variations, the allele of *Vp-1Ba* was identified to be associated with weak seed dormancy and susceptibility to PHS. Conversely, other variants, *Vp-1Bb*, *Vp-1Bc*, *Vp-1Bd*, *Vp-1Be* and *Vp-1Bf*, were distributed in highly PHS-resistant wheat varieties. However, no allelic variation has been found in the *Vp-1D* ortholog.

Improving embryo-based dormancy in cultivars is essential to reduce the susceptibility to sprouting damage. Dormancy is governed by multiple genes as well as environmental influences, making it challenging to investigate these genes. Hence, QTL analysis has become the preferred method for analyzing dormancy and germination-related genes. Gao et al. (2013) reviewed that several studies have identified QTLs associated with PHS on all 21 chromosomes in the wheat genome. One of the major QTL for grain dormancy, termed as *QPhs.ocs-3A.1*, has been identified on the short arm of chromosomes 3A by a study conducted by Osa et al. (2003), using hybrid lines from a cross between high PHS-resistant Japanese spring wheat line Zenkoujikomugi and Chinese spring wheat line, which showed a remarkable effect on PHS. Nakamura et al. (2011) have identified a gene *TaMFT*, a homolog of the *MFT* gene that involved in the regulation of seed dormancy during physiological maturity, co-localized with the QTL *QPhs.ocs-3A.1* on chromosome 3A. Some of the QTLs located on chromosome 4A coincide with the R gene that controls the seed coat colour to affect the PHS tolerance. A QTL located on chromosome 5D acts independently of the seed coat colour but is strongly associated with the PHS tolerance in Hard white wheat (*Triticum aestivum* L.) (Fofana et al., 2009). These findings demonstrate

that the QTL analysis has been instrumental in identifying specific genetic regions and candidate genes associated with PHS resistance, paving the way for targeted breeding efforts to develop wheat varieties with improved dormancy characteristics and reduced susceptibility to PHS.

1.3.3.3 The role of phytohormones

Plant hormones, ABA and gibberellic acid (GA) act antagonistically and directly related to the expression of germination and dormancy (Bewley, 1997). During seed development, ABA promotes dormancy, while GA induces germination in non-dormant seeds. ABA is the main factor responsible for the primary dormancy in seeds. During early seed development, ABA is necessary to sustain the embryos in a developmental mode until they are fully matured and encourages the accumulation of storage reserve for successful germination and successive seedling establishment (Kermode, 1990). Generally, during early seed development, the level of ABA remains lower, then increases and peaks during the mid-development stage when storage reserves are formed. Later, during the grain maturation stage, the ABA amount precipitously declines (Bewley & Black, 1994; Kermode, 1995). In wheat, two peaks of ABA accumulation have been identified during seed development (Suzuki et al., 2000). The first peak arises around 25 days after pollination, while the second peak arises around 35-40 days after pollination (Chono et al., 2013; Suzuki et al., 2000), and the accumulation of ABA during the late stage of maturation is salient for seed dormancy.

Synthesis and catabolism rates modulate the endogenous ABA level in seeds/tissues. Numerous enzymes catalyze ABA biosynthesis during seed maturation, mainly 9-cis-

epoxycarotenoid dioxygenase (NCED) and zeaxanthin epoxidase (ZEP). On the contrary, ABA catabolism by ABA 8'-hydroxylase enzyme (ABA 8'OH) is encoded by specific members of the *CYP707A* gene family, which leads to ABA hydroxylation at the 8' position (Nambara et al., 2010). Seeds alter their sensitivity to ABA during the different stages of the seed life cycle. Studies have revealed that the decrease in seed ABA content during AR occurs mainly through hydroxylation of ABA and loss of sensitivity to the ABA, leading to the loss of seed dormancy in *Arabidopsis* (*Arabidopsis thaliana*) and barley (*Hordeum vulgare*) (Barrero et al., 2009; Okamoto et al., 2006). A study by Chono et al. (2013) reported that reducing ABA catabolism through mutations of the ABA 8'-hydroxylase gene (*TaABA8'OH1*) may lead to germination inhibition in field-grown wheat. However, in wheat seeds, dormancy is associated with the sensitivity to ABA than the endogenous ABA level (Morris et al., 1989; Walker-Simmons, 1987). Exogenous application of physiological concentrations of ABA is known to inhibit germination in imbibed non-dormant (ND) seeds (Garcarrubio, Legaria, & Covarrubias, 1997; Gonai, 2003). In *Arabidopsis*, the availability of energy and metabolites was restricted by exogenous ABA to inhibit germination (Garcarrubio, Legaria, & Covarrubias, 1997). Moreover, exogenous ABA has the ability to impede the action of various hydrolytic enzymes that weaken the tissues surrounding the embryo, thus obstructing radical protrusion (Bewley, 1997; Leubner-Metzger, Fründt, & Meins, 1996). A study by Walker-Simmons (1987) revealed that wheat embryos of PHS resistance cultivars continue to show sensitivity to the exogenously applied ABA even upon grain desiccation, while the ABA sensitivity of wheat embryos of PHS susceptible cultivars diminishes upon grain desiccation.

GAs are endogenous growth regulators associated with plant growth and diverse developmental functions in different stages of the plant life cycle, namely stem elongation, regulation of pollen development, flowering and fruit development, dormancy decay and promotion and maintenance of seed germination (Davies, 1995). Currently, 136 distinct GAs have been discovered and termed as GA₁-GA₁₃₆, but only a few bioactive forms were identified, such as GA₁, GA₃, GA₄ and GA₇. These bioactive GAs are accompanied by deactivation products of the active forms of GAs or presumably inactive GA precursors (Sponsel & Hedden, 2010), which serve as reservoirs of GAs that can be converted into active forms as needed by the plant.

The balance between GA synthesis and inactivation regulates the endogenous bioactive concentration of GAs in plants. Geranylgeranyl diphosphate (GGDP) serves as a common precursor of bioactive GAs synthesized via a multistep process (Yamaguchi, 2008). Terpene synthases (TPSs), Cytochrome P450 monooxygenases (P450s), and 2-oxoglutarate-dependent dioxygenases (2ODDs), localized in plastids, the endomembrane system and the cytosol, respectively, are the classes of enzymes that are associated with the biosynthesis of bioactive GAs in plants (Hedden & Thomas, 2012; Yamaguchi, 2008). At the final stage of GA biosynthesis, the reaction is catalyzed by two 2ODD enzymes, GA 20-oxidase (GA20ox) and GA 3-oxidase (GA3ox), encoded by gibberellin oxidase gene families, *GA20ox* and *GA3ox*, respectively. Development and environmental cues moderate the *in vivo* concentrations of bioactive GAs at the sites of action, and GA catabolism is crucial for maintaining these GA levels in plants. The deactivation of GAs is mainly regulated by the GA 2-oxidase enzyme encoded by the *GA2ox* gene family (Hedden & Thomas, 2012; Yamaguchi & Kamiya, 2000; Yamaguchi, 2008). Upon release, GA

promotes the destruction of the negative regulators of GA signaling called DELLA proteins via the ubiquitin-proteasome pathway, revoking DELLA-mediated repression of GA responses (Hauvermale et al., 2012; Silverstone et al., 2001), including seed germination.

Endogenous active GA accumulation is usually higher during embryo development, deactivates during seed maturity, and increases again at the beginning of seed germination, just before radicle formation (Ogawa et al. 2003). In the natural environment, seed germination is stimulated by GAs in response to favourable environmental conditions. Upon imbibition, the embryo releases GAs, which play a vital role by inhibiting the effect of ABA and stimulating the secretion of hydrolytic enzymes such as α -amylases to mobilize food reserves in the starchy endosperm to increase the growth potential of the embryo (Bewley, 1997). GAs were found to be responsible for stimulating the expression of genes associated with cell expansion and modification to reduce the mechanical barrier provided by the seed coat by the enzymatic weakening of the tissues surrounding the radicle (Finkelstein et al., 2008). It has been reported that ABA and GA exhibit a mutual antagonistic regulation that suppresses each hormone's biogenesis. High accumulation of ABA and low GA levels maintain seed dormancy, while low ABA and high GA accumulation stimulate seed germination (Seo et al., 2009; Shu et al., 2013; Shu et al., 2016); thus, ABA/GA balance is pivotal to determining the seed's fate.

In addition to ABA and GA, nearly all other plant hormones, like auxins, ethylene (ET), brassinosteroid (BR), jasmonates (JAs), cytokinin (CK) and salicylic acid (SA), are involved in the regulation of seed dormancy and germination (Finkelstein et al., 2008;

Kucera et al., 2005; Shu et al., 2016). Understanding the roles of these hormones and their crosstalk is crucial for preventing PHS in agricultural practices.

Auxin is another primary hormone in higher plants, which entails many plant developmental processes due to different environmental cues such as apical dominance, root and stem tropisms, and arranging cell division (Balzan, Johal, & Carraro, 2014; Zhao, 2010). Recent studies have revealed that auxin participates in cross-talk with ABA to suppress seed germination. For instance, Belin et al. (2009) reported that the ABA suppresses the elongation of the embryonic axis by downregulating the *AUXIN INDUCIBLE* gene (*AXR/IAA*) expression in *Arabidopsis thaliana*. Moreover, a study conducted by Ramaih, Guedira, & Paulsen (2003) revealed that alteration to the auxin sensitivity in wheat caryopses during AR could hinder the germination of wheat seeds, thus impeding PHS.

ET is a known dormancy inhibitor which stimulates seed germination by acting against the effect of ABA. ET generation in the seeds begins with imbibition and increases with germination advancement. The radicle protrusion is concomitant with the peak of the ET emission (El-Maarouf-Bouteau et al., 2014; Kepczynski, Rudnicki, & Khan, 1977; Matilla, 2000; Matilla & Matilla-Vazquez, 2008; Satoh, Takeda, & Esashi, 1984). However, a recent study conducted by Sun et al. (2019) using non-dormant wheat genotype RL4452 discovered that ET does not affect radicle protrusion in wheat but controls post-germination seedling growth through endospermic starch degradation via modulation of ABA/GA balance through metabolism and signaling.

BRs are plant steroid hormones that regulate numerous developmental and physiological responses in plants, including plant growth and cell division, reduced root elongation, epinasty, and plant resistance to pathogens and diseases (Ali et al., 2013; Ikekawa & Takatsuto, 1984; Salchert et al., 1998; Wang, 2011). Previous studies conducted on *Arabidopsis* (Steber & McCourt, 2001), barley (*Hordeum vulgare* L.) (Kartal et al., 2009), sorghum (Vardhini & Rao, 2003), *Ailanthus altissima* (Li, Zhang, & Li, 2005) seeds provide evidence to confirm that BRs play a role in the stimulation of germination. BRs mainly regulate seed germination by counteracting the effect of ABA through the *MFT*-mediated pathway (Steber & McCourt, 2001; Xi et al., 2010) and increasing protein and proline contents (Vardhini & Rao, 2003). Chitnis et al. (2014) reported that the dormancy decay in imbibed AR wheat is associated with the increased synthesis and signaling of BR, thereby promoting seed germination by antagonizing the effect of ABA.

Jasmonic acid (JA) and its conjugates methyl ester, methyl jasmonate (MeJA) and jasmonyl isoleucine (JA-Ile), together called JAs, are cyclopentanone compounds derived from fatty acid metabolism (Pirbalouti, Sajjadi, & Parang, 2014). The action of JAs on seed dormancy and germination are contradictory and remain unclear. JA and MeJA act as stimulators of seed germination in dormant seeds, while in non-dormant seeds, their action inhibits germination (Creelman & Mullet, 1997). Coronatine insensitive1 (*COI1*), an F-box protein, is vital in all responses of JAs (Ellis & Turner, 2002). Barrero et al. (2009) discovered that the jasmonate-related genes involved in the biosynthesis of JAs, *Jasmonate 12-oxophytodienoic acid reductase* and *Allene oxide synthase*, were upregulated in coleorhiza, which consequently associated with the germination of AR barley. JAs have shown an antagonistic effect with ABA during wheat seed germination

by repressing the ABA biosynthesis genes, activating ABA-inactivating genes, and alleviating seed dormancy in dormant wheat seeds (Jacobsen et al., 2013). Contrarily, however, Nambara et al. (2010) reported that seed germination is delayed by exogenous JA application. Mutations in jasmonate signaling factors, *COII*, and *JASMONATE INSENSITIVE4 (JIN4)* cause hypersensitivity to ABA during the germination of AR barley (Ellis & Turner, 2002), promoting seed dormancy.

CKs exist as nucleobase, nucleotide, and nucleoside forms, and biologically active CKs are isopentenyladenine (iP), trans isomer of zeatin (tZ), and dihydrozeatin (dihydroZ) *in vivo*. CKs play a vital role in the development of cereal grains. Precipitously elevated CK levels have been observed in developing maize, wheat, rice, and barley grains right after the anthesis (Morris et al., 1993). Studies have shown that CKs counteract the effect of ABA during seed dormancy alleviation and germination in *Arabidopsis* (Wang et al., 2011) and lettuce (Khan, 1968) seeds. Moreover, CKs enhance the activity of GA by reversing the inhibitory effect on α -amylase synthesis from ABA during barley (Khan & Downing, 1968) and wheat (Eastwood, Tavener, & Laidman, 1969) seed germination.

SA is a well-known endogenous signaling molecule associated with the plant's defence mechanism against pathogens. Moreover, recent studies discovered that exogenously applied SA blocks germination under normal conditions in barley seeds by suppressing the α -amylase expression induced by GA (Xie et al., 2007). However, under stress conditions such as salinity, exogenous application of SA promotes the alleviation of germination arrest in *Arabidopsis* (Lee, Kim, & Park, 2010; Rajjou et al., 2006), broad bean (*Vicia faba* L.) (Anaya et al., 2018) and wheat (Dolatabadian, Modarres Sanavy, & Sharifi, 2009) via an

antioxidant pathway, accomplished by reducing the activity of antioxidative enzymes (CAT), peroxidase, superoxide dismutases (SODs), and polyphenol oxidase, thereby reducing the oxidative damage. Nevertheless, Chitnis et al. (2014) revealed that SA stimulates the germination in AR wheat even under natural conditions, suggesting that the SA signaling might contribute to the regulation of ROS levels, which accumulate due to the dormancy release of seeds by AR, thus encouraging the germination.

Concisely, all the other phytohormones, auxins, ET, BR, JAs, CK and SA are involved in seed dormancy and germination regulation by mediating the ABA/GA balance.

1.3.3.4 The role of α -amylase

Three types of natural amylases have been found in organisms, termed α -amylase (EC 3.2.1.1), β -amylase (EC 3.2.1.2) and γ -amylase (EC 3.2.1.3). These amylases break down starch molecules by hydrolyzing different sites on the molecule. α -Amylase belongs to the glycoside hydrolase 13 family and acts on random sites to cleave α -1,4 glycosidic bonds on the amylose chains to yield maltose and maltotriose, and on amylopectin chains to yield glucose, maltose and dextrin. β -Amylase belongs to glycoside hydrolase family 14 and cleaves the second α -1,4 glycosidic bond in the starch molecule to yield two maltose molecules simultaneously. γ -Amylase hydrolyzes the last α -1,4 glycosidic and α -1,6 glycosidic bonds in the starch molecule to yield glucose molecules (Rani, Rana, & Datt, 2015). α -Amylase and β -amylase are active amylases found in seeds. The action of these two amylases, together with the debranching enzyme and α -glucosidase, is crucial for complete starch degradation (Sun & Henson, 1991), which is vital for providing the necessary energy and nutrients for seed germination and early seedling growth.

α -Amylase engages in many physiological processes in plants, including seed germination, where α -amylase in the aleurone degrades the endosperm starch reserve to generate energy for the germination process (Akazawa & Hara-Mishimura, 1985; Beck & Ziegler, 1989). Ritchie et al. (2000) revealed that approximately 70% of newly synthesized and secreted enzymes from the aleurone are α -amylases. GA biosynthesis initiates in the embryo prior to α -amylase expression. Synthesized active GAs are then transported to the aleurone to trigger the secretion of α -amylase into the endosperm to catalyze starch hydrolysis (Fincher, 1989). The orchestrated interaction of GA synthesis, α -amylase secretion, and starch hydrolysis ensures the growing embryo acquires the energy and nutrients needed to fuel its growth during seed germination.

β -Amylase accumulates in soluble and bound forms during the grain development stage. The vast majority of β -amylase accumulates in inactive, bound form in the starchy endosperm, where the enzyme is deposited as a component of the protein matrix on the periphery of the starch granules to protect from premature attack by α -amylase (Ziegler, 1999). Goswami, Jain, & Paul (1977) reported that free β -amylase hydrolyzes starch during the first 24 h of germination in wheat, and during the next 24 h, α -amylase synthesized *de novo* acts concertedly with some of the β -amylase that converts from the inactive form. However, the activity of β -amylase dwindles at the later germination stage when α -amylase becomes predominant.

Right after the water absorption to an adequate level, α -amylase activity increases in seeds. PHS-resistant and sensitive varieties showed a significant difference in α -amylase activity in wheat. Therefore, the correlation between α -amylase and PHS in wheat is noteworthy

(Gao et al., 2013). Genes, *α -Amy1*, *α -Amy2* and *α -Amy3* are the three different classes of α -amylase genes identified, located on chromosomes 6, 7 and 5, respectively, in hexaploid wheat (Baulcombe et al., 1987; Huttly et al., 1988). However, these genes are differentially expressed (Marchylo, Kruger, & MacGregor, 1984). Sargeant (1980) has identified two α -amylase isozymes in wheat. At the onset of germination (1st-2nd days), the α -amylase-1 isozyme is more active and abundant, whereas, after the third day of germination, the α -amylase-2 isozyme became active and abundant. However, α -amylase-3 isozyme only became abundant in developing grains (Baulcombe et al., 1987). Studies have discovered that α -amylase/subtilisin inhibitors restrain seed germination in wheat (Mundy, Hejgaard, & Svendsen, 1984; Henry et al., 1992), and α -amylase-1/subtilisin inhibitors have shown increased PHS tolerance in barley varieties (Yuan et al., 2005; Gao et al., 2013). These findings suggest that the regulation of α -amylase activity, the differential expression of α -amylase genes, and the presence of α -amylase inhibitors are important factors that influence seed germination and PHS susceptibility in wheat and related cereal crops. Understanding these characteristics can benefit breeding programmes aiming to generate PHS-resistant cultivars.

1.4 Role of reactive oxygen species and reactive nitrogen species in plants and the regulation of seed germination and dormancy

1.4.1 Reactive oxygen and nitrogen species

Reactive oxygen species (ROS) and reactive nitrogen species (RNS) are two groups of highly reactive molecules containing oxygen and nitrogen, respectively, which are often

called reactive oxygen and nitrogen species (RONS) collectively. RONS are by-products of metabolism, and RONS that bear unpaired electrons are called free radicals (Weidinger & Kozlov, 2015). For instance, superoxide ($O_2^{\bullet-}$), peroxy (RO_2^{\bullet}), hydroxyl ($\bullet OH$), and alkoxy ($RO\bullet$) are some oxygen-derived free radicals. Ozone (O_3), singlet oxygen (1O_2), hypochlorous acid (HOCl), and hydrogen peroxide (H_2O_2) are some examples of oxygen-derived non-radicals, which give rise to chain reactions that easily convert into radicals or oxidizing agents. Nitric oxide (NO^{\bullet}), peroxynitrite ($ONOO\bullet$), and nitrogen dioxide (NO_2^{\bullet}) are some nitrogen-derived RNS that are generated in plants (Bedard & Krause, 2007), which play crucial roles in plant signaling, stress responses, and regulation of growth and development.

1.4.2 ROS and RNS production sites in plants

The generation of ROS is a cascade of reactions that commence with the partial reduction of oxygen to $O_2^{\bullet-}$ radicals. Because of the instability and reactivity, $O_2^{\bullet-}$ radicals act as primary precursors of various ROS and mediate chain reactions (Thannickal & Fanburg, 2000; Zeng et al., 2017). The dismutation of $O_2^{\bullet-}$ produces H_2O_2 via an enzymatic pathway catalyzed by superoxide dismutase (SOD) at low pH. Subsequently, H_2O_2 is either fully reduced by converting to water or partially reduced by $O_2^{\bullet-}$ to $\bullet OH$ (Liochev & Fridovich, 1999).

1.4.2.1 NADPH oxidases in the plasma membrane

Numerous intracellular locations contribute to the total RONS content under normal and stress conditions (Minibaeva & Gordon, 2003). An essential function of Respiratory Burst Oxidase Homologs (RBOHs), designated as Nicotinamide Adenine Dinucleotide

Phosphate oxidases (NOXs) localized in the plasma membrane, has recently been identified as a crucial signaling hub in the ROS gene network of plants (Suzuki et al., 2011). NOXs are the most studied ROS-generating enzymes integrating numerous signal transduction pathways with ROS signaling. The electron transport from the cytosolic Nicotinamide Adenine Dinucleotide Phosphate (NADPH) to extracellular oxygen is catalyzed by NADPH oxidase, resulting in $O_2^{\cdot-}$ radicals (Minibaeva and Gordon, 2003). Different *Rboh* genes have been discovered in rice (Groom et al., 1996), tomato (Amicucci, Gaschler, & Ward, 1999), potato (Yoshioka et al., 2001), apple (Cheng et al., 2020) and tobacco (Yoshioka et al., 2003), whereas Arabidopsis NOXs are encoded by a multigenic family with ten *AtRboh* genes (Mittler et al., 2004; Torres & Dan, 2005). NOXs in plants have homology with the mammalian *gp91^{phox}* domain of the respiratory burst oxidases. However, in contrast to mammalian NOXs, plants consist of an additional N-terminal region, which contains regulatory regions, such as EF-hands, that bind calcium (Ca^{2+}) and phosphorylation domains necessary for the function of the plant oxidases (Groom et al., 1996; Keller et al., 1998). Ca^{2+} influx into the cytoplasm is involved in the activation of RHOs. Conformational changes in EF-hand motifs were stimulated by the increase in cytosolic Ca^{2+} , which helps Ca^{2+} binding (Ogasawara et al., 2008). Phosphorylation of Ca^{2+} -dependent protein kinases (CDPKs) was found to be controlled by Ca^{2+} , which in turn regulates the RHOs' activity and ROS production (Kobayashi et al., 2007). However, Levine et al. (1996) demonstrated that H_2O_2 activates Ca^{2+} channels, implying that Ca^{2+} mediates ROS production upstream and downstream events.

1.4.2.2 Other intracellular locations of RONS generation

Mitochondria are deemed to be one of the key players in ROS production. H_2O_2 and $\text{O}_2^{\cdot-}$ are generated in mitochondria during the mitochondrial electron transport chain (mtETC) (Navrot et al., 2007). Complex I and Complex III in mtETC are mainly responsible for producing ROS (Møller, Jensen, & Hansson, 2007; Noctor, De Paepe, & Foyer, 2007). Oxygen converts to $\text{O}_2^{\cdot-}$ in mitochondrial complex I, and reverse electron flow from complex III further increases the production (Turrens, 2003). Nevertheless, compared to mammalian mitochondria, the relative contribution to ROS production in plant mitochondria in photosynthetic plants is diminutive (Purvis, 1997). Mitochondria are an intracellular source of NO^{\cdot} , and the production rate varies with the intra-mitochondrial oxygen concentration (Alvarez et al., 2003). NO^{\cdot} is produced as a byproduct of the breakdown of arginine (Arg) to citrulline, which is catalyzed by enzyme nitric oxide synthases (NOSs). In mammals, NOS has been discovered in the mitochondrial matrix (Alvarez et al., 2003; Ghafourifar & Richter, 1997). However, the data for NOS in plants is controversial and debatable, and NOS genes equivalent to those found in animals have not been identified and characterized in plants. Studies have identified that mtETC reduces nitrite to NO^{\cdot} , especially to survive under conditions such as hypoxic or anoxic periods (Gupta, Stoimenova, & Kaiser, 2005; Planchet et al., 2005). Additionally, a study by Gupta & Kaiser (2010) demonstrated that NO^{\cdot} production in root mitochondria only occurs by nitrite reduction on the mitochondrial membrane but not via NOS in the mitochondrial matrix and depends on nitrite content. The location of mitochondria and the external stimuli in plants determines NO^{\cdot} generation in mitochondria (Gupta, Stoimenova, & Kaiser, 2005). Igamberdiev & Hill (2004) revealed that under low oxygen conditions, NO^{\cdot} production

could maintain the energetics in the plant mitochondria. NO^* is produced by reducing nitrite through a cyclic reaction where nitrate acts as an intermediate electron acceptor. Eventually, NO^* is reduced back to nitrate by a hypoxically-induced class 1 hemoglobin, contributing to the oxidation of NADPH. The production of NO^* is stimulated by H_2O_2 content in mitochondria (El-Maarouf-Bouteau & Bailly, 2008). Generated NO^* can react with $\text{O}_2^{\cdot-}$ resulting in ONOO^{\bullet} (Alvarez et al., 2003; Ghafourifar & Richter, 1997; Giulivi, Poderoso & Boveris, 1998), a potent nitrating agent and an oxidant.

Photosynthesis utilizes CO_2 , water, and light energy to generate food and oxygen in chloroplasts. However, inefficient light energy utilization under an oxygen-rich environment inevitably yields ROS via photosystem I (PSI) and photosystem II (PSII) along the thylakoid membrane (Asada, 2006; Khorobrykh et al., 2020). Excess photons trapped in PSII activate the chlorophylls in the light-harvesting complex, where these excited chlorophylls transfer the absorbed energy to the oxygen, producing highly reactive $^1\text{O}_2$ (Asada, 2006; Triantaphylidès & Havaux, 2009). The leakage of PSII-derived electrons to oxygen via ineffective photochemical and non-photochemical quenching (NPQ) in the PSI electron transfer complex leads to the production of $\text{O}_2^{\cdot-}$ at PSI (Havaux, Strasser & Greppin, 1991). Moreover, the electron acceptor side of the PSII generates $\text{O}_2^{\cdot-}$ due to electron leakage, which dismutase to H_2O_2 , whereas H_2O_2 is produced by incomplete water oxidation on the electron donor side of PSII. Subsequently, generated H_2O_2 was further reduced to more dangerous $^{\bullet}\text{OH}$ (Pospisil, 2016). Mehler (1951) discovered the photoreduction of oxygen to H_2O_2 in PSI. The electron transfer from excited PSI reduces NADP^+ to NADPH, which ultimately reduces the final electron acceptor, CO_2 , in the

Calvin cycle (Mehler, 1951). However, a part of the electron flow diverts from ferredoxin to oxygen, giving rise to the $O_2^{\bullet-}$ radicals.

Peroxisomes are another major site of intracellular H_2O_2 production due to their integral oxidative metabolism. H_2O_2 -producing flavin-oxidases and CAT are well-known protein constituents identified in peroxisomes (del Río et al., 2006; Palma et al., 2009). Peroxisomal matrix and peroxisomal membrane are the two sites involved in the production of $O_2^{\bullet-}$ in peroxisomes. Oxidation of xanthene and hypoxanthine to uric acid, which is catalyzed by xanthine oxidase in the peroxisomal matrix, generates $O_2^{\bullet-}$ radicals (Halliwell & Gutteridge, 2000). Additionally, the peroxisomal membrane is composed of many major and minor peroxisomal membrane polypeptides (PMPs). NADPH-dependent small ETC with three major integral peroxisomal membrane polypeptides termed PMP18, PMP29 and PMP32, according to their molecular masses, 18KD, 29KD and 32KD, respectively, is responsible for $O_2^{\bullet-}$ production. PMP18, PMP29 and PMP32 were proposed as cytochrome b, peroxisomal NADPH: cytochrome P450 reductase and monodehydroascorbate reductase (MDHAR), respectively. Nicotinamide adenine dinucleotide (NADH) is used as an electron donor by PMP18 and PMP32 to produce $O_2^{\bullet-}$ radicals, whereas PMP29 depends on NADPH as an electron donor (López-Huertas et al., 1999). Reducing glutathione (GSH) by NO^{\bullet} generates another RNS, S-nitrosoglutathione (GSNO), in peroxisomes (del Río et al., 2006; Durzan & Pedroso, 2002). Furthermore, $ONOO^{\bullet}$ and peroxynitrous acid can be produced by the reaction of NO^{\bullet} with $O_2^{\bullet-}$, and $ONOO^{\bullet}$ rapidly decomposes to generate $^{\bullet}OH$ and NO^{\bullet}_2 (Durzan and Pedroso, 2002), which are high oxidizing agents.

Additionally, apoplast (Hu et al., 2006; Podgórska, Burian, & Szal, 2017), endoplasmic reticulum (ER) (Duan et al., 2010; Mittler, 2002; Zeeshan et al., 2016) and cell walls (Higuchi, 2006; Lüthje & Martinez-Cortes, 2018) are involved in the production of RONS, especially under the stress conditions in plants.

1.4.3 Enzymatic and non-enzymatic antioxidant mechanisms of ROS/RNS scavenging in plants

Virtually all biological molecules, including lipids, DNA, and proteins, are susceptible to ROS damage, affecting cell functions due to the high reactivity and toxicity (Gill & Tuteja, 2010; Møller et al., 2007). It has been estimated that 1-2% of consumed oxygen generates ROS in various sub-cellular locations in plants (Bhattacharjee, 2005). Numerous antioxidative defence mechanisms scavenge ROS under steady-state conditions. However, various biotic and abiotic stress factors can disturb the balance between ROS production and scavenging, leading to oxidative bursts that damage the structure and function of the cell mainly by lipid peroxidation, oxidation of proteins and damaging DNA (Foyer & Noctor, 2005). Finally, cellular damage and death can be caused by the overproduction of ROS due to stress conditions (Gill & Tuteja, 2010), potentially affecting plant growth and development. Enzymatic and non-enzymatic mechanisms are included in the ROS-scavenging system to thwart stress-induced ROS accumulation.

1.4.3.1 Enzymatic antioxidant mechanisms of ROS/RNS scavenging in plants

The antioxidant enzymes work synergistically and interactively in different sites of plant cells to detoxify ROS in the enzymatic mechanisms. SOD (E.C.1.15.1.1), glutathione peroxidase (GPX, EC 1.11.1.9), CAT (EC 1.11.1.6), ascorbate peroxidase (APX, EC

1.11.1.11), guaiacol peroxidase (GOPX, EC 1.11.1.7), dehydroascorbate reductase (DHAR, EC 1.8.5.1), MDHAR (EC 1.6.5.4), glutathione reductase (EC 1.6.4.2), and glutathione S-transferase (GST, EC 2.5.1.18) are some enzymatic ROS scavengers (Mittler et al., 2004). The coordination of these enzymes is crucial for plant survival and adaptation to changing conditions.

The $O_2^{\bullet -}$ radicals are moderately reactive, and the life span is very concise. Besides converting into more reactive and toxic ROS species, the damage caused by $O_2^{\bullet -}$ itself to the cell components and biological molecules is minute (Halliwell, 2006; Møller et al., 2007). However, the elimination of generated $O_2^{\bullet -}$ is essential to maintain the redox homeostasis in the cell. As the first line of defence, SOD dismutates $O_2^{\bullet -}$ into more stable H_2O_2 and oxygen, thereby decreasing the chance of $\bullet OH$ radical formation. SODs are metalloenzymes and classified according to their metal co-factor, manganese (Mn-SOD), copper/zinc (Cu/Zn-SOD) and iron (Fe-SOD). These SODs are confined in different cellular compartments to carry out $O_2^{\bullet -}$ dismutation (Mittler, 2002). Their compartmentalization within the cell attests to the accuracy and efficacy of the plant's antioxidant defence system.

H_2O_2 in low concentration acts as a signaling molecule stimulating tolerance to various biotic and abiotic stresses, whereas high H_2O_2 concentration leads to programmed cell death (Quan et al., 2008). Enzymatic scavengers CAT, GPX, APX, and GOPX detoxify H_2O_2 by converting it to water and oxygen.

CAT is a tetrameric heme-containing enzyme mainly located in peroxisomes to catalyze H_2O_2 dismutation into water and oxygen (Mittler, 2002). However, Mhamdi et al. (2010)

reported that CAT enzymes are located in other subcellular compartments such as mitochondria, chloroplast and the cytosol. APX localizes in chloroplast and the cytosol and eliminates H_2O_2 by reducing it to water and dehydroascorbate (DHA), using ascorbic acid as a reducing agent via the ascorbate-glutathione cycle (AsA-GSH) and the water-water cycle. In contrast to CAT, APX is an efficient scavenger due to its higher affinity to H_2O_2 and wide distribution, consisting of at least five isomers confined to different subcellular locations (Noctor & Foyer, 1998; Sharma & Dubey, 2004). GOPX is a heme-containing enzyme that detoxifies excess H_2O_2 using aromatic compounds such as guaiacol and pyragallol as electron donors. GOPX is active in the extracellular locations (cell wall) and intracellular locations, such as the cytosol and vacuole, and utilizes H_2O_2 during both normal metabolism and stress conditions. Therefore, GOPX is considered a key enzyme in maintaining the H_2O_2 equilibrium in plant cells (Asada, 1999). GPXs are Cys-containing antioxidant enzymes, mainly localized in the cytosol and mitochondria, that catalyzes the reduction of H_2O_2 into water and oxygen via the oxidation of reduced glutathione (GSH) into glutathione disulfide (GSSH). In addition to H_2O_2 , GPX can effectively detoxify lipid peroxides to lipid alcohols (Noctor et al., 2002), thereby maintaining cell redox homeostasis.

DHAR and MDHAR are responsible for regenerating the cellular ascorbic acid pool. These enzymes are vital for sustaining H_2O_2 scavenging activity by APX. DHAR utilize GSH as an electron donor to convert DHA to ascorbic acid (Eltayeb et al., 2007), whereas MDHAR regenerates ascorbic acid from the short-lived monodehydro ascorbate, using NADPH as a reducing agent (Mittler, 2002). Glutathione reductase is a crucial component of the AsA-GSH cycle, which catalyzes the reduction of GSSG to GSH using NADPH as a reductant;

thereby, it is vital to maintain the GSH pool. In general, Glutathione reductase is predominantly located in the chloroplasts. However, recent studies revealed that mitochondria and cytosol contain a small amount of glutathione reductase enzymes (Creissen et al., 1994; Edwards, Rawsthorne, & Mullineaux, 1990). GSTs are a large and highly diverse group of ubiquitous enzymes predominantly found in the cytoplasm. Microsomal, nuclear, plastidic, and apoplastic isoforms of GST have been identified by recent studies (Frova, 2003). GSTs contribute to the conjugation of GSH with various electrophilic and hydrophobic xenobiotic substrates.

1.4.3.2 Non-enzymatic antioxidant mechanisms of ROS/RNS scavenging in plants

In the non-enzymatic homeostasis system, low molecular mass antioxidants such as ascorbate (AsA), GSH, carotenoids, tocopherols, and flavonoids regulate RONS (Gill & Tuteja, 2010). $^1\text{O}_2$ is the first excited electron state of oxygen and a highly reactive oxidizing agent that can oxidize various biological molecules, including proteins, lipids, pigments and DNA (Hatz, Lambert, & Ogilby, 2007; Krieger-Liszkay, Fufezan, & Trebst, 2008; Wagner et al., 2004). Triantaphylidès et al. (2008) documented that $^1\text{O}_2$ was responsible for more than 80% of the non-enzymatic lipid peroxidation in Arabidopsis leaf tissues. However, apart from the deleterious effect, $^1\text{O}_2$ functions as a signaling molecule, activating many stress-response pathways by upregulating defence response genes (Krieger-Liszkay, Fufezan, & Trebst, 2008; op den Camp et al., 2003). It is well established that $^1\text{O}_2$ equilibrium is maintained by efficiently quenching $^1\text{O}_2$ via a non-enzymatic pathway, mainly using β -carotene, plastoquinone or tocopherol (Gill & Tuteja, 2010), ultimately protecting cellular components from oxidative damage.

The non-enzymatic scavenging pathway detoxifies RNS, and some free radicals are involved in RNS scavenging. NO^\bullet is one of the critical RNSs generated in plants. NO^\bullet acts as a signal molecule and controls physiological processes, including seed germination (Domingos et al., 2015), lateral root development (Correa-Aragunde, Graziano, & Lamattina, 2004), and stress responses such as pathogen attack (Mur et al., 2012; Ye et al., 2013). Moreover, major plant hormones such as auxin (Kramer & Bennett, 2006), CK (Shao, Wang, & Shanguan, 2010) and JA (Liu et al., 2005) have been found to act synergistically with NO^\bullet radicals. Ascorbic acid, flavonoids, melatonin, oxygen, Fe^{2+} and O_2^\bullet are some endogenous NO^\bullet scavengers in plants. Thiols, flavonoids, phenolic acids, Zn-SH groups, iron/sulphur centers, GSH, ascorbic acid, and melatonin are some scavengers of ONOO^- and NO^\bullet_2 (Arnao & Hernández-Ruiz, 2019). This intricate interplay between signaling molecules and antioxidants emphasizes the complexity of plant stress responses and strategies for adaptation. Properties and antioxidant scavengers of major ROS are listed in Table 1.

The most reactive ROS identified *in vivo* is $^\bullet\text{OH}$ radical. Almost any constituent of cells, including all biological molecules, is susceptible to damage by $^\bullet\text{OH}$ radicals. However, no enzymatic or non-enzymatic mechanism has been discovered that effectively quenches $^\bullet\text{OH}$ (Das & Roychoudhury, 2014; Pinto et al., 2003); thereby, excessive accumulation ultimately leads to cell death.

Table 1: Properties and antioxidant scavengers of major ROS

ROS	Properties	Enzymatic/Non-enzymatic Antioxidants
$O_2^{\cdot-}$	Moderately reactive Concise life span Good reductant	Enzymatic SOD Non-enzymatic Ascorbic acid
H_2O_2	Oxidant High diffusability	Enzymatic CAT, GPX, APX, GOPX Non-enzymatic Ascorbic acid
1O_2	Highly reactive oxidizing agent	Non-enzymatic β -carotene, Plastoquinone, Tocopherol
$ONOO^{\cdot-}$	Good oxidant Short-lived	Non-enzymatic Thiols, Flavonoids, Phenolic acids, Zn-SH groups, Iron/sulphur centers, GSH, Ascorbic acid, Melatonin
ROO^{\cdot}	High diffusability Low oxidizing ability compared to $\cdot OH$	Non-enzymatic Phenolic acids, Tocopherol

1.4.4 ROS-mediated reversible and irreversible protein modifications

Proteins are one of the major cellular targets of the oxidative species (Levine et al., 1994). Proteins have numerous biological functions, and post-translational modifications (PTMs) are vital to control the stability, conformation and localization of the protein (Hashiguchi & Komatsu, 2017). Plants depend on various PTMs to expand protein function to survive in the environment (Glazer et al., 1975). PTMs mediated by ROS are termed oxidative PTMs. Apart from $\cdot OH$ radicals, all the other ROS react specifically with proteins and have a low oxidation rate. However, being the most reactive ROS, $\cdot OH$ radicals react non-specifically with proteins with a high and constant oxidation rate (Davies, 2005). In contrast, RNS, including NO^{\cdot} -involved in PTMs, are termed nitrosative PTMs. These

oxidative and nitrosative modifications alter the enzymatic and binding properties of the protein, leading to various functional changes (Stadtman, 1992). The studies have identified more than 400 types of PTMs that affect protein function (Khoury, Baliban, & Floudas, 2011). Among these, phosphorylation, ubiquitination, and acetylation are the prominent and most frequent PTMs.

Each amino acid goes through a minimum of three types of PTMs. However, some amino acids, including Lysine (Lys), Cysteine (Cys) and Serine (Ser), were found to undergo more than ten types of PTMs (Ramazi & Zahiri, 2021). Generally, these modifications can be classified into two categories: i) irreversible PTMs and ii) reversible PTMs (Stadtman & Levine, 2003).

Phosphorylation, ubiquitylation, methylation, and glycosylation are some of the most studied reversible protein modifications (Ramazi & Zahiri, 2021). A phosphate group from adenosine triphosphate is transferred to the target amino acid residue in phosphorylation; kinase enzymes catalyze this reaction. Usually, Cys, Ser, Threonine (Thr), Tyrosine (Tyr) and Histidine (His) residues are prone to phosphorylation (Panni, 2019; Skamnaki et al., 1999). Ubiquitylation is a versatile PTM that predominantly occurs on Lys; however, all amino acids can undergo ubiquitylation, where a covalent bond forms with the residue and the C-terminal of an active ubiquitin protein (Bhogaraju & Dikic, 2016). Methylation is a PTM that occurs by the addition of a methyl group to the target residue. Nitrogen-containing side chains of Arg and Lys undergo methylation often, especially on nuclear proteins such as histone (Huang et al., 2018; Ramazi, Allahverdi, & Zahiri, 2020). The addition of carbohydrates by covalent bonds to the protein via amino acid residues is

known as glycosylation. This complex, enzyme-directed reaction is catalyzed by the glycosyltransferase enzyme, which occurs more often on Ser, Thr, Asn and tryptophan (Trp) residues (Huang et al., 2018) and is vital for protein stability, folding, and cellular recognition processes.

Post-translational thiol modifications of Cys residues are facile, highly selective, and considered a putative mechanism of cell responses to RONS (Go et al., 2011). It is increasingly apparent that the RONS-mediated reversible thiol modifications are vital for the dynamic modulation of protein function. Cys is a sulphur-containing amino acid within proteins with the formula $\text{HOOC-CH(-NH}_2\text{)-CH}_2\text{-SH}$ (Biteau, Labarre, & Toledano, 2003; Jacob, Holme, & Fry, 2004) and is more susceptible to oxidation from RONS.

However, not all Cys thiol (Cys-SH) groups are prone to redox modifications, and the reactivity varies according to the physiological function and endogenous redox environment (Waszczak et al., 2015). It is noted that the reactivity of the individual Cys residue depends on the ability to form the thiolate anions (Cys-S⁻), which are more reactive than the Cys-SH. H₂O₂ predominantly causes thiolate anion formation, and the reaction depends on the pK_a of the sulphur atom and the pH of the surrounding solution. Protonated thiols will dominate if the pK_a of the sulphur atom is higher than the pH of the surrounding solution. Conversely, the lower pK_a of the sulphur atom compared to the pH of the surrounding solution leads to the formation of Cys-S⁻ (Harris & Turner, 2002). Furthermore, one-electron oxidants such as O₂^{•-} and [•]OH radicals can oxidize Cys-SH to generate thiyl radicals (Cys-S[•]). Subsequently, these Cys-S[•] and Cys-S⁻ undergo further

modifications (Winterbourn & Hampton, 2008), including the highly unstable, reversible sulfenic acid (Cys-SOH, S-sulfenation) formation.

Two-electron oxidants such as H_2O_2 , ONOO^- , hypohalites and halo amines can generate Cys-SOH directly from Cys-SH as the first form of Cys thiol oxidation, which can dramatically affect protein function (Poole, Karplus, & Claiborne, 2004; Poole & Nelson, 2008). Furthermore, non-radical species, including peroxynitrites (ONOOH) and hypobromous (HOBr) or hypochlorous (HOCl) acids, can react with Cys-SH to generate Cys-SOH. The presence of excess oxidants can further oxidize Cys-SOH into sulfinic acid (Cys-SO₂H) and sulfonic acid (Cys-SO₃H) forms (Finkel, 2012; Roos & Messens, 2011), which are irreversible modifications and can lead to permanent changes in protein structure and function.

RNS is involved in protein S-nitrosylation. Covalent attachment of NO^\bullet to Cys-SH is termed S-nitrosylation and is considered a critical modification that regulates protein activities by various mechanisms, including stability, conformation change, subcellular localization, and protein-protein interaction (Foster et al., 2003; Hess et al., 2005; Astier et al., 2011). However, NO^\bullet does not directly react with Cys-SH by itself. NO^\bullet derivatives, S-nitrosothiols, are involved in the reaction (Dahm, Moore, & Murphy, 2006). Additionally, NO^\bullet and its derivatives can be involved in the range of reactions that produce Cys-SO₃H from Cys-SH.

S-glutathionylation (Cys-S-S-GSH) has recently gained increasing attention as a major Cys modification that occurs under oxidative stress conditions (Xiong et al., 2011). S-glutathionylation can occur by various pathways. I) Low molecular weight, major cellular

antioxidant thiol, GSH, can react with partially oxidized (activated) protein sulphhydryls such as Cys-S[•], Cys-SOH, and protein S-nitrosothiol (S-nitrosated protein), forming a disulfide bridge between the Cys residue and the glutathione tripeptide. II). Through disulfide exchange between protein Cys-SH and GSSG (Biswas, Chida, & Rahman, 2006; Ghezzi, 2005). III). The reaction of intermediate S-nitrosothiols such as GSNO with Cys-SH (Rinalducci, Murgiano, & Zolla, 2008). S-glutathionylation is a redox-sensitive, reversible covalent modification that leads to functional changes in the target proteins (Zweier, Chen, & Druhan, 2011) and protects from irreversible and permanent damage (Coan et al., 1992); thus, it serves as a means to restore protein function under oxidative stress conditions.

Amide or amine can react with Cys-SOH to form a sulfenylamide (Cys-S-N), and condensation with another Cys-SOH leads to the formation of thiosulfinate (Cys-S(O)S-Cys) (Claiborne et al., 1993). Alternatively, Cys-SOH can be modified by forming disulphide bonds with free protein thiols intramolecular or intermolecular (Cys-S-S-Cys/ Cys-S-S-Cys'), termed as S-cysteinylation (McDonagh, 2012). These reversible formations stabilize the protein structure under oxidative stress (Savitsky & Finkel, 2002). Persulfidation (Cys-SSH), the interaction of H₂S with Cys-SOH, is another reversible Cys modification that prevents further oxidation of Cys-SOH to Cys-SO₂H or Cys-SO₃H (Cuevasanta et al., 2015). Moreover, high oxygen conditions preferentially lead to the disulfide bond formation between Cys-S⁻ and Cys-S[•], resulting in O₂^{•-} as a by-product (Wardman & von Sonntag, 1995; Winterbourn, 1993), further increasing oxidative stress.

Carbonylation is the most frequent ROS-mediated irreversible protein PTM that leads to protein degradation. Carbonylation is a stepwise process commenced by the oxidative attack of the ROS species to the side chains of Arg, His, Proline (Pro), Thr, and Lys residues, converting it to reactive, unsaturated aldehyde or ketone groups. Subsequently, these aldehyde or ketone groups can react with Cys residue to form carbonyl adducts. Johansson, Olsson, & Nyström (2004) have discovered the carbonylated proteins in all the life cycle stages in Arabidopsis. This modification is unrepairable and readily detectable as the modification occurs on multiple amino acid residues on selected protein targets (Stadtman, 1992; Stadtman & Levine, 2003; Tola, Jaballi, & Missihoun, 2021; Yan, 2009); thus, it is widely used as a biomarker indicating protein oxidation.

1.4.5 Evidence for the redox regulation of seed dormancy and germination

The synthesis of RONS in seeds depends on the metabolical and physiological state of the seed (Jeevan et al., 2015; Foyer et al., 2017). RONS are continuously generated in seeds in all the stages of the seed life cycle, from embryogenesis to germination or dry seed storage and seed aging (Bailly, El-Maarouf-Bouteau, & Corbineau, 2008). At the onset of germination, activation of metabolism immediately after imbibition generates ROS in the seed. Rapid oxygen consumption, the restrictions to gaseous diffusion by the seed coat and dense internal structures lead to an internal deficiency of oxygen, thus developing anaerobic conditions that limit oxidative respiration in the seeds until radical protrusion, where aerobic respiration reinstates subsequently. Moreover, the hypoxic condition promotes RNS production, mainly NO[•] from nitrate and nitrite via fermentation (Bykova et al., 2015), which can have various regulatory roles in seed germination.

H₂O₂ content is higher at the beginning of the seed development, probably due to the high moisture content and metabolic activities. During the desiccation phase, followed by early seed development, the content of H₂O₂ decreases and later vastly increases in hydrated seeds during germination (Oracz et al., 2007). Nevertheless, even under the desiccated environment, AR seeds displayed a high accumulation of H₂O₂. Leubner-Metzger (2004) suggested that the mature seed might contain hydrated pockets within cells and tissues, which aid the metabolic production of ROS even under dry conditions. Moreover, ROS can be generated via non-enzymatic reactions such as the Amadori and Maillard (Esashi et al., 1993; Murthy & Sun, 2000; Sun & Leopold, 1995) and lipid peroxidation in dry seeds (Finch-Savage, 2013; Wilson and McDonald, 1986). Concisely, RONS show a dual nature in seed physiology as cell signaling molecules that regulate the cellular signaling pathways or as baneful molecules that obliterate cell function, especially under stress conditions (Bailly, El-Maarouf-Bouteau, & Corbineau, 2008). The balance between these roles is crucial for seed development, dormancy, and germination.

The antioxidant defence mechanism is crucial to maintaining the RONS equilibrium in seeds. High RONS accumulation can occur due to insufficient antioxidant control, which provokes extensive oxidative damage to the biomolecules, eventually leading to cell death and ultimately affecting the seed's viability (Kranter et al., 2010). Recent studies show that the tight regulation of RONS production and scavenging is vital for seed germination and dormancy alleviation.

Upon imbibition, the seeds activate the antioxidant system (De Gara, Pinto, & Arrigoni, 1997; Tommasi et al., 2001). For instance, studies have revealed that the embryos of the

dry seeds of wheat (De Gara, Pinto, & Arrigoni, 1997) and pine (*Pinus pinea* L., Tommasi et al., 2001) completely lack AsA and APX enzyme but contain a small amount of DHA. These are essential constituents in the H₂O₂ scavenging system. However, *de novo* AsA biosynthesis is initiated during early germination (after 8-10 hours of germination). The APX enzyme appears simultaneously, and the activity escalates parallel to the AsA production. These studies revealed that the stored DHA reduces to AsA via an enzymatic pathway during the lag period until AsA biosynthesis reinstates.

Moreover, Tommasi et al. (2001) examined the GSH content in dry pine seeds and during the early seed germination in the same study. They revealed that the glutathione present as a GSH/ GSSG pool in the dry seeds, and during the first 24 h of germination, reduction of GSSG increases the GSH level. Furthermore, this study observed a progressive increase of the glutathione reductase enzyme in the embryo and the endosperm, which impeded the effect of generated ROS due to the hypoxic conditions. CAT enzyme was reported to play a crucial role in seed germination by regulating H₂O₂. According to Ishibashi et al. (2017), upon imbibition, the CAT expression level in dormant barley seeds was higher than in non-dormant seeds. Moreover, CAT activity increased prior to the radical protrusion in germinating *Arabidopsis*, soybean, and sunflower seeds (Bailly, 2004; Gallardo et al., 2001; Puntarulo et al., 1991). These evidences suggests that CAT activity is essential in the early stages of seed germination to regulate H₂O₂ levels and prevent oxidative damage.

H₂O₂ and [•]OH are well-known ROS involved in seed germination and dormancy alleviation. Being the most stable ROS, H₂O₂ easily migrates through membranes via aquaporins over relatively long distances (Kibinza et al., 2011). The redox studies with

dormant and non-dormant seeds revealed that upon imbibition, the level of H₂O₂ accumulated in non-dormant seeds was higher than in dormant seeds in *Arabidopsis* (Leymarie et al., 2011), barley (Ishibashi et al., 2017) and sunflower (Bailly, El-Maarouf-Bouteau, & Corbineau, 2008). Therefore, it is apparent that the accumulation of controlled and critical levels of H₂O₂ was linked to the high germination potential of seeds.

Bailly, El-Maarouf-Bouteau, & Corbineau (2008) further proposed that the interplay between the ROS and hormone signaling pathways leads to alterations of cellular redox status or gene expressions promoting seed dormancy alleviation. More studies confirmed the influence of ROS on hormone balance, favouring the dormancy alleviation and germination of the seeds. Ishibashi et al. 2017 reported that H₂O₂ regulated the level of ABA by the ABA catabolism enzyme, ABA-8'-hydroxylase, and the activity of the enzyme in non-dormant seeds was higher compared to the dormant seeds. They found that the activity of the NADPH oxidase, which is involved in ROS production, displayed a lower level in dormant seeds than in non-dormant barley seeds. Moreover, H₂O₂ was found to be involved in the GA biosynthesis and/or GA signaling pathways, activating the production and/or the activity of GA, which leads to dormancy alleviation in *Arabidopsis* (Leymarie et al., 2011; Liu et al., 2010) and barley seeds (Bahin et al., 2011). However, in sunflower seeds, ROS has been implicated with ABA signaling pathways at the transcriptional level (El-Maarouf-Bouteau et al., 2013). A study by Bykova et al. (2011a) identified a higher reduction of ABA- and GA-responsive redox-sensitive proteins in dormant wheat seeds compared to non-dormant wheat seeds. This study suggested that ROS and hormones compete for dormancy alleviation and subsequent germination. These results suggest that

regulating hormonal pathways by ROS, especially H_2O_2 , is vital for dormancy release and seed germination.

H_2O_2 accumulates in seeds during AR, leading to embryonic dormancy alleviation or seed aging. ROS-mediated dormancy release can occur via protein modifications and ABA/ GA signaling. Predominantly, protein carbonylation of specific embryo proteins has been identified as vital for dormancy alleviation during AR (Oracz et al., 2007). Moreover, Müller et al. (2009) discovered that NADPH oxidase mutant *Arabidopsis* seeds (*atrbohB* mutants) displayed low protein oxidation and failed to after-ripen, thus indicating NADPH oxidase plays a significant role in seed AR in *Arabidopsis* seeds. If the conditions are favourable after the AR period, the seeds can germinate once the dormancy is broken.

However, prolonged storage of seeds can lead to seed aging. Reduced seed germination and the deprivation of seed viability are common repercussions of seed aging. Production and progressive ROS accumulation in dry conditions are deleterious for seeds. Bailly, El-Maarouf-Bouteau, & Corbineau (2008) introduced an “oxidative window for germination” concept, where they have shown that after the AR stage, ROS affects the viability of the seeds due to the oxidative damage of biomolecules during ageing or continuous desiccation.

RNS, predominantly NO^* , was suggested to be involved in seed germination. It was reported that an increase in ROS accumulation during dormancy alleviation could induce NO^* production, which can act in addition to H_2O_2 in the same signaling pathway for seed germination (El-Maarouf-Bouteau and Bailly, 2008; Liu et al., 2010). Studies have revealed that the NO^* is an endogenous dormancy regulator in seeds and grains. For

instance, dormancy release of Arabidopsis (Bethke et al., 2004; Bethke, Libourel, & Jones, 2005), barley (Bethke et al., 2004) and lettuce (Beligni & Lamattina, 2000) seeds was found to be associated with NO[•], whereas high NO[•] accumulation was observed in germinating seeds of the soybean (Caro & Puntarulo, 1999) and switchgrass (*Panicum virgatum* L.; Sarath et al., 2007) seeds. It has been reported that the NO[•] accumulation leads to the rapid decline of ABA via ABA catabolism, thus vital for breaking the dormancy and, subsequently, germination (Liu et al., 2009). According to Bethke et al. (2007), during dormancy release, NO[•] was perceived by aleurone cells along with ABA and GA signaling in Arabidopsis, where NO[•] perception was upstream to GA signaling. Moreover, Zanardo et al. (2005) reported that the NO[•] has a dual nature in canola seeds, where seed germination was stimulated, but root growth was suppressed by NO[•]. Furthermore, the findings of Albertos et al. (2015) suggested that S-nitrosylation, the major PTM by NO[•], of abscisic acid-insensitive 5 protein (ABI5) at Cys-153 stimulates the degradation of ABA and promotes seed germination in Arabidopsis.

In some species, such as Arabidopsis, tomato, and tobacco, germination is restrained by the mechanical resistance imposed by the micropylar endosperm that covers the radicle tip. Endosperm weakening mediated by ROS is found to be crucial for the germination of these seeds (Finch-Savage & Leubner-Metzger, 2006; Kucera, Cohn, & Leubner-Metzger, 2005). Müller et al. (2009) suggested that [•]OH radicals produced from NADPH oxidase and/ or Fenton reaction can oxidize the cell wall polysaccharides, resulting in endosperm rupture.

Recent studies have shown the importance of NADPH oxidase activity in seed germination and dormancy alleviation. Leymarie et al. (2012) reported that the NADPH oxidase mutants of Arabidopsis were highly dormant. Moreover, according to Ishibashi et al. (2017), dormant barley seeds displayed a lower NADPH oxidase activity in contrast to non-dormant seeds upon imbibition, and the H₂O₂ accumulation was concomitant. It is demonstrated that suppressing the NADPH oxidase activity of the plasma membrane delays seed germination (Sarath et al., 2007). Diphenylene iodonium (DPI) is a lipophilic reagent identified as an NADPH oxidase inhibitor that impairs the production of O₂^{•-} in plasma membranes. The studies on barley seed germination by Ishibashi et al. (2010, 2015) indicated that the DPI treatment suppressed the GA biosynthesis and ABA catabolism in embryos and the early induction of α -amylase by GA in aleurones, thus potentially suppressing seed germination. Furthermore, DPI has shown inhibitory effects on radical protrusion and root elongation in germinating rice seeds, where the effect was notably eliminated after transferring the seedlings to water from DPI (Li et al., 2017). These findings confirm that NOXs play a critical role in seed germination and dormancy alleviation.

1.5 Proteomic approaches to study seed dormancy, germination and redox control

Proteomics is the systematic analysis of the protein complements of the genome known as proteome (Pandey & Mann, 2000). Genomic studies help to understand the biology of organisms and provide valuable insights about the structure and function of a gene in living organisms. Plant proteomes are highly complex and dynamic. Proteins are a prime

component for signaling, and biochemical pathways and precise investigations are vital to reveal molecular mechanisms underlying plant growth, development, and interactions with the environment (Chen & Harmon, 2006). Through unraveling the intricate dynamics and interactions of the proteome, researchers can achieve a more profound comprehension of the molecular processes underlying these critical stages in plant development. This knowledge can have significant implications for agriculture and crop management.

Proteomics of dormancy and germination has been studied in many plants, including *Arabidopsis* (Gallardo et al., 2002), rice (*Oryza sativa*) (Kim et al., 2009; Yang et al., 2007), barley (*Hordeum vulgare*) (Finnie et al., 2002), mung bean (*Vigna radiata*) (Ghosh & Pal, 2012), and wheat (He et al., 2015; Kamal et al., 2009; Mak et al., 2009). A study by Bykova et al. (2011a) provided evidence for the dynamic differences that occur during the dormancy alleviation of wheat in the redox-sensitive proteome using a thiol-specific proteomics approach. The studies of Mak et al. (2009) revealed that there was a higher abundance of proteins involved in protein degradation and protein folding, cytoskeletal activities, and energy metabolism-related enzymes during the first three days of germination of the wheat embryo; simultaneously, the abundance of β -amylase, protease inhibitors, peroxidases, alcohol dehydrogenase, and ADP-glucose phosphorylase decreased.

Proteomic studies provide a quantitative and qualitative estimation of proteins, and current technologies aid in analyzing various functional aspects, such as PTM, subcellular localization, and protein-protein interactions (Chen & Harmon, 2006). Currently, a wide range of methods, reagents, instrumentation, and data analysis tools are available (Pandey

& Mann, 2000) to design an experiment to investigate various aspects of proteins and their roles in biological processes.

1.5.1 Two-dimensional gel electrophoresis-based proteomics

Gel electrophoresis has traditionally been the primary analytical technique used in proteomics studies. Electrophoresis can separate macromolecules, such as proteins, in a sample according to size, charge, and conformation (Smithies, 2012). Two types of high-performance electrophoretic separation techniques of proteins were available initially, which used utterly different separation parameters: molecular mass and isoelectric point (Rabilloud & Lelong, 2011). The first technique is zone electrophoresis of proteins with sodium dodecyl sulfate (SDS) (Laemmli, 1970). This is the most used technique for protein identification. The second technique is associated with denaturing isoelectric focusing, as described by Gronow & Griffiths (1971). Those two techniques, in combination, gave rise to the two-dimensional polyacrylamide gel electrophoresis (2D-PAGE) technique.

As the name implies, 2D-PAGE separates the proteins in two steps: proteins are separated in gel according to the isoelectric point (pI), and then, SDS-PAGE separates proteins according to the molecular mass (O'Farrell 1975). However, this order is not mandatory. Tuszynski, Buck, & Warren (1979) have identified the reverse order for the studies. A stain is used to visualize the proteins in the gel, such as coomassie brilliant blue and silver nitrate, which binds to the protein's basic, aromatic amino acids (De St. Groth, Webster, & Datyner, 1963) and attaches covalently cross-linked to the proteins (Rabilloud, 1990), respectively. In 2D gel-based proteomics, spot selection is used to perform quantitative analysis, which is vital for downstream mass spectrometry analysis. By spot selection, a

minimal portion of the proteins in the samples will need to be analyzed (Rabilloud & Lelong, 2011); thus, it allows for a more targeted approach to protein identification and quantification in quantitative proteomics experiments.

Along with the ability to obtain a final quantitative analytical image, reproducibility and robustness, and low consumption of mass spectrometer time are some of the significant advantages of the 2D-PAGE technique that make this technique popular.

1.5.2 Quantitative shotgun-based proteomics technique

The scale of proteomic studies has dramatically expanded by the shotgun proteomics technique with MS. The most distinctive feature of this technique is that it aids in identifying, quantifying, and characterizing thousands of proteins and their PTMs in a complex mixture (Fonslow & Yates, 2012). It has applications in various areas of biology, including biomarker discovery, drug development, and understanding cellular processes at the protein level.

In a typical shotgun proteomics experiment, the peptide mixture is fractionated by protease, separated in high-performance liquid chromatography (HPLC), and subjected to LC-MS/MS analysis. The procedure for protein identification has two main steps: peptide identification and protein inference. Peptide identification is accomplished by comparing theoretical tandem mass spectra derived from the *in silico* digestion of a protein database with the identified tandem mass spectra generated from peptide fragmentation of the sample. Protein inference is obtained by allocating peptide sequences to proteins (Zhang et al., 2013). This technique's major drawback is the limited detection of low-abundance peptides because abundant peptides are favoured in the MS-MS acquisition (van Vliet,

2014). Compared to the 2D gels, the shotgun strategy is powerful and has increased the overall data throughput. However, both approaches remain complementary (Nesvizhskii & Aebersold, 2005) by providing different types of information about the proteome, making them valuable tools in proteomic studies.

1.5.3 Quantitative redox proteomics

Recently, due to the development of MS technology, there has been significant attention to ‘gel-free’ proteomics. In these methods, proteins are submitted for enzymatic digestion, and the resulting mixture of peptides is separated and analyzed by MS. Two approaches are used for quantifying peptides: i) label-free quantification; ii) stable-isotope labeling quantification. These techniques determine the relative abundance of the proteins in two or more biological samples by the ratio of ion intensities in each sample (Deracinois et al., 2013), enabling the simultaneous quantification of multiple samples.

In the label-free quantification, the comparing samples are prepared individually and analyzed separately by MS-MS. These techniques use either a comparison of mass spectrometric signal intensities or a comparison of spectral counting (Bondarenko, Chelius, & Shaler, 2002; Liu, Sadygov, & Yates, 2004). These label-free quantification techniques require minimal sample preparation (Deracinois et al., 2013) and, therefore, are cost-effective compared to stable isotopic labeling methods.

Isotope labeling quantification techniques are based on the characteristic labeling of proteins or peptides using metabolic, chemical or enzymatic labels (Schulze & Usadel, 2010). In this technique, the different stable isotopes have the same physical properties but different masses; thus, depending on the isotope used, two peptides tagged with these

different isotopes will undergo the same ionization and be detected in the same spectrum with a mass shift. MS easily detects the mass shift. The relative quantity of each peptide is calculated as a ratio, where ratio 1 represents the equal amount of each peptide and ratio imbalance represents the overabundance of one of the peptides. MS-detected mass shifts are combined in the advanced algorithms of search engines (Deracinois et al., 2013), supplying information about the relative abundance of proteins or peptides across different conditions or samples.

Metabolic labeling includes labeling with ^{13}C or ^{15}N and Stable Isotope Labeling by Amino acids in Cell culture (SILAC). However, metabolic labeling is limited to cell cultures. In contrast, chemical and enzymatic labeling can be used for all biological samples, and Isotope-Coded Protein Labeling (ICPL), Isotope-Coded Affinity Tags (ICAT), Isobaric Tags for Relative and Absolute Quantification (iTRAQ) and Tandem Mass Tags (TMT) are some examples. (Abdallah et al., 2012; Deracinois et al., 2013). Many redox proteome analyses have been successfully accomplished by TMT labeling (Rauniyar & Yates, 2014). TMT labels are amine-specific reagents, and quantification is attained via intensity comparison of the reporter ion. The approach provide major advantages, including the higher sensitivity level and the reduction of MS spectra complexity due to sample multiplexing.

Cys-specific Iodoacetyl Isobaric Tandem mass tags (iodoTMT) have recently been employed in PTM studies (Araki et al., 2016; Pan et al., 2014). IodoTMT warrants selective labeling and relative quantitation of Cys-containing peptides from up to six samples. Every sample designated for analysis undergoes trypsin digestion and is then marked with a single

iodoTMT label. IodoTMT tags irreversibly label free sulfhydryl groups on Cys residues. Each iodoTMT tag contains a sulfhydryl-reactive iodoacetyl reactive group, a mass-neutral spacer arm and a mass reporter, and each six-plex reagent has the same nominal mass (457.33Da) containing five variable isotope-coded positions (Pan et al., 2014). Mass reporters readily detach from the parent molecules, thus generating reporter ions with unique m/z values (126-131) under collision-induced dissociation. Relative intensities of reporter ions accomplish the quantification of the selected peptide, and protein identification of specific peptide fragment ions in the spectra can be made by searching in a database. This technique conserves a significant amount of time by allowing parallel proteomic analysis of six different samples with high sensitivity (Pan et al., 2014), making iodoTMT an efficient and sensitive technique for proteomic analysis.

1.6 Objectives of the project

In order to develop wheat varieties resistant to PHS, it is important to understand the exact molecular mechanisms underlying wheat seed dormancy and germination resistance. In this study, we used the thiol-specific proteomics approach in conjunction with pharmacological treatment to understand the role of ROS generation and post-translational thiol modifications in either induction or suppression of germination and embryo growth in imbibed non-dormant wheat seeds. The detailed roles of these Cys-PTM proteins are critical for modelling metabolic reprogramming mediated by RONS production. In the present study, the identification and quantitation of reversible Cys-PTMs in wheat tissue-specific proteomes were conducted in order to distinguish the thiol redoxomes for germination suppression in freshly-harvested (FH) and after-ripened (AR) white-seeded

spring wheat using three non-dormant Doubled Haploid (DH) lines (ND-AR, ND-AN, and ND-BQ) and one parent line (AC Karma). The objectives of this research were as follows:

1) To explore the impact of oxidative stress induced by the application of DPI and DPI combined with the phytohormone ABA, and exogenous ABA alone on either suppression or induction of germination in freshly harvested and after-ripened wheat seeds with a non-dormant genotype.

Milestones 01: Investigate the physiological changes in germination resistance of freshly harvested seeds under different DPI, ABA and DPI combined with ABA treatments.

Milestone 02: Investigate the physiological changes in germination resistance of after-ripened seeds under different DPI, ABA, and DPI combined with ABA treatment conditions.

Milestone 03: Compare the effect of different concentrations of DPI, ABA and DPI combined with ABA on physiological changes in germination resistance in FH and AR seeds

2) To investigate the redox-sensitive sources of PHS resistance in wheat seed embryos and aleurones and examine the role of reversible protein thiol-redox PTMs in response to the inhibition of ROS production and externally applied ABA in freshly-harvested and after-ripened seeds.

Milestones 01- Identify and quantify of Cys Thiol Redox Modified Proteins (RMPs) and Cys-containing Differentially Abundant Proteins (CysDAPs) in FH and AR embryos and aleurones by Iodoacetyl Tandem Mass Tags (iodoTMT)-based labeling approach.

Milestone 02: Identify and quantify unique and common significant RMPs found in embryo and aleurone tissues of DPI-treated and DPI in the presence of ABA-treated seeds after the differential blocking of redox-active protein thiols with IAA (Approach I).

Milestone 03: Identify and quantify unique and common significant CysDAPs found in embryo and aleurone tissues of seeds treated with DPI and DPI in the presence of ABA after the reduction of all redox-active protein thiols with DTT (Approach II).

3) To characterize the role of ROS generation, redox and phytohormonal signaling in the synergistic developmental and metabolic reprogramming in the embryo and aleurone tissues during seed imbibition.

Milestone 01: Functionally annotate the identified and quantified RMPs and CysDAPs from approaches I and II in FH and AR embryos and aleurones.

Milestone 02: Compare the thiol-containing proteins identified from approaches I and II in FH and AR embryos.

Milestone 03: Compare the thiol-containing proteins identified from approaches I and II in FH and AR aleurones.

Milestone 04: Compare the RMPs in FH and AR wheat kernels identified using the approach I that quantifies oxidative changes in reversible Cys PTMs (IAA and iodoTMT differential alkylation).

Milestone 05: Compare the CysDAPs in FH and AR wheat seeds in approach II that quantify differential protein abundance changes (DTT reduction and iodoTMT labeling).

2 Materials and Methods

2.1 Plant material and seed sampling procedure

Non-dormant (ND) lines of spring wheat (*Triticum aestivum* L.) DH population derived from the cross 94C15/9014 = 8021-V2 (high PHS resistance, white seed coat) X AC Karma (low PHS resistance, white seed coat) segregating transgressively for dormancy phenotype were used in this study. Non-dormant (ND) DH lines AA016AR (ND-AR), AA016BQ (ND-BQ), and AB015AN (ND-AN), and the parent line AC Karma developed by the Agriculture and Agri-Food Canada breeding program based in Semiarid Prairie Agricultural Research Centre were selected for the analysis. All experimental work was conducted at Morden Research and Development Centre, Agriculture and Agri-Food Canada (MRDC, Manitoba, AAFC).

Plants were grown in climate-controlled growth chambers (Figure 1). From each DH line, 24 seeds were randomly selected and placed in dry conditions in individual paper bags at room temperature (RT) for 24 hours prior to planting. Twelve pots were made for each seed line using the steps outlined below. The following formula was used to prepare the potting mixture: soil to soilless LB2 professional growing mix at a ratio of 1:1. One layer of tissue paper was added at the bottom of the pot, and a thin layer of peat moss was added on top of the tissue paper. The soil mix was added on top of the peat. Prepared pots were transferred to the growth chambers and watered. Per pot, two seeds were sown and incubated at 15°C with 16 hr day-light at 50% relative humidity. The temperature was raised to 18°C eight weeks after seeding and to 21°C at ten weeks after seeding. Natural

light was supplemented with 100W high-pressure sodium lamps. Fertilizer (Plant-Prod 20–20–20, 500 ml of 15 g/L per pot, daily) was applied during watering.



Figure 1: Cultivation of spring wheat (*Triticum aestivum* L.) DH lines in the climate-controlled growth chambers at Agriculture and Agri-Food Canada based in Morden Research and Development Centre.

Heads on the primary and secondary tillers were harvested at physiological maturity, the critical stage for imposing maximum dormancy (Nyachiro et al., 2002). The harvested heads were dried in a forced air oven at 35°C for 5 days to reduce the grain moisture content and then immediately stored in paper envelopes at -20°C to halt any further metabolic activity until further use (Bykova et al., 2011b).

Half of the FH seeds were stored in the dark at RT in paper envelopes to obtain AR seeds. Seeds stored at -20°C immediately after harvest to preserve the maximum dormancy were used as FH seed materials and seeds stored for after-ripening at RT for dormancy decay for more than 2 years or -20°C for more than 4 years were used as AR seed materials throughout this study. The seed materials AR at RT were stored at -20°C during the experiment to cease further after-ripening.

2.2 Germination resistance tests

2.2.1 Germination assay for freshly-harvested seeds

This assay was performed to determine the level of retained dormancy in freshly harvested (FH) seeds. FH kernels from the three DH lines and the parent line were surface sterilized for 5 minutes in 1% "No Damp" solution (2.5% oxine benzoate fungicide stock solution, Plant Products Co. Ltd.) before being rinsed three times with milli-Q water. The seeds were then soaked in 4 ml of milli-Q water and incubated in the dark for 2 hours at 15°C. The seeds were then placed the crease facing down in a sterile Petri plate (20 seeds per plate) on a sterile Whatman #3 filter paper hydrated with 6 mL of milli-Q water and incubated in the dark for 21 days at 15°C and 40% relative humidity. Plates were examined daily for germination analysis. Seeds were counted as germinated and removed when the emergence of the coleorhiza beyond the seed coat was visible. Un-germinated seeds were treated with 0.5 mM GA in water on the 21st day, and their viability was tested for another 5 days (Bykova et al., 2011a). The Germination Resistance (GR) index was calculated as described by Gordon (1971), where t_1 , t_2 , t_i = first, second, and i th days of the test, and n_1 ,

n_2, n_i =total number of grains germinating by the above mentioned times, which calculates the time at which half of the seeds germinated.

$$GR = \frac{\frac{t_1}{2}(n_1) + \frac{t_2 + t_1}{2}(n_2 - n_1) + \dots + \frac{t_i + t_{i-1}}{2}(n_i - n_{i-1})}{n_i} \text{ hours}$$

2.2.2 Germination resistance tests of non-dormant FH and AR seeds treated with DPI, ABA, and DPI in the presence of ABA and water as a control

The germination resistance of FH and AR wheat seeds was tested using DPI [Diphenyleneiodonium chloride, Sigma D2926- 10 mg, soluble in Dimethylsulfoxide (DMSO)], ABA (Sigma A1049, 100 mg, soluble in methanol), DPI in the presence of ABA, and water treatments. Seeds from 2015, 2017 and 2019 seed increases stored at -20°C for 2 years and 5 months, 5 months, and 2 months, respectively, immediately after the harvesting process were used as FH seed materials. In order to test the GR in FH white-seeded spring wheat, three Biological Replicates (BioReps) were performed using seeds from 2015, 2017, and 2019 seed increases, and three Technical Replicates (TechReps) were performed using seeds from the 2015 FH seed increase. AR wheat seeds from 2013 (after-ripened at -20°C for four years and two months) and 2017 (after-ripened at RT for two years and five months) seed increases were used as AR seed material for this experiment. BioReps were performed using 2013 and 2017 AR seed materials, along with two TechReps using the 2017 AR seed increase.

In this assay, six treatments were used to check the germination resistance index of the ND-DH lines, ND-AN, ND-AR, ND-BQ and one parent line, AC Karma. The treatments used were:

- I) Treatment 01- Water (Control)
- II) Treatment 02- 50 μ M ABA
- III) Treatment 03- 150 μ M DPI
- IV) Treatment 04-300 μ M DPI
- V) Treatment 05- 600 μ M DPI
- VI) Treatment 06- 150 μ M DPI + 50 μ M ABA

From each seed line of FH and AR seed material, 20 seeds were surface sterilized in a tube with 1% "No Damp" solution (2.5% oxine benzoate fungicide stock solution, Plant Products Co. Ltd.) for 5 minutes before being rinsed three times with Milli-Q water. The seeds were then treated with 4 mL treatment solutions and incubated in the dark for 2 hours at 15°C. Later, the seeds were placed crease facing down in a sterile Petri plate, on a sterile Whatman #3 filter paper hydrated with the same treatment solution (4 mL), and incubated in the dark for 21 days at 15°C and 40% relative humidity. The same procedure as described above in the germination assay for FH seeds was used to calculate the germination resistance index for each seed line in each treatment solution. Two treatments that delivered the highest GR in these seed lines were chosen for the iodoTMT analysis procedure.

2.2.3 Germination resistance tests to control the effect of different solvent concentrations used in pharmacological treatments of non-dormant wheat kernels

In GR tests, DMSO and methanol were used as solvents to prepare DPI and ABA treatment solutions, respectively. Experiments were carried out to examine the effect of DMSO, methanol, and DMSO combined with methanol concentrations that were used in the corresponding DPI, ABA, and DPI combined with ABA treatments on the GR of FH and AR non-dormant DH lines, as well as the parent line (Table 2).

The effect of DMSO combined with methanol solvent concentrations corresponding to the 150 μ M DPI + 50 μ M ABA treatment on GR was investigated using FH and AR DH lines (ND-AN, ND-AR, and ND-BQ) and AC Karma parent as seed material. Water treatment was used as the control in this experiment. For FH seeds, three BioReps were performed using 2015, 2017 and 2019 seed increases, stored at -20°C for 2 years and 5 months, 5 months, and 2 months, respectively, whereas two TechReps from the 2017 seed increase (after-ripened for 2 years and 5 months at RT) and one replicate from the 2013 seed increase (after-ripened for 4 years and 2 months at -20°C), were used to check the GR in AR seed material in this experiment. The GR index was calculated using the same procedure as described in the previous GR tests.

Another experiment was carried out using seeds from the 2006 seed increase that had been stored at -20°C for nearly ten years. In this experiment, different DPI concentrations and one ABA concentration were used, along with the corresponding DMSO and methanol solvent concentrations to assess the GR (Table 2).

Table 2: Treatments, solvent controls and percentage of DMSO and methanol concentrations of solvents used in treatment and control experiments

Treatment	Solvent	DMSO (%v/v)	Methanol (%v/v)
Water (Control)	-	-	-
150 μ M DPI	DMSO	1.5%	-
Solvent control for 150 μ M DPI	DMSO	1.5%	-
300 μ M DPI	DMSO	3%	-
Solvent control for 300 μ M DPI	DMSO	3%	-
600 μ M DPI	DMSO	6%	-
Solvent control for 600 μ M DPI	DMSO	6%	-
1.2 mM DPI	DMSO	12%	-
Solvent control for 1.2 mM DPI	DMSO	12%	-
1.5 mM DPI	DMSO	15%	-
Solvent control for 1.5 mM DPI	DMSO	15%	-
1 mM ABA	Methanol	-	3.34%
Solvent control for 1 mM ABA	Methanol	-	3.34%
150 μ M DPI + 50 μ M ABA	DMSO+ Methanol	1.5%	0.17%
Solvent control for 150 μ M DPI + 50 μ M ABA	DMSO+ Methanol	1.5%	0.17%

2.2.4 **Statistical analysis for GR tests with DPI, ABA, DPI combined with ABA and water treatments of FH and AR wheat seeds from non-dormant DH lines**

The values obtained for GR were statistically analyzed using Minitab Statistical Software, version 21.1.0 (Minitab, LLC., 2021), to check the physiological changes in GR of seeds with ND genotypes under DPI, ABA, DPI combined with ABA, and water treatment

conditions on FH and AR wheat kernels. First, the GR values obtained for FH and AR seed lines in these treatments were analyzed separately for statistical differences. One-way ANOVA tests were run on each seed line separately to determine whether there were any significant differences in GR values between the DPI, ABA, DPI combined with ABA, and control treatments. Moreover, one-way ANOVA tests were run for each treatment separately to see if there were any significant differences in GR values between AC Karma, ND-AR, ND-AN, and ND-BQ seed lines. FH and AR data were subjected to two-way ANOVA tests to determine statistical significance and to compare the physiological changes in GR between FH and AR seeds from ND wheat DH lines and the parent in response to DPI and ABA treatments.

One-way ANOVA tests were run on each seed line individually to see how different solvent concentrations affected GR in FH and AR, ND-DH lines, and the parent. In all ANOVA tests, P-values of 0.05 or less were considered significantly different. Furthermore, to obtain grouping information, the ANOVA tests were followed by pairwise/multiple comparisons using Tukey's range test with a 95% confidence level. For perspicuity, values obtained for GR were graphically depicted to show the statistical differences using Microsoft Excel, version 2016 (Microsoft, 2016).

2.3 Experimental design for identification and quantitation of Cys Thiol Redox Modified Proteins (RMPs) and Cys-containing Differentially Abundant Proteins (CysDAPs) by iodoacetyl Tandem Mass Tags (iodoTMT)-based labeling approach

2.3.1 Treatments for non-dormant white-seeded spring wheat DH Lines

Throughout the iodoTMT labeling-based redox proteomic experiments, only the FH and AR DH lines, ND-AN, ND-AR, and ND-BQ from the 2017 seed increase were used as seed material. Seeds from each DH line were subjected to three treatments: i) Water-reference, ii) 600 μ M DPI, and iii) 150 μ M DPI + 50 μ M ABA (Figure 2). For each DH line, 25 seeds were surface sterilized for 5 minutes in 1% "No Damp" solution (2.5% oxine benzoate fungicide stock solution, Plant Products Co. Ltd.). The surface sterilized seeds were rinsed five times with Milli-Q water before being immersed into 4.0 mL of the treatment solutions and incubated in the dark for 2 hours at 15°C and 40% relative humidity. Seeds were placed crease facing down in a 9-cm sterile Petri plate on a sterile Whatman #3 filter paper soaked with 4ml of each treatment solution. These Petri plates were incubated in the dark for 48 hours at 15°C.

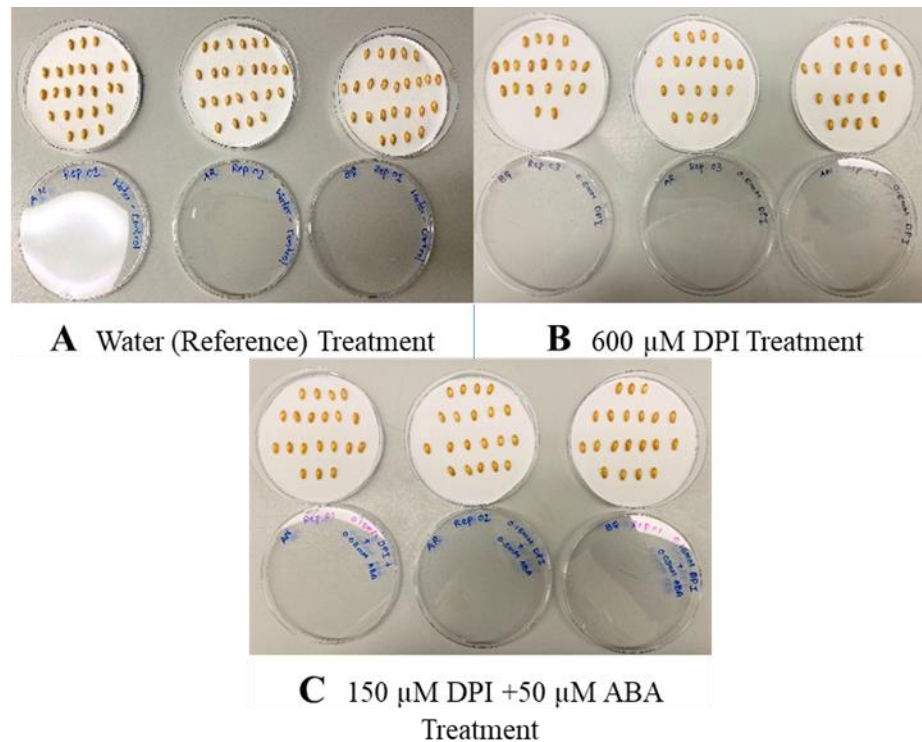


Figure 2: Treated wheat kernels from DH lines after 48h incubation at 15°C in a representative replicate experiment. A. The control treatment with water; B. 600 μ M DPI treatment; C. 150 μ M DPI + 50 μ M ABA treatment

2.3.2 Dissection of embryo and aleurone tissues and extraction of proteins from FH and AR pharmacologically treated seeds

The seeds in the incubated Petri plates were used to prepare protein extractions. Altogether, 30 bulked seeds from each treatment (10 seeds from each DH line) were used for the aleurone and embryo protein extractions. Two differential redoxome analysis approaches were performed for each treatment and the reference control in each embryo and aleurone sample (Figure 3).

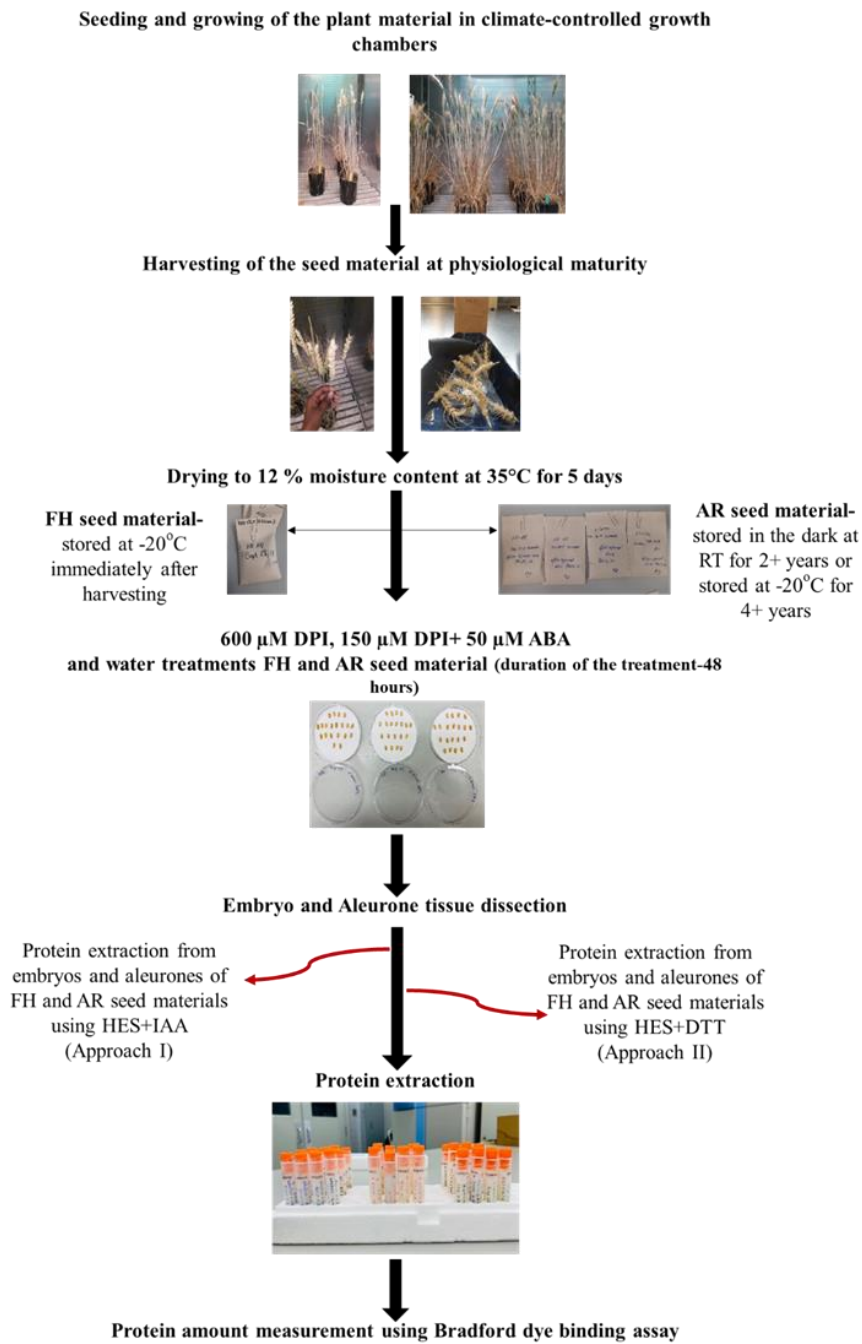


Figure 3: Workflow diagram of the procedures for protein extraction from embryo and aleurone tissues of wheat seeds using DH lines with marginally non-dormant phenotype.

For the first approach (Approach I), during protein extraction, one part of each embryo and aleurone sample from the treatment experiment was supplemented with IAA alkylating reagent (Iodoacetamide, Bio-Rad Laboratories, Mississauga, Ontario, Canada #163-2109), which was followed by protein precipitation and reduction by DTT (Dithiothreitol, Bio-Rad Laboratories, Mississauga, Ontario, Canada, #161-0611). In the second approach (Approach II), the second part of the isolated embryo and aleurone samples was treated in parallel with DTT reducing reagent only during protein extraction. Two types of HES buffer [50 mM HEPES, 1 mM EDTA, 0.1% SDS, 1x Protease Inhibitor cocktail (Roche, Complete tablets) (pH=8.0)] containing either 200 mM IAA (HES+IAA) or 20 mM DTT (HES+DTT) were used for protein extractions. NaOH was used to adjust the pH of the HES buffer, and the buffer was degassed before adding IAA or DTT.

Embryos from pharmacologically treated seeds were excised with a sterilized scalpel and immediately placed in 1.5 mL Eppendorf tubes containing the extraction buffer HES+DTT/HES+IAA before being quickly frozen in liquid N₂. After removing the embryo, the ventral side of the seed along the crease was incised with a scalpel to reveal the aleurone and placed in a beaker with HES+DTT/HES+IAA extraction buffer. The aleurone was cleaned twice by gently scraping the endosperm off with the tip of a sterilized scalpel and washing it in a small beaker containing HES+DTT/HES+IAA extraction buffer. Cleaned aleurone layers were collected and quickly frozen in liquid N₂ in 1.5 mL Eppendorf tubes. The frozen embryos and aleurone layers were then removed from the liquid N₂, and the buffer was drained using filter papers. The intact embryos and aleurone layers were then ground into a fine powder with liquid N₂ using a mortar and pestle. A total of 2.5mL of HES+DTT/HES+IAA extraction buffer was added while grinding and transferred to a 5 mL Eppendorf

tube at the end. The Eppendorf tubes with the extracted samples were then vortexed for 1 hour at 550 rpm at RT, followed by sonication on ice with the sonicator (QSONICA Ultrasonic processor), five cycles of five seconds with five seconds intervals, at power 4. Sonicated samples were immediately frozen in liquid N₂ and vortexed (550 rpm) at RT for 15 minutes to thaw. Then, the samples were extracted by vortexing (550 rpm) for 1 hour at 37°C in the dark and centrifuged at 10,000 g for 30 minutes at 22°C using a Sorvall RC-6 Plus Refrigerated Centrifuge (Thermo Fisher Scientific). The supernatant was collected in 5 ml Eppendorf tubes and stored at -80°C for future research. The pellets were stored in Eppendorf tubes at -80°C, and the extraction process was repeated the next day with 1ml of extraction buffer, either with HES+DTT or with HES+IAA. The supernatant was then collected and combined with the first supernatant to yield approximately 3 mL of protein extract of embryos and aleurones, which was then frozen at -80°C. Three protein extractions were obtained at the end of this procedure from the two germination inhibition treatments [DPI-IAA/ DPI-DTT and (DPI+ABA)-IAA/ (DPI+ABA-DTT)] and the reference treatment (Water-IAA/ Water-DTT) per FH or AR, embryos and aleurones in each approach. The protein concentrations in the extractions were determined using the Bradford assay.

2.3.3 Bradford assay to determine the protein concentration of extracts from FH and AR, embryos and aleurones

The Bradford dye-binding assay (Bio-Rad Laboratories) was used to determine the concentration of solubilized proteins. The Coomassie Brilliant Blue G-250 dye is bound to proteins in the solution, which converts the dye's doubly protonated red cationic form to

the stable unprotonated blue form under acidic conditions (Bradford, 1975; Reisner et al., 1975). The lyophilized Bovine Serum Albumin (BSA), stored at 4°C in a 2 mg/ml concentrated solution, was used as the standard. From the original BSA standard, a concentrated solution of 20 µg/ml was prepared for a BSA stock solution.

In disposable cuvettes, one blank solution with 800 µl of water and seven dilutions of BSA standards with different protein concentrations ranging from 2.5 to 20 µg/ml was prepared for the standard curve. Then, 200 µl of Protein Assay Dye Reagent Concentrate (dye, phosphoric acid, and methanol solution; Bio-Rad Laboratories) was added to each standard and incubated at RT (23°C) for at least 5 minutes. Following the same procedure, sample protein solutions were prepared using the extracted protein fractions.

The Spectrophotometer (UV-Visible, Ultrospec 3000, Amersham Pharmacia Biotech Inc.) was then used to measure the absorbance at 595 nm. To obtain the linear regression formula, the absorbance values at 595 nm were plotted on the y-axis against the values of standard diluted protein concentrations in µg/ml on the x-axis, and the protein concentrations in the extracted protein fractions of embryos and aleurones in FH and AR seeds were determined based on linear function range of the standard curve.

2.3.4 Preparation of the FH and AR, embryo and aleurone protein extractions for iodoTMT labeling

Using Bradford Assay measurements, volumes containing 120 µg of proteins were aliquoted from the embryo and aleurone protein extractions and precipitated with 8 volumes of 100% (v/v) ice-cold acetone containing 0.07% DTT (Figure 4). These tubes

were kept overnight at -20°C . This step eliminates unreacted IAA from the HES+IAA samples. Subsequently, the samples were centrifuged at 10,000 g for 30 minutes at 4°C .

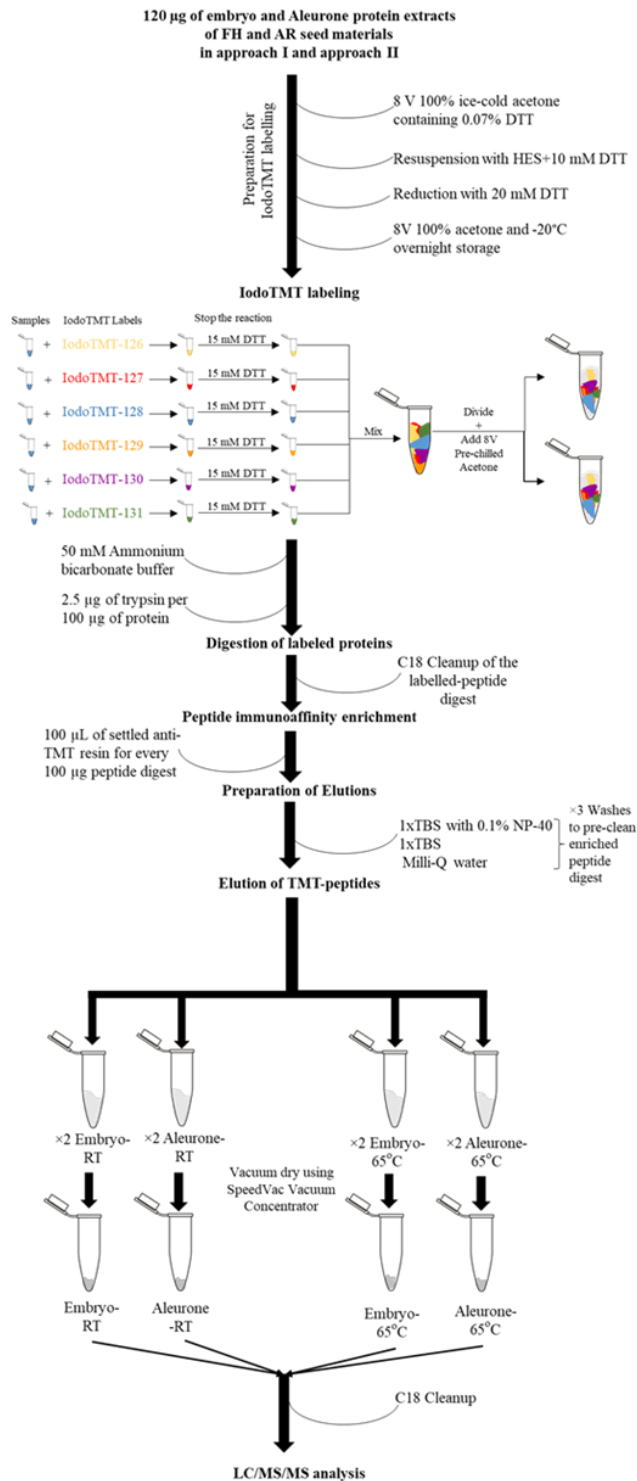


Figure 4: Workflow diagram of the iodoTMT labeling procedure of protein extracts from seed tissues of DH wheat lines. Eppendorf Tube Clip Art from Wang, 2011 was used.

Then, the supernatant was removed, and the pellets were air-dried. Meanwhile, the HES buffer was prepared using the previous method described on page 61 but without the Protease inhibitor cocktail (Roche, Complete tablets). Pellets were resuspended in HES+DTT buffer and vortexed at 500 rpm for 2 hours at 4°C. For the reduction step, a 0.5M DTT stock solution was prepared, and 4.8 µL was added to each Eppendorf tube (20mM DTT final concentration) containing the samples and incubated for 1hr at 56°C. The samples were treated with 8 V (1 mL) of 100% (v/v) acetone and stored overnight at -20°C to remove DTT. Following that, the samples were centrifuged at 10,000 g for 30 minutes at 4°C, washed with acetone, and stored at -20°C overnight.

2.3.5 IodoTMT labeling procedure

After the acetone precipitation overnight at -20°C, the samples were centrifuged at 4°C for 30 minutes at 10,000 g. After, the supernatant was removed, and the pellets were air-dried briefly until the acetone evaporated (around 10-15 min). The pellets were then resuspended in 120 µL HES buffer and vortexed at 1,000 rpm for 1 hour at RT. Meanwhile, six iodoTMT reagents (0.2 mg, Thermo Fisher Scientific) were prepared by adding and mixing 10 µL of LC/MS grade methanol and centrifuging at 1500 g for 1 minute to solubilize the reagent.

The samples were then mixed with the dissolved iodoTMT reagents, quickly spun down, and incubated at 37°C for 1 hour, protected from light. To avoid potential artifactual effects from labels and protein-specific tag biases, the matrix in Table 3 was used to balance the

embryo and aleurone samples in each biological replicate through randomization of isobaric labeling tags. The same matrix was used in the BioReps of FH and AR protein extractions. The experiments with FH embryo and aleurone samples were performed in three BioReps with two Experimental Replicates (ExpReps) and three TechReps each (TechReps), a total of 18 replicates for each experiment. The experiments with AR embryo and aleurone samples were performed in three BioReps and three TechReps each (TechReps), a total of 9 replicates for each experiment.

At the end of the incubation period, 4 μ L of freshly prepared 0.5 M DTT was added to 15 mM DTT final concentration and mixed into each sample tube to quench the reaction. Equal amounts of six reactions were then mixed in 5 mL Eppendorf LoBind tubes (134 μ L \times 6 = 804 μ L), divided into two tubes (402 μ L each), and 8 V (3216 μ L) of pre-chilled acetone (-20°C) was added for protein precipitation overnight at -20°C.

Table 3: IodoTMT labeling matrix showing the allocation of biological replicate experiments with FH and AR, embryo and aleurone protein extracts to labeling tags.

Samples	TMT Label		
	Biological Replicate 1	Biological Replicate 2	Biological Replicate 3
Embryo-sixplex			
Water-Embryo-IAA	126	131	129
Water-Embryo-DTT	127	130	128
600 μ M DPI-Embryo-IAA	128	129	127
600 μ M DPI-Embryo-DTT	129	128	126

150 μ M DPI + 50 μ M ABA -Embryo-IAA	130	127	131
150 μ M DPI + 50 μ M ABA -Embryo-DTT	131	126	130
Aleurone-sixplex			
Water-Aleurone-IAA	126	131	129
Water-Aleurone-DTT	127	130	128
600 μ M DPI-Aleurone-IAA	128	129	127
600 μ M DPI-Aleurone-DTT	129	128	126
150 μ M DPI + 50 μ M ABA -Aleurone-IAA	130	127	131
150 μ M DPI + 50 μ M ABA -Aleurone-DTT	131	126	130

2.3.6 Digestion of iodoTMT labeled proteins

After the acetone precipitation, samples were centrifuged at 10,000 g for 30 minutes at 4°C. The tubes were carefully inverted to decant acetone without disturbing the pellets, and the pellets were allowed to air-dry for 10 minutes. The pellets were re-dissolved with 360 μ L of 50 mM ammonium bicarbonate buffer (Fluka), pH 8.0, to reconstitute proteins. At this point, each embryo and aleurone protein extraction had two Eppendorf LoBind tubes with 360 μ g labeled proteins in one technical replicate. These two tubes were combined, yielding one embryo and one aleurone labeled protein extracts, each containing 720 μ g proteins from combined samples.

For digestion, 2.5 μ g of trypsin was used per 100 μ g of protein. For this amount of labeled proteins, a trypsin vial (Thermo Fisher Scientific) containing 20 μ g of trypsin was used. Before use, the trypsin in these vials was resuspended in a 20 μ L trypsin storage solution

and kept on ice for 5 minutes. The volume containing 720 μg labeled proteins was then transferred into the prepared trypsin vials, mixed thoroughly, and returned to the 5 mL Eppendorf LoBind tubes. The samples were then incubated at 37°C overnight for protein digestion.

2.3.7 C18 clean-up of the peptide digests

Following the digestion, samples were acidified with 4 μL of 10% TFA. Pierce C18 spin columns (Thermo Fisher Scientific) were used to clean-up the peptide mixtures in the samples. The C18 clean-up procedure was primarily comprised of three steps. i) conditioning of the spin columns; ii) binding and washing of labeled peptides; and iii) preparing desalted peptide eluates.

i) Conditioning of the spin columns started with removing the white caps from the bottom of the spin columns, placing the columns in 2 mL tubes and centrifuging at 5,000 g for 1 minute to remove the solution and pack the resin material. The columns were then loaded with 300 μL of 100% acetonitrile (ACN) and spun at 5,000 g for 1 minute before the ACN flow-through was discarded. Afterwards, the columns were washed twice with 0.1% (v/v) FA (Formic acid in water, Fisher LS-118-1).

ii) Binding and washing of peptides proceeded with loading 300 μL of the peptide samples and centrifuging at 1,500 g for 1 minute. Another 300 μL of samples were added, centrifuged at 1,500 g for 1 minute, and the process was repeated with the remaining samples (the total volume in each sample was 720 μL). The flow-through was saved and frozen at -80°C. The columns were then placed in new 2 mL

Eppendorf LoBind tubes, and 300 μL of 0.1% FA was loaded onto each spin column before being centrifuged at 1,500 g for 1 minute. This step was repeated twice, for a total of three washes, and the washes were saved and stored in the -80°C freezer.

iii) Preparation of desalted peptide eluates was done by inserting the spin columns into 1.5 ml tubes and loading them with 300 μL of the elution buffer containing 1.5% (v/v) FA and 66% (v/v) ACN in water. The columns were centrifuged at 1,500 g for 1 minute, and the eluates were collected into 1.5 ml Eppendorf tubes. Following the same procedure, three elutions were repeated, eluates were collected and freeze-dried. Finally, freeze-dried eluates were kept in the -80°C freezer until further use.

2.3.8 Enrichment of iodoTMT reagent-labeled peptide digests

TMT-labeled peptides were captured and affinity purified using anti-TMT resin (Thermo Fisher Scientific). For every 100 μg of peptide digest of samples labeled with iodoTMT reagent, 100 μL of settled resin was used. After thoroughly mixing the resin, 1440 μL slurry was added in a 2 mL tube for 720 μL of proteins and centrifuged at 500 g for 0.5 minutes. After removing the slurry buffer, 800 μL of 1xTBS (tert-butyldimethylsilyl) containing 50 mM Tris-HCl (hydrochloric acid) and 150 mM NaCl (sodium chloride) was added and vortexed. The tubes were then spun at 500 g for 0.5 minutes, and the TBS-containing supernatant was removed. This procedure was repeated twice more with 800 μL 1xTBS. The lyophilized peptides were then resuspended in 720 μL of 1x TBS, and 10 μL of each sample was saved for non-enriched sample analysis and stored at -80°C. The

samples were transferred to the resin tube and thoroughly mixed by inverting. Then, the Eppendorf LoBind tubes containing the samples were put on the platform shaker overnight for incubation at 4°C.

2.3.9 Preparation of eluates after anti-TMT resin incubation

After overnight incubation with anti-TMT resin, samples were divided into three Pierce spin columns (Thermo Fisher Scientific) with large frits and centrifuged at 500 g for 0.5 minutes (one sample contained approximately 1500 µl resin and sample). The flow-through was combined and stored at -80°C in separate tubes for the embryo and aleurone samples. The anti-TMT resin containing captured peptides was washed as follows:

- i) Wash 1 - Each column received 270 µL of 1xTBS containing 0.1% NP-40, incubated at RT for 30 minutes, and centrifuged at 500 g for 0.5 minute. The flow-through solution was saved in a 5 mL tube labeled as 1xTBS +0.1% NP-40 wash. This washing step was repeated twice, but the incubation time for each wash was reduced to 2 minutes. All of the flow-through of the washes was collected in the same tube and stored at -80°C.
- ii) Wash 2 - The resin was then washed three times with 1xTBS. For the first wash, 270 µL of 1xTBS was added to each tube, incubated at RT for 15 minutes, and centrifuged at 500 g for 0.5 minutes. The flow-through solution was collected in a 5 mL tube labelled as 1xTBS wash. Two more washes were performed while incubating for only 2 minutes, and the flow-through was collected and stored at -80°C.

iii) Wash 3 - The resin was then washed three times with milli-Q water (270 μ l per tube). Similar to the previous step, the first wash was incubated for 15 minutes and centrifuged at 500 g for 0.5 minute. The other two washes were only incubated for 2 minutes. The flow-through was combined and stored at -80°C in a 5 mL tube.

Following the washing steps, four elutions of bound peptides from the resin were prepared at two different temperatures. The TMT elution buffer (Thermo Fisher Scientific) was used in this step to elute the captured TMT-labeled peptides in the anti-TMT resin:

For the first elution, 270 μ L of elution buffer was added to the spin column, vortexed (500 rpm) at RT for 15 minutes, and spun at 500 g for 0.5 minute. The eluates for each sample were collected into one 2 mL tube (total volume 810 μ L from three spin columns per sample). The elution was repeated with 270 μ L of elution buffer, resulting in a total combined volume of 1620 μ L.

The second elution was performed at RT using the same procedure as described for elution 1. Finally, elutions 1 and 2 were combined in a single tube to obtain the final eluate at RT (final volume approximately 3200 μ L).

For the third elution step, 270 μ L of elution buffer was added to the spin column, vortexed (500 rpm) at 65°C for 15 min and spun at 500 g for 0.5 minutes. The eluates for each sample were collected into another 2 mL tube (total volume 810 μ L from three spin columns per sample). The previous step was repeated with another 270 μ L of elution buffer. These two elutions were combined in one tube to get elution 3 (total volume 1620 μ L).

The same procedure as Elution 3 was followed to collect Elution 4 at 65°C (total volume 1620 μ L). The elutions 3 and 4 were combined in one tube to get the final eluate at 65°C (final volume approximately 3200 μ L).

Ultimately, four elutions were obtained from embryo and aleurone labeled peptide samples. These enriched peptide digests were dried using the SpeedVac Vacuum Concentrator (Thermo Fisher Scientific).

2.3.10 C18 clean-up and NanoLiquid Chromatography Tandem Mass Spectrometry (nanoLC-MS/MS) analysis of enriched embryo and aleurone peptide digests

The vacuum-dried pellets were resuspended in 300 μ L of buffer A (0.1% FA) and vortexed for 30 minutes at RT. Prior to the automated nanoLiquid Chromatography Tandem Mass Spectrometry (nanoLC-MS/MS) analysis, the resuspended pellets were cleaned using the C18 clean-up procedure as previously described. The peptide digests were analyzed in a data-dependent acquisition (DDA) mode using the Q-Exactive™ Hybrid Quadrupole-Orbitrap Mass Spectrometer (Thermo Fisher Scientific) connected on-line with EASY-nLC 1000 system (Thermo Scientific).

For FH and AR embryo and aleurone protein extracts, biological replicates, experimental replicates, and TechReps were performed to increase the accuracy and reliability of statistical analysis in the experimental work with iodoTMT labeling. For the FH embryo and aleurone protein extractions, two ExpReps were performed. Each experimental replicate consisted of 3 biological replicates, and each biological/ experimental replicate was subjected to nanoLC-MS/MS analysis in 3 technical replicates. Protein extractions

from AR embryo and aleurone samples were subjected to three biological replicates, which were subjected to nanoLC-MS/MS analysis in three TechReps each. Figure 4 depicts the workflow of the iodoTMT labeling procedure.

2.3.11 Database searching, and comparative quantitative and statistical analysis

The raw nano LC-MS/MS data files were analyzed using MASCOT™ search engine version 2.4.1 (Matrix Science, London, UK), configured with Mascot Daemon 2.3.2 (Matrix Science, London, U.K) software for automated data processing and Mascot Distiller 2.4 (Matrix Science, London, U.K) for extraction of MS/MS spectra and generation of peak lists (Figure 5). For the peptide/ protein identifications and modification analysis, the peak lists were searched in MASCOT™ against two databases, the International Wheat Genome Sequencing Consortium (IWGSC) RefSeq v.1.1 HC genome assembly and in-house customized and annotated wheat EST databases (EST) that is more specific to Canadian wheat cultivars. The following MASCOT™ MS/MS Ion Search parameters were used: I) quantitation with Sixplex iodoacetyl Tandem Mass Tag® with purity corrections according to manufacturer specifications (Thermo Scientific); II) trypsin as digestion enzyme with maximum one missed cleavage; III) monoisotopic mass values; IV) precursor peptide ions mass tolerance at 10 ppm; and fragment ions mass tolerance at 0.02 Da; V) fixed modification with iodoTMT6plex (C); VI) variable modifications: carbamidomethyl (C), deamidation (NQ), oxidation (M); VII) precursor peptide charge states +1, +2, +3; and +4; VIII) instrument type ESI-FTICR. Proteins and PTMs were identified using *Triticum aestivum* EST and IWGSC sequence matches.

Scaffold Q+ software, version 4.10.0 (Proteome Software Inc., Portland, OR), was used to validate protein and peptide matches from the MASCOT search engine and to perform iodoTMT-based comparative quantitative and statistical analysis. Peptides containing iodoTMT Cys modifications were chosen with a protein identification probability threshold of 99.0%, a minimum number of peptides of one, peak quantitation as centroided peak intensity, and a peptide threshold of 95.0%. For the quantitative analysis at the peptide level, two non-parametric statistical tests, the Mann-Whitney test and the Permutation test, were used with a $p \leq 0.05$ significance level. Ultimately, Scaffold Q+ quantitative peptide reports were exported into Microsoft Excel 2016 (Microsoft, 2016) for further data analysis and organization.

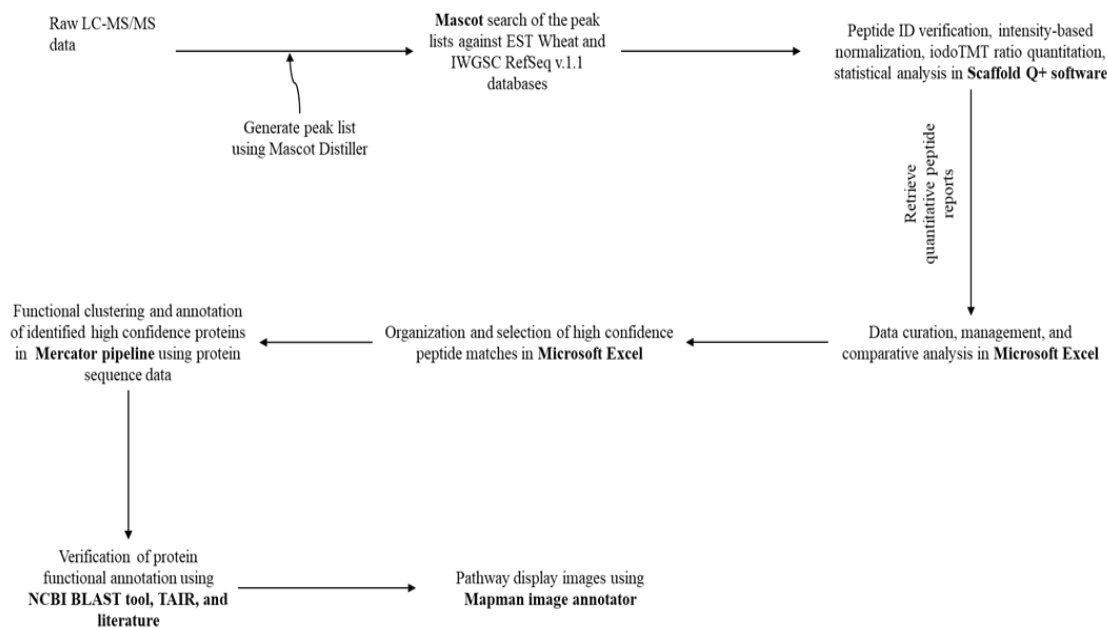


Figure 5: Data processing workflow of the raw data obtained from the nanoLC-MS/MS analysis for identification and quantitation of thiol-containing proteins in embryo and aleurone tissues of FH and AR seeds from DH wheat lines.

2.3.12 The data analysis strategy, further data curation and organization of quantitative peptide reports

Throughout the data analysis, FH and AR, embryo and aleurone peptide reports were analyzed separately. The files were further organized by removing the carbamidomethyl (+57) modification containing peptide lines, and all cluster groupings were removed. For clarity, the quants were given the sample category labels, water-DTT; water-IAA; DPI-IAA; DPI-DTT; (DPI+ABA)-IAA; and (DPI+ABA)-DTT. The Fold Change (FC) values expressed as Log₂ ratios were calculated with water treatments as control categories and non-parametric statistical tests Mann Whitney and Permutation were performed in Scaffold Q+ software package version 4.7.3 (Proteome Software, Inc, Portland, OR) with $p \leq 0.05$ significance level for statistical analysis within each category and for each peptide. Separate comparisons were made for two different approaches with IAA and DTT sample treatments. The DPI-IAA, (DPI+ABA)-IAA, or DPI-DTT, (DPI+ABA)-DTT redox or protein abundance changes were compared to the corresponding references, either Water-IAA or Water-DTT, respectively.

The FC was selected as significant using the following stringency criteria: I) At least one statistical method was given the test P-Value ≤ 0.05 . II) The average value representing available replicates reached $-0.6 \geq \text{Log}_2 \geq +0.6$, or minimum absolute value of 1.5 FC. III) At least three BioReps were present with the same - or + sign (up-regulated or down-regulated). If the values for multiple BioReps were available for peptides, at least two values equal or higher than $\text{Log}_2 \pm 0.6$ with similar signs of the average value were taken as significant. IV) The values for BioReps with opposite signs were taken as insignificant,

provided that Log_2 was below the significance threshold $-0.6 < \text{Log}_2 < + 0.6$. V) A minimum of two BioReps were accepted with the same sign, providing the values for other BioReps were missing. Reference missing was taken as a positive value in comparisons to support other positive values.

Finally, high-confidence unique peptides belonging to DPI-IAA, (DPI+ABA)-IAA, DPI-DTT, and (DPI+ABA)-DTT treatment categories, and common peptides belonging to both DPI-IAA, (DPI+ABA)-IAA (common-IAA) or DPI-DTT, (DPI+ABA)-DTT (common-DTT) treatment categories were identified and listed separately for further analysis.

2.3.13 The database search of protein sequences and functional annotation of the identified proteins

For the functional interpretation and protein grouping, complete protein sequences were used in the Mercator pipeline for automated sequence annotation (Figure 5). Protein sequences were either taken directly from the IWGSC RefSeq v. 1.1 database, or for the EST sequences, the homologous protein sequences were used based on annotations in the in-house EST database.

The high-confidence protein sequences identified in the unique and common treatment categories were functionally annotated using the web server Mercator pipeline. In this study, two versions of the Mercator pipeline were used for functional annotation: Mercator version 3.6 (Lohse et al., 2014) and Mercator4 version 2.0 (Schwacke et al., 2019). In Mercator version 3.6, the following database parameters were assigned to the search: I) TAIR: TAIR Release 10; II) PPAP: SwissProt/UniProt Plant Proteins; III) CHLAMY: JGI

Chlamy release 4 Augustus models; IV) ORYZA: TIGR5 rice proteins; V) KOG: Clusters of orthologous eukaryotic genes database (KOG); VI) CDD: Use conserved domain database; VII) IPR: Include InterPro scan (long runtime); VIII) BLAST_CUTOFF: 50; IX) MULTIPLE: Allow multiple bin assignments; X) CONSERVATIVE: Consider the "unassigned" bin with equal weight when assigning bin codes; XI) ANNOTATE: Append database annotation to mapping. Finally, functional annotation and mapping files from both Mercator versions were acquired, and annotations were manually combined to obtain the final functional annotations of the proteins in each unique and common treatment category. The National Center for Biotechnology Information (NCBI) BLAST tool (Proteins-NCBI, 2004), TAIR, and literature were used to verify protein functional annotations. To obtain a clearer picture, the Image Annotator of Mapman version 3.5.1R2 was used to generate pathway display images (Usadel et al., 2009) of the treatment categories containing a greater number of proteins. The software was run using data files with Log2 FC values created in Microsoft Excel (Microsoft, 2016), mapping files retrieved from Mercator Pipeline, and a pathway image created in Microsoft PowerPoint, version 2016 (Microsoft, 2016).

3 Results

3.1 Germination resistance of non-dormant seeds treated with an inhibitor of cell redox metabolism and ABA phytohormone

3.1.1 Changes in germination resistance of seeds with non-dormant genotypes under DPI, ABA, and DPI combined with ABA treatment conditions

Different concentrations of ABA and DPI were applied to seeds from three ND-DH lines (ND-AR, ND-AN, and ND-BQ) and one parent line (AC Karma) of white-seeded spring wheat, and the germination resistance (GR) of seeds was assessed. FH and AR seeds were used for these experiments. Three BioReps were performed using seeds from 2015, 2017, and 2019 seed increases and three TechReps were performed from the 2015 FH seed increase to check the GR in FH white-seeded spring wheat. Before being tested, these FH seeds were stored at -20°C for 5 months (2015 seed increase), 2 years and 5 months (2017 seed increase), and 2 months (2019 seed increase) directly after the harvesting process. AR seeds were taken from the 2013 seed increase (stored at -20°C for four years and two months) and the 2017 seed increase (stored at RT for two years and five months). BioReps were performed using 2013 and 2017 AR seed materials for AR seeds, along with two TechReps using the 2017 AR seed increase.

3.1.1.1 Physiological changes in germination resistance of freshly harvested seeds under different DPI, ABA and DPI combined with ABA treatments

In our GR experiment with the FH seeds, GR for the water (control) remained lower compared to all other treatments used in this experiment, with values of 4.39 days, 2.54 days, 2.76 days, 3.90 days in AC Karma, ND-AR, ND-AN and ND-BQ, respectively (Figure 6A). A significant difference in GR was observed in treatments with DPI compared to the water (control). DPI was used in the range of 150 μ M to 600 μ M, and increased DPI concentration gradually increased the grain GR in all three ND-DH lines and the parent line. Among the five treatments used, 150 μ M DPI combined with 50 μ M ABA treatment showed the highest effect on grain GR of 19.34 days (AC Karma, 4.4-fold increase), 17.00 days (ND-AR, 6.7-fold increase), 13.15 days (ND-AN, 4.8-fold increase) and 16.41 days (ND-BQ, 4.2-fold increase), which was followed by 600 μ M DPI treatment. There was no statistically significant difference detected in GR between these two treatments, which was consistent in every seed line. No significant differences were found in the GR of FH seeds from all three DH lines with ND genotypes under the 50 μ M ABA treatment compared to the water (control). The ungerminated seeds were treated with 0.5 mM GA on the 21st day and incubated for five more days to check their viability. All the ungerminated seeds in the treatment solutions germinated after the GA treatment; thus, it is apparent that the DPI and ABA-induced GR in the seeds was reversible in this white-seeded spring wheat population.

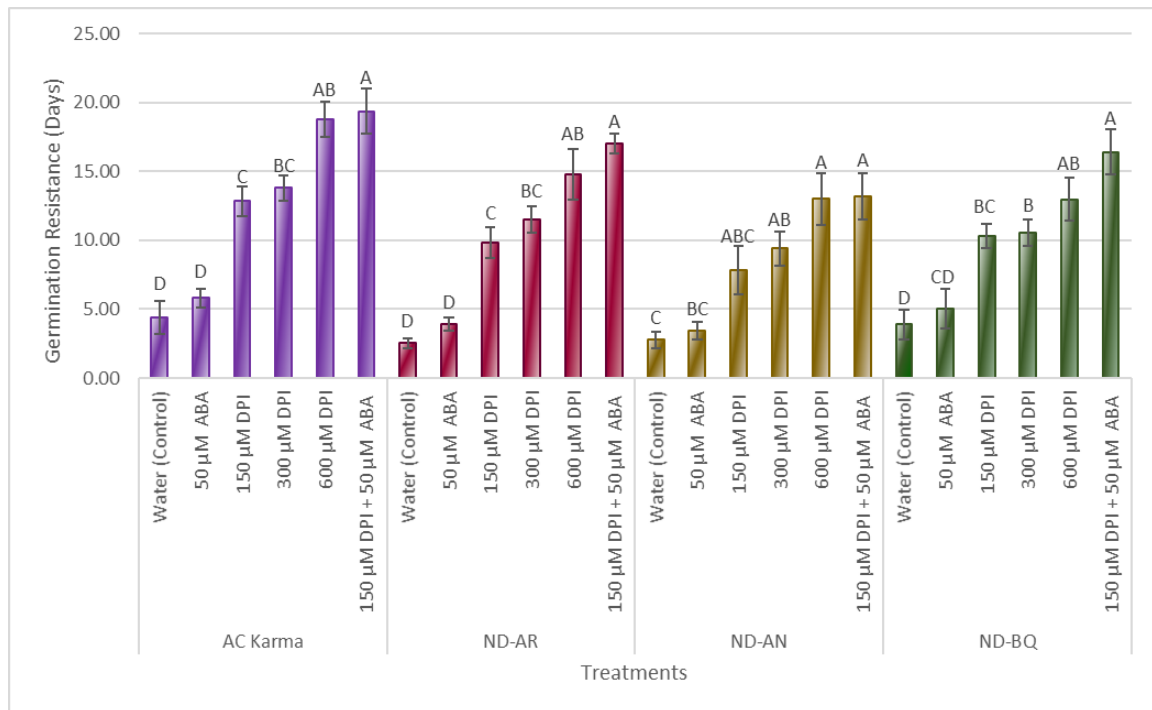


Figure 6A: Comparison of germination resistance in freshly harvested (stored at -20°C) wheat (*Triticum aestivum* L.) kernels treated with different concentrations of ABA, DPI and DPI in the presence of ABA. One parent line (AC Karma) and three non-dormant doubled haploid (DH) lines (ND-AR, ND-AN, and ND-BQ) of spring wheat DH population derived from the cross 94C15/9014 = 8021-V2 (high PHS resistance, white seed coat) X AC Karma (low PHS resistance, white seed coat) were used as a seed source. Three biological replicates were performed using seeds from 2015, 2017, and 2019 seed increases and three technical replicates were performed from the 2015 FH seed increase to check the GR. Mean germination resistance values \pm standard error are shown. One-way ANOVA test and pairwise/ multiple comparisons using Tukey's range test with a 95% confidence level were used for statistical analysis. Mean values followed by different letters in each seed line are significantly different at $P \leq 0.05$ level.

3.1.1.2 Physiological changes in germination resistance of after-ripened seeds under different DPI, ABA, and DPI combined with ABA treatment conditions

Similar to the FH experiment, ND-DH lines (ND-AR, ND-AN, and ND-BQ) and one parent line (AC Karma) were used to assess the GR of the AR wheat (*Triticum aestivum* L.) kernels (Figure 6B). Values for GR of the water (control) were 1.26 days (AC Karma), 0.53 days (ND-AR), 1.23 days (ND-AN) and 1.04 days (ND-BQ). Water (control) displayed a lower value for GR in AC Karma, ND-AR and ND-AN seed lines compared to other treatments. However, the GR of the water (control) was higher than that of the 50 μ M ABA treatment (0.90 days, 0.9-fold decrease) of the ND-BQ seed line. With the DPI concentration increase, the GR of AR kernels increased progressively. However, unlike the FH kernels, AR kernels reacted differently to the same DPI and ABA concentrations. For AR kernels from all DH lines and the parent, 150 μ M DPI combined with 50 μ M ABA treatment did not result in higher grain GR. The treatment with 600 μ M DPI was the most effective in AR wheat kernels, resulting in the highest grain GR of 3.25 days (2.6-fold increase), 3.37 days (6.4-fold increase), 3.75 days (3.0-fold increase), 2.80 days (2.7-fold increase) in AC Karma, ND-AR, ND-AN and ND-BQ, respectively, followed by 300 μ M DPI treatment in every seed line. A significant difference in GR was observed in treatment with 600 μ M DPI compared to the water (control) in AC Karma, ND-AR and ND-AN lines. However, there were no statistically significant differences in treatment with 600 μ M DPI compared to the water (control) in the ND-BQ seed line. Overall, there were no statistically significant differences in GR between ABA, lower concentrations of DPI (less

than 600 μM DPI), and DPI combined with ABA treatments compared to the water (control) in each seed line in AR kernels, indicating that after ripening of the seeds decreased, the DPI and ABA responsiveness in the seed of ND lines from white-seeded spring wheat DH population.

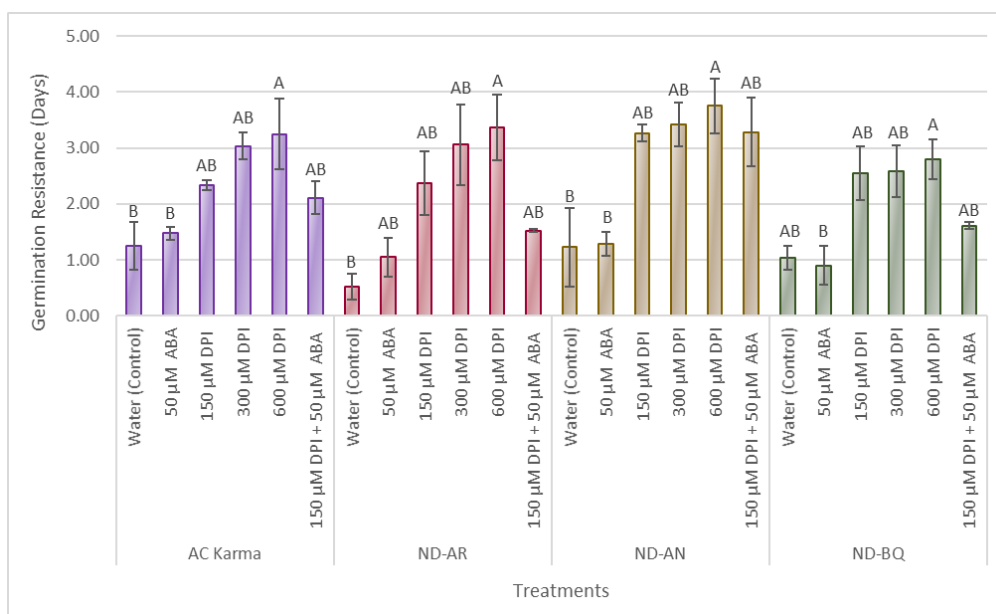


Figure 6B: Comparison of germination resistance in after-ripened wheat (*Triticum aestivum* L.) kernels treated with different concentrations of ABA, DPI and DPI in the presence of ABA. One parent line (AC Karma) and three non-dormant DH lines (ND-AR, ND-AN, and ND-BQ) of spring wheat DH population derived from the cross 94C15/9014 = 8021-V2 (high PHS resistance, white seed coat) X AC Karma (low PHS resistance, white seed coat) were used as a seed source. Seeds were after-ripened prior to the treatment experiments. Two biological replicates were performed using AR seed material from the 2013 seed increase (stored at -20°C for four years and two months) and the 2017 seed increase (stored at RT for two years and five months), and two technical replicates were performed using 2017 AR seed increase. Mean germination resistance values \pm standard error are shown. One-way ANOVA test and pairwise/ multiple comparisons using Tukey's range test with a 95% confidence level were used for statistical analysis. Mean values followed by different letters in each seed line are significantly different at $P \leq 0.05$ level.

3.1.2 Comparison of physiological changes in GR between FH and AR seeds from non-dormant wheat DH lines in response to DPI and ABA treatments

In FH wheat kernels, the moderately non-dormant parent line (AC Karma) showed the highest grain GR repeatedly in every treatment with the values of 4.39 days (control), 5.80 days (50 μ M ABA, 1.3-fold increase), 12.85 days (150 μ M DPI, 2.9-fold increase), 13.79 days (300 μ M DPI, 3.1-fold increase), 18.79 days (600 μ M DPI, 4.3-fold increase), 19.34 days (150 μ M DPI combined with 50 μ M ABA, 4.4-fold increase) (Figure 7A). Under conditions with higher DPI and DPI combined with ABA concentrations, ND-AR displayed the greatest GR compared to the other DH lines, ND-AN and ND-BQ. Nevertheless, there was no significant difference in GR between seed lines under most treatment conditions except for 300 μ M DPI treatment of FH wheat kernels. Upon treatment with 300 μ M DPI, there was a significant difference in the GR of AC Karma seeds compared to the GR of ND-AN seeds.

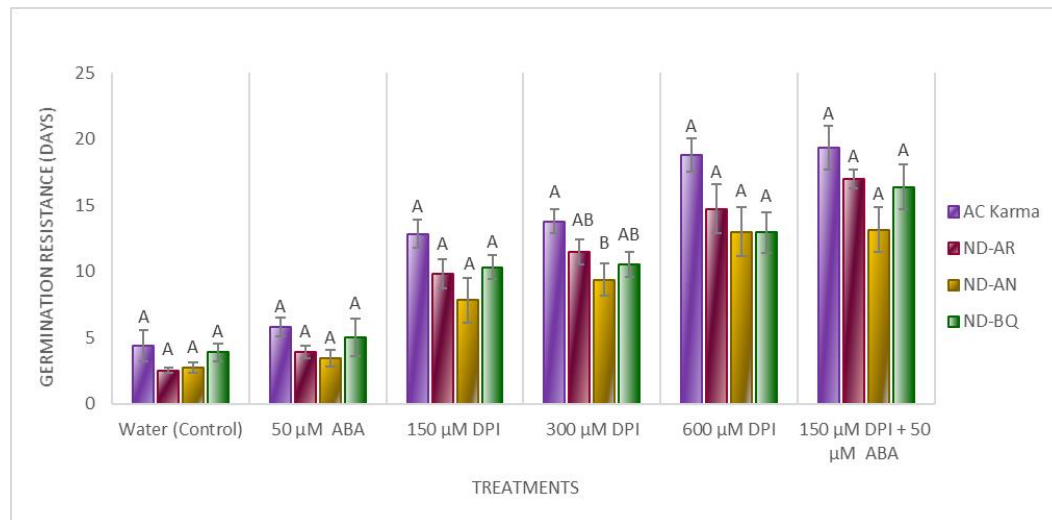


Figure 7A: Comparison of germination resistance in freshly harvested (stored at -20°C) wheat (*Triticum aestivum* L.) kernels after each experimental treatment. Three biological replicates were performed using seeds from 2015, 2017, and 2019 seed increases and three technical replicates were performed from the 2015 FH seed increase to check the GR. Mean germination resistance values \pm standard error are shown. One-way ANOVA test and pairwise/ multiple comparisons using Tukey's range test with a 95% confidence level were used for statistical analysis. Mean values followed by different letters in each treatment are significantly different at $P \leq 0.05$ level.

However, in AR wheat kernels, the responsiveness of the parent line (AC Karma) to the treatment with different concentrations of ABA, DPI, and DPI combined with ABA was dramatically lower with the values of 1.48 days (50 μM ABA, 1.2-fold increase), 2.33 days (150 μM DPI, 1.9-fold increase), 3.03 days (300 μM DPI, 2.4-fold increase), 3.25 days (600 μM DPI, 2.6-fold increase), 2.11 days (150 μM DPI combined with 50 μM ABA, 1.7-fold increase) (Figure 7B). Seeds from the ND-AN DH line exhibited the highest mean values of grain GR under the DPI and DPI combined with ABA treatment conditions as compared to those in other lines with values of 3.27 days (150 μM DPI, 2.7-fold increase),

3.42 days (300 μ M DPI, 2.8-fold increase), 3.75 days (600 μ M DPI, 3.0-fold increase), 3.28 days (150 μ M DPI combined with 50 μ M ABA, 2.7-fold increase). Similar to the responses in FH kernels, AC Karma seeds achieved marginally higher GR in water (control) and 50 μ M ABA treatment compared to the other three DH lines with a mean value of 1.26 days and 1.48 days, respectively. However, the AR wheat kernels showed no significant differences in GR between the seed lines under all tested conditions.

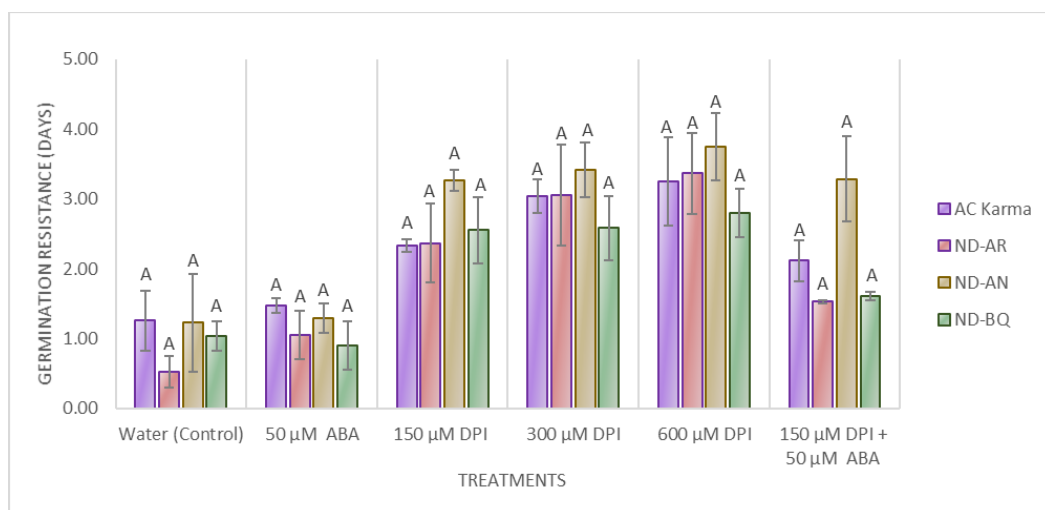


Figure 7B: Comparison of germination resistance in AR wheat (*Triticum aestivum* L.) kernels after each experimental treatment. Seeds were after-ripened prior to the treatment experiments. Two biological replicates were performed using AR seed material from the 2013 seed increase (stored at -20°C for four years and two months) and the 2017 seed increase (stored at RT for two years and five months), and two technical replicates were performed using 2017 AR seed increase. Mean germination resistance values \pm standard error are shown. One-way ANOVA test and pairwise/multiple comparisons using Tukey's range test with a 95% confidence level were used for statistical analysis. Mean values followed by different letters in each treatment are significantly different at $P \leq 0.05$ level.

3.1.3 Comparison of the effect of different concentrations of DPI, ABA and DPI combined with ABA on physiological changes for GR in FH and AR seeds

Comparison of the GR between the FH wheat kernels and AR wheat kernels manifests the responsiveness to DPI and DPI in the presence of ABA of the AR wheat kernels diminished through the after-ripening process in the seeds of spring wheat DH lines with ND genotypes. In contrast to all treatments conducted in this study, the highest values for GR in FH wheat kernels were 19.34 days (AC Karma, 4.4-fold increase), 17.00 days (ND-AR, 6.7-fold increase), 13.15 days (ND-AN, 4.8-fold increase) and 16.41 days (ND-BQ, 4.2-fold increase), while the highest values for GR in AR wheat kernels were reached only up to 3.25 days (AC Karma, 2.6-fold increase), 3.37 days (ND-AR, 6.4-fold increase), 3.75 days (ND-AN, 3.0-fold increase), 2.80 days (ND-BQ, 2.7-fold increase), providing a drastic difference in GR between FH and AR seeds in general (Figure 8). Persistently, the values for GR during the water (control) and 50 μ M ABA treatments in FH kernels remained slightly higher in every seed line compared to AR kernels, but no significant difference in repose to the ABA treatment was detected between the FH and AR kernels. Similarly, compared to the water (control), the GR of seeds after 50 μ M ABA treatments were consistently higher in both FH and AR kernels but not significantly different compared to the water (controls) in each seed line tested. In seeds from AC Karma, ND-AR and ND-BQ lines, the GR of AR kernels treated with different DPI and DPI in the presence of ABA concentrations were essentially similar to the GR values measured during the water (control) treatments of both AR and FH wheat kernels, indicating that the AR

wheat kernels were unresponsive to DPI in the treatment experiments. Thus, DPI and DPI combined with ABA treatments contributed to the increase in grain GR only in FH wheat kernels, resulting in a significant difference as compared to the GR in AR wheat kernels during the same treatments of seeds from DH lines tested.

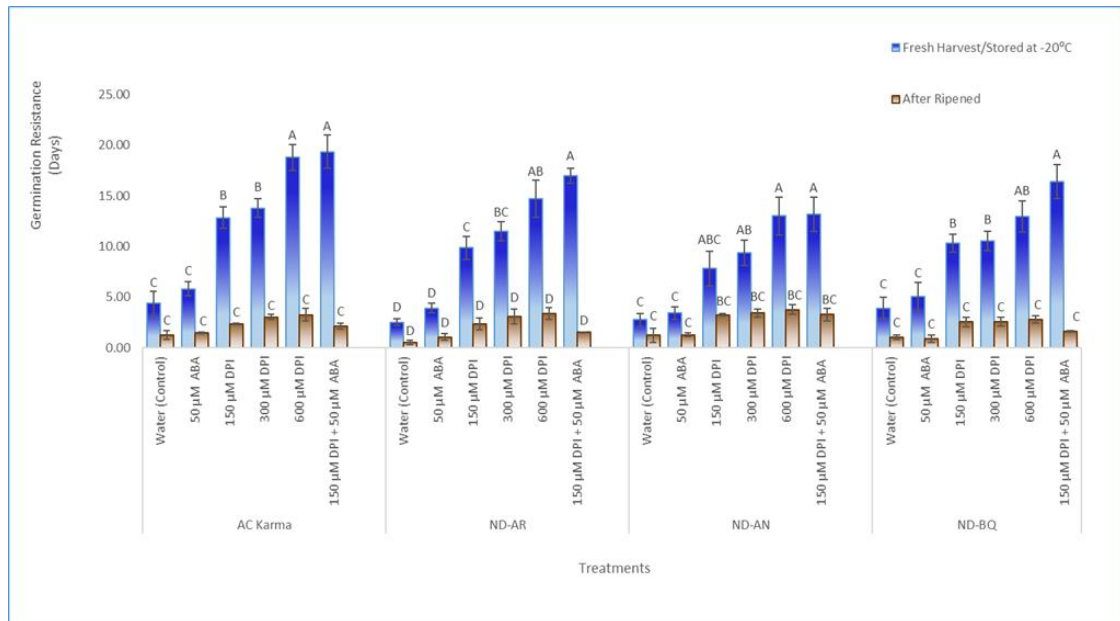


Figure 8: Effect of treatments with DPI, ABA and DPI in the presence of ABA on germination resistance in FH and AR wheat (*Triticum aestivum* L.) kernels. Three biological replicates were performed using seeds from 2015, 2017, and 2019 seed increases and three technical replicates were performed from the 2015 FH seed increase to check the GR in FH seeds. Seeds were after-ripened prior to the treatment experiments. Two biological replicates were performed using AR seed material from the 2013 seed increase (stored at -20°C for four years and two months) and the 2017 seed increase (stored at RT for two years and five months), and two technical replicates were performed using 2017 AR seed increase to check the GR in AR seeds. Mean germination resistance values \pm standard error are shown. Two-way ANOVA test and pairwise/ multiple comparisons using Tukey's range test with a 95% confidence level were used for statistical analysis. Mean values followed by different letters in each seed DH line are significantly different at $P \leq 0.05$ level.

3.1.4 Effect of solvents on germination resistance of seeds from non-dormant DH lines and AC Karma parent

DMSO and methanol solvents were used to prepare DPI and ABA treatment solutions in GR tests. Therefore, the control experiments were conducted using FH and AR seeds to check the solvent effect of DMSO, methanol and DMSO combined with methanol at concentrations corresponding to the DPI, ABA and DPI combined with ABA treatments for the GR assay, respectively. The concentrations of DMSO, methanol and DMSO combined with methanol in each treatment and control solution are listed in Table 2.

The 150 μ M DPI combined with 50 μ M ABA treatments were tested with the same concentration of DMSO (1.5%) combined with methanol (0.17%) solvent control treatments of both FH (Figure 9A) and AR (Figure 9B) white-seeded spring wheat lines. For FH seeds, three BioReps were performed using FH seeds from 2015, 2017 and 2019 seed increases, stored at -20°C for 5 months, 2 years and 5 months, and 2 months, respectively. Two TechReps from the 2017 seed increase (after-ripened for 2 years and 5 months at RT) and one replicate from the 2013 seed increase (after-ripened for 4 years and 2 months at -20°C), were used as the AR seed material for the experiment.

In FH seeds, values for the GR of water (control) in FH seeds were 4.39 days, 2.54 days, 2.76 days, and 3.90 days in AC Karma, ND-AR, ND-AN and ND-BQ, respectively (Figure 9A). Values for the GR of DMSO combined with methanol solvent control in FH seeds were 8.48 days (1.9-Fold increase), 10.48 days (4.1-Fold increase), 5.54 days (2.0-Fold increase) and 10.73 days (2.8-Fold increase) in AC Karma, ND-AR, ND-AN and ND-BQ, respectively. Compared to the water (control), DMSO concentrations of 1.5% combined

with 0.17% methanol significantly affected the GR of ND-AR and ND-BQ DH lines but did not significantly affect the AC Karma parent and ND-AN DH line in FH seeds. Nevertheless, all seed lines displayed a lower GR in the solvent control of 1.5% DMSO combined with 0.17% methanol compared to the corresponding DPI combined with ABA treatment, and the GR values were significantly different.

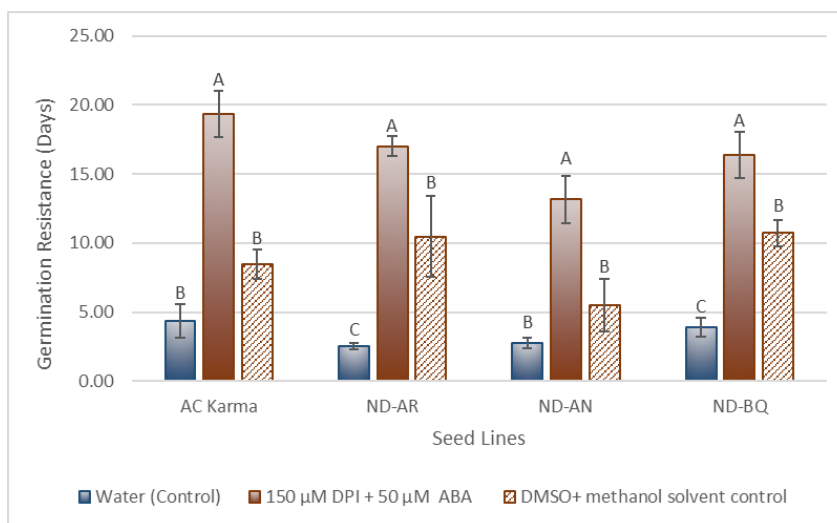


Figure 9A: Effect of DMSO combined with methanol solvent on germination resistance in FH (stored at -20°C) (*Triticum aestivum* L.) kernels at concentrations of 1.5% and 0.17%, respectively, used during the treatment with DPI in the presence of ABA. Blue, dark brown and pattern (brown) bars represent the GR values for water (control), DPI combined with ABA treatment and corresponding DMSO combined with methanol solvent control, respectively. Three biological replicates were performed using seeds from 2015, 2017, and 2019 seed increases and three technical replicates were performed from the 2015 FH seed increase to check the GR. Mean germination resistance values \pm standard error are shown. One-way ANOVA test and pairwise/multiple comparisons using Tukey's range test with a 95% confidence level were used for statistical analysis. Mean values followed by different letters in each seed DH line are significantly different at $P \leq 0.05$ level.

These results indicate that DMSO and methanol in the treatment solution used throughout the entire GR assay contributed to the inhibition of germination in all FH seeds of ND-DH lines used in this experiment, and some seed lines could be more sensitive to the DMSO and methanol in the treatment solution. However, compared to the level of germination inhibition by the corresponding DPI in the presence of ABA treatment, germination inhibition by the solvent control was lower in these FH seed lines.

In AR seeds, values for the GR of the water (control) were 1.26 days (AC Karma), 0.53 days (ND-AR), 1.23 days (ND-AN) and 1.04 days (ND-BQ), whereas values for the GR of the DMSO combined with methanol solvent control were 2.26 days (AC Karma, 1.8-fold increase), 1.85 days (ND-AR, 3.5-fold increase), 2.35 days (ND-AN, 1.9-fold increase) and 1.98 days (ND-BQ, 1.9-fold increase) (Figure 9B). Similar to the FH seeds, the GR of AR seeds from DH lines and parent remained low compared to the GR in DPI combined with ABA treatments with similar DMSO combined with methanol concentrations. Nevertheless, all AR seeds from ND-DH lines tested showed no significant differences between water (control), treatment and solvent control. Therefore, it is apparent that the sensitivity to the DMSO and methanol in the treatment solution in AR seeds was lower and provided little effect on the germination inhibition of AR seeds; hence, the after-ripening of seeds affects the responsiveness to DMSO and methanol, as well as DPI and ABA.

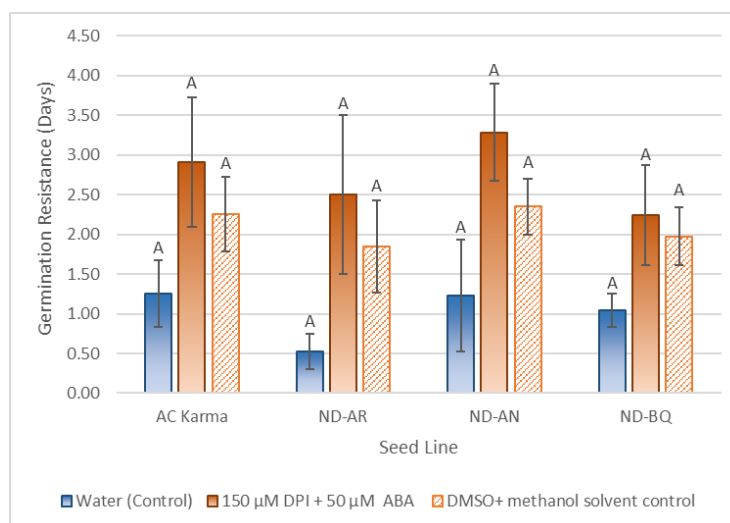


Figure 9B: Effect of DMSO combined with methanol solvent on germination resistance response in AR (*Triticum aestivum* L.) kernels at concentrations of 1.5% and 0.17%, respectively, used during the treatment with DPI in the presence of ABA. Blue, orange and pattern (orange) bars represent the GR values for water (control), DPI combined with ABA treatment and corresponding DMSO combined with methanol solvent control, respectively. Seeds were after-ripened prior to the treatment experiments. Two biological replicates were performed using AR seed material from the 2013 seed increase (stored at -20°C for four years and two months) and 2017 seed increase (stored at RT for two years and five months), and two technical replicates were performed using 2017 AR seed increase to check the GR in AR seeds. Mean germination resistance values \pm standard error are shown. One-way ANOVA test and pairwise/ multiple comparisons using Tukey's range test with a 95% confidence level were used for statistical analysis. Mean values followed by different letters in each seed DH line are significantly different at $P \leq 0.05$ level.

Another experiment was conducted using AR AC Karma seeds from the 2006 seed increase stored at -20°C for nearly ten years. DMSO concentrations in treatments and solvent controls ranging from 1.5% to 15% were used throughout the GR experiment (Table 2). The values for GR in DMSO control solutions remained lower than those during the DPI treatments. However, the higher concentrations of DPI, such as 1.2 mM DPI and 1.5 mM

DPI solutions, irreversibly inhibited the germination of the AC Karma kernels (Figure 9C). The addition of 0.5 mM GA did not reverse the effect of DPI on GR, indicating that extremely high DPI concentrations affect the viability of seeds. In the solvent control treatments, kernels were viable and germinated after the induction with 0.5 mM GA at the same DMSO concentrations with 12% and 15% of DMSO used for the DPI treatments. Hence, it is apparent that the DMSO at lower concentrations in the treatment solutions provided little effect on the GR of these AR seeds that were subject to a slow after-ripening process under -20 °C low-temperature conditions. High ABA concentration (1mM ABA) and the solvent methanol (at 3.34%) in the treatment solutions were tested, and there were no differences in the values of GR between the treatments with high ABA, solvent and water controls (Figure 9C). These results demonstrate that there was no effect of either ABA or methanol solvent, even at very high concentrations, 20-fold higher than that used for the experimental treatments.

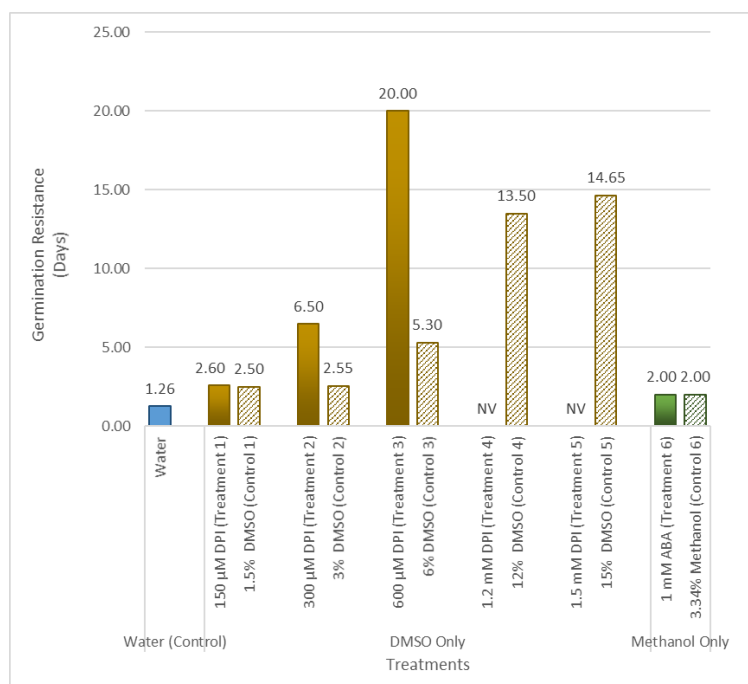


Figure 9C: Effects of DMSO or methanol individual solvents on germination resistance response in kernels (*Triticum aestivum* L.) subjected to slow after-ripening process under $-20\text{ }^{\circ}\text{C}$ low-temperature conditions at different concentrations used during the treatment with either DPI or ABA, respectively. Gold and pattern (gold) bars represent the GR values for DPI combined with ABA treatment and corresponding DMSO combined with methanol solvent control, respectively. Green and green pattern bars represent the GR values for ABA treatment and corresponding methanol solvent control, respectively.

Overall, low concentrations of DMSO, methanol and DMSO combined with methanol in the treatment solutions (up to at least 3%) provided no effect on the GR of seeds from all tested lines compared to the treatment solutions with similar concentrations. A previous study by Zhang et al. (2015) demonstrated that high concentrations of DMSO induce the accumulation of hydrogen peroxide. These solvent control experiments further demonstrate the sensitivity of FH seeds to the redox changes and induction of oxidative stress conditions.

3.2 Identification and quantitation of Cys Thiol Redox Modified Proteins (RMPs) and Cys-containing Differentially Abundant Proteins (CysDAPs) by Iodoacetyl Tandem Mass Tags (iodoTMT)-based labeling approach

Two different treatments were used in the thiol-redox proteomics experiment, 600 μ M DPI and 150 μ M DPI in the presence of 50 μ M ABA (DPI+ABA) with water as a reference for the identification and differential quantitative analysis of reversible Cys modifications in embryo and aleurone tissues from FH and AR wheat kernels. Two differential redoxome analysis approaches were conducted for each treatment and the reference control (Figure 3). In the first differential approach (Approach I), one part of each embryo and aleurone sample from the treatment experiment was supplemented with IAA to block free thiols and followed by DTT reduction during protein extraction. In the second approach (Approach II), the second part of the isolated embryo and aleurone samples was treated in parallel with DTT only during protein extraction. Redox-Modified Proteins (RMPs) found differentially labeled between water-IAA to water-DTT (references) showed all reversibly oxidized Cys PTMs. Samples treated with DTT only showed all RMPs with endogenous Cys PTMs that were reversibly oxidized at the time of extraction and that were reduced with DTT. Therefore, all samples reduced with DTT, such as DPI-DTT and (DPI+ABA)-DTT, were completely reduced controls of the protein thiol content in these experiments.

The approach I was used to identify and quantify the oxidized protein thiols with reversible Cys redox PTMs present in the sample at the time of protein extraction. This workflow consisted of five major steps that help preserve the endogenous oxidative state of the Cys

PTMs: i) blocking of free, active Cys thiols (Cys-SH) via alkylation using IAA; ii) reduction of reversible Cys PTMs to newly formed Cys-SH using DTT; iii) labeling of proteins containing regenerated Cys-SH groups in each sample with different iodoTMT reagents; iv) anti-TMT affinity enrichment of iodoTMT-labeled peptides from sixplex combined protein digests; v) nanoLC-MS/MS analysis for quantification. IAA is a known alkylating reagent commonly used in proteomic studies for the identification and quantification of reversible Cys PTMs such as S-nitrosylation (S-NO), S-sulfenylation (S-OH), S-cysteinylation (Cys-S-S-Cys), S-glutathionylation (Cys-S-S-GSH), S-acylation, S-sulfhydration (Cys-S-SH), as well as intra- and intermolecular disulfide bonds (Bykova & Rampitsch, 2013). Use of IAA prior to reduction blocks the free protein Cys-SH groups present in vivo at the time of protein extraction and eliminates the artefactual oxidation resulting in the formation of disulfide bonds and other redox PTMs by covalent addition of a carbamidomethyl group. An indirect readout of reversible Cys PTMs at the time of protein extraction was provided by the newly generated Cys-SH (Willems et al., 2020). Comparisons with the reference (Water-IAA) were conducted in each experimental treatment. Any unique differences in RMPs between Water-IAA and DPI-IAA (Unique RMPs in DPI-IAA) displayed the effect of DPI on Cys PTMs in response to the DPI blocking the germination in wheat kernels (Figure 10). The unique differences in RMPs between Water-IAA and (DPI+ABA)-IAA (Unique RMPs in (DPI+ABA)-IAA) exhibited the effect of the hormone ABA on Cys PTMs in the presence of DPI for the blocking of germination. Proteins found in both categories (Common RMPs in DPI-IAA and (DPI+ABA)-IAA) were considered as the Cys PTMs only affected by DPI, which occurred due to the blocking of germination by DPI.

Approach II was used to identify and quantify changes in the total available thiol content resulting from either irreversible Cys PTMs such as Cys sulfinic (Cys-SO₂H) and sulfonic (Cys-SO₃H) acids, which are associated with oxidative damage (decreased thiol content, inactive redox proteins destined to degradation), or from alterations in protein abundance (increased or decreased thiol content). The workflow consisted of four major steps: i) reduction of all reversible Cys PTMs using DTT; ii) labeling of proteins containing regenerated and native Cys-SH groups in each sample with different iodoTMT reagents; iii) and anti-TMT affinity enrichment of iodoTMT-labeled peptides from sixplex combined protein digests; iv). nanoLC-MS/MS analysis for quantification. Comparisons with the reference (Water-DTT) were conducted in each experimental treatment. Any differences in Cysteine-containing Differentially Abundant Proteins (CysDAPs) between Water-DTT and DPI-DTT (Unique CysDAPs in the DPI-DTT category) displayed the effect of DPI on irreversible Cys PTMs and the abundance of Cys-containing proteins in response to DPI blocking of germination in wheat seeds (Figure 10). Differences in CysDAPs between Water-DTT and (DPI+ABA)-DTT (Unique CysDAPs in (DPI+ABA)-DTT category) exhibited the effect of DPI in the presence of ABA on irreversible Cys PTMs and the abundance of Cys-containing proteins upon blocking of germination in wheat seeds. Proteins found in both categories (Common CysDAPs in DPI-DTT and DPI+ABA-DTT) represent the Cys PTMs that were irreversibly oxidized and Cys-containing proteins that changed in their abundance due to blocking of germination by DPI.

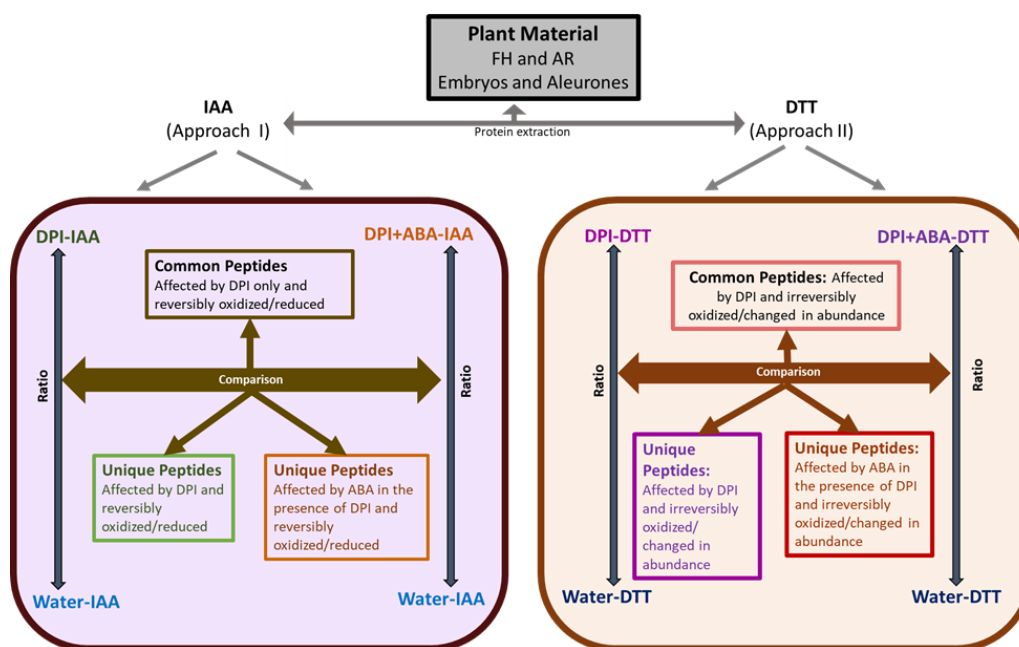


Figure 10: Strategy for comparative analysis in the iodoTMT labeling experiment. The quantitative redox strategy was comprised of two approaches: (i) Approach I - analysis of the reversibly oxidized or reduced thiol fraction in FH and AR embryos and aleurones during the germination inhibition by the DPI and DPI combined with ABA treatment; (ii) Approach II – evaluation of the total thiol content that irreversibly oxidized/ changed in abundance in FH and AR embryos and aleurones during the germination inhibition by the DPI and DPI combined with ABA treatment. The quantitative analysis of changes in the absolute quantity of oxidized fraction for a given redox-active Cys during the treatment experiments was done pairwise using water treatment as a reference. The ratios of the Cys reporter ions in the completely reduced by DTT/ labeled samples calculated between the treatments and the water reference reflect changes in the abundance level of redox-active proteins.

3.2.1 Unique significant RMPs found in embryo and aleurone tissues of DPI-treated seeds after the differential blocking of redox-active protein thiols with IAA (DPI-IAA)

3.2.1.1 Unique significant RMPs found in freshly harvested embryos in the DPI-IAA category

In FH embryos, we identified a total of 124 unique RMPs with Cys-labeled peptides that significantly changed in relative abundance and up-regulated (more reduced) after DPI treatment as compared to the water control ($FC < -1.5$, $p < 0.05$) (Supplementary Table S1). These RMPs were functionally assigned into 26 major functional groups (FGs) (Figures 19A and 19B). Altogether, 173 unique Cys modification sites were identified in a total of 131 unique peptides. Unique, multiple differentially Cys-labeled peptides were recognized in 6 RMPs, with the highest number of 3 labeled peptides, which belonged to the small ribosomal subunit (SSU) processome-associated component RACK1 protein in the ribosome biogenesis sub-functional group (sub-FG), protein biosynthesis FG. The other 118 RMPs were detected with a single peptide containing redox-active Cys. However, 6 of those RMPs, such as ketol-acid reductoisomerase (amino acid metabolism FG), mRNA-translocation factor (eEF2, protein biosynthesis FG), globulin-1 (development FG), contained multiple peptides with modifications other than Cys such as deamidation and methionine oxidation.

Protein biosynthesis was the most abundant FG detected, representing 18.5% of the total RMPs, including RMPs strongly related to ribosome biogenesis sub-FG (12.9% of the total RMPs identified in this category) (Figure 11A). There were many less abundant FGs with

only one protein corresponding to 0.8% of the total identified RMPs, namely nucleotide metabolism, coenzyme metabolism, secondary metabolism, cell cycle organization, RNA biosynthesis, photosynthesis, cell wall organization, protein translocation, solute transport, and multi-process regulation.

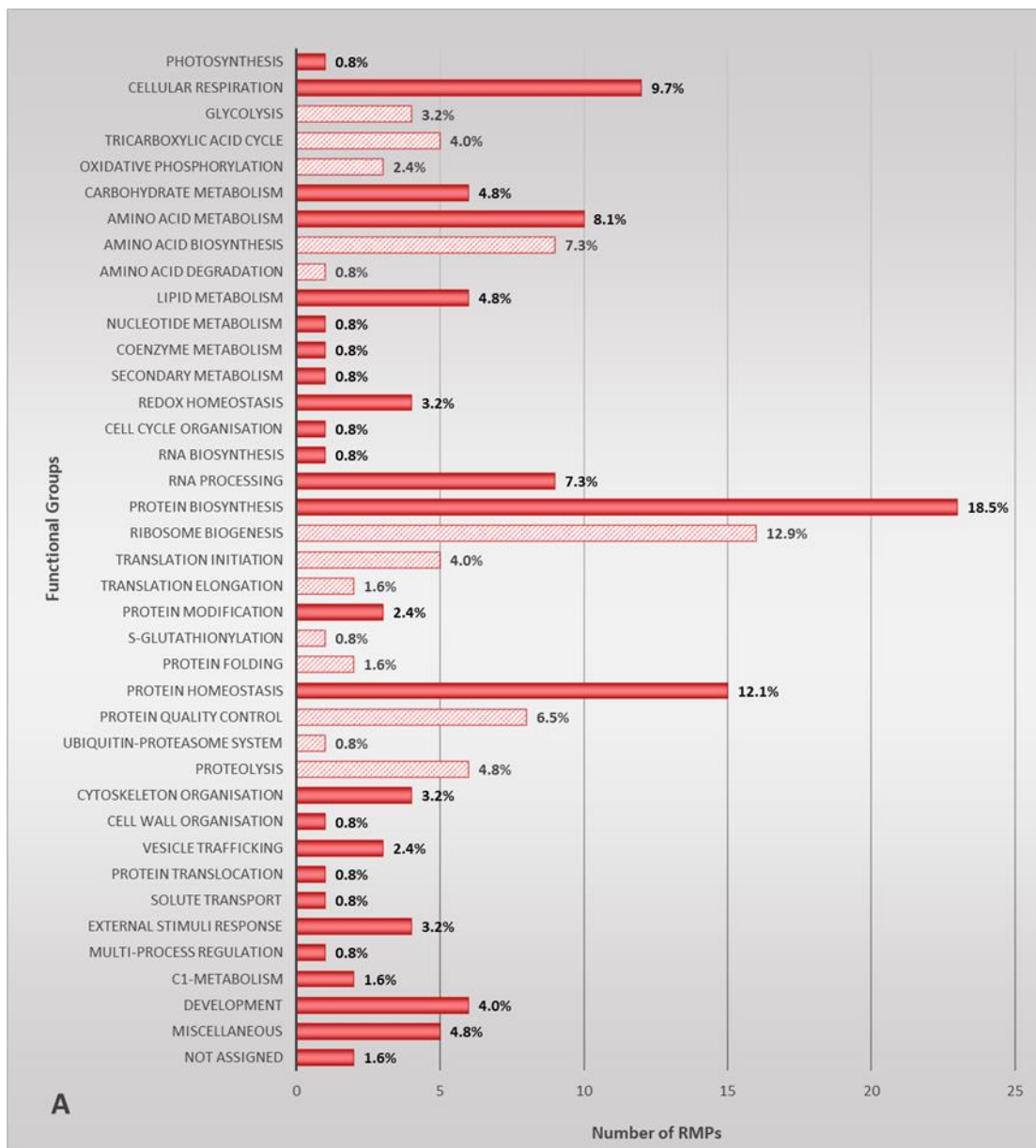


Figure 11A: Functional annotation of unique significant redox-modified proteins (RMPs) ($FC \leq -1.5$, $p < 0.05$) found in FH embryos from DPI-treated seeds and after the differential blocking of free thiol-containing redox proteins with IAA in the DPI-IAA category. Red bars show the number of RMPs with Cys-labeled oxidized peptides down-regulated in relative abundance (up-regulated in the absolute quantity of the reduced fraction) after DPI treatment as compared to the control (water) in each major functional group ($FC \leq -1.5$). Pattern bars (red) show the number of RMPs in the sub-functional group ($FC \leq -1.5$).

A high number of RMPs were found for cellular respiration, amino acid metabolism, protein homeostasis and RNA processing FGs, representing 9.7%, 8.1%, 12.1%, and 7.3% of the total RMPs, respectively. Within these FGs, a high number of RMPs with redox-responsive peptides were related to the tricarboxylic acid cycle (TCA; cellular respiration FG), amino acid biosynthesis (amino acid metabolism FG), and protein quality control (protein homeostasis FG) pathways (Figure 11B). Among those, succinate-CoA ligase (2-fold decrease in the oxidation level), ketol-acid reductoisomerase (approximately 3-fold decrease in the oxidation level), heat shock class-C-I protein (approximately 2-fold decrease in the oxidation level) were highly up-regulated in the level of reduced fraction of RMPs identified in cellular respiration FG, amino acid metabolism FG, and protein homeostasis FG, respectively.

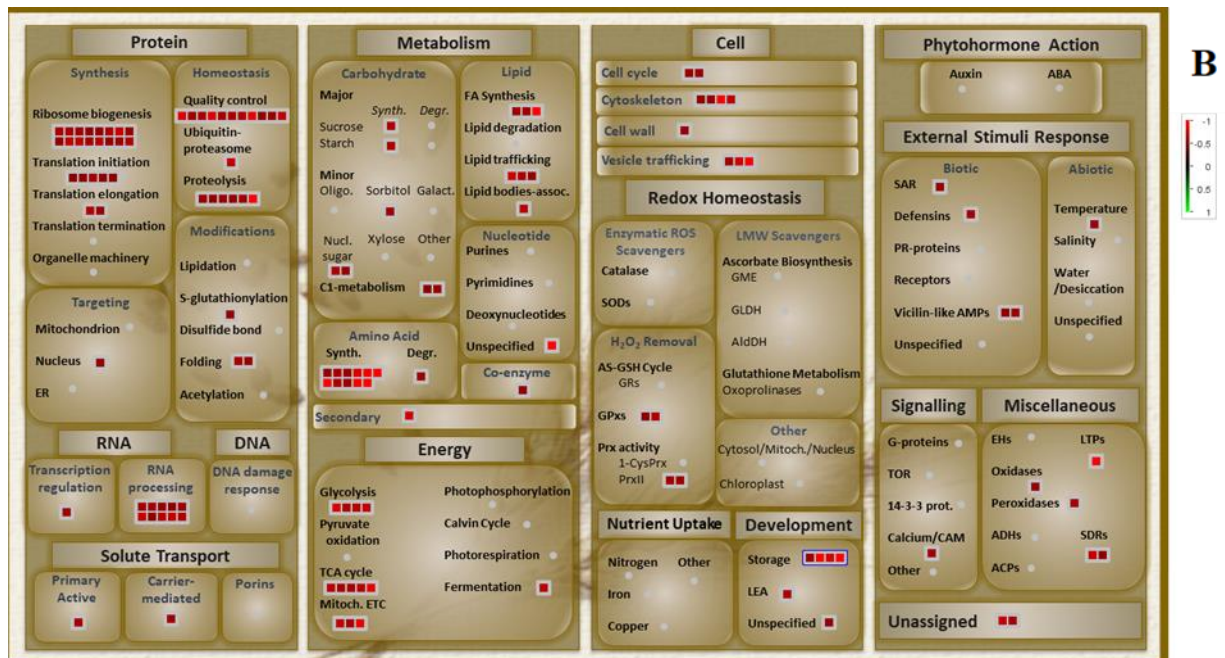


Figure 11B: Mapman visualization of the unique significant redox-modified proteins (RMPs) and their functional groups found in FH embryos from DPI-treated seeds and after the differential blocking of free thiol-containing redox proteins with IAA in the DPI-IAA category. Protein thiol-redox changes (squares) in the corresponding biological pathways are colored according to their log₂ of fold change ratios.

Peptides, DccQQLADINNEWcR and SQVLQQSTYQLLQELccQ from dimeric alpha-amylase inhibitor (miscellaneous FG) and 91 alpha-gliadin GLi2-LM2-17 (development FG) proteins, respectively, were the most significantly changed (down-regulated in labeling and thus the level of oxidation) peptides found in this category showing an approximately 4-fold decrease in the oxidation level compared to that of the control.

3.2.1.2 Unique significant RMPs found in after-ripened embryos in the DPI-IAA category

Only three unique RMPs with Cys-labeled peptides that significantly changed in relative abundance ($-1.5 > FC > +1.5$, $p < 0.05$) in response to the DPI treatment, belonging to 3 different FGs were identified compared to that of the water control in AR embryos (Supplementary Table S2). Among these, two proteins, endochitinase (external stimuli response FG) and gamma-gliadin B protein (development FG), showed up-regulated reduction levels (were down-regulated in the abundance of labeled peptides), while component beta type-2 of 26S proteasome protein (protein homeostasis FG) was found to be more oxidized (with down-regulated reduction level) during treatment with DPI as compared to the control. Five Cys modifications on three peptides were detected, and no multiple peptides were found in these RMPs.

3.2.1.3 Unique significant RMPs found in FH aleurones in the DPI-IAA category

Two RMPs belonging to protein biosynthesis FG with one significantly modified Cys-containing peptide per protein ($FC < -1.5$, $p < 0.05$) were identified as responding to the DPI treatment in FH aleurones as compared to the control (Supplementary Table S3).

3.2.1.4 Unique significant RMPs found in AR aleurones in the DPI-IAA category

In AR aleurone, one peptide with two Cys modifications was found to have a significantly up-regulated level of reduced thiols ($FC < -1.5$, $p < 0.05$) after the DPI treatment as compared to the control. The RMP, N2-acetylornithine aminotransferase, belongs to the amino acid metabolism FG (Supplementary Table S4).

3.2.2 Unique significant RMPs found in embryo and aleurone tissues of seeds treated with DPI in the presence of ABA after the differential blocking of redox-active protein thiols with IAA (DPI+ABA)-IAA category

3.2.2.1 Unique significant RMPs found in FH embryos in (DPI+ABA)- IAA category

In FH embryos, 61 Cys modification sites in 46 peptides corresponding to a total of 45 RMPs were significantly up-regulated ($FC < -1.5$, $p < 0.05$) in the level of reduced thiols after DPI in the presence of ABA treatment as compared to the control (Supplementary Table S5). These RMPs were assigned to 16 major FGs (Figures 12A and 12B). Fructose kinase, which belongs to carbohydrate metabolism FG, was the only protein recognized with multiple unique peptides (2 peptides). Three FGs, cellular respiration, lipid metabolism and protein biosynthesis, were found to have the highest number of proteins, with 13.3% of total RMPs identified in this group, while 7 FGs were represented by the lowest number of proteins (one protein per FG) with 2.2% of the total RMPs in this category, namely redox homeostasis FG, DNA damage response FG, cytoskeleton organization FG, photosynthesis FG, vesicle trafficking FG and miscellaneous FG.

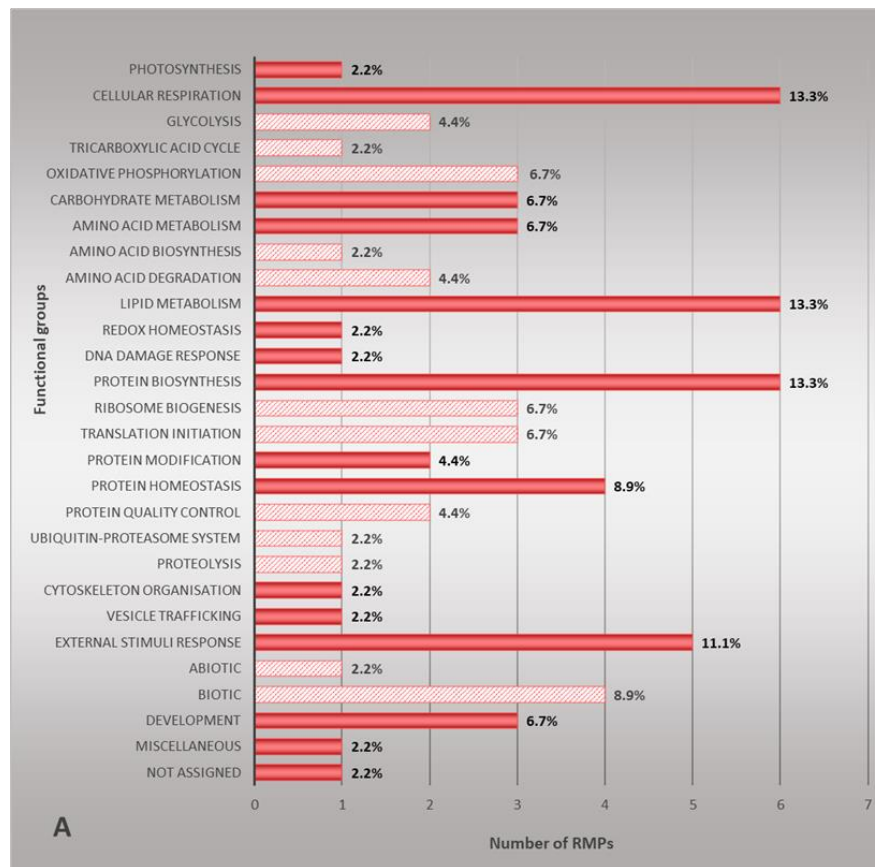


Figure 12A: Functional annotation of the unique significant RMPs ($FC \leq -1.5$, $p < 0.05$) found in FH embryos from seeds treated with DPI in the presence of ABA and after the differential blocking of thiol-redox proteins with IAA, in the (DPI+ABA)-IAA category. Red bars show the number of RMPs with an up-regulated level of the reduced peptide fractions in each major functional group ($FC \leq -1.5$) after the DPI combined with ABA treatment as compared to the control. Pattern bars (red) show the number of RMPs in the sub-functional groups ($FC \leq -1.5$).

The peptide with sequence QPQQPFPQPQQPQqSFPQQQPSLIQQSLQQQLNPcK from gamma-gliadin protein showed an approximately 3-fold increase in the reduction level in this category. The RMPs from other functional pathways TCA cycle (cellular respiration FG), oxidative phosphorylation (cellular respiration FG), Chaperonin containing T-

complex polypeptide (CCT) folding complex (cytoskeleton organization), PR-protein (external stimuli response FG), storage protein (development FG) were each identified by one redox-responsive peptide with over 2-fold increase in the relative amount of the reduced fraction upon the treatment with DPI in the presence of ABA (Figure 12B). The RMPs related to the lipid trafficking and biotic stress (external stimuli response FG) showed a higher number of redox-responsive peptides (4 peptides per functional sub-group and per protein) that changed in relative abundance (up-regulated in the reduction level and decrease in the absolute quantity of the oxidized fraction) in response to the DPI in the presence of ABA treatment as compared to the control.

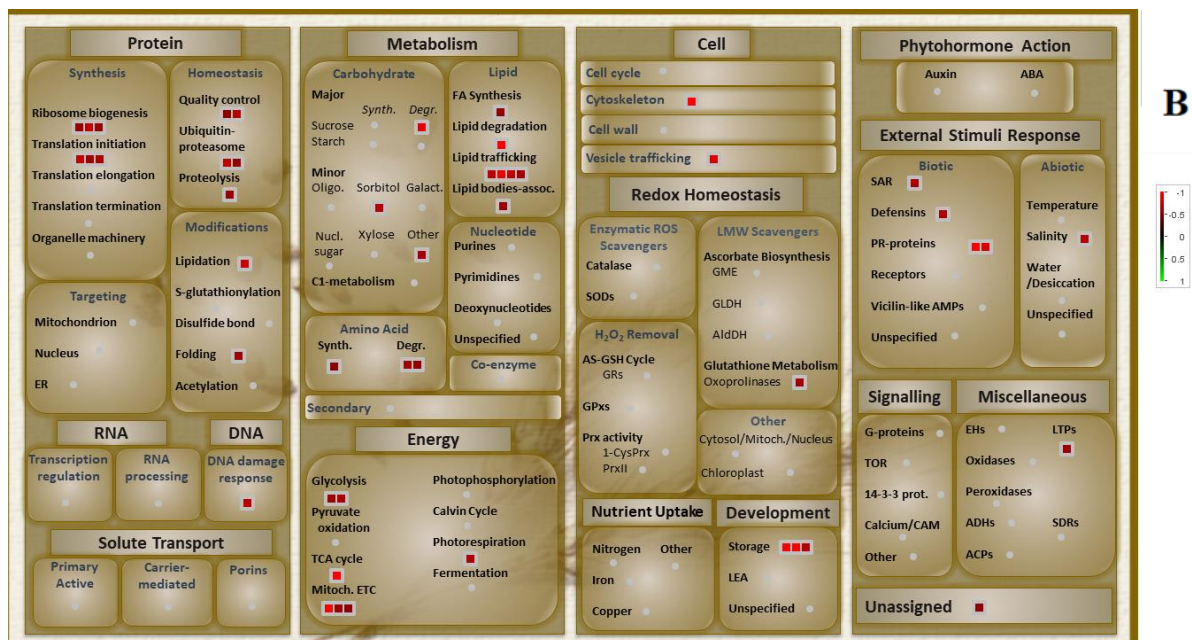


Figure 12B: Mapman visualization of the unique significant RMPs and their functional groups found in FH embryos from seeds treated with DPI in the presence of ABA and after the differential blocking of thiol-redox proteins with IAA, in the (DPI+ABA)-IAA category. Protein thiol-redox changes (squares) in the corresponding biological pathways are colored according to their log₂ of fold change ratios.

3.2.2.2 Unique significant RMPs found in AR embryos in (DPI+ABA)- IAA category

Twelve redox-modified Cys residues in nine peptides corresponding to nine significant RMPs ($-1.5 > FC > +1.5$, $p < 0.05$) were found to change in redox levels in AR embryos during DPI treatment in the presence of ABA as compared to the control (Supplementary Table S6). These nine RMPs were annotated into six major FGs (Figure 13). Out of 9 proteins, redox peptides from six proteins were up-regulated in the reduction level, such as mitochondrial NAD-dependent malate dehydrogenase (mMDH, cellular respiration FG), scaffold protein (ISU) (coenzyme metabolism FG), gamma-gliadin (development FG). The other three proteins, betaine-aldehyde dehydrogenase, P450s (secondary metabolism) and caffeoyl-CoA 3-O-methyltransferase (CcoA-OMT) (cell wall organization FG), were down-regulated in the level of the reduced fraction.

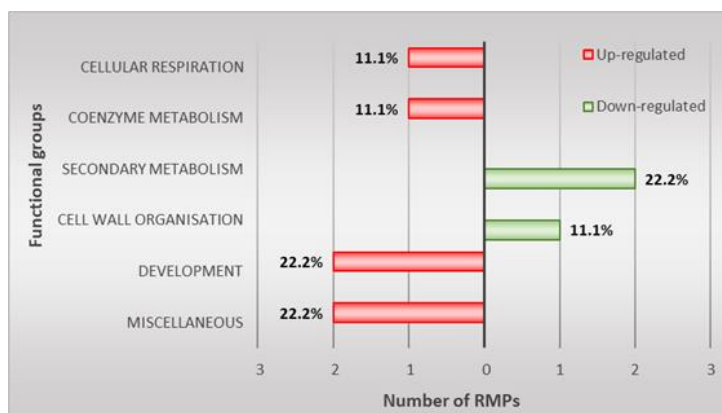


Figure 11: Unique significant RMPs found in AR embryos from seeds treated with DPI in the presence of ABA, and after the differential blocking of thiol-redox proteins with IAA, in the (DPI+ABA)-IAA category. Functional annotation of unique significant RMPs ($-1.5 \geq FC \geq +1.5$, $p < 0.05$). Red bars and green bars show the number of RMPs with the up-regulated ($FC \leq -1.5$) or down-regulated ($FC \geq 1.5$) level of the reduced peptide fractions for each major functional group, respectively, after the DPI combined with ABA treatment as compared to the control water treatment.

3.2.2.3 Unique significant RMPs found in FH aleurones in (DPI+ABA)- IAA category

A total of 176 RMPs significantly up-regulated in the reduction level ($FC < -1.5$, $p < 0.05$) (Supplementary Table S7), which belonged to 23 major FGs, were identified in FH aleurones during DPI treatment in the presence of ABA as compared to the control (Figure 14A). Altogether, 255 unique (309 in all quantified peptides) Cys redox sites were detected on a total of 196 unique peptides (211 total peptides with other modifications such as deamidation and methionine oxidation). Among these, multiple unique peptides were recognized in 17 proteins, with the highest of 4 unique redox active peptides belonging to dimeric alpha-amylase inhibitor protein (miscellaneous FG). The other 159 proteins were identified with only a single unique peptide, whereas 17 of those had peptides with modifications other than Cys. Miscellaneous FG was the most abundant FG, with 21.6% of the total proteins in this group, followed by the external stimuli response and development FGs (15.3% of the total proteins in this group) (Figure 14A), represented mostly by the biotic stress response proteins (Figure 14B).

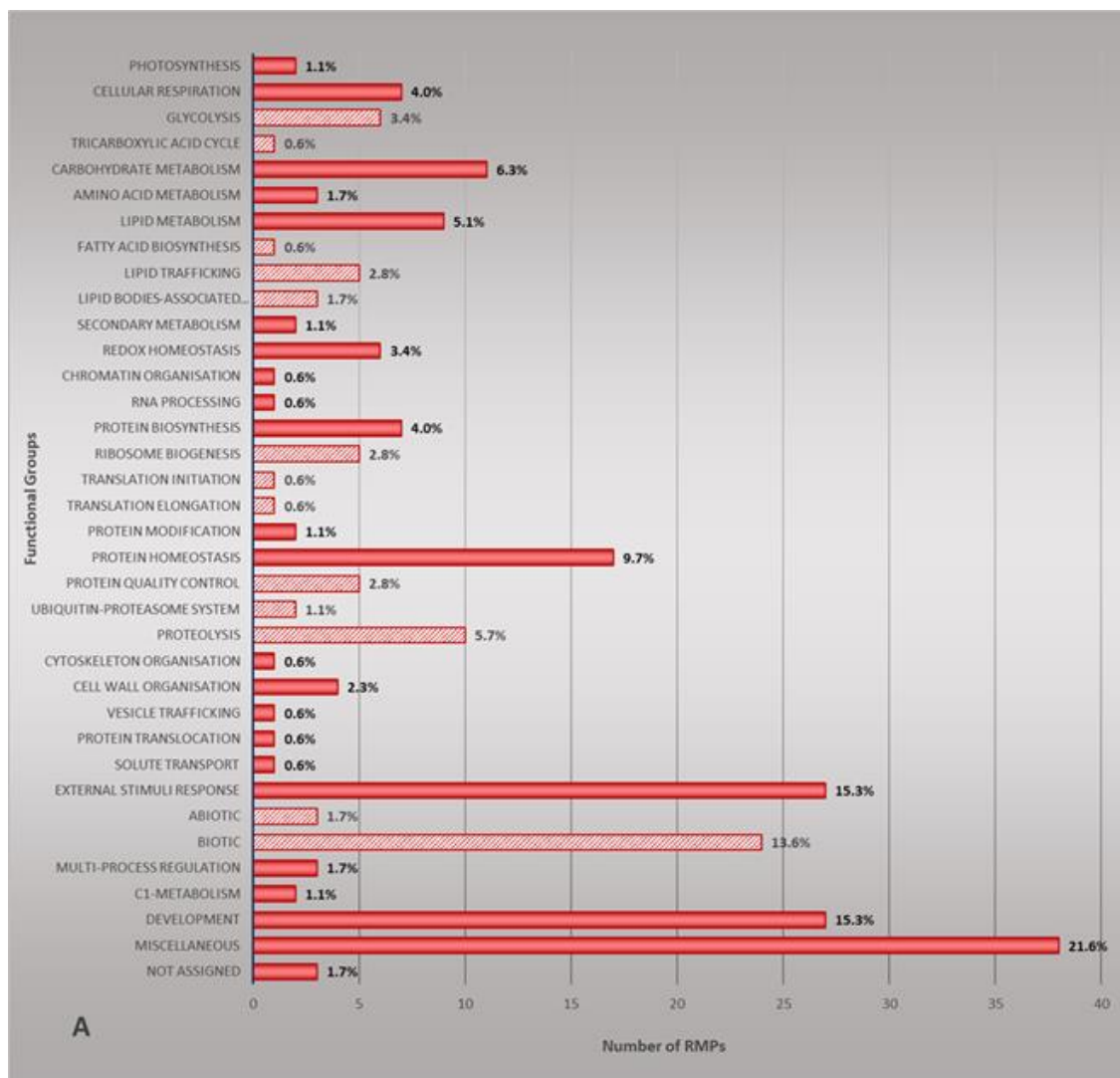


Figure 14A: Functional annotation of unique significant RMPs ($FC \leq -1.5$, $p < 0.05$) found in FH aleurones from seeds treated with DPI in the presence of ABA, and after the differential blocking of thiol-redox proteins with IAA, in the (DPI+ABA)-IAA category. Red bars show the number of RMPs with an up-regulated level of the reduced peptide fractions in each major functional group ($FC \leq -1.5$) after the DPI combined with ABA treatment as compared to the control. Pattern bars (red) show the number of RMPs in the sub-functional group ($FC \leq -1.5$).

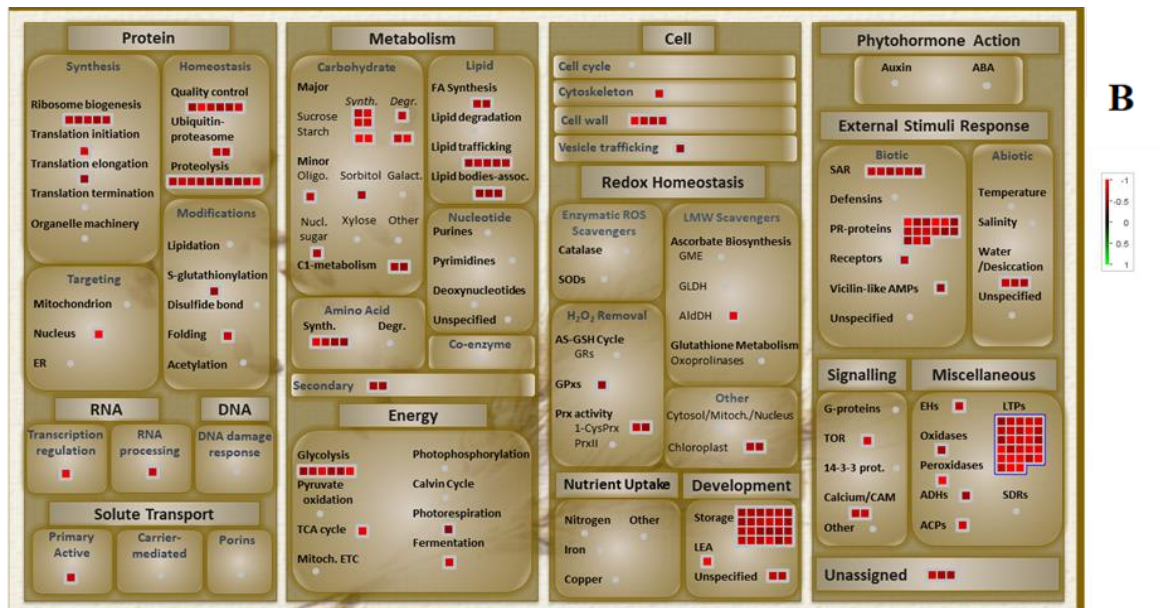


Figure 14B: Mapman visualization of the unique significant RMPs and their functional groups found in FH aleurones from seeds treated with DPI in the presence of ABA, and after the differential blocking of thiol-redox proteins with IAA, in the (DPI+ABA)-IAA category. Protein thiol-redox changes (squares) in the corresponding biological pathways are colored according to their log₂ of fold change ratios.

The peptide with sequence ELY_nASQHcR from alpha-amylase/trypsin inhibitor CM2 protein, the peptide with sequence cGDLSSMLR from the dimeric alpha-amylase inhibitor protein and another peptide with sequence ccDNcNSWSGAQFcDDVGPK from the wound-induced protease inhibitor proteins in the miscellaneous FG, and the peptide sequences LLPEATVVAEDVSGMPVLCr and ILPEATVVAEDVSGMPVLCr from isoforms of starch branching enzyme in the carbohydrate metabolism FG were found to be highly up-regulated with an approximately 3-fold increase in the relative amount of the reduced fraction. Many least abundant FGs were detected, with only one protein corresponding to 0.6% of the total RMPs in this treatment category, such as chromatin organization, RNA processing, and cytoskeleton organization. A high number of non-

specific Lipid Transfer Proteins (nsLTPs, miscellaneous FG), seed storage proteins (development FG), and Pathogenesis-related (PR) proteins (external stimuli response FG) were identified by redox peptides that changed in relative abundance (up-regulated in the reduction level and decrease in the absolute quantity of the oxidized fraction) in response to the DPI in the presence of ABA treatment in this category (Figure 14B). Among those, redox peptides belonging to alpha-amylase/trypsin inhibitor CM3 from miscellaneous FG, wheatwin-2 and xylanase inhibitor TL-XI (PR proteins) from external stimuli response FG, and low molecular weight glutenin subunit from development FG were identified with over 2-fold increase in the relative amount of the reduced fraction upon the treatment of DPI in the presence of ABA as compared to the water control.

3.2.2.4 Unique significant RMPs found in AR aleurones in (DPI+ABA)- IAA category

A total of 9 unique RMPs significantly down-regulated in the reduction level ($FC > +1.5$, $p < 0.05$) belonging to 3 major FGs were identified in AR aleurones during DPI treatment in the presence of ABA as compared to the control (Supplementary Table S8, Figure 15). Altogether, 24 Cys modification sites in nine peptides were detected. Miscellaneous FG showed the highest number of proteins changed in the redox level in this category, including isoforms of alpha-amylase/trypsin inhibitor proteins.

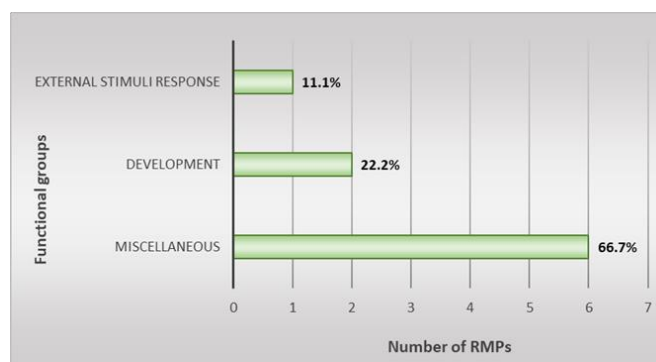


Figure 12: Unique significant RMPs found in AR aleurones from seeds treated with DPI in the presence of ABA, and after the differential blocking of thiol-redox proteins with IAA, in the (DPI+ABA)-IAA category. Functional annotation of unique significant RMPs ($FC \geq 1.5$, $p < 0.05$). Green bars show the number of RMPs with the downregulated level of the reduced peptide fractions in each major functional group ($FC \geq 1.5$) after the DPI combined with ABA treatment as compared to the control.

3.2.3 Common RMPs found in embryo and aleurone tissues of seeds treated with DPI and DPI in the presence of ABA after the differential blocking of redox-active protein thiols with IAA in both DPI-IAA and (DPI+ABA)-IAA categories (Common-IAA)

3.2.3.1 **Common RMPs found in FH embryos in both DPI-IAA and (DPI+ABA)-IAA categories**

In FH embryos, a total of 436 RMPs significantly up-regulated in the level of reduced fraction ($FC < -1.5$, $p < 0.05$) (Supplementary Table S9) belonging to 30 major FGs were identified as common to both DPI-IAA and (DPI+ABA)-IAA treatments (Figure 16A and 16B). A total of 56 proteins were detected with multiple unique peptides among the redox up-regulated RMPs, while other 380 proteins were detected only with a single unique peptide sequence. A total of 621 Cys modification sites in 505 unique peptides were

changing in the absolute quantity of the oxidized fraction. Interestingly, all peptides commonly responding to both treatments showed a significant decrease in the absolute quantity of the oxidized fraction and, therefore, accumulation of a reduced fraction during induction of oxidative stress and inhibition of germination.

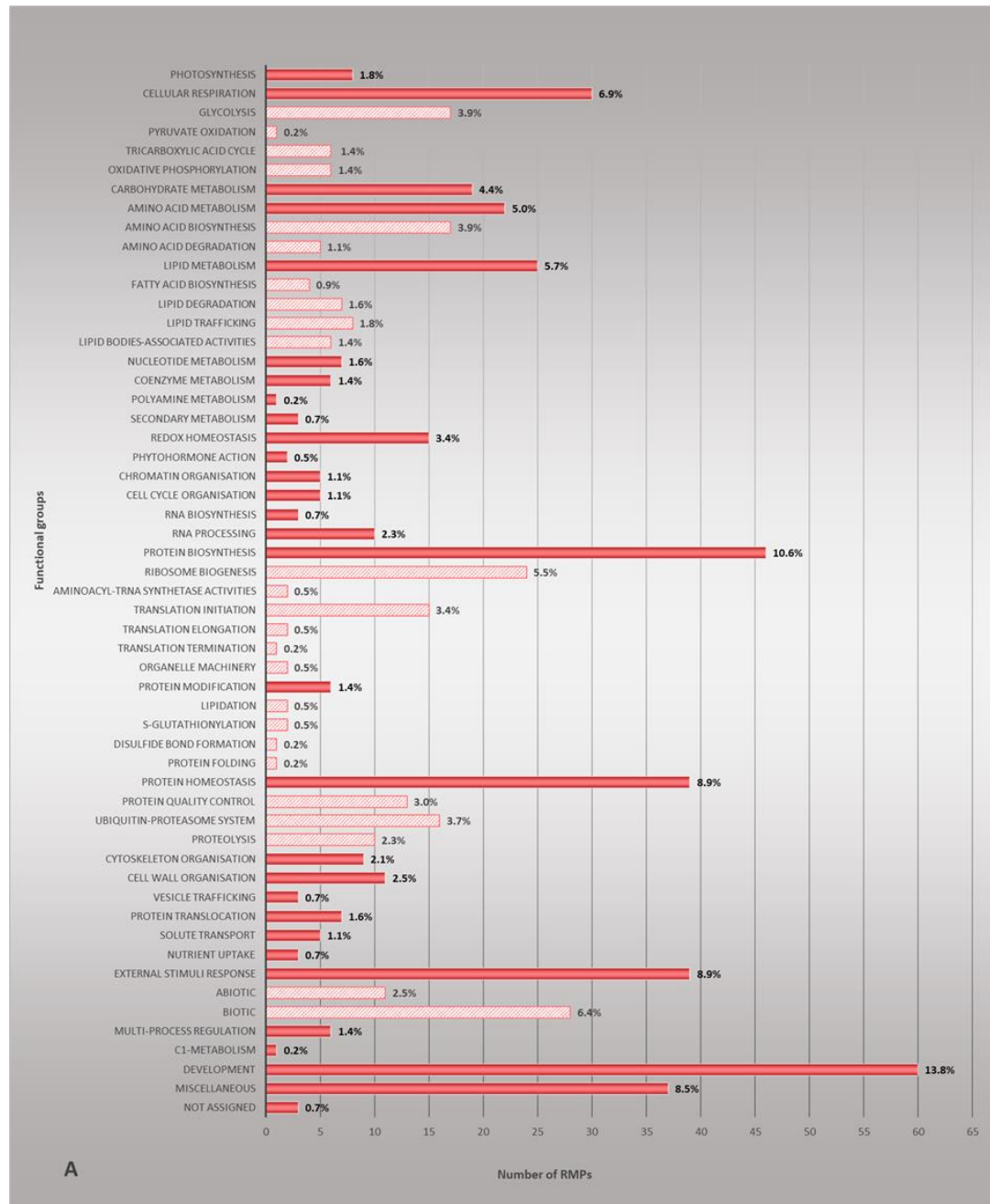


Figure 16A: Functional annotation of common significant RMPs ($FC \leq -1.5$, $p < 0.05$) found in FH embryos from seeds treated with either DPI or DPI in the presence of ABA, and after the differential blocking of thiol-redox proteins with IAA, common in DPI-IAA and (DPI+ABA)-IAA categories. Red bars show the number of RMPs identified with the up-regulated level of the reduced peptide fractions in each major functional group ($FC \leq -1.5$) after the DPI or DPI+ABA treatment as compared to the control. Pattern bars (red) show the number of RMPs in the sub-functional group ($FC \leq -1.5$).

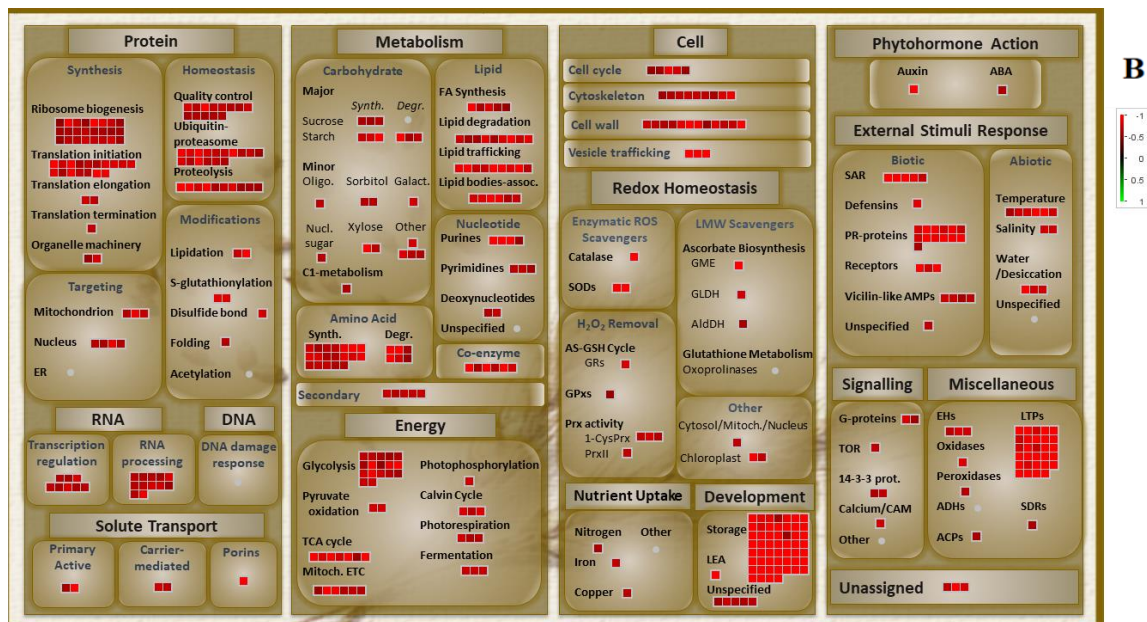


Figure 16B: Mapman visualization of the common significant RMPs and their functional groups found in FH embryos from seeds treated with either DPI or DPI in the presence of ABA, and after the differential blocking of thiol-redox proteins with IAA, common in DPI-IAA and (DPI+ABA)-IAA categories. Protein thiol-redox changes (squares) in the corresponding biological pathways are colored according to their log₂ of fold change ratios.

The highest unique peptide count (5 unique Cys-containing peptides) was observed in eEF2 protein in translation elongation sub-FG, protein biosynthesis FG. Four unique redox-responsive peptides were found in platform ATPase (CDC48) (protein homeostasis FG), whereas three unique redox-responsive peptides were detected in proteins such as carbamoyl-phosphate synthase, isomers of alanine aminotransferase (amino acid

metabolism FG), eIF3 mRNA-to-PIC binding complex (protein biosynthesis FG), dimeric alpha-amylase inhibitor (development FG) (Supplementary Table S9). Other proteins such as beta 1,3 glucan hydrolases (PDCB) (protein modification FG), low molecular weight glutenin subunit, and gamma-gliadin (development FG) were found to have multiple peptides with the same sequence but different modifications such as methionine oxidations. Development was the most abundant FG, representing 13.8% of the total identified proteins responding to both treatments DPI and DPI in the presence of ABA (Figure 16A). A high number of redox-responding proteins was found for protein biosynthesis, protein homeostasis, external stimuli and stress response, miscellaneous enzymes, cellular respiration, lipid and amino acid metabolism FGs, represented by 10.6%, 8.9%, 8.9%, 8.5%, 6.9%, 5.7%, and 5.0% of the total RMPs, respectively. Polyamine metabolism and C1-metabolism were the least abundant functional groups, with a percentage of 0.2% of the total proteins.

Approximately 5.7% of the peptides in the (DPI+ABA)-IAA category showed a dramatic increase in the absolute quantity of the reduced fraction (decrease in the absolute quantity of the oxidized fraction), in the range of 4-fold to 15-fold change, while only 1.4% of peptides in the DPI-IAA category showed a high increase in the absolute quantity of the reduced fraction, between 4-fold to 8-fold change in the reduction level. Hence, for the majority of highly responsive peptides, changes in the reduction level found in the DPI-IAA treated sample were further enhanced by the addition of DPI in the presence of ABA during the imbibition and treatment of seeds. These RMPs with highly redox-responsive peptides included a number of seed storage (development FG), bifunctional protease inhibitors and nsLTPs (miscellaneous FG), one PR protein (external stimuli response FG),

a subunit of E3 ubiquitin ligase (protein homeostasis FG), and mMDH (cellular respiration FG) (Figure 16B). Only 1.2% of the thiol-redox active peptides were highly up-regulated in both categories ($FC > 4$), such as the peptide sequence TLPNMcNVYVRPDcSTINAPFASIVAGISGQ from gamma-gliadin protein (development FG), which displayed an approximately 15-fold and approximately 8-fold increase in the reduction level in (DPI+ABA)-IAA and DPI-IAA categories, respectively.

3.2.3.2 Common RMPs found in AR embryos in both DPI-IAA and (DPI+ABA)-IAA categories

Only one RMP significantly up-regulated in the quantity of the reduced fraction ($FC < -1.5$, $p < 0.05$), methylthioribulose-1-phosphate dehydratase (amino acid metabolism FG) and one RMP significantly down-regulated in the quantity of the reduced fraction ($FC > +1.5$, $p < 0.05$), protease (LON) (protein homeostasis FG), were detected as common in both (DPI+ABA)-IAA and DPI-IAA categories in AR embryos (Supplementary Table S10). Each protein contained one peptide, and altogether, 3 Cys modification sites were identified with two Cys modifications on the peptide of LON protease.

3.2.3.3 Common RMPs found in FH aleurones in both DPI-IAA and (DPI+ABA)-IAA categories

Ten RMPs significantly up-regulated in the reduction level ($FC < -1.5$, $p < 0.05$) (Supplementary Table S11), which belonged to 5 major FGs, were identified in FH aleurones upon both treatments with DPI and DPI in the presence of ABA (Figure 17). Among these RMPs, three proteins contained two unique thiol-responsive peptides each, and 24 Cys modification sites on 13 peptides were identified. Miscellaneous FG was the

most enriched with identified RMPs (60.0% of the total proteins found in this experimental group). In the (DPI+ABA)-IAA category, the majority of common thiol-responsive peptides from RMPs showed a higher increase in the reduction level FC (up to 3-fold change) compared to that in the DPI-IAA category, such as the peptide sequences, NYVEEQAcR, DYVEQQAcR and LYccQELAEISQQcR from isomers of alpha-amylase/trypsin inhibitor proteins (miscellaneous FG). The redox-active IAcYVTIR peptide from 50S ribosomal protein L5 (protein biosynthesis FG) was the most up-regulated in the reduction level peptide detected in the (DPI+ABA)-IAA category with over 3-fold increase.

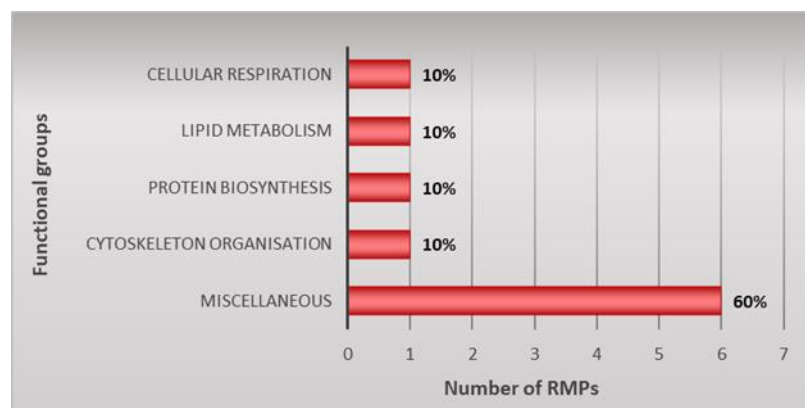


Figure 13: Common significant RMPs found in FH aleurones from seeds treated with either DPI or DPI in the presence of ABA, and after the differential blocking of thiol-redox proteins with IAA, common in DPI-IAA and (DPI+ABA)-IAA categories. Functional annotation of unique significant RMPs ($FC \geq \pm 1.5$, $p < 0.05$). The red bars show the number of RMPs with up-regulated level of the reduced peptide fractions in each major functional group ($FC \leq -1.5$) found after the DPI and DPI+ABA treatment as compared to the control.

3.2.3.4 Common RMPs found in AR aleurones in both DPI-IAA and (DPI+ABA)-IAA categories

In AR aleurones, a single peptide with three Cys redox modification sites corresponding to the avenin-like protein s1 was the only redox-modified peptide identified as common to both (DPI+ABA)-IAA and DPI-IAA categories (Supplementary Table S12). The peptide was significantly down-regulated in the reduction level ($FC > +1.5$, $p < 0.05$).

3.2.4 Unique significant CysDAPs found in embryo and aleurone tissues of seeds treated with DPI after the reduction of all redox-active protein thiols with DTT, (DPI- DTT) category

3.2.4.1 Unique significant CysDAPs found in FH embryos in the DPI-DTT category

Altogether, 50 peptides with 81 Cys residues corresponding to a total of 49 significant unique CysDAPs ($-1.5 > FC > +1.5$, $p < 0.05$) (Supplementary Table S13), which belonged to 10 major FGs, changed in abundance during the treatment with DPI as compared to the control (Figure 18A and 18B). Among these CysDAPs, four proteins belonging to lipid metabolism FG, protein biosynthesis FG, and development FG were down-regulated in abundance, and the other 45 CysDAPs were up-regulated in abundance upon DPI-mediated inhibition of seed germination. Multiple peptides were identified in 9 up-regulated CysDAPs, but only one CysDAP had two unique peptide sequences, and the other 8 CysDAPs had peptides with methionine oxidations and glutamine deamidation.

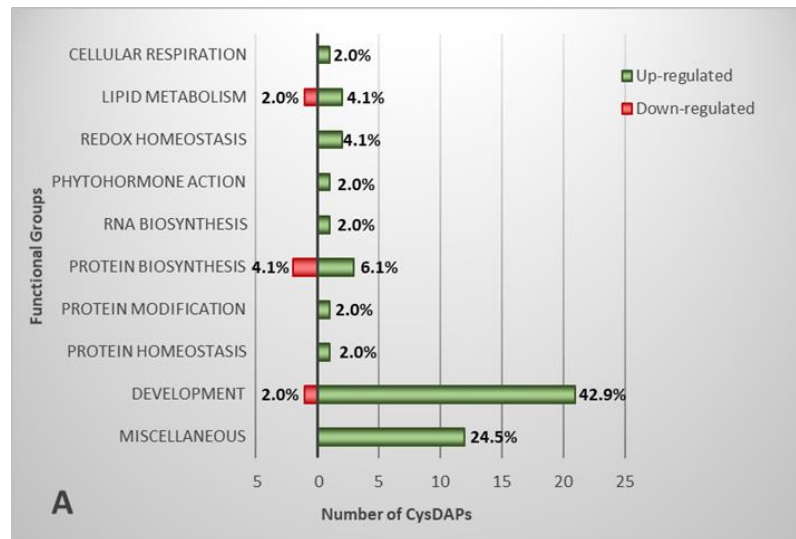


Figure 18A: Functional annotation of unique significant CysDAPs ($-1.5 \geq FC \geq +1.5$, $p < 0.05$) found in FH embryos from seeds treated with DPI, and after the complete reduction of thiol-redox proteins with DTT, in the DPI-DTT category. Red bars show the number of CysDAPs with the down-regulated level of redox-active protein thiols in each major functional group ($FC \leq -1.5$), while green bars show the number of CysDAPs with the up-regulated level of redox-active protein thiols (alteration in protein abundance) in each major functional group ($FC \geq 1.5$) after the treatment with DPI as compared to the control.

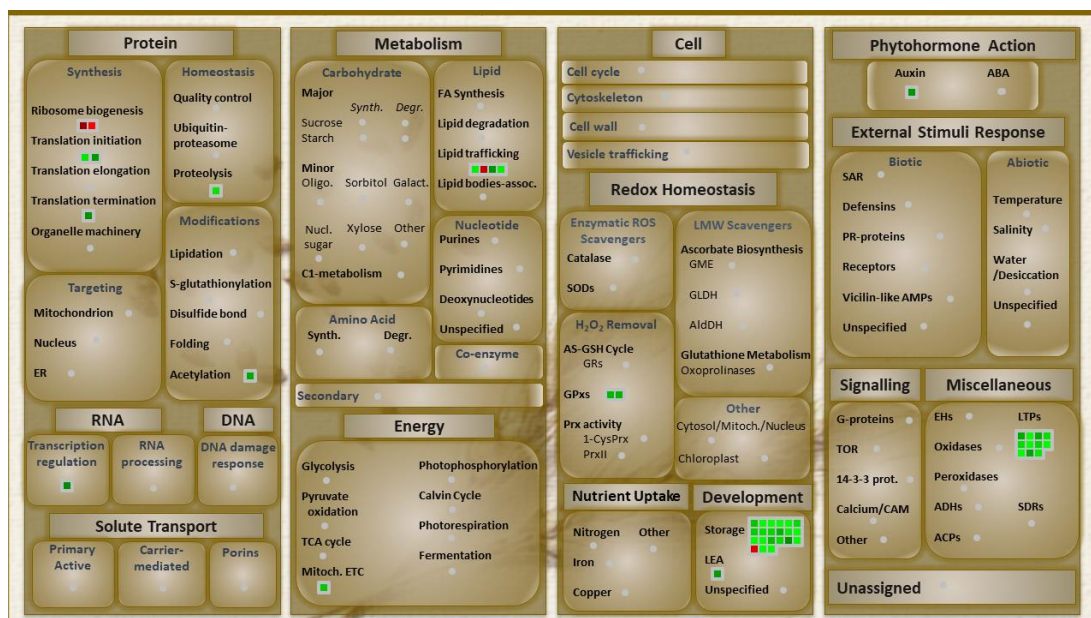


Figure 18B: Mapman visualization of the unique significant CysDAPs and their functional groups found in FH embryos from seeds treated with DPI, and after the complete reduction of thiol-redox proteins with DTT, in the DPI-DTT category. Protein thiol-redox changes (squares) in the corresponding biological pathways are colored according to their log₂ of fold change ratios.

A total of 44.9% CysDAPs belonged to the development FG, including the peptide with sequence TLPTMcNVYVSPDcSTINAPFANIVVGIGGQ from gamma-gliadin protein identified with a higher FC (approximately 4-fold increase in abundance) (Figure 18A). The miscellaneous FG, the second most enriched FG in a number of CysDAPs (24.5% of the total proteins in this category), contained up-regulated proteins such as alpha-amylase inhibitor protein and dimeric alpha-amylase inhibitor (FC>3-fold increase in abundance). Almost all the CysDAPs changed in abundance in development FG were storage proteins, and all the CysDAPs recognized in the miscellaneous FG were nsLTPs (Figure 18B). Cellular respiration, RNA biosynthesis, protein modification, protein homeostasis, and phytohormone action FGs were represented by only one protein (2.1% of the total proteins in this category), up-regulated in abundance. Five CysDAPs from protein biosynthesis FG, three and two CysDAPs from lipid metabolism, and redox homeostasis FGs, respectively, were changing in abundance upon DPI treatment.

3.2.4.2 Unique significant CysDAPs found in AR embryos in DPI- DTT category

Only four unique CysDAPs significantly up-regulated in abundance (FC > +1.5, p < 0.05), which belonged to each FG, carbohydrate metabolism, amino acid metabolism, nucleotide metabolism and development, were detected in AR embryos during DPI treatment as

compared to the control in this category (Supplementary Table S14). Each CysDAP was detected with one redox-active peptide, and altogether, 7 Cys residues were identified. The peptide with sequence LGcSALAQAFDQIGNDcPDIEDVPYLK from formylglycinamide ribonucleotide synthase protein displayed the highest change in abundance, an approximately 3-fold increase in this category.

3.2.4.3 Unique significant CysDAPs found in FH aleurones in DPI- DTT category

Altogether, 27 Cys residues in a total of 12 peptides corresponding to 11 significant unique CysDAPs ($-1.5 > FC > +1.5$, $p < 0.05$) that belonged to 3 major FGs, lipid metabolism FG, miscellaneous FG, and development FG changed in abundance during treatment with DPI as compared to the control in FH aleurones (Supplementary Table S15, Figure 19). Out of 11 CysDAPs, 2 CysDAPs were down-regulated in abundance, while the other nine CysDAPs were up-regulated in abundance. Miscellaneous FG (72.7% of the total CysDAPs in this category) was the most enriched FG detected upon DPI-mediated germination inhibition in FH aleurones, which contained an isoform of alpha-amylase/trypsin inhibitor with multiple unique peptides (2 peptides).

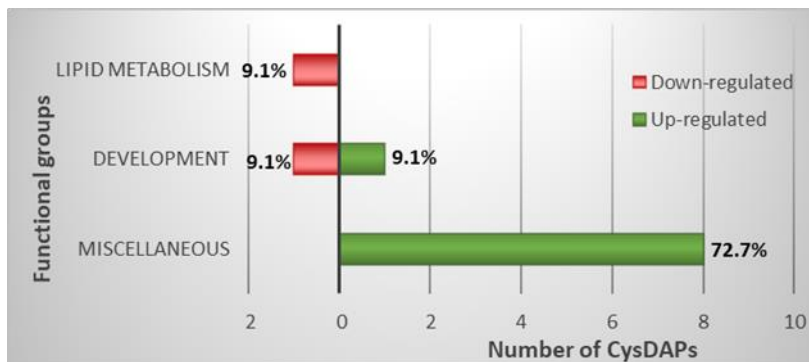


Figure 14: Unique significant CysDAPs found in FH aleurones from seeds treated with DPI, and after the complete reduction of thiol-redox proteins with DTT, in the DPI-DTT category. Functional annotation of unique significant CysDAPs ($-1.5 \geq FC \geq +1.5$, $p < 0.05$). Red bars show the number of CysDAPs with the down-regulated level of redox-active protein thiols in each major functional group ($FC \leq -1.5$), while green bars show the number of CysDAPs with the up-regulated level of redox-active protein thiols (alteration in protein abundance) in each major functional group ($FC \geq 1.5$) after treatment with DPI as compared to the control.

3.2.4.4 Unique significant CysDAPs found in AR aleurones in DPI- DTT category

In AR aleurones, nine unique significant CysDAPs ($-1.5 > FC > +1.5$, $p < 0.05$) belonging to 6 major FGs, with 7 CysDAPs down-regulated and 2 CysDAPs up-regulated in abundance, were identified upon the treatment with DPI, as compared to the control in this category (Supplementary Table S16, Figure 20). Altogether, 20 Cys residues in 9 unique peptides were detected. Besides these Cys residues, gamma-gliadin B in development FG was identified with an oxidized methionine residue. A total of 44.4% CysDAPs in this category belonged to the development FG, including gamma gliadin and gliadin-like avenin storage proteins. No unique multiple peptides were detected in this category.

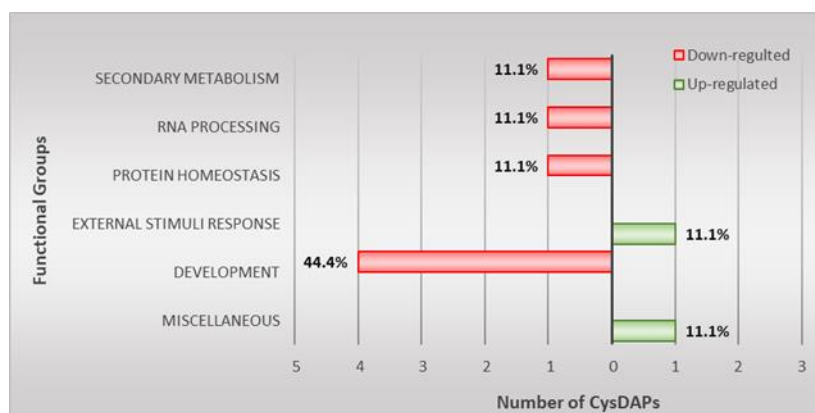


Figure 15: Unique significant CysDAPs found in AR aleurones from seeds treated with DPI, and after the complete reduction of thiol-redox proteins with DTT, in the DPI-DTT category. Functional annotation of unique significant CysDAPs ($-1.5 \geq FC \geq +1.5$, $p < 0.05$). Red bars show the number of CysDAPs with the down-regulated level of redox-active protein thiols in each major functional group ($FC \leq -1.5$), while green bars show the number of CysDAPs with the up-regulated level of redox-active protein thiols (alteration in protein abundance) in each major functional group ($FC \geq 1.5$) after treatment with DPI as compared to the control.

3.2.5 Unique significant CysDAPs found in embryo and aleurone tissues of seeds treated with DPI in the presence of ABA after the reduction of all redox-active protein thiols with DTT, (DPI+ABA)-DTT category

3.2.5.1 Unique significant CysDAPs found in FH embryos in the (DPI+ABA)-DTT category

A total of 194 significant unique CysDAPs ($-1.5 > FC > +1.5$, $p < 0.05$), which belonged to 29 major FGs, were found to change in abundance during treatment with DPI in the presence of ABA as compared to the control in FH embryos (Supplementary table S17, Figure 21A). Among these CysDAPs, 193 proteins were up-regulated, while only one protein, Voltage-gated Anion Channel (VDAC, $FC > 2$) belonging to solute transport FG, was down-regulated in abundance (Figure 21B). Altogether, 277 Cys residues were identified in a total of 212 unique peptides. Multiple unique peptides were recognized in 15 CysDAPs, with the highest of 4 peptides belonging to scaffolding component PP2A-phosphatase protein, cell cycle organization FG. Three unique peptides were detected in eEF2 belonging to translation elongation sub-FG, protein biosynthesis FG. Other 179

CysDAPs were identified with a single unique peptide. Among those, 4 CysDAPs were detected with methionine oxidations and glutamine deamidation.

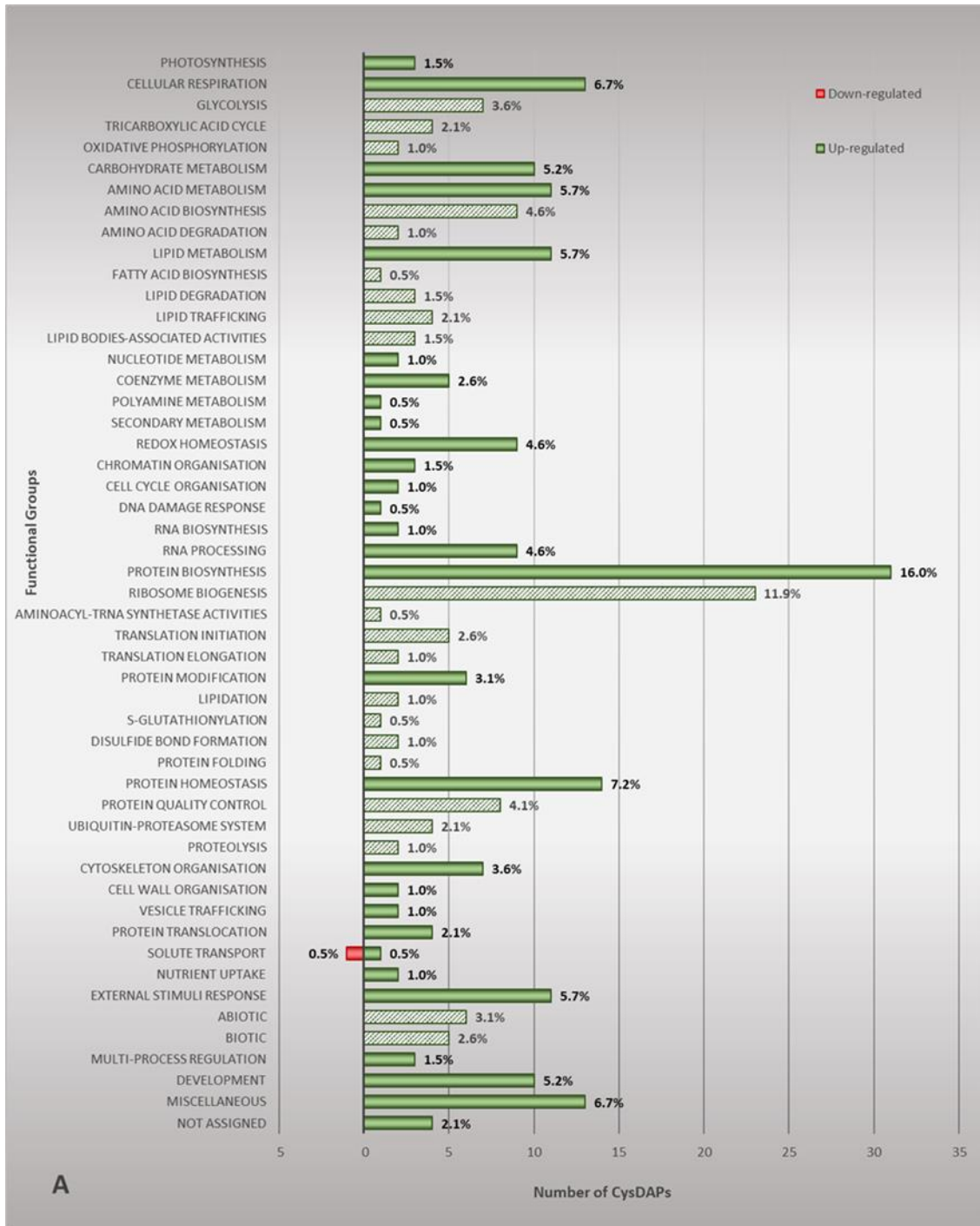


Figure 21A: Functional annotation of unique significant CysDAPs ($-1.5 \geq FC \geq +1.5$, $p < 0.05$) found in FH embryos from seeds treated with DPI in the presence of ABA, and after the complete reduction of thiol-redox proteins with DTT, in (DPI+ABA)-DTT category. Red bars show the number of CysDAPs with the down-regulated level of redox-active protein thiols in each major functional group ($FC \leq -1.5$), whereas green bars show the number of CysDAPs with the up-regulated level of redox-active protein thiols (alteration in protein abundance) in each major functional group ($FC \geq 1.5$) after treatment with DPI in the presence of ABA as compared to the control. Pattern bars (Green) show the number of CysDAPs in the sub-functional group ($FC \geq 1.5$).

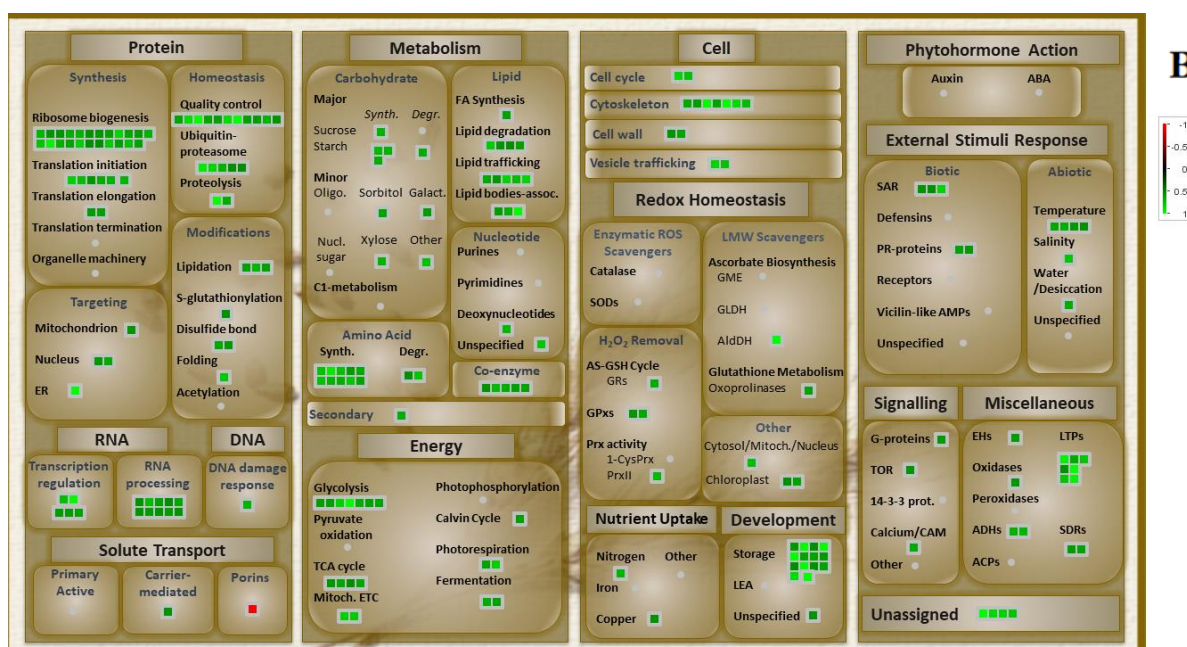


Figure 21B: Mapman visualization of the unique significant CysDAPs and their functional groups found in FH embryos from seeds treated with DPI in the presence of ABA, and after the complete reduction of thiol-redox proteins with DTT, in (DPI+ABA)-DTT category. Protein thiol-redox changes (squares) in the corresponding biological pathways are colored according to their log₂ of fold change ratios.

The peptide with the sequence SQMLWQSScHVMQQQccQQLPR from low-molecular-weight glutenin subunit protein (Development FG) and the peptide with sequence FYNSEFHTASFcLPSFAR from spermidine synthase (polyamine metabolism FG) were

found to be highly up-regulated in abundance with more than 3-fold increase upon the blocking of germination with DPI in the presence of ABA.

Protein biosynthesis FG was the most enriched with CysDAPs, representing 16.0% of the total CysDAPs in this category (Figure 21A). This FG contained proteins up-regulated in abundance belonging to ribosome biogenesis, aminoacyl-tRNA synthetase activities, translation initiation and translation elongation sub-FGs. Protein homeostasis was the second FG most enriched with CysDAPs, which were up-regulated in abundance (7.2% of the total CysDAPs in this category). Cellular respiration, carbohydrate metabolism, amino acid metabolism, lipid metabolism, redox homeostasis, RNA processing, external stimuli response, development, and miscellaneous FGs contained a high number of CysDAPs up-regulated in relative abundance by 6.7%, 5.2%, 5.7%, 5.7%, 4.6%, 4.6%, 5.7%, 5.2% and 6.7% of the total CysDAPs found in this category, respectively. Polyamine metabolism, secondary metabolism, and DNA damage response were represented by only one protein (0.5%) up-regulated in abundance. A high number of CysDAPs that changed in abundance upon germination inhibition by DPI in the presence of ABA treatment were related to ribosome biogenesis, protein quality control, and seed storage protein sub-groups (Figure 21B).

3.2.5.2 Unique significant CysDAPs found in AR embryos in the (DPI+ABA)-DTT category

A total of 6 significant unique CysDAPs containing altogether 8 Cys residues ($-1.5 > FC > +1.5$, $p < 0.05$) assigned to 6 different FGs were identified in AR embryos upon DPI treatment in the presence of ABA as compared to the control (Supplementary Table S18,

Figure 22). Among these, 5 CysDAPs were down-regulated in abundance, while only one CysDAP, chaperone (Hsp60) (protein homeostasis FG), was up-regulated in abundance (1.6-fold increase) during germination inhibition due to DPI treatment combined with ABA. Among these down-regulated CysDAPs, P450s (secondary metabolism FG) with the peptide sequence ALDMTELLGGYASDFVcR and ATP-Binding Cassette (ABC, protein biosynthesis FG) with the peptide sequence LINQVAQEIWVcENQAVTR showed a significant decrease in abundance (over 2-fold change).

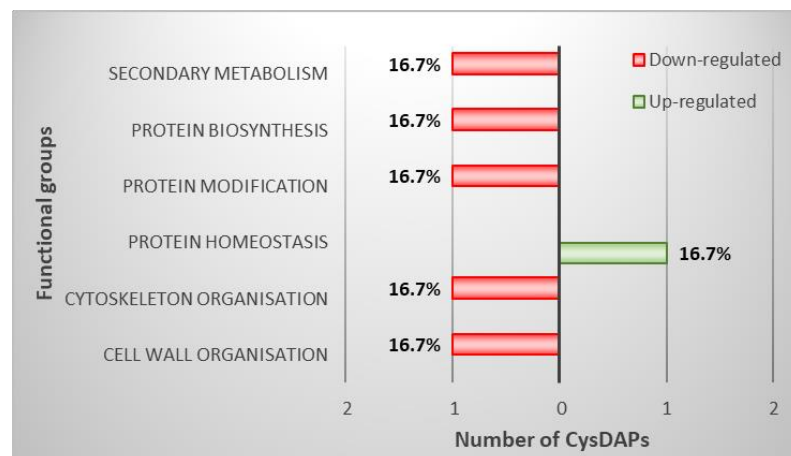


Figure 16: Unique significant CysDAPs found in AR embryos from seeds treated with DPI in the presence of ABA, and after the complete reduction of thiol-redox proteins with DTT, in (DPI+ABA)-DTT category. Functional annotation of unique significant CysDAPs ($-1.5 \geq FC \geq +1.5$, $p < 0.05$). Red bars show the number of CysDAPs with the down-regulated level of redox-active protein thiols in each major functional group ($FC \leq -1.5$), whereas green bars show the number of CysDAPs with the up-regulated level of redox-active protein thiols (alteration in protein abundance) in each major functional group ($FC \geq 1.5$) after treatment with DPI in the presence of ABA as compared to the control.

3.2.5.3 Unique significant CysDAPs found in FH aleurones in the (DPI+ABA)-DTT category

A total of 22 significant unique CysDAPs ($-1.5 > FC > +1.5$, $p < 0.05$) belonging to 8 major FGs were identified in FH aleurones upon the treatment with DPI in the presence of ABA as compared to the control (Supplementary Table S19, Figure 23). Out of 22, five CysDAPs were down-regulated in abundance, while 17 CysDAPs were up-regulated in abundance. Altogether, 35 Cys residues were identified in a total of 22 unique peptides. The development FG was the most enriched FG (36.4% of the total CysDAPs found in this category). It contained up-regulated CysDAPs, including storage proteins alpha/beta-gliadin and gamma-gliadin, with over a 2-fold increase in abundance. Almost all down-regulated CysDAPs showed over 2-fold decrease in abundance in this category and belonged to lipid metabolism, external stimuli response and miscellaneous FGs. Although unique multiple peptides were not detected in this category, methionine oxidations and glutamine deamidation were detected in peptide sequences from isoforms of gamma-gliadin protein and alpha/beta-gliadin A-II that belonged to the development FG.

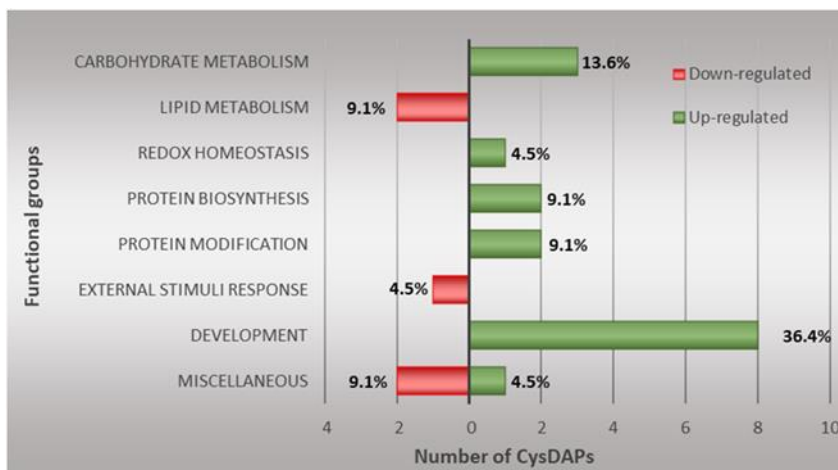


Figure 17: Unique significant CysDAPs found in FH aleurones from seeds treated with DPI in the presence of ABA, and after the complete reduction of thiol-redox proteins with DTT, in (DPI+ABA)-DTT category. Functional annotation of unique significant CysDAPs ($-1.5 \geq FC \geq +1.5$, $p < 0.05$). Red bars show the number of CysDAPs with the down-regulated level of redox-active protein thiols in each major functional group ($FC \leq -1.5$), whereas green bars show the number of CysDAPs with the up-regulated level of redox-active protein thiols (alteration in protein abundance) in each major functional group ($FC \geq 1.5$) after treatment with DPI in the presence of ABA as compared to the control.

3.2.5.4 Unique significant CysDAPs found in AR aleurones in the (DPI+ABA)-DTT category

A total of 19 significant unique CysDAPs ($-1.5 > FC > +1.5$, $p < 0.05$) belonging to 5 major FGs changed in abundance upon the treatment with DPI in the presence of ABA as compared to the control in AR aleurones (Supplementary Table S20, Figure 24). Among these CysDAPs, sucrose synthase (carbohydrate metabolism FG) was the only protein found to be up-regulated in abundance, while the other 18 CysDAPs were down-regulated in abundance during the germination inhibition by DPI in the presence of ABA. Altogether, 42 Cys residues in 21 peptides were identified. Multiple unique peptides were detected in 2 CysDAPs, isoforms of alpha-amylase inhibitor proteins in the miscellaneous FG. Another isoform of alpha-amylase inhibitor protein was detected with glutamine deamidation. The miscellaneous FG was found to have the highest number of CysDAPs (73.7% of the total CysDAPs found in this category) that down-regulated in abundance, including one CysDAP, an isoform of alpha-amylase inhibitor, that displayed a 2-fold decrease in abundance in response to DPI combined with ABA treatment.

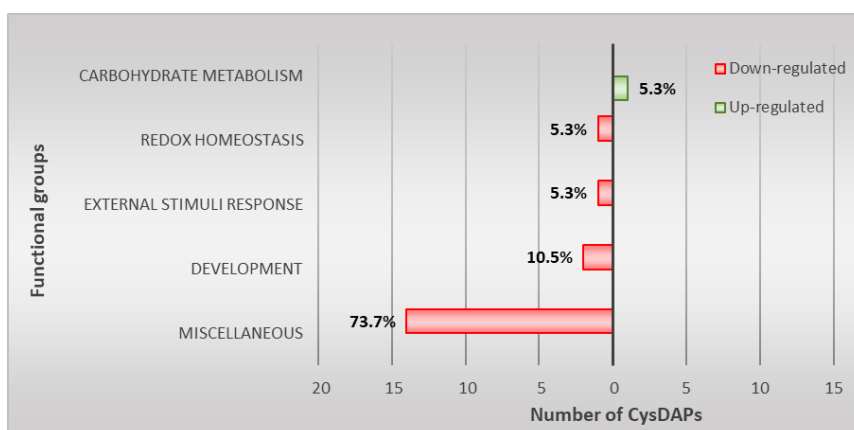


Figure 18: Unique significant CysDAPs found in AR aleurones from seeds treated with DPI in the presence of ABA, and after the complete reduction of thiol-redox proteins with DTT, in (DPI+ABA)-DTT category. Functional annotation of unique significant CysDAPs ($-1.5 \geq FC \geq +1.5$, $p < 0.05$). Red bars show the number of CysDAPs with the down-regulated level of redox-active protein thiols in each major functional group ($FC \leq -1.5$), while green bars show the number of CysDAPs with the up-regulated level of redox-active protein thiols (alteration in protein abundance) in each major functional group ($FC \geq 1.5$) after treatment with DPI in the presence of ABA as compared to the control.

3.2.6 Common CysDAPs found in embryo and aleurone tissues of seeds treated with DPI or DPI in the presence of ABA after the reduction of all redox-active protein thiols with DTT, both DPI-DTT and (DPI+ABA)-DTT categories (Common-DTT)

3.2.6.1 Common CysDAPs found in FH embryos in both DPI-DTT and (DPI+ABA)-DTT categories

A total of 119 unique significantly up-regulated CysDAPs ($FC > +1.5$, $p < 0.05$) belonging to 26 major FGs were identified as common to both DPI and DPI combined with ABA treatments in FH embryos (Supplementary Table S21, Figure 25A). Among these, 5 CysDAPs were detected with unique multiple peptides, whereas platform ATPase

(CDC48) belonging to the ubiquitin-proteasome system sub-FG, protein homeostasis FG, was found to have the highest multiple unique peptide count (3 peptides). Other 114 CysDAPs were detected only with a single peptide, whereas 6 of those had peptides with oxidized methionine and deamidated glutamine residues. Altogether, 178 Cys residues were identified in 125 peptides corresponding to the identified CysDAPs.

The development FG was found to be the most enriched FG, representing 23.5% of the total identified CysDAPs responding to both treatments, DPI and DPI in the presence of ABA. The external stimuli response FG was the second most enriched FG in a number of CysDAPs, representing 10.1% of the total identified CysDAPs in this category. Nucleotide metabolism, photosynthesis, polyamine metabolism, secondary metabolism, chromatin organization, cell cycle organization, DNA damage response, protein modification, cytoskeleton organization, cell wall organization, vesicle trafficking, protein translocation, and solute transport FGs were represented by only one protein (0.8% of the total identified CysDAPs in this category) up-regulated in abundance. A high number of CysDAPs up-regulated in abundance was found for cellular respiration, lipid metabolism, redox homeostasis, RNA processing, protein biosynthesis, protein homeostasis and miscellaneous FGs, represented by 6.7%, 5.9%, 5.0%, 5.0%, 6.7%, 5.9% and 7.6% of the total CysDAPs, respectively (Figure 25A).

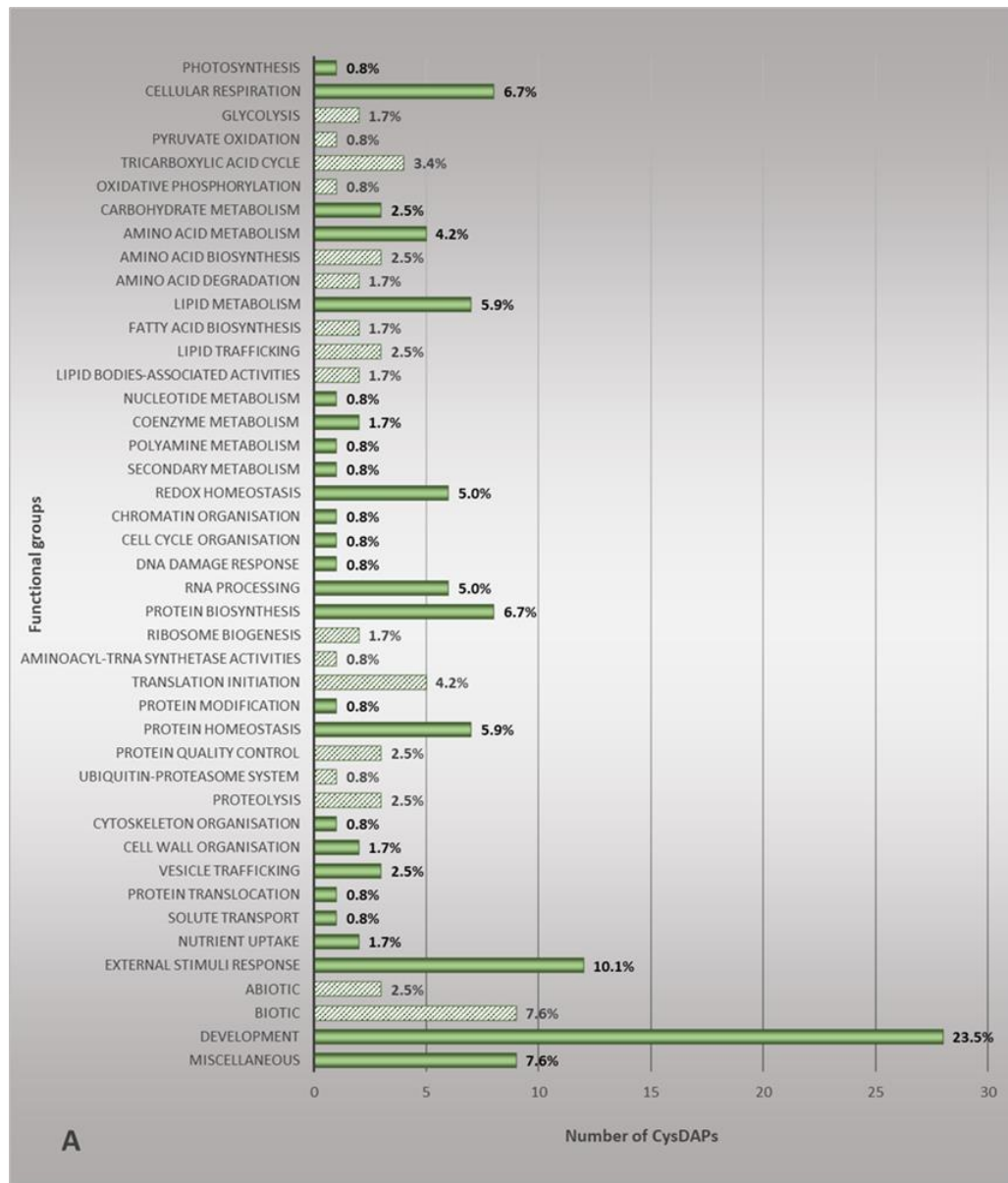


Figure 25A: Functional annotation of common significant CysDAPs ($FC \geq 1.5$, $p < 0.05$) found in FH embryos from seeds treated with either DPI or DPI in the presence of ABA, and after the complete reduction of thiol-redox proteins with DTT, in both DPI-DTT and (DPI+ABA)-DTT categories. Green bars show the number of CysDAPs with the up-regulated level of redox-active protein thiols (alteration in protein abundance) in each major functional group ($FC \geq 1.5$) after treatment as compared to the control. Pattern bars (green) show the number of CysDAPs in the sub-functional group ($FC \geq 1.5$).

The peptide sequence IASGLScPK from PR protein (Purothionin A-II, External stimuli response FG) and the peptide sequence SQVLQQSTYQLLQELccQ from alpha/beta-gliadin protein (development FG) were found to be highly up-regulated in abundance in the range of a 4-fold to 7-fold increase, in both DPI-DTT and (DPI+ABA)-DTT categories. Apart from those peptides, one peptide sequence SQVLQQSTYQLVQQLccQQLWQIPEQSR from alpha-gliadin protein (development FG) was found to be highly up-regulated in abundance only in the DPI-DTT category with approximately 6-fold increase. A number of seed storage (development FG) and nsLTPs (miscellaneous FG) were found to be highly up-regulated in abundance after DPI and DPI in the presence of ABA treatments during the germination inhibition (Figure 25B).

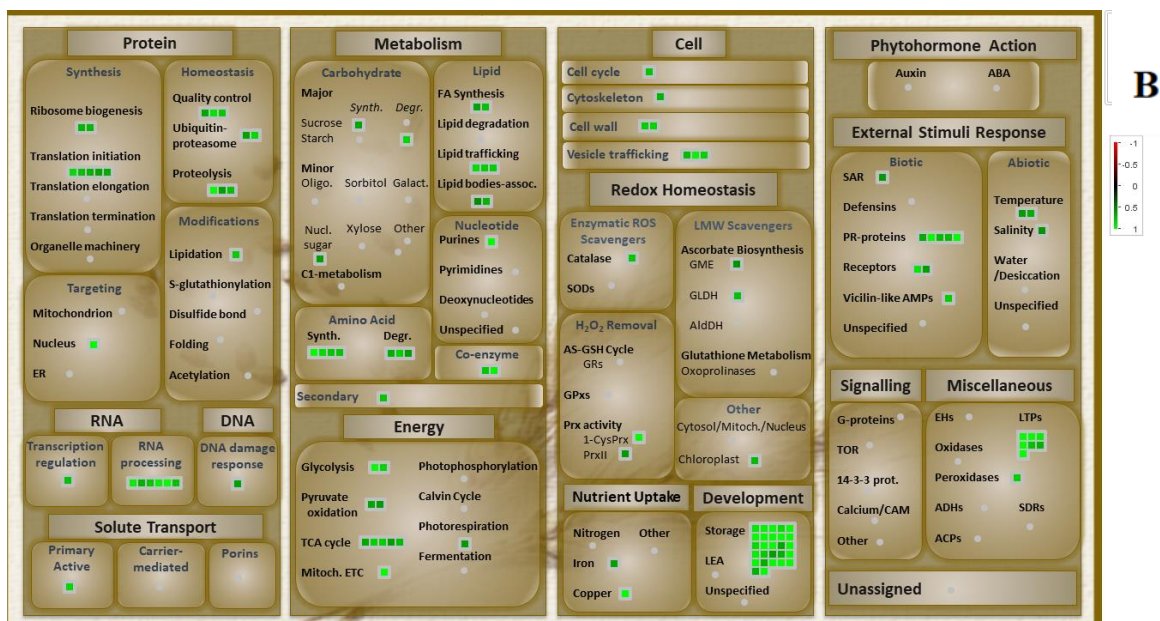


Figure 25B: Mapman visualization of the common significant CysDAPs and their functional groups found in FH embryos from seeds treated with either DPI or DPI in the presence of ABA, and after the complete reduction of thiol-redox proteins with DTT, in both DPI-DTT and (DPI+ABA)-DTT categories. Protein thiol-redox changes (squares) in the corresponding biological pathways are colored according to their log₂ of fold change ratios.

3.2.6.2 Common CysDAPs found in AR embryos in both DPI-DTT and (DPI+ABA)-DTT categories

Upon the germination inhibition by DPI and DPI in the presence of ABA treatments in AR embryos, one peptide with one Cys residue corresponding to 60S acidic ribosomal protein P3, which belonged to the protein biosynthesis FG, was significantly down-regulated with a 1.5-fold decrease ($FC < -1.5$, $p < 0.05$) in both DPI-DTT and (DPI+ABA)-DTT categories (Supplementary Table S22).

3.2.6.3 Common CysDAPs found in FH aleurones in both DPI-DTT and (DPI+ABA)-DTT categories

In FH aleurones, only two significantly up-regulated CysDAPs ($FC > +1.5$, $p < 0.05$), avenin-like b1 and gamma gliadin, both belonging to the development FG, were detected as common to both DPI-DTT and (DPI+ABA)-DTT categories (Supplementary Table S23). Each CysDAP contained a single peptide with multiple Cys residues (A total of 6 Cys residues)

3.2.6.4 Common CysDAPs found in AR aleurones in both DPI-DTT and (DPI+ABA)-DTT categories

In AR aleurones, avenin-like protein s1 (development FG) was the only significantly down-regulated common CysDAP ($FC < -1.5$, $p < 0.05$) identified in these categories with 3 Cys residues in one peptide (Supplementary Table S24). Peptides with the same sequence from the same CysDAP were found with oxidized methionine residues.

3.3 Comparison of the thiol-containing proteins identified in FH and AR wheat kernels in each approach

3.3.1 Comparison of the RMPs in FH and AR wheat kernels identified using the approach I that quantifies oxidative changes in reversible Cys PTMs (IAA and iodoTMT differential alkylation)

In this experimental approach, the total number of RMPs detected in AR wheat kernels was constantly lower compared to the total number of RMPs in FH wheat kernels in both embryo (Figure 26A) and aleurone (Figure 26B) samples in all unique and common DPI-IAA and (DPI in the presence of ABA)-IAA categories. Proteins identified in the DPI-IAA category contained the redox-modified peptides with reversible Cys-PTMs induced by DPI during the germination inhibition.

In embryos of FH wheat kernels in the DPI-IAA category, a total of 124 RMPs that significantly changed in relative abundance ($FC < -1.5$, $p < 0.05$) (Supplementary Tables S1) were identified, while only 3 RMPs significantly changed in relative abundance ($-1.5 > FC > +1.5$, $p < 0.05$) were detected in embryos of AR wheat kernels (Supplementary Tables S2). Altogether, 173 redox-modified Cys sites in 131 peptides were identified in FH embryos, while only five redox-modified Cys sites in 3 peptides were identified in AR embryos during the germination inhibition by the DPI treatment.

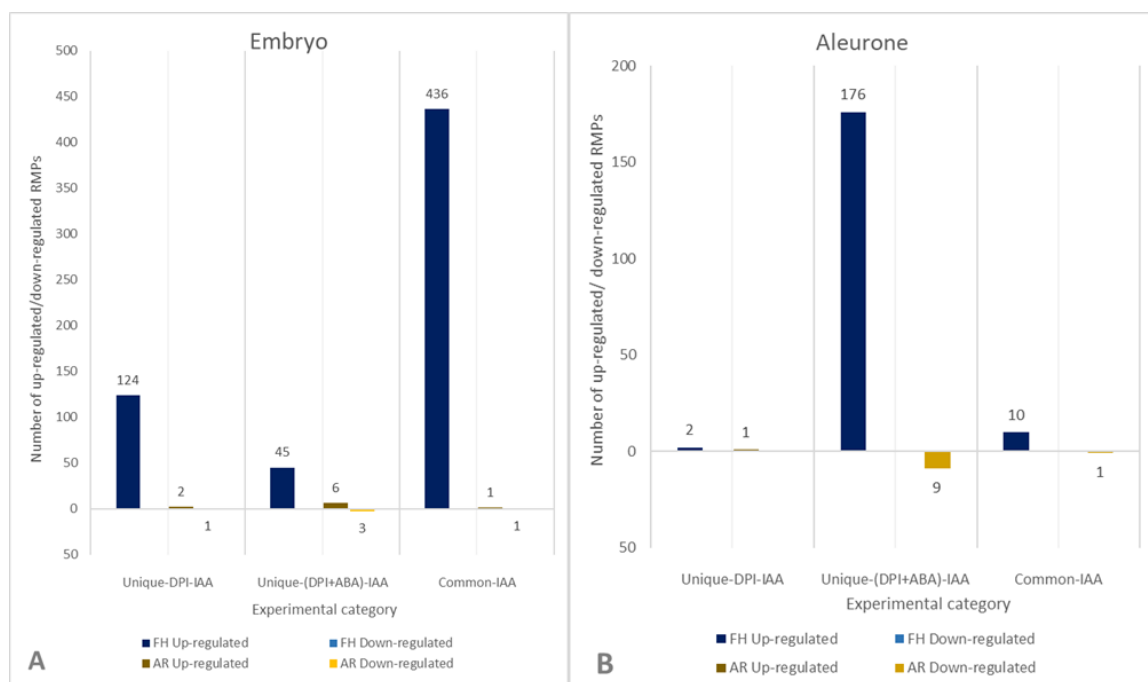


Figure 19: (A) Comparison of the total number of RMPs found in FH and AR embryos in the approach I (IAA category) (B) Comparison of the total number of RMPs found in FH and AR aleurones in the approach I (IAA category). Blue and brown color bars represent the total number of RMPs found in FH and AR seed material, respectively. Unique-DPI-IAA denotes unique RMPs found in the DPI-IAA category. Unique-(DPI+ABA)-IAA denotes unique RMPs found in (DPI+ABA)-IAA category. Common-IAA denotes the common RMPs found in both DPI-IAA and (DPI+ABA)-IAA categories.

All the thiol-responsive peptides from RMPs identified in FH embryos showed up-regulated reduction levels (lower relative oxidation levels) (Figure 26A, Table 4) in the 1.5-fold to 4.0-fold change range. Out of three RMPs identified in AR embryos, 2 RMPs, endochitinase (external stimuli response FG) and gamma-gliadin B protein (development FG), were up-regulated in reduction level, while the other RMP, component beta type-2 of 26S proteasome (protein homeostasis FG) was down-regulated in reduction level (more oxidized) (Figure 26B, Table 4). The RMPs found in AR embryos were related to protein

homeostasis, external stimuli response, and development FGs only. On the other hand, in FH embryos, a high diversification of FGs was observed (Figures 19A and 19B). Among these FGs, protein biosynthesis showed the highest abundance ratio (18.5% of total RMPs identified in the DPI-IAA category) in FH embryos. An isomer of dimeric alpha-amylase inhibitor protein and alpha-gliadin protein were the most significantly changed (down-regulated in labeling and thus the level of oxidation) RMPs found in the DPI-IAA category in FH embryos showing an approximately 4-fold decrease in the oxidation level in response to DPI in the treatment compared to that of the control. However, no common RMPs significantly changing in relative abundance in both FH and AR embryos could be detected (Table 4). The peptides and their Cys modifications found in AR embryos were absent in FH embryos, indicating that the response to the DPI of AR wheat kernels was distinct from that of the FH wheat kernels.

In FH aleurones, two RMPs, 30S ribosomal protein S7 and 40S ribosomal protein S12 belonging to protein biosynthesis FG, were up-regulated in the reduction level ($FC < -1.5$, $p < 0.05$) (Table 4, Figure 26B, Supplementary Tables S3) in response to DPI treatment. In AR aleurones though, only one RMP, N2-acetylornithine aminotransferase belonging to the amino acid metabolism FG, up-regulated in the reduction level ($FC < -1.5$, $p < 0.05$) was identified as responding to the DPI treatment as compared to the control (Table 4, Figure 26B, Supplementary Tables S4). Altogether, two redox-modified Cys sites in 2 unique peptides were identified in FH aleurones, whereas two redox-modified Cys sites in 1 peptide were detected in AR aleurones. However, no common RMPs that were significantly changing in relative abundance in both FH and AR aleurones were identified in this category (Table 4).

Table 4: Number of the unique up- and down-regulated (in the level of the reduced fraction), and common RMPs in FH and AR wheat kernels identified using the approach I (IAA and iodoTMT differential alkylation)

Treatment Category	Embryo				Total common RMPs identified in both FH and AR embryos	Aleurone				Total common RMPs identified in both FH and AR aleurones
	FH		AR			FH		AR		
	Up-regulated	Down-regulated	Up-regulated	Down-regulated		Up-regulated	Down-regulated	Up-regulated	Down-regulated	
DPI-IAA	124	-	2	1	0	2	-	1	-	0
(DPI+ABA)-IAA	45	-	6	3	0	176	-	-	9	4
Common-IAA	436	-	1	1	0	10	-	-	1	0

Cys-PTMs found in unique RMPs of the (DPI+ABA)-IAA category were affected by the ABA phytohormone in the presence of DPI and reversibly redox modified during germination inhibition. Redox peptides from 45 RMPs were significantly up-regulated in the reduction level as compared to the control ($FC < -1.5$, $p < 0.05$) in the range of 1.5-fold to approximately 3-fold change in FH embryos (Table 4, Figure 26A, Supplementary Table S5), while only nine RMPs were found to change in redox levels ($-1.5 > FC > +1.5$, $p < 0.05$) in AR embryos. Among those 9 RMPs, redox peptides from 6 RMPs showed up-regulated reduction levels, whereas redox peptides in 3 RMPs showed down-regulated reduction levels (Table 4, Figure 26A, Supplementary Table S6). In FH embryos, 61 redox-

modified Cys sites in 46 peptides were detected, while in AR embryos, 12 modified Cys sites in 9 peptides were identified upon the germination inhibition by DPI in the presence of ABA treatment. However, no changes in RMPs could be identified in common (overlapping) between FH and AR embryos (Table 4). Three FGs, cellular respiration, lipid metabolism, and protein biosynthesis, displayed the highest number of RMPs (13.3% of total RMPs identified in this category) in FH embryos (Figures 20A and 20B), while secondary metabolism, development and miscellaneous FGs were more enriched with RMPs (22.2% of total RMPs identified in this group) in AR embryos (Figure 13). One of the isomers of gamma-gliadin protein in development FG was highly up-regulated RMP found in FH embryos with approximately a 3-fold increase in the reduction level. P450s protein in secondary metabolism FG was a highly down-regulated protein (approximately a 2.0-fold decrease in the reduction level) detected in AR embryos.

In aleurones, the highest number of RMPs was detected in the unique (DPI+ABA)-IAA category in contrast to the other two categories, unique DPI-IAA and Common-IAA, in both FH and AR samples (Figure 26B). A total of 176 RMPs up-regulated in the reduction level ($FC < -1.5$, $p < 0.05$) in the range of 1.5-fold to approximately 3-fold increase were identified in FH aleurones (Supplementary Table S7), while only nine RMPs down-regulated in the reduction level ($FC > +1.5$, $p < 0.05$) in the range of 1.5-fold to 2.2-fold decrease, were detected in AR aleurones (Supplementary Table S8, Table 4) upon DPI in the presence of ABA treatment. In FH aleurones, 255 redox-modified Cys sites were assigned to 196 peptides, whereas 24 redox-modified Cys sites in 9 peptides were identified in AR aleurones. Miscellaneous FG was the most enriched FG with a high number of RMPs in both FH aleurones (21.6% of the total RMPs identified in this category) (Figure 14A)

and AR aleurones (66.7% of the total RMPs identified in this category) (Figure 15). An isomer of alpha-amylase/trypsin inhibitor (miscellaneous FG) was highly up-regulated RMP (approximately 3-fold increase in the reduction level) found in FH aleurones, whereas avenin-like b1 protein (development FG) was highly down-regulated protein found in AR aleurones (2.2-fold decrease in the reduction level). The peptide with sequence SLVLQTLPSMcNVYVPPEcSIMR from gamma-gliadin protein and the peptides with sequences DccQQLADINNEWcR, LYccQELAEIPQQcR, DccQQLADISEWcR from three isomers of alpha-amylase inhibitors changed in the reduction level in both FH and AR aleurones (Supplementary Table S25, Table 4). These thiol-responsive peptides were up-regulated in the reduction level in the FH aleurones, while down-regulated in the reduction level in AR aleurones, indicating differential redox responses upon seed development and/or aging.

Reversible thiol PTMs in RMPs, common to both DPI-IAA and (DPI+ABA)-IAA treatments in the common-IAA category in embryos and aleurones, were affected by DPI blocking germination and by the induction of general oxidative stress response. A remarkable difference was observed in the number of RMPs detected in FH embryos as compared to AR embryos (Figure 26A), which demonstrates the abundance of redox proteins highly responsive to the general oxidative stress in FH but not in AR embryos. Two RMPs belonging to two FGs, amino acid metabolism and protein homeostasis, were only detected in AR embryos (Supplementary Table S10), while 436 common RMPs significantly up-regulated in the reduction level after treatments as compared to the control ($FC < -1.5$, $p < 0.05$) (Supplementary Table S9) belonging to diverse FGs were identified in FH embryos (Figures 24A and 24B). Among those two RMPs detected in AR embryos,

one RMP, methylthioribulose-1-phosphate dehydratase (amino acid metabolism FG), was up-regulated in the relative quantity of the reduced fraction ($FC < -1.5$, $p < 0.05$), and the other RMP, LON (protein homeostasis FG) was down-regulated in the quantity of the reduced fraction ($FC > +1.5$, $p < 0.05$) (Table 4, Figure 26A). A total of 505 peptides with 621 thiol modification sites increased in the absolute quantity of the reduced fraction, in the range of 1.5-fold to an approximately 15-fold change, in FH embryos, while only 2 peptides with three thiol modifications were identified in AR embryos. Development FG showed the highest protein abundance ratio in FH embryos (13.8% of RMPs identified in this category), which included dramatically up-regulated in the reduction level isomer of gamma-gliadin protein that displayed approximately 15- and 8-fold changes in (DPI+ABA)-IAA and DPI-IAA categories, respectively (Supplementary Table S9). However, the RMPs identified in AR embryos did not significantly change in the redox level in FH embryos (Table 4).

Altogether, ten RMPs up-regulated in the reduction level ($FC < -1.5$, $p < 0.05$) were detected in FH aleurones, while only one RMP down-regulated in the reduction level was identified ($FC > +1.5$, $p < 0.05$) in AR aleurones common to both DPI-IAA and (DPI+ABA)-IAA treatments in the common-IAA category (Figure 26B, Table 3). Altogether, 24 redox-modified Cys sites in 13 peptides were detected in FH aleurones (Supplementary Table S11), while only three redox-modified Cys sites in 1 peptide were identified in AR aleurones (Supplementary Table S12). In FH aleurones, the thiol-responsive peptides from RMPs in the (DPI+ABA)-IAA category changed in the reduction level FC in the range of 1.5-fold to 3.0-fold change. The majority of RMPs in the (DPI+ABA)-IAA category showed a higher increase in the reduction level (up to 3-fold

change) compared to that in the DPI-IAA category, where the thiol-responsive peptides from RMPs increased in the reduction level in the range of 1.5-fold to 1.7-fold. For instance, component RPL11 of LSU proteome protein belonging to protein biosynthesis FG showed an increase of the reduction level up to 3.2-fold in the DPI+ABA-IAA category and 1.7-fold in the DPI-IAA category. However, in AR aleurones, the thiol-responsive peptide from the RMP in (DPI+ABA)-IAA and DPI-IAA categories showed a lower level of decrease in the reduction level, approximately 1.7- and 1.6-fold change, respectively. Miscellaneous FG was the most enriched FG with identified RMPs (60.0% of the total proteins found in this experimental group) in FH aleurones (Figure 17). The RMP identified in AR aleurones, avenin-like protein s1, belonged to the development FG. However, no RMPs were identified in common for both FH and AR aleurones (Table 4).

3.3.2 Comparison of the CysDAPs in FH and AR wheat seeds in approach II that quantifies differential protein abundance changes (DTT reduction and iodoTMT labeling)

In the experimental approach II, the number of proteins with significant changes in abundance in FH embryos and aleurone samples were higher than that in AR embryos and aleurones, and the majority of CysDAPs were found in FH embryos (Figure 27A). However, a prodigious difference was not observed between the number of CysDAPs in FH aleurones versus AR aleurones (Figure 27B).

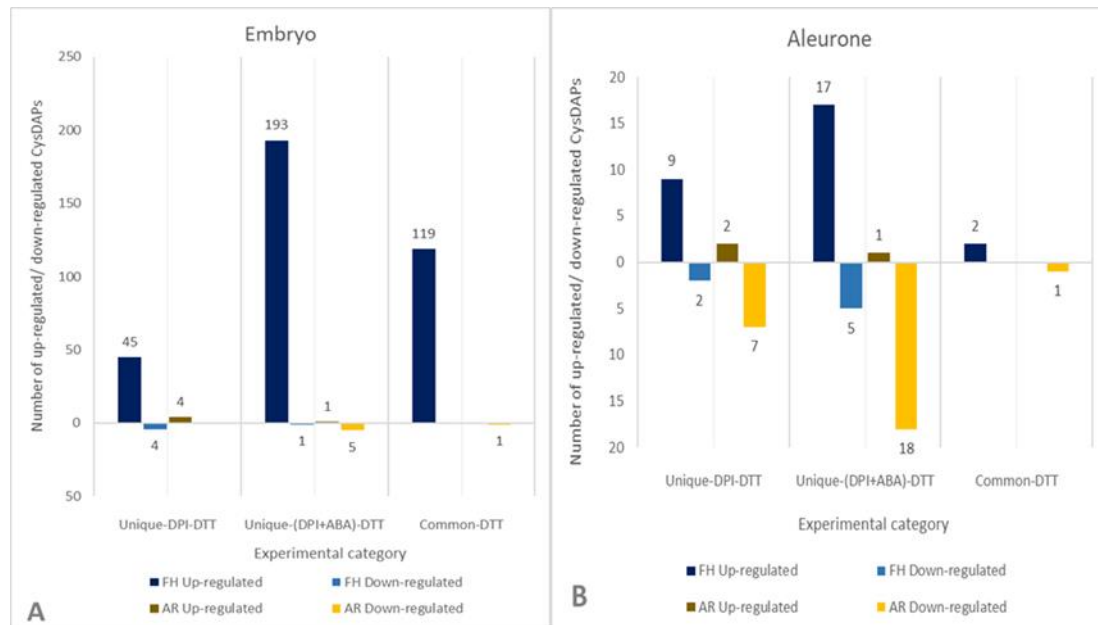


Figure 20: (A) Comparison of the total number of CysDAPs found in FH and AR embryos in approach II (DTT category) (B) Comparison of the total number of CysDAPs found in FH and AR aleurones in approach II (DTT category). Blue and brown color bars represent the total number of CysDAPs found in FH and AR seed material, respectively. Unique-DPI-DTT denotes unique CysDAPs found in the DPI-DTT category. Unique-(DPI+ABA)-DTT denotes unique CysDAPs found in (DPI+ABA)-DTT category. Common-DTT denotes the common CysDAPs found in both DPI-DTT and (DPI+ABA)-DTT categories.

The unique proteins found in the DPI-DTT category displayed the effect of DPI on irreversible Cys-PTMs and the abundance of Cys-containing proteins during germination inhibition in FH and AR wheat seeds. Altogether, 49 CysDAPs (45 up-regulated CysDAPs and 4 down-regulated CysDAPs) were changed in abundance ($-1.5 > FC > +1.5$, $p < 0.05$) in FH embryos, while only 4 CysDAPs changed in abundance ($FC > +1.5$, $p < 0.05$) in the AR embryos during the germination inhibition by DPI (Figure 27A). A total of 45 CysDAPs increased in abundance (up-regulated CysDAPs), and a total of 4 CysDAPs decreased in abundance (down-regulated CysDAPs) in the FH embryos upon the DPI

treatment (Table 5). The fold change of the CysDAPs up-regulated in abundance ranged between 1.5- to approximately 4-fold, and down-regulated in abundance ranged between 1.5- to 2-fold in FH embryos in the DPI-DTT category (Supplementary Table S13). All four CysDAPs identified in the AR embryos were up-regulated in abundance, and the FC ranged between 1.5-fold to approximately 3-fold (Supplementary Table 14). No CysDAPs changed in abundance in both FH and AR embryos (Table 5). CysDAPs identified in the DPI-DTT category in FH embryos were assigned to 10 major FGs, and the development FG was the most enriched FG (44.9% of the total CysDAPs in this category) (Figure 18A), including highly up-regulated storage proteins, gamma-gliadin and alpha-amylase inhibitor protein (Figure 18B), with approximately 4.0-fold increase. However, CysDAPs identified in AR embryos belonged to 4 major FGs, and storage proteins were not significantly changing in abundance. Only one Late Embryogenesis Abundant protein (LEA protein) was significantly up-regulated with an approximately 2.0-fold increase in abundance. Formylglycinamide RN synthase was the highly enriched CysDAP found to be increased in abundance in AR embryos with an approximately 3.0-fold increase.

In aleurones, 11 CysDAPs ($-1.5 > FC > +1.5$, $p < 0.05$) were identified in FH aleurones, while 9 CysDAPs ($-1.5 > FC > +1.5$, $p < 0.05$) were identified in AR aleurones in the DPI-DTT category. Among these 11 CysDAPs, nine CysDAPs were up-regulated in abundance, and two were down-regulated in abundance in FH aleurones, whereas 2 CysDAPs were up-regulated in abundance and 7 CysDAPs were down-regulated in abundance in AR aleurones during the germination inhibition by DPI (Figure 27B, Table 5). Thus, the majority of CysDAPs detected in FH aleurones increased in abundance, whereas most CysDAPs detected in AR aleurones decreased in abundance. All these identified CysDAPs

in both FH (Supplementary Table S15) and AR aleurones (Supplementary Table S16) changed in abundance in the range of 1.5-fold to 2-fold change, and there were no common CysDAPs enriched in both FH and AR aleurones in response to the DPI treatment (Table 5). In FH aleurones, most of the CysDAPs belonged to miscellaneous FG (72.7% of the total CysDAPs in this category) (Figure 19), while development FG was the most enriched FG (44.4% of the total CysDAPs in this category) in AR aleurones (Figure 20) in response to the DPI treatment.

Table 5: Number of unique up- and down-regulated (in the level of the reduced fraction), and common CysDAPs in FH and AR wheat kernels identified using the approach II (complete DTT reduction and iodoTMT labeling)

Treatment Category	Embryo				Total common CysDAPs identified in both FH and AR embryos	Aleurone				Total common CysDAPs identified in both FH and AR aleurones
	FH		AR			FH		AR		
	Up-regulated	Down-regulated	Up-regulated	Down-regulated		Up-regulated	Down-regulated	Up-regulated	Down-regulated	
DPI-DTT	45	4	4	-	0	9	2	2	7	0
(DPI+ABA)-DTT	193	1	1	5	1	17	5	1	18	3
Common-DTT	119	-	-	1	0	2	-	-	1	0

CysDAPs found in (DPI+ABA)-DTT category were affected by the treatment with external ABA phytohormone in the presence of DPI. A noticeable difference was observed in the total CysDAPs identified in the (DPI+ABA)-DTT category in FH embryos versus AR embryos. A total of 194 CysDAPs changed in abundance ($-1.5 > FC > +1.5$, $p < 0.05$) in FH embryos, while only 6 CysDAPs changed ($-1.5 > FC > +1.5$, $p < 0.05$) in AR embryos. Only one CysDAP identified in FH embryos decreased in abundance (down-regulated, 2-fold decrease), while all other 193 CysDAPs increased in abundance (up-regulated) (Figure 27A, Table 5) within the FC range of 1.5-fold to approximately 4-fold (Supplementary Table S17). Nevertheless, the majority of CysDAPs decreased in abundance in the range of 1.5-fold to 2.3-fold in AR embryos upon treatment with DPI in the presence of ABA (Supplementary Table S18). Only one CysDAP was up-regulated in abundance with a 1.6-fold increase, while the other 5 CysDAPs were down-regulated in abundance in AR embryos (Figure 27A, Table 5). CysDAPs identified in FH embryos in this category belonged to 29 major FGs (Figure 21A). The most enriched FG was the protein biosynthesis FG, with 16.0% of the total CysDAPs identified in FH embryos in response to germination inhibition by DPI in the presence of ABA. Low-molecular-weight glutenin subunit protein in development FG was highly up-regulated in abundance (approximately 4-fold increase) within the category in FH embryos (Figure 21B). In contrast, CysDAPs belonging to only six major FGs were enriched in AR embryos (Figure 22). Among the prominent CysDAPs, ABC protein in protein biosynthesis FG displayed the largest fold change and decreased in abundance (by 2.3-fold) due to the germination inhibition by DPI in the presence of ABA in AR embryos. The peptide with sequence TQNVSAcQAVANIVK from the CCT1 subunit alpha of CCT chaperonin folding

complex showed changes in abundance in both FH and AR embryos in response to the DPI in the presence of ABA (Table 5, Supplementary Table S26). However, this protein was increased in abundance in FH embryos, while it was decreased in abundance in AR embryos.

A total of 22 CysDAPs and 19 CysDAPs changed in abundance in FH and AR aleurones, respectively ($-1.5 > FC > +1.5$, $p < 0.05$), upon the DPI in the presence of ABA treatment. CysDAPs that were up- and down-regulated in abundance were detected in both FH and AR aleurones (Figure 27B). A total of 17 CysDAPs were up-regulated in abundance, and five were down-regulated in abundance in FH aleurones, whereas one CysDAP was up-regulated and 18 CysDAPs were down-regulated in abundance in AR aleurones during the germination inhibition by DPI in the presence of ABA (Table 5). Thus, the majority of CysDAPs detected in FH aleurones increased in abundance, whereas almost all CysDAPs detected in AR aleurones decreased in abundance. The up-regulated and down-regulated CysDAPs in FH aleurones increased and decreased in abundance, respectively, in the range of 1.5-fold to 2.5-fold FC (Supplementary Table 19). In contrast, down-regulated CysDAPs in AR aleurones decreased in abundance in the range of 1.5- to 2.0-fold change (Supplementary Table 20). The enriched CysDAPs in FH (Figure 23) and AR (Figure 24) aleurones belonged to 8 and 5 major FGs, respectively. Development FG (36.4% of total CysDAPs identified in this category) and miscellaneous FG (73.7% of total CysDAPs identified in this category) comprised the highest number of CysDAPs that changed in abundance in FH and AR aleurones, respectively. Three CysDAPs displayed changes in abundance in both FH and AR aleurones (Table 5). The same peptide with sequence LQELVNLVVVcGDHGK from sucrose synthase in carbohydrate metabolism FG was up-

regulated in abundance in both FH and AR aleurones. However, in the other two CysDAPs, different unique peptide sequences were redox responding in either FH or AR aleurones. In CysDAPs from the miscellaneous FG, dimeric alpha-amylase inhibitor peptides with sequences EccQQLADISEWcR and EHGvQEGQAGTGAFPScR were down-regulated in abundance in both FH and AR aleurones, respectively, while in the isomer of alpha-amylase inhibitor protein peptides with sequence LQcVGSQVPEAVLR and DccQQLADINNEWcR were up-regulated in abundance in FH aleurones and down-regulated in AR aleurones, respectively (Supplementary Table S26).

CysDAPs identified as common to both DPI-DTT and (DPI+ABA)-DTT in the common-DTT category were affected by DPI and by the induction of general oxidative stress response that resulted in irreversible protein oxidation and changes in protein abundance that blocked seed germination. A conspicuous difference in the number of CysDAPs in FH versus AR embryo samples was observed in the common-DTT category. A total of 119 CysDAPs up-regulated in abundance ($FC > +1.5$, $p < 0.05$) were identified in FH embryos, while only one CysDAPs down-regulated in abundance ($FC < -1.5$, $p < 0.05$) was detected in AR embryos (Figure 27A). CysDAPs in FH embryos up-regulated in abundance in the range from 1.5-fold to 7.3-fold increase and 1.5-fold to 6.6-fold increase upon the treatment with DPI in the presence of ABA and DPI alone, respectively (Supplementary Table S21). The CysDAP common to both DPI-DTT and (DPI+ABA)-DTT categories in AR embryos displayed a 1.5-fold decrease upon the treatment with DPI alone and DPI in the presence of ABA (Supplementary Table S22). However, there were no CysDAPs common in both FH and AR embryos in this category (Table 5). CysDAPs enriched in FH embryos in this category belonged to 29 major FGs (Figure 25A). The majority of CysDAPs enriched in

FH embryos that were common to both DPI-DTT and (DPI+ABA)-DTT categories belonged to development FG (23.5% of total CysDAPs identified in this category) (Figure 25B), which included alpha/beta-gliadin protein highly up-regulated in abundance with 7.3-fold and 6.6-fold increase in (DPI+ABA)-DTT and DPI-DTT categories, respectively. The only CysDAP identified in the AR embryos that were common to both (DPI+ABA)-DTT and DPI-DTT categories belonged to protein biosynthesis FG.

Altogether, two CysDAPs up-regulated in abundance ($FC > +1.5$, $p < 0.05$) were identified in FH aleurones, while one CysDAP down-regulated in abundance ($FC < -1.5$, $p < 0.05$) was identified in AR aleurones (Figure 27B, Table 5) after both DPI alone and DPI in the presence of ABA treatments. These CysDAPs, detected in FH (Supplementary Table 23) and AR (Supplementary Table 24) aleurones, belonged to the development FG. An isomer of avenin-like protein was found to have redox peptides up-regulated in FH aleurones, but down-regulated in AR aleurones upon treatments with DPI alone and DPI in the presence of ABA. However, no CysDAPs with similar thiol-responsive peptide sequences were identified as common to both FH and AR aleurones (Table 5).

3.4 Comparison of the thiol-containing proteins identified from the approach I and II in FH and AR wheat kernels

3.4.1 Comparison of the thiol-containing proteins identified from approaches I and II in FH and AR embryos

3.4.1.1 Comparison of the thiol-containing proteins identified from approaches I and II in FH embryos

In FH embryos, we identified a total of 131 unique peptides corresponding to 124 unique RMPs that were significantly up-regulated in relative abundance (more reduced) after DPI treatment as compared to the water control ($FC < -1.5$, $p < 0.05$) in the DPI-IAA category (Figure 28A, Supplementary Tables S1). These RMPs were functionally assigned into 26 major FGs (Figure 11A). However, only 50 thiol-responsive peptides corresponding to 49 significant unique CysDAPs ($-1.5 > FC > +1.5$, $p < 0.05$), which belonged to 10 major FGs, changed in abundance during treatment with DPI as compared to the control in DPI-DTT category (Supplementary Tables S13). Altogether, 44 CysDAPs were up-regulated in abundance, while only 4 CysDAPs were down-regulated in abundance (Figure 28A). Proteins belonging to the protein biosynthesis FG contained the highest number of RMPs (Figure 11B), with 18.5% of the total RMPs identified in the DPI-IAA category, including RMPs strongly related to the ribosome biogenesis sub-FG (12.9%). Nevertheless, the development FG displayed a higher amount of Cys-containing proteins (Figure 18B) that change in abundance (44.9% of the total CysDAPs in the DPI-DTT category) (Figure 18A). Altogether, five proteins with identical Cys-containing peptides that changed in both the redox and protein abundance levels were found in FH embryos (Table 6). The peptide with

sequence YKDQGFELAFPcNQFGGQEPGTNEEIVQFAcTR from GPX enzyme (redox homeostasis FG), the peptide with sequence DTQDLLVEccVEFINLLSSESNDVcSR from nuclear transcription factor Y protein (RNA biosynthesis FG), the peptides with sequences TLPTMcSVNVPVYGTTTIVPFGVGTR and TLPTmcNVNVPLYETTTSVPL from low-molecular-weight glutenin subunit (development FG) were up-regulated in both the reduction and protein abundance levels in FH embryos. The peptide with sequence STLAGHGGYVNAVAVSPDGSLcASGGK from associated component RACK1 of SSU proteome (protein biosynthesis FG) was found to be up-regulated in the reduction level but down-regulated in protein abundance during the germination inhibition by DPI in FH embryos (Supplementary Table S27). Two isomers of GPX were enriched in both DPI-IAA and DPI-DTT categories with identical Cys sites and peptide sequences, with or without missed cleavage for one of the peptides. Other 118 RMPs from the DPI-IAA category and 43 CysDAPs identified in the DPI-DTT category changed in response to the DPI treatment either in the thiol-redox level or in protein abundance, respectively. The peptide with sequence DccQQLADINNEWcR from dimeric alpha-amylase inhibitor (miscellaneous FG) and the peptide with sequence IPIcDISFNLK from alpha-gliadin GLI2-LM2-17 (development FG) proteins were the most significantly changing (down-regulating in the iodoTMT labeling, thus in the level of oxidation) RMPs found only in DPI-IAA category, and showing an approximately 4-fold decrease in the oxidation level compared to that of the control. The peptide with sequence TLPTMcNVYVSPDcSTINAPFANIVVGIGGQ from gamma-gliadin protein (development FG) was highly enriched CysDAP identified only in the DPI-DTT category, and it increased in abundance with approximately 4-fold change.

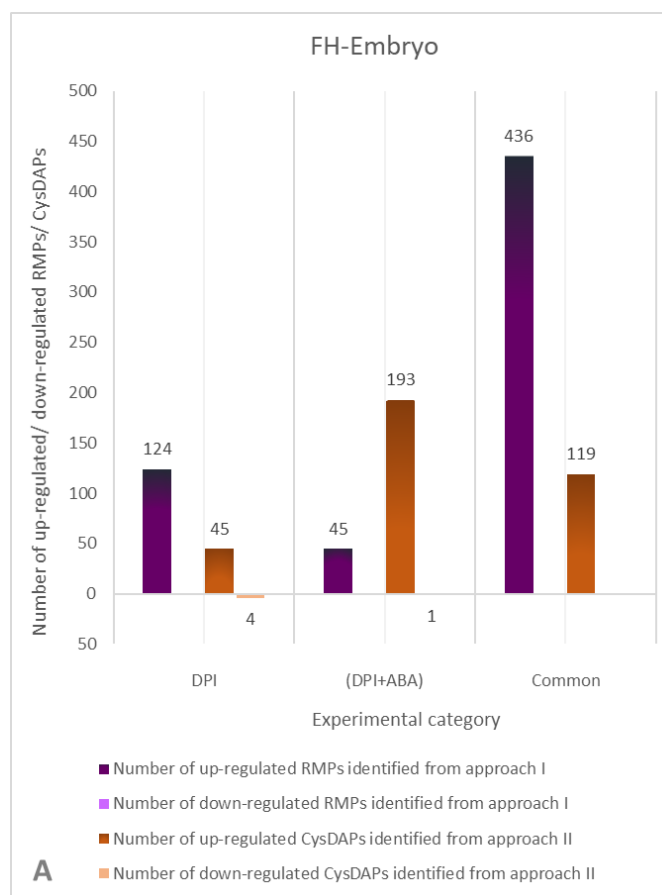


Figure 28A: Comparison of the thiol-containing proteins identified from the approach I (IAA category) and II (DTT category) in FH embryos. Purple and orange color bars represent the total number of RMPs and CysDAPs found in FH/AR embryos, respectively. DPI denotes unique thiol-containing proteins found in the DPI-IAA and DPI-DTT categories in FH/AR embryos. (DPI+ABA) denotes unique thiol-containing proteins found in (DPI+ABA)-IAA and (DPI+ABA)-DTT categories in FH/AR embryos. Common denotes the common thiol-containing proteins found in both common-IAA and common-DTT categories in FH/AR embryos.

In FH embryos treated with DPI in the presence of ABA, 46 active thiol-containing peptides (Supplementary Tables S5) corresponding to a total of 45 RMPs (Figure 28A) that were assigned to 16 major FGs (Figure 12A) changed significantly ($FC < -1.5$, $p < 0.05$) in the level of reduced thiols in (DPI+ABA)-IAA category. A total of 212 unique Cys-

containing peptides (Supplementary Tables S17) from 194 significant unique CysDAPs ($-1.5 > FC > +1.5$, $p < 0.05$) belonging to 29 major FGs (Figure 21A) changed in abundance in (DPI+ABA)-DTT category as compared to the water control. All RMPs identified in the (DPI+ABA)-IAA category were up-regulated in the reduction level. Except for one CysDAP, which was down-regulated in abundance, all other CysDAPs identified in the (DPI+ABA)-DTT category were increased in abundance in response to the ABA phytohormone in the presence of DPI (Figure 28A). Three FGs, cellular respiration, lipid metabolism and protein biosynthesis, were found to have the highest number of proteins that changed in the reduction level (Figure 12B) with 13.3% of total RMPs identified in (DPI+ABA)-IAA category, whereas protein biosynthesis FG was the most enriched in a number of CysDAPs (Figure 21B), with 16.0% of total CysDAPs identified in (DPI+ABA)-DTT category. Altogether, 29 proteins changed only in the redox level, 178 proteins were found to be changing only at the level of protein abundance, and 16 proteins were identified with changes in both the redox level and protein abundance during the germination inhibition by DPI in the presence of ABA in FH embryos (Table 6). Among these 16 proteins that were identified as common to both (DPI+ABA)-IAA and (DPI+ABA)-DTT categories, 14 proteins had identical thiol-responsive peptide sequences, while two proteins consisted of unique peptide sequences (Supplementary Table S27). NADH-ubiquinone oxidoreductase subunit (cellular respiration FG), aldose reductase (carbohydrate metabolism FG), phosphoglycerate dehydrogenase and fumarylacetoacetate hydrolase (FAH, amino acid metabolism FG), lipid-transfer proteins (2 proteins) and steroleosin dehydrogenase (lipid metabolism FG), oxoprolinase (redox homeostasis FG), 60S ribosomal protein L22 and component eIF3b of eIF3 mRNA-to-PIC binding complex

(protein biosynthesis FG), beta 1,3 glucan hydrolases and protein folding catalyst (cyclophilin) (protein modification FG), CCT7 subunit eta of CCT chaperonin folding complex (cytoskeleton organization FG), one PR protein and dirigent (DIR) (external stimuli response FG) are the proteins that were identified in both (DPI+ABA)-IAA and (DPI+ABA)-DTT categories upon germination inhibition by the phytohormone in the presence of DPI in FH embryos.

In FH embryos, a total of 505 redox-active peptides (Supplementary Table S9) corresponding to 436 RMPs (Figure 28A) that significantly changed in the level of reduced fraction ($FC < -1.5$, $p < 0.05$) and belonged to 30 major FGs, were identified as common to both DPI-IAA and (DPI+ABA)-IAA treatments (Figure 16A). A total of 125 thiol-responsive peptides (Supplementary Table S21) corresponding to 119 CysDAPs (Figure 28A) that significantly changed in abundance ($FC > +1.5$, $p < 0.05$) and belonged to 26 major FGs (Figure 25A), were identified as common to both DPI-DTT and (DPI+ABA)-DTT treatments. All RMPs identified in the common-IAA category were up-regulated in the reduction level. All CysDAPs assigned to the common-DTT category were up-regulated in abundance during the germination inhibition by DPI and DPI in the presence of ABA treatments. Among the proteins identified in both common-IAA and common-DTT categories, 99 thiol-containing peptides corresponding to a total of 95 proteins were changing in the redox level as well as in protein abundance in response to the inhibition of germination by DPI (Table 6). Among these proteins, three proteins, large subunit of carbamoyl phosphate synthetase heterodimer (amino acid metabolism FG), spermidine synthase (polyamine metabolism FG) and A1-class protease (pepsin) (protein homeostasis FG), were identified with unique peptide sequences, whereas other 92 proteins were

identified with identical peptide sequences in both common-IAA and common-DTT categories (Supplementary Table S27). Altogether, four proteins, aconitase (cellular respiration FG), platform ATPase (protein homeostasis FG), a PR protein (external stimuli response FG), and dimeric alpha-amylase inhibitor (miscellaneous FG), were found with multiple peptide sequences that changed in both the redox level and protein abundance. A total of 341 RMPs changed only in the reduction level, and 24 CysDAPs were found to be differentially abundant only in FH embryos (Table 6). Thus, the majority of peptides that increased in abundance increased in the redox level in FH embryos in response to the DPI-mediated inhibition of germination.

3.4.1.2 Comparison of the thiol-containing proteins identified from approaches I and II in AR embryos

In AR embryos, only three unique RMPs (two up-regulated RMPs and one down-regulated RMP, Figure 28B) with three Cys-labeled peptides that significantly changed in the reduction level ($-1.5 > FC > +1.5$, $p < 0.05$) were identified in the DPI-IAA category, compared to that of the water control (Supplementary Tables S2). On the other hand, only four unique thiol-responsive peptides corresponding to four CysDAPs (Figure 28B) that significantly changed in abundance ($FC > +1.5$, $p < 0.05$) were detected in the DPI-DTT category compared to that of the water control (Supplementary Tables S14) in AR embryos in response to the DPI treatment. Redox-modified proteins enriched in the DPI-IAA category belonged to 3 FGs: protein homeostasis, external stimuli response, and development. In comparison, proteins that changed in abundance in the DPI-DTT category in AR embryos belonged to 4 FGs: carbohydrate metabolism, amino acid metabolism,

nucleotide metabolism, and development. However, no proteins were identified as common to both DPI-IAA and DPI-DTT categories (Table 6); thus, proteins identified in AR embryos either changed in the redox level or the protein abundance during the germination inhibition by DPI.

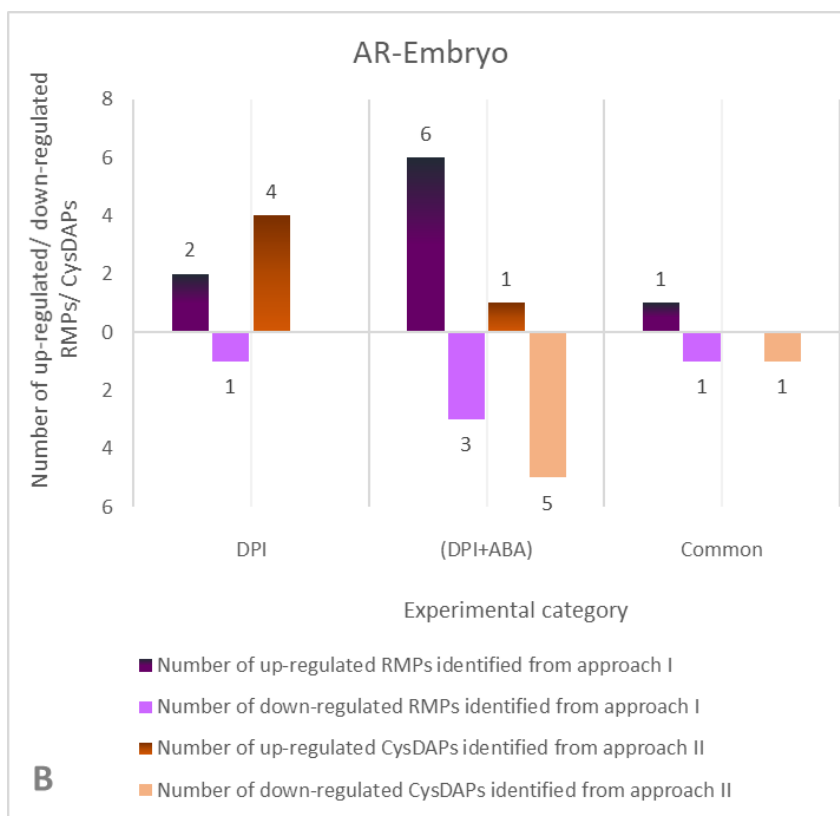


Figure 28B: Comparison of the thiol-containing proteins identified from the approach I (IAA category) and II (DTT category) in AR embryos. Purple and orange color bars represent the total number of RMPs and CysDAPs found in FH/AR embryos, respectively. DPI denotes unique thiol-containing proteins found in the DPI-IAA and DPI-DTT categories in FH/AR embryos. (DPI+ABA) denotes unique thiol-containing proteins found in (DPI+ABA)-IAA and (DPI+ABA)-DTT categories in FH/AR embryos. Common denotes the common thiol-containing proteins found in both common-IAA and common-DTT categories in FH/AR embryos.

Table 6: Number of thiol-containing proteins identified in approaches I and II that changed in the redox level only, protein abundance only and in both redox and abundance levels in FH and AR embryos

Number of thiol-containing proteins Treatments	FH embryos			AR embryos		
	Change in the redox level and abundance	Change in the redox level only	Change in protein abundance only	Change in the redox level and abundance	Change in the redox level only	Change in protein abundance only
DPI	6	118	43	0	3	4
DPI in the presence of ABA	16	29	178	1	8	5
Common to both DPI and DPI in the presence of ABA	95	341	24	0	2	1

In response to the DPI in the presence of ABA treatment in AR embryos, nine peptides (Supplementary Tables S6) corresponding to nine significant RMPs ($-1.5 > FC > +1.5$, $p < 0.05$) (six up-regulated RMPs and 3 down-regulated RMPs, Figure 28B) that belonged to 6 FGs (Figure 13) were found to be changing in the redox levels. A total of 6 thiol-responsive peptides (Supplementary Tables S18) corresponding to six significant unique CysDAPs ($-1.5 > FC > +1.5$, $p < 0.05$) (one up-regulated CysDAP and 5 down-regulated CysDAPs, Figure 28B), and belonging to 6 FGs (Figure 22) changed in protein abundance.

Among these identified peptides in AR embryos, the peptide with sequence ALDMTELLGGYASDFVcR from P450s (secondary metabolism FG) changed in both redox level (down-regulated in the reduction level) and protein abundance (decreased in abundance) upon the DPI in the presence of ABA treatment (Table 6, Supplementary Table S27).

Upon the germination inhibition by DPI and DPI in the presence of ABA treatments in AR embryos, only one RMP, methylthioribulose-1-phosphate dehydratase (amino acid metabolism FG) with one unique redox-modified peptide, that was significantly up-regulated in the quantity of the reduced fraction ($FC < -1.5$, $p < 0.05$), and one RMP, LON (protein homeostasis FG) with one unique redox modified peptide that was significantly down-regulated in the quantity of the reduced fraction ($FC > +1.5$, $p < 0.05$), were detected as common in both (DPI+ABA)-IAA and DPI-IAA categories (Supplementary Tables S10). Altogether, two peptides corresponding to two proteins changed in the redox level (one up-regulated RMP and one down-regulated RMP, Figure 28B), whereas one peptide corresponding to one CysDAP, 60S acidic ribosomal protein P3 (1.5-fold decrease in both categories), which belonged to the protein biosynthesis FG, was significantly down-regulated in protein abundance ($FC < -1.5$, $p < 0.05$) in common to both DPI-DTT and (DPI+ABA)-DTT categories in AR embryos (Supplementary Tables S22). There were no proteins detected with changes in both the redox level as well as in protein abundance that would be common to both common-IAA and common-DTT categories in response to the DPI inhibition of germination (Table 6).

3.4.2 Comparison of the thiol-containing proteins identified from approaches I and II in FH and AR aleurones

3.4.2.1 Comparison of the thiol-containing proteins identified from approaches I and II in FH aleurones

In FH aleurones, two RMPs (Figure 29A) belonging to the protein biosynthesis FG with one significantly modified Cys-containing peptide per protein ($FC < -1.5$, $p < 0.05$) were identified in the DPI-IAA category (Supplementary Tables S3), whereas 12 peptides corresponding to 11 significant unique CysDAPs ($-1.5 > FC > +1.5$, $p < 0.05$) changed in abundance as response to the DPI treatment in DPI-DTT category (Supplementary Tables S15). These identified RMPs were up-regulated in the reduction level. Out of 11 CysDAPs identified, two CysDAPs were down-regulated in abundance, while the other nine CysDAPs were up-regulated in abundance during inhibition of germination by DPI treatment (Figure 29A). The proteins that changed in the redox level belonged to the protein biosynthesis FG, and proteins that changed in protein abundance belonged to the lipid metabolism FG, miscellaneous FG and development FG (Figure 19). However, the proteins identified in FH aleurones in this category changed either in protein abundance or the redox level but not both upon the treatment with DPI (Table 7).

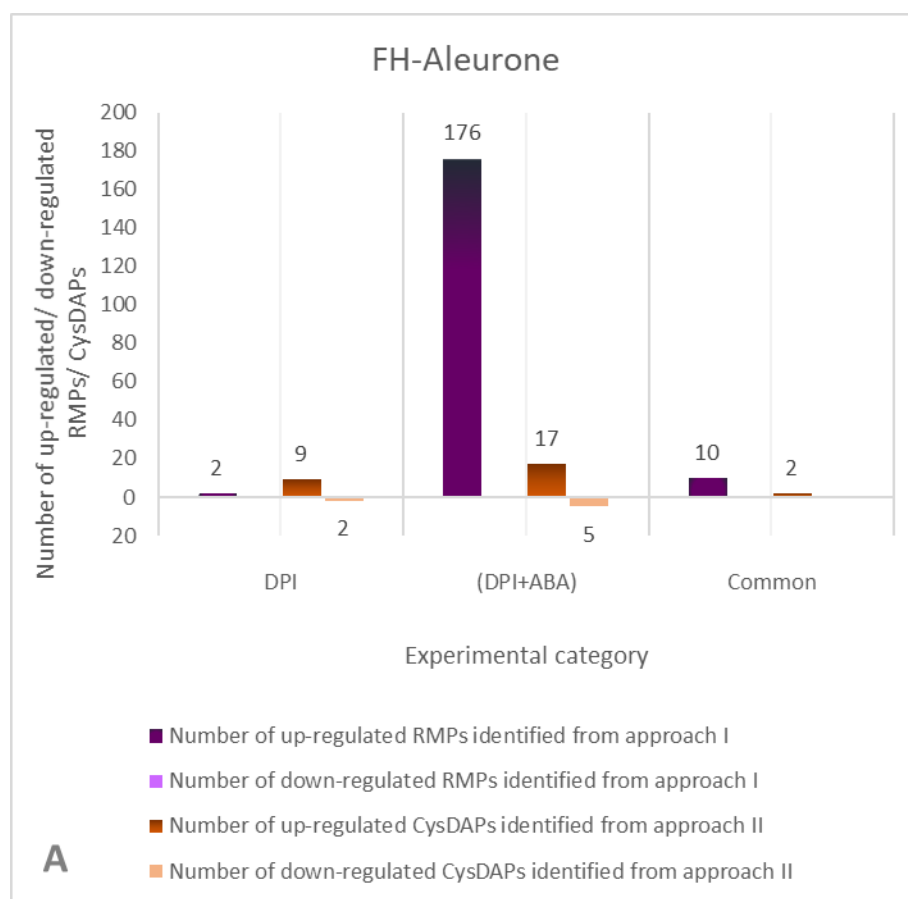


Figure 29A: Comparison of the thiol-containing proteins identified from the approach I (IAA category) and II (DTT category) in FH aleurones. Purple and orange color bars represent the total number of RMPs and CysDAPs found in FH/AR aleurones, respectively. DPI denotes unique thiol-containing proteins found in the DPI-IAA and DPI-DTT categories in FH/AR aleurones. (DPI+ABA) denotes unique thiol-containing proteins found in (DPI+ABA)-IAA and (DPI+ABA)-DTT categories in FH/AR aleurones. Common denotes the common thiol-containing proteins found in both common-IAA and common-DTT categories in FH/AR aleurones.

Upon the treatment with DPI in the presence of ABA, a total of 196 redox-active peptides (Supplementary Tables S7) corresponding to 176 unique RMPs ($FC < -1.5$, $p < 0.05$), which belonged to 23 major FGs (Figure 14A), were identified with changes in the redox

level, while a total of 22 thiol-responsive peptides (Supplementary Tables S19) corresponding to 22 significant unique CysDAPs ($-1.5 > FC > +1.5$, $p < 0.05$), which belonged to 8 major FGs (Figure 23), were changing in abundance in FH aleurones. All RMPs were found to be up-regulated in the reduction level, whereas, out of 22 CysDAPs, five CysDAPs were down-regulated in abundance, and 17 CysDAPs were up-regulated in abundance in response to the DPI in the presence of ABA (Figure 29A). Miscellaneous FG was the most abundant FG (Figure 14B) in the (DPI+ABA)-IAA category, with 21.6% of the total proteins that changed in the redox level, while the majority of the proteins that changed in abundance in (DPI+ABA)-DTT category belonged to the development FG (36.4% of the total CysDAPs found in this category). Altogether, seven proteins with similar peptide sequences were found with changes in both the redox level and protein abundance in response to the inhibition of germination by ABA phytohormone in the presence of DPI in FH aleurones (Table 7, supplementary Table S28).

Among those, the peptides with sequences FSFcFDGLHGVAGAYAK from cytosolic phosphoglucomutase (cPGM) and LQELVNLVVVcGDHGK from Sucrose synthase (carbohydrate metabolism FG), the peptide with sequence TVFVNFmDLcK from component eIF2-beta of eIF2 Met-tRNA binding factor complex (protein biosynthesis FG), the peptide with sequence LQcVGSQVPEAVLR from alpha-amylase inhibitor protein (miscellaneous FG), the peptides with sequences SLVLQTLPTMcNVYVPPEcSIIK, and SLVLQTLPSmcNVYVPPEcSIMR from isomers of gamma-gliadin (development FG) were found to be up-regulated in the reduction level and up-regulated in protein abundance in FH aleurones (Supplementary Table S28). The peptide with sequence EccQQLADISEWcR from an alpha-amylase inhibitor was up-regulated in the reduction

level but down-regulated in protein abundance. Other 169 RMPs identified in the (DPI+ABA)-IAA category changed in the redox level only, while the other 15 CysDAPs identified in the (DPI+ABA)-DTT category changed only in protein abundance in FH aleurones during the germination inhibition by DPI in the presence of ABA.

Upon the germination inhibition by DPI and DPI in the presence of ABA treatments in FH aleurones, 13 redox-active peptides (Supplementary Tables S11) corresponding to 10 RMPs, assigned to 5 major FGs (Figure 17), were significantly up-regulated in the reduction level ($FC < -1.5$, $p < 0.05$) (Figure 29A) in both DPI-IAA and (DPI+ABA)-IAA categories. In contrast, two peptides (Supplementary Tables S23) corresponding to two CysDAPs that belonged to a single FG were significantly up-regulated in abundance ($FC > +1.5$, $p < 0.05$) (Figure 29A) in both DPI-DTT and (DPI+ABA)-DTT categories. However, there were no proteins found with changes in both the redox level as well as protein abundance in response to the inhibition of germination by DPI treatment (Table 7). Proteins belonging to the miscellaneous FG were the most enriched among the identified RMPs (60.0% of the total proteins identified in the common-IAA category), whereas proteins that changed in abundance in the common-DTT category only belonged to the development FG.

3.4.2.2 Comparison of the thiol-containing proteins identified from approaches I and II in AR aleurones

In AR aleurones, one peptide corresponding to the RMP N2-acetylornithine aminotransferase belonging to the amino acid metabolism FG had a significantly up-

regulated level of reduced thiols ($FC < -1.5$, $p < 0.05$) in DPI-IAA category after the DPI treatment as compared to the control (Figure 29B, Supplementary Tables S4).

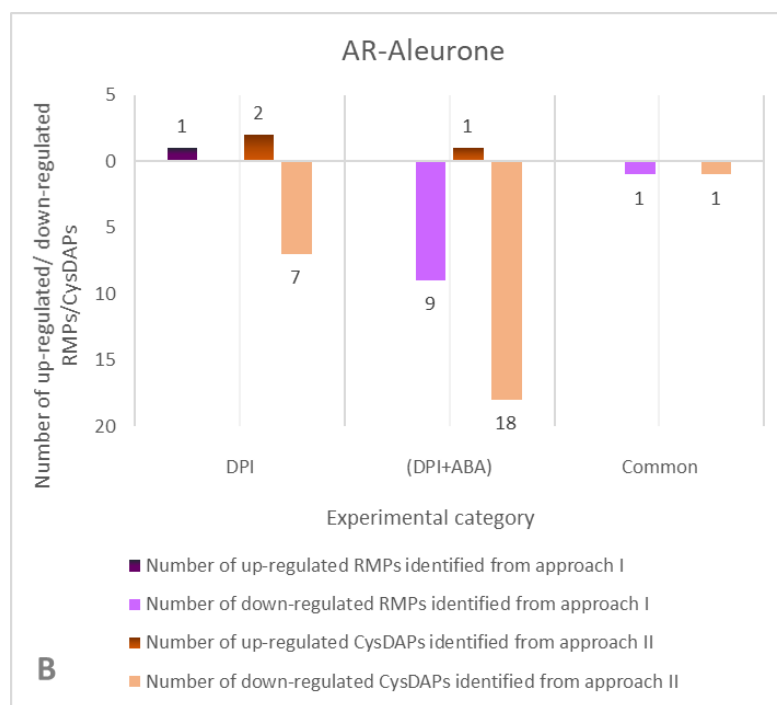


Figure 29B: Comparison of the thiol-containing proteins identified from the approach I (IAA category) and II (DTT category) in AR aleurones. Purple and orange color bars represent the total number of RMPs and CysDAPs found in FH/AR aleurones, respectively. DPI denotes unique thiol-containing proteins found in the DPI-IAA and DPI-DTT categories in FH/AR aleurones. (DPI+ABA) denotes unique thiol-containing proteins found in (DPI+ABA)-IAA and (DPI+ABA)-DTT categories in FH/AR aleurones. Common denotes the common thiol-containing proteins found in both common-IAA and common-DTT categories in FH/AR aleurones.

In the DPI-DTT category, nine thiol-responsive peptides (Supplementary Tables S16) corresponding to nine significant CysDAPs ($-1.5 > FC > +1.5$, $p < 0.05$), assigned to 6 major FGs (Figure 20) were identified upon the treatment with DPI, as compared to the control. Out of the nine CysDAPs identified in the DPI-DTT category, seven proteins were

down-regulated in abundance, while two proteins were up-regulated in abundance (Figure 29B), and the majority of CysDAPs belonged to the development FG. However, these proteins detected in AR aleurones were not changing in both the redox level and protein abundance upon the germination inhibition by DPI treatment (Table 7).

Table 7: Number of the thiol-containing proteins identified in approaches I and II that changed in the redox level only, protein abundance only and in both redox and abundance levels in FH and AR aleurones

Number of thiol-containing proteins Treatments	FH aleurones			AR aleurones		
	Change in the redox level and abundance	Change in the redox level only	Change in protein abundance only	Change in the redox level and abundance	Change in the redox level only	Change in protein abundance only
DPI	0	2	11	0	1	9
DPI in the presence of ABA	7	169	15	4	5	15
Common to both DPI and DPI in the presence of ABA	0	10	2	1	0	0

During the inhibition of germination by DPI in the presence of ABA in AR aleurones, a total of 9 redox-active peptides (Supplementary Tables S8) corresponding to 9 RMPs were significantly down-regulated in the reduction level ($FC > +1.5$, $p < 0.05$) (Figure 29B) in

(DPI+ABA)-IAA category, whereas 21 thiol-responsive peptides (Supplementary Tables S20) corresponding to 19 significant unique CysDAPs ($-1.5 > FC > +1.5$, $p < 0.05$) (one up-regulated CysDAP and 18 down-regulated CysDAPs, Figure 29B) were changing in abundance in (DPI+ABA)-IAA category. In each category, these RMPs and CysDAPs were assigned to 3 (Figure 15) and 5 (Figure 24) major FGs, respectively. A high number of enriched proteins in AR aleurones belonged to the miscellaneous FG in both (DPI+ABA)-IAA and (DPI+ABA)-DTT categories. Among the proteins enriched in both categories, four proteins with identical peptide sequences, the peptides with sequences DccQQLAHISEWcR and QQccGELANIPQQcR from two isomers of dimeric alpha-amylase inhibitors and the peptides with sequences DccQQLADINNEWcR and LYccQELAEISQQcR from two isomers of alpha-amylase inhibitor proteins, which belongs to miscellaneous FG were found with changes in both the redox level (down-regulated in the reduction level) and protein abundance (decrease in abundance) in response to the treatment with ABA phytohormone in the presence of DPI (Table 7, Supplementary Table S28). Altogether, five proteins changed in the redox level only, while 15 proteins changed in protein abundance only in AR aleurones in response to the inhibition of germination by DPI in the presence of ABA.

In AR aleurones, avenin-like protein s1 that belonged to the development FG was the only identified protein that significantly changed in both the redox level ($FC > +1.5$, $p < 0.05$) (Supplementary Table S12) and protein abundance ($FC < -1.5$, $p < 0.05$) (Supplementary Table S24) in response to DPI and DPI in the presence of ABA treatments in both common-IAA and common-DTT categories. This protein was found to be down-regulated in the reduction level in the common-IAA category and down-regulated in protein abundance in

the common-DTT category during the germination inhibition by DPI (Figure 29B, Supplementary Table S28). A single thiol-responsive peptide with sequence SmcSIYIPVQcPAPTTYNIPLVATYTGGAc corresponding to the enriched protein was detected in both categories. Another modification, methionine oxidation, was observed along with the modified thiol residues in this identified peptide sequence. However, the peptides with the same sequence but with modified thiol residues only were found to be changing in protein abundance in the common-DTT category.

4 Discussion

Cereal germination is followed by a substantial shift in the redox status of seed proteins (Alkhalfioui et al., 2007). Many studies have reported that the ROS-based trigger is essential for the germination of a variety of seeds such as *Arabidopsis thaliana* (Leymarie et al., 2011), wheat (Bykova et al., 2011a), rice (Bhattacharjee, Chakrabarty, Kora, & Roy, 2022), soybean (Ishibashi et al., 2012), maize (Hite, Auh, & Scandalios, 1999), and tomato (Morohashi, 2002), where ROS function as regulators of the germination process. An "oxidative window for germination" was postulated by Bailly et al. (2008), which demonstrated that seed germination only occurs when the seed ROS level reaches a point that is sufficient for facilitating ROS signaling and hindered when this level of ROS is either insufficient or excessive. The reduction of ROS accumulation in seeds upon imbibition has resulted in delayed germination in barley (Ishibashi et al., 2015) and *Trichilia dregeana* (Moothoo-Padayachie et al., 2016). In this study, we used

pharmacological treatments to displace the redox and phytohormonal balance in tissues of wheat seeds with high germination potential and identify thiol-redox responding proteins involved in the suppression of germination via reciprocal signaling between the ROS and phytohormones. Seeds with highly ND genotypes were treated with DPI, an inhibitor of flavin oxidoreductases and inducer of the general oxidative stress response, and with ABA dormancy-promoting hormone, on their own or combined. Treatment with DPI was shown to suppress cell redox metabolism via inhibition of NADPH oxidase-dependent ROS production (Riganti et al., 2004), inhibition of mitochondrial Complex I (Bykova et al., 1999; Bykova & Møller, 2001), and alteration of ROS-mediated signal transduction pathways.

The Interplay between NADPH Oxidase, Exogenous ABA, and DPI Regulates Germination Sensitivity in Non-dormant White-Seeded Spring Wheat, Exhibiting Distinct Patterns in FH and AR Seeds

Plant NOXs, known as respiratory burst oxidase homologues (RBOHs), play a vital role in ROS generation. Multiple NOX family members that play specific roles in important processes during plant growth and development were described in different plant species (Hu et al., 2018 and references therein). Several studies have discovered that the administration of DPI, an inhibitor of NADPH oxidase, inhibited the germination of *Arabidopsis* (Müller et al., 2009), barley (Ishibashi et al., 2015), and cress (Müller et al., 2009) seeds. In addition, Leymarie et al. (2011) reported that the NADPH oxidase mutants of *Arabidopsis thaliana* were deeply dormant. NADPH oxidase catalyzes the transfer of an electron from NADPH to molecular oxygen and generates $O_2^{\bullet-}$, which can dismutate to H_2O_2

and O_2 either via the enzymatic reaction of SOD or via spontaneous disproportionation at low pH (Møller et al., 2007; Marino et al., 2012). Impaired enzyme activity of NOXs hinders the production of O_2^- (Cross & Segal, 2004). In our study, the non-dormant FH white-seeded spring wheat displayed delayed germination following DPI application, as compared to the water control (Figure 6A). However, the treatment using a combination of ABA and DPI was effective for germination suppression in FH wheat seeds. The dormancy phytohormone ABA suppresses seed germination and promotes endogenous dormancy in seeds (Finch-Savage & Leubner-Metzger, 2006). The sensitivity of seeds to externally administered ABA across different species varies. Arabidopsis seeds were demonstrated to be responsive to exogenous ABA, which inhibited seed germination by limiting the accessibility of energy and metabolites (Garcarrubio, Legaria, & Covarrubias, 1997). However, according to Bykova et al. (2011a), wheat seeds demonstrated insensitivity to the externally applied ABA treatment alone, which was consistent with our experiment with FH non-dormant wheat seeds (Figure 6A). Therefore, the synergistic effect of DPI and ABA resulted in greater sensitivity to ABA, which in turn increased the germination suppression effect on non-dormant FH wheat seeds. According to Ishibashi et al. (2015), ABA inhibited the activity of NADPH oxidase in barley embryos, leading to a decrease in ROS levels. The enhanced germination suppression observed in our study after treatment with ABA in the presence of DPI demonstrated the link between the production of ROS, cellular redox metabolism and sensitivity to external ABA in FH wheat seeds. However, the addition of GA to the treated non-dormant FH wheat seeds eradicated the inhibitory effect of DPI alone as well as DPI in the presence of ABA. Therefore, the impacts of these compounds exert a reversible effect on the repression of cellular metabolism, suggesting

that the biochemical processes and signal transduction pathways are shared and are involved in phytohormonal regulation.

On the other hand, in contrast to the FH non-dormant seeds, the AR non-dormant wheat seeds did not demonstrate substantial suppression of germination after treatments with high concentrations of DPI and ABA in the presence of DPI (Figures 6B & 8). AR is defined as an increase in the sensitivity of seed perception to environmental variables that promote germination while diminishing or restricting sensitivity to those that repress germination. (Finch-Savage & Leubner-Metzger, 2006). The results obtained in our study for AR seeds supported the above statement by demonstrating a reduced perception of exogenous ABA application and NADPH oxidase inhibitor, DPI, which were involved in germination suppression in FH seeds.

Dynamic Thiol-Based Cysteine Redox Modifications and Protein Abundance Changes were Identified During Germination Suppression in Non-Dormant White-Seeded Spring Wheat Population

Proteins can undergo numerous PTMs after being synthesized in ribosomes, affecting the folding, stability, and conformation, hence affecting the chemical characteristics and biological function of target proteins. These PTMs are vital for gene expression, cellular signaling, and plant enzyme kinetics (Friso & van Wijk, 2015; Navrot, Finnie, Svensson, & Hägglund, 2011). Cys has been recognized as a highly conserved amino acid that frequently occurs in protein functional sites (Marino & Gladyshev, 2010). For many proteins, the regulation of their activities depends on the thiol groups of the Cys residues that are engaged in the active center and/or folding of the protein (Poole, 2015; Ulrich &

Jakob, 2019). Several previous studies demonstrated that proteins present in an oxidized state in dry seeds are transformed into reduced forms following imbibition (Kobrehel et al., 1992; Rhazi, Cazalis, & Aussenac, 2003; Yano, Wong, Cho, & Buchanan, 2001). In this study, changes to the embryo and aleurone redoxomes during germination suppression in FH and AR non-dormant seeds from white-seeded DH population in response to the treatment with either a high concentration of DPI or ABA in the presence of DPI were investigated. Two different approaches were employed; the reversible thiol-based Cys redox modifications were analyzed using approach I, and protein abundance changes, including the changes resulting from irreversible Cys PTMs, were revealed using approach II (Figure 10).

Differential Thiol-Redox Regulation and Changes in Protein Abundance were Observed in FH and AR Embryos and Aleurones During ABA-Induced Germination Inhibition in the Presence of DPI

Among the thiol-containing proteins discovered by approach I of our study in FH embryos, a substantial majority of thiol-responsive proteins found to be redox-regulated via reversible thiol-specific PTMs during ABA-mediated inhibition of germination were related to the cellular respiration, protein biosynthesis, and biotic and abiotic stress responses representing 13.3% of the total RMPs (Figure 12A). Moreover, according to our results using approach II, a higher number of thiol-containing proteins involved in protein biosynthesis (16.0% of total CysDAPs) were changing in abundance as a result of the ABA treatment in the presence of DPI in FH embryos (Figure 21A).

In FH aleurones, during the germination inhibition in response to the ABA treatment in the presence of DPI, a high number of thiol-based proteins that annotated to miscellaneous FG, were found to be redox-regulated via reversible thiol-specific PTMs, representing 21.6% of total RMPs identified (Figure 14A), and the development FG comprised a high number of CysDAPs representing 36.4% of total CysDAPs identified (Figure 23). Miscellaneous FG was the most prevalent FG in AR aleurones during the germination inhibition by the phytohormonal treatment in the presence of DPI, accounting for 66.7% of total RMPs identified (Figure 15) and 73.7% of total CysDAPs identified (Figure 24).

Altogether, 16 thiol-containing proteins were identified from peptides that were both thiol-redox regulated and changed in abundance during ABA-induced germination inhibition in the presence of DPI in FH embryos (Table 7, Supplementary Table 27). Those proteins were associated with diverse functional groups, including cellular respiration, photosynthesis, carbohydrate metabolism, amino acid metabolism, protein homeostasis, redox homeostasis, and development (Figure 30).

However, in AR embryos, only one thiol-containing protein associated with secondary metabolism was identified from a peptide that was thiol-redox regulated and changed in abundance during ABA-induced germination inhibition in the presence of DPI. In FH and AR aleurones, seven and four thiol-containing proteins were identified from peptides that were thiol-redox regulated and changed in abundance during ABA-induced germination inhibition in the presence of DPI, respectively (Table 7, Supplementary Table 27).

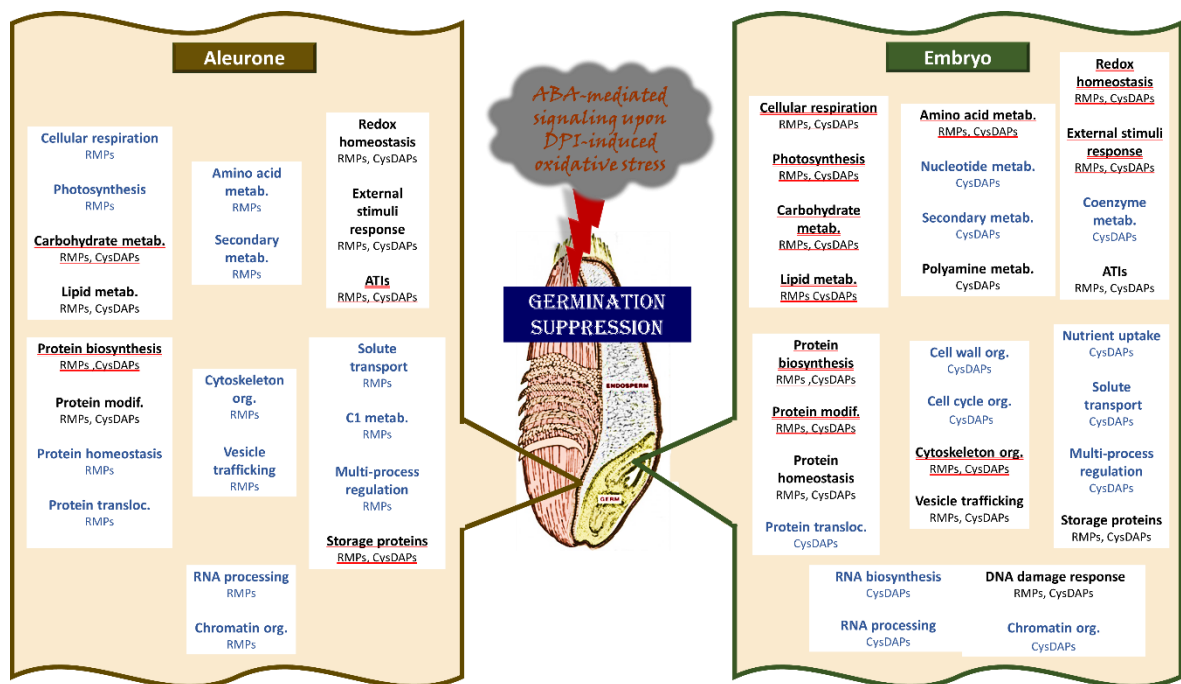


Figure 21: Functional distribution of embryo and aleurone thiol-redoxomes during ABA-mediated germination suppression in the presence of DPI in DH lines of non-dormant FH white-seeded spring wheat. Blue letters represent functional groups identified either in the (DPI+ABA)-IAA or (DPI+ABA)-DTT categories. Black letters represent functional groups found in both the (DPI+ABA)-IAA and (DPI+ABA)-DTT categories. Red underline indicate the functional groups identified with common peptides in the (DPI+ABA)-IAA and (DPI+ABA)-DTT categories. Image of the wheat kernel retrieved by <https://eatwheat.org/learn/wheat-kernels-2/> on 8th July 2023.

Enzymes/ Proteins Associated with Energy Metabolism were Thiol-redox Regulated and Changed in Abundance in FH and AR Wheat Embryos During ABA-Mediated Germination Inhibition: Insights from Cellular Respiration, Photorespiration and Carbohydrate Metabolism

The redox status in the cell and energy metabolism are inextricably interrelated. Chloroplasts and mitochondria are the sites of the key redox processes that govern energy metabolism in photosynthetic cells. The study by Nietzel et al. (2019) discovered a rapid

activation of mitochondrial respiration following the imbibition of *Arabidopsis* seeds. In addition, the study revealed that a swift change in the thiol-redox environment, from an oxidized to a more reduced state, happened concurrently in the mitochondrial matrix. In the present study, in FH embryos, cellular respiration was one of the FGs with the highest number of RMPs with reversible thiol-redox modifications (13.3% of the total RMPs) identified responding to the treatment with ABA under the condition of DPI-mediated changes in redox metabolism (Figure 12A). During the germination inhibition in FH embryos, thiol-responsive peptides that belonged to the proteins associated with glycolysis, TCA cycle, and oxidative phosphorylation were redox-regulated by the hormonal treatment in the presence of DPI (Figure 12B). Thiol-containing CysDAPs associated with the Calvin cycle, glycolysis, TCA cycle, and oxidative phosphorylation were identified in FH embryos based on redox-active peptides upon ABA-mediated germination inhibition in the presence of DPI (Figure 21B). Among these proteins, one peptide with one redox-modified Cys site corresponding to the component NQO3 protein of NADH dehydrogenase complex (complex I) was up-regulated in the reduction level and abundance during the germination inhibition by ABA in the presence of DPI. NADH dehydrogenase complex is a flavin mononucleotide and iron-sulphur-containing complex associated with ETC in oxidative phosphorylation. Complex I of the ETC is one of the major sources of mitochondrial ROS (Møller, Jensen, & Hansson, 2007). A few other peptides associated with the components of this complex, component NDUFA2 and component NDUFA2, were discovered to be only reversibly redox-regulated during the treatment (Supplementary Table S5).

In our study, mMDH was one of the enzymes found to be thiol-redox regulated during germination inhibition by both the high concentration of DPI treatment and the ABA treatment in the presence of DPI (Supplementary Table S9). One peptide with one redox-modified Cys site belonging to this enzyme was discovered to be significantly up-regulated in the reduction level in both DPI only and DPI in the presence of ABA treatments in FH embryos. However, the reduction level of this enzyme after the ABA treatment in the presence of DPI was higher (6.3-fold increase) in contrast to the treatment with the high concentration of DPI (3.6-fold increase). Interestingly, during the ABA-mediated germination suppression, exactly the same peptide with one redox-modified Cys site that corresponded to the same mMDH enzyme identified in the FH embryos was discovered to be up-regulated in the reduction level in AR embryos (Supplementary Table S6). However, the reduction level of the peptide in FH embryos was substantially higher compared to the AR embryos (1.7-fold increase), and mMDH was the only enzyme related to cellular respiration identified as reversibly thiol-redox-regulated RMP in AR embryos. The mMDH enzyme is a TCA cycle component that catalyzes the reversible oxidation of malate to oxaloacetate while reducing the NAD^+ pool. According to a proteomic study, one of the mMDH isoforms, mMDH1, was found to be significantly accumulating during the germination of Arabidopsis seeds (Fu et al., 2005). Furthermore, according to Sew et al. (2016), loss of mMDH activity in Arabidopsis resulted in altered seed metabolism, affecting seed maturation and post-germination growth. The increased reduction level of this enzyme may be related to the stronger germination suppression observed in the FH wheat seeds in response to the ABA treatment in the presence of DPI. Changes in the AR

seeds suggest that this enzyme is essential for responses to general oxidative stress during wheat seed germination.

Thiol-containing peptides from enzymes associated with photorespiration were found to be thiol-redox-regulated and changed in abundance in FH embryos in response to the germination inhibition by ABA in the presence of DPI. During ABA-mediated germination suppression in the presence of DPI, one peptide with one redox-modified Cys site corresponding to the glyoxylate/hydroxypyruvate reductase (GHPR) enzyme was found to be up-regulated in both reduction level and protein abundance in FH embryos. GHPR are highly conserved enzymes with dual activity, which convert hydroxypyruvate to D-glycerate and reduce glyoxylate to glycolate (Lassalle et al., 2016). The photorespiratory glycolate-glyoxylate cycle is aided by the enzyme GHPR. Photorespiration in seeds contributes to the synthesis of signaling molecules such as H_2O_2 , which has a central role in the regulation of cellular redox homeostasis, particularly in response to developmental and environmental cues (Carvalho et al., 2022; Foyer, Bloom, Queval, & Noctor, 2009). The up-regulation of the peptide that belonged to the GHPR enzyme in response to ABA and redox changes suggests a potential role for GHPR in mediating the germination response and maintaining redox homeostasis in seeds.

The metabolic pathways for energy generation include the metabolism of carbohydrates. In FH embryos, thiol-responsive peptides corresponding to the proteins associated with carbohydrate metabolism were found to be redox-regulated and changed in abundance upon ABA in the presence of DPI treatment during germination inhibition. Among those, one peptide with one redox-modified Cys site corresponding to the aldose reductase

enzyme was up-regulated in both reduction level and abundance upon ABA-mediated germination inhibition. Aldose reductases are members of the aldo-keto reductase superfamily of enzymes found in plants and animals. Using NADPH as a cofactor, this enzyme catalyzes the initial step in the polyol pathway, which converts glucose into sorbitol. Aldose reductase is the rate-limiting enzyme of the polyol pathway and operates as an additional route of glucose metabolism that performs in parallel with glycolysis under normal glucose homeostasis. Aldose reductase is known to promote oxidative stress by lowering the NADP/NADPH ratio and competing for NADPH with glutathione reductase (Ramana, 2011). Mature seeds of cereals, including rice, barley, oat, maize and wheat, have been found to contain aldose reductase. It was reported that the aldose reductase protein levels steadily declined during the rice seed germination and reached a minimum by the fifth day upon imbibition. Additionally, exogenous ABA treatment increased the aldose reductase activity in vegetative tissues in rice (Karuna Sree, Rajendrakumar, & Reddy, 2000). The current study revealed that the exogenous ABA application in the presence of DPI increased the aldose reductase enzyme protein abundance and the absolute quantity of the reduced fraction of redox-modified Cys site in FH embryos in these ND wheat seeds. The redox-active Cys187 site is located in immediate proximity to one of 18 hydrogen bonds (Gln188), comprising the highly conserved NADPH cofactor binding site (Olsen et al., 2008). Therefore, Cys187 in wheat aldo-keto reductase of the 4C family could contribute to the perception of changes in the redox microenvironment, resulting in conformational changes in the NADPH binding site affecting the enzyme function.

Sucrose is the principal product of photosynthesis in plants and is involved in a wide range of developmental and metabolic activities such as energy metabolism, carbohydrate

metabolism, and storage protein accumulation. When the photosynthetically generated carbon export from the chloroplast is absent, the sucrose biosynthesis pathway depends on the byproducts of starch degradation, which involve cPGM enzyme activity (Fettke et al., 2009; Stitt & Zeeman, 2012). In the present study, one peptide with one redox-modified Cys site corresponding to the cPGM enzyme was found to be up-regulated in both the reduction level and protein abundance in FH aleurones in response to the germination inhibition by ABA treatment in the presence of DPI. Furthermore, with ABA-mediated germination suppression in the presence of DPI, one peptide with one redox-modified Cys site belonging to the sucrose synthase involved in sucrose degradation was observed to be up-regulated at both the reduction and protein abundance levels in FH aleurones. The same peptide with one Cys site corresponding to the sucrose synthase enzyme was found to be up-regulated in abundance in AR aleurone upon ABA-mediated germination inhibition in the presence of DPI (Supplementary Table S20). Interestingly, this was the only protein that increased in abundance in both FH and AR aleurones under the same conditions, indicating that the redox response of the cPGM enzyme was not related to the germination suppression but rather to the general response to treatment.

Thiol-redox Regulation of the Proteins/Enzymes Associated with the Protein Biosynthesis, Ribosome Biogenesis, and Protein Modification in Wheat Embryos and Aleurones During ABA-Mediated Germination Inhibition

In this study, another pivotal FG that exhibited a high number of thiol-containing proteins in FH embryos was protein biosynthesis FG. The majority of thiol-redox regulated RMPs [13.3% of total RMPs identified] and CysDAPs that changed in abundance [16.0% of total

CysDAPs identified] during ABA-mediated germination suppression in the presence of DPI were associated with protein biosynthesis. Protein synthesis is essential for cell function and tends to occur in three subcellular compartments: cytoplasm, plastids, and mitochondria. Approximately 75% of proteins are synthesized in the cytoplasm, 20% in the chloroplast, and only a minimal amount in the mitochondria. In each subcellular compartment, proteins are synthesized by different mechanisms. As a result, plant cells contain three types of ribosomes, three groups of tRNAs, and three sets of protein synthesis factors (Sun, 2005), which reflects the complexity of protein synthesis machinery in these cells. This complexity allows plants to adapt and regulate protein synthesis under different conditions and in response to various environmental cues.

In FH embryos, the majority of the CysDAPs identified in protein biosynthesis FG upon ABA-mediated germination inhibition were related to ribosome biogenesis (Figure 21B). For instance, many CysDAPs related to the large ribosomal subunit (LSU) and small ribosomal subunit (SSU) proteomes increased in abundance upon ABA-mediated germination inhibition in FH embryos. Among these, one peptide with one redox-modified Cys site corresponding to the component RPL22 of chloroplast LSU proteome associated with the ribosome biogenesis was found to be both thiol-redox regulated (up-regulated in the reduction level) and changed in protein abundance (increased) in FH embryos in response to the ABA treatment in the presence of DPI. In FH aleurones, one peptide with one redox-modified Cys site corresponding to the component RPL11 of the LSU proteome was identified to be up-regulated in the reduction level during the germination suppression in both treatments with the high concentration of DPI and ABA in the presence of DPI (Supplementary Table S11). The reduction level of this peptide showed more dramatic

changes (3.2-fold increase) during the ABA-mediated germination suppression in the presence of DPI as compared to the changes after the treatment with the high concentration of DPI (1.7-fold increase).

Moreover, two unique peptides with one Cys site in each corresponding to the eIF3b component of the Pre-Initiation Complex (PIC) module associated with the translation initiation were up-regulated in both the reduction level and protein abundance in FH embryos upon ABA-mediated germination inhibition in the presence of DPI. In FH aleurones, one peptide with one redox-modified Cys site corresponding to the eIF2-beta component of the PIC module was up-regulated in the reduction level and the abundance under the same treatment conditions.

Upon ABA-mediated germination inhibition, thiol-responsive proteins involved in protein modification, such as S-glutathionylation, disulfide bond formation, protein folding, and lipidation, were found to be thiol-redox regulated and/or changed in abundance in FH embryos, FH aleurones, and AR embryos. Glycosylphosphatidylinositol (GPI) is a prevalent PTM used to anchor proteins to the outer surface of the plasma membrane in eukaryotes. In *Arabidopsis*, nearly 200 GPI-anchored proteins have been discovered (Borner, Lilley, Stevens, & Dupree, 2003). In the current study, one peptide with two redox-modified Cys sites corresponding to beta 1,3-glucan hydrolases (PDCB) associated with the GPI anchor addition was up-regulated in both the reduction level and abundance in response to germination inhibition by ABA treatment in the presence of DPI in FH embryos. Additionally, the abundance of another peptide with two thiols, corresponding to a different isoform of the PDCB enzyme, was increased in FH embryos under the same

conditions of germination inhibition in the presence of ABA and DPI (Supplementary Table S17). In plants, the plasmodesmata apertures, which span the cell wall and interconnect adjacent cells, accumulate 1,3-beta-glucans (callose) to physically constrict and regulate cytoplasmic exchange (Han & Kim, 2016). PDCBs are callose-binding proteins localized in the neck zone of plasmodesmata (Simpson et al., 2009). Changes in plasmodesmal permeability could disrupt the distribution of small molecular size metabolites such as Ca^{2+} , ROS, sucrose, and glucosinolate in the metabolic pathways (Han & Kim, 2016; Radford, Vesk, & Overall, 1998). In *Arabidopsis*, elevated *PDCB1* gene expression resulted in an increased callose buildup surrounding plasmodesmata, bending the plasma membrane inward and forming a constricted neck region, reducing the free space available for the passage of molecules (Simpson et al., 2009). Several studies have reported that the physical and physiological stresses induce callose deposition at plasmodesmata to regulate the plasmodesmata flow (Beffa & Meins, 1996; Botha & HM Cross, 2000; Sivaguru et al., 2000; Ueki & Citovsky, 2005). It is reported that the cellular redox status controls callose deposition on the plasmodesmata, which changes the symplastic permeability (Stonebloom et al., 2012). Moreover, during viral exposure, ABA has been found to promote callose deposition at plasmodesmata to limit viral cell-to-cell migration (Iriti & Faoro, 2008; Alazem, He, Moffett, & Lin, 2017) and exogenous ABA application has been shown to induce callose deposition in rice (Liu et al., 2017) and *Arabidopsis* (Oide et al., 2013). The influx of Ca^{2+} into the cytoplasm is necessary for the activation of NOXs. The increased germination suppression observed with FH seeds following the ABA treatment in the presence of DPI may be partially attributed to the restriction of the plasmodesmatal flow.

In FH embryos, cyclophilin (CYP) that participates in the folding of target proteins through their peptidyl-prolyl cis-trans isomerase activity was identified as responsive to ABA treatment in the presence of DPI (Romano, Horton, & Gray, 2004). ABA has been discovered to up-regulate the expression of the CYP gene in *Solanum commersonii* (Meza-Zepeda et al., 1998). In addition, the analysis of *Arabidopsis* knock-out mutants impaired in the *CYP20-3* gene indicated that they were hypersensitive to oxidative stress conditions (Dominguez-Solis et al., 2008). In the present study, one peptide with one thiol-modified Cys site corresponding to the CYP protein was up-regulated in both the redox level and abundance upon the ABA-mediated germination inhibition in the presence of DPI in FH embryos. Another peptide was up-regulated in the reduction level in FH aleurones in response to the ABA treatment in the presence of DPI during germination inhibition. This peptide contained a single redox-modified Cys site corresponding to a distinct CYP isomer.

Enzymes/Proteins Related to Amino Acid Metabolism, Lipid Metabolism and Secondary Metabolism were Thiol-Redox Regulated and Changed in Abundance in Response to ABA-Mediated Germination Inhibition with DPI in Wheat Embryos and Aleurones

Thiol-responsive proteins related to amino acid metabolism were detected in FH embryos and aleurones. In FH embryos, one peptide with one redox-modified Cys site corresponding to the 3-phosphoglycerate dehydrogenase 1 (PGDH1) enzyme associated with amino acid biosynthesis and one peptide with two redox-modified Cys sites corresponding to the FAH enzyme associated with amino acid degradation were discovered to have decreased oxidation levels and increased protein abundance levels upon ABA-

mediated germination inhibition in the presence of DPI. The first step in the phosphorylated pathway of Ser biosynthesis in plastids is catalyzed by PGDH. According to recent research, the phosphorylation pathway is essential for maintaining plant metabolism and growth (Cascales-Minana et al., 2013; Toujani et al., 2013). Notably, PGDH was found to be thioredoxin (Trx)-linked in the germination of model legume *Medicago truncatula* seeds (Alkhalfioui et al., 2007). Recent research has identified PGDH as a thiol-based redox-regulated enzyme in *Arabidopsis* (Yoshida et al., 2020). The study discovered that one isoform of *Arabidopsis* PGDH, PGDH1 enzyme, has the ability to physically interact with redox-regulatory components such as Trx via the mixed disulfide bond, and the enzyme activity increased upon the reduction of Cys residues involved in the formation of disulfide bond. However, under non-reducing conditions, the formation of intramolecular disulfide bonds between Cys residues reduced PGDH enzyme activity in *Arabidopsis* (Yoshida et al., 2020). The PGDH1 protein from wheat embryos identified in this study is homologous to the *Arabidopsis* PGDH1 isoform and has 82% identity to AT4G34200.1 protein sequence (BLAST score 928, E value 0.0).

Moreover, in PGDH1 from wheat embryos, increased reduction and peptide abundance levels were revealed for the Cys residue identical to the conserved Cys86 in AT4G34200.1 that was shown to be involved in the disulfide bond formation (Yoshida et al., 2020). Therefore, this study provides evidence for the potential activation of PGDH1 enzymatic activity and increased capacity for the PGDH1 contribution to the phosphorylated pathway in response to oxidative stress and ABA-driven suppression of germination in wheat embryos. Another enzyme, FAH, catalyzes the hydrolysis of fumarylacetoacetate into fumarate and acetoacetate, the final step in the Tyr breakdown pathway. Previous research

by Han et al. (2013) discovered that the disruption of FAH activity triggered cell death in *Arabidopsis* mutant deficient in *short-day sensitive cell death1 (sscd1)* gene encoding FAH and suggested that the Tyr degradation pathway is critical for plant viability. Loss of FAH activity in *Arabidopsis* resulted in an increased ROS buildup and less pronounced up-regulation of specific ROS-scavenging genes under salt stress conditions due to the accumulation of Tyr degradation intermediates (Huang et al., 2018). This indicates the significance of Tyr degradation in maintaining redox homeostasis and responding to plant stress. Our findings suggest that FAH may become active and contribute to Tyr breakdown in response to oxidative stress and ABA-mediated germination inhibition in wheat embryos.

A high number of thiol-responsive proteins representing 13.3% of the total RMPs identified after the ABA in the presence of DPI treatment in FH embryos were associated with changes in the lipid metabolism, and nsLTPs were shown to be prevalent in this functional category. The nsLTPs were found to be thiol-redox responding as well as changing in protein abundance in FH aleurone. Various nsLTPs play crucial roles in numerous biological processes *in planta* by transporting different phospholipids across the membrane (Liu et al., 2015). Drought and salt stress strongly activated several nsLTP genes in wheat, indicating their potential roles in influencing responses to abiotic stress conditions (Fang et al., 2020). In the present study, two peptides with four redox-modified Cys sites, corresponding to two isoforms of nsLTPs, were discovered to be up-regulated at both the reduction and abundance levels during ABA-induced germination inhibition in the presence of DPI in FH embryos. However, nsLTPs were not identified as redox-regulated or changed in abundance in AR embryos and AR aleurone.

Steroleosin dehydrogenase is an enzyme that is associated with lipid metabolism. In the present study, one peptide with one redox-modified Cys site corresponding to the steroleosin dehydrogenase was identified to be up-regulated in both the reduction level and abundance upon ABA-mediated germination inhibition in FH embryos. In FH aleurones, one peptide with one redox-modified Cys site corresponding to the different isoform of the steroleosin dehydrogenase was up-regulated in the reduction level in response to the hormonal treatment in the presence of DPI during germination inhibition. Steroleosins are NADPH-dependent proteins discovered on the exterior of lipid bodies and have a role in cytoplasmic signaling in seed plants (Lin, Tai, Peng, & Tzen, 2002). Sterol-binding dehydrogenases aid in the mobilization of lipid bodies during the germination of seeds and are engaged in signal transduction in a variety of plant tissues (van der Schoot, Paul, Paul, & Rinne, 2011). Increased expression of steroleosin genes has been identified in imbibed *Arabidopsis* seeds, rice seed embryos and endosperm (Umate, 2012), and maturing sesame seeds (Lin, Tai, Peng, & Tzen, 2002), indicating the importance of the enzyme in the early stages of seed germination. Our findings imply that steroleosin dehydrogenase responds to ABA treatment and oxidative stress during germination inhibition.

Secondary metabolites contribute to the regulation of plant growth, development, interaction with the environment and defence (Erb & Kliebenstein, 2020). In this study, thiol-responsive proteins linked with secondary metabolic pathways that changed in the redox state and/or abundance level during germination suppression in response to ABA treatment in the presence of DPI were discovered in FH embryos, FH aleurones, and AR embryos.

P450s are enzymes involved in both secondary and primary metabolic pathways. The P450 enzymes are substrate-promiscuous, heme-thiolate enzymes that are widely dispersed and catalyze a wide range of oxidative processes (Bernhardt, 2006; O'Reilly, Köhler, Flitsch, & Turner, 2011). In AR embryos, one peptide with one redox-modified Cys site corresponding to the P450 enzyme associated with the glucosinolate biosynthesis pathway was both down-regulated in the reduction level and in abundance upon ABA-mediated germination inhibition. Glucosinolates are secondary plant metabolites that have a role in plant stress responses (Bednarek et al., 2009; Schlaeppli et al., 2008; Wittstock & Halkier, 2000). According to Meier, Ehbrecht, and Wittstock (2019), after 24 hours of stratification, the glucosinolate concentration increased in germinating *Arabidopsis* seeds. Our results suggest that exogenous ABA treatment under oxidative stress may reduce the accumulation of glucosinolate in non-dormant AR wheat seeds, although no suppression of germination could be observed.

Thiol-Redox Modifications and Abundance Changes were Observed in the Proteins/Enzymes Related to Cellular Redox Homeostasis and Cytoskeleton Dynamics due to the Oxidative stress Induced by DPI in the Presence of ABA

The oxidation or reduction of numerous redox-active species, which are involved in various metabolic activities, determines the cellular redox state (Foyer & Noctor, 2009). The antioxidant defence mechanism is vital to maintaining redox homeostasis in cells. Ohkama-Ohtsu et al. (2008) proposed a novel GSH degradation mechanism in *Arabidopsis*. The 5-oxoprolinase enzyme, which hydrolyzes 5-oxoproline to glutamate in an ATP-dependent process, was identified as a component of this pathway (Ohkama-Ohtsu et al., 2008). As a

component of the AsA-GSH cycle, GSH detoxifies photosynthetically produced H_2O_2 (Noctor & Foyer, 1998). GSH performs redox reactions via the thiol residue of the GSH tripeptide, which allows it to operate as a regulator of redox homeostasis (Foyer & Noctor, 2005). In the present study, one peptide with two thiol-modified Cys sites corresponding to the 5-oxoprolinase was up-regulated in both the reduction level and abundance upon ABA-mediated germination inhibition in the presence of DPI in FH embryos.

The cytoskeleton is regarded as the cell's backbone as it provides the cell with its form and structure (Zheng & Oegema et al., 2008). It is essential for modulating inter-and intracellular transport, as well as for cell division and differentiation (Rao et al., 1997). The cytoskeletal components have been identified as being involved in signal transduction and influencing gene transcription in response to external stimuli (Damanian et al., 2010). A component of the CCT chaperonin folding complex was identified as thiol-based, reversibly redox-regulated RMP, as well as CysDAP in FH embryos. The CCT chaperonin is a 1000 kDa hetero-oligomeric ATP-dependent high-molecular-mass protein complex composed of eight subunits (CCT1-CCT8) (Ahn et al., 2019; Joachimiak et al., 2014). It was previously demonstrated that CCT aids in the folding of numerous proteins, including the abundant cytoskeletal proteins actin and tubulin, which form microfilament and microtubule assemblies (Grantham, Brackley, & Willison, 2006). CCT chaperonin activity is essential for cytoskeleton protein homeostasis (proteostasis) (Grantham, 2020; Lundin, Leroux, & Stirling, 2010), and in mammalian cells, full CCT activity is required for proper cell growth and division (Grantham, Brackley, & Willison, 2006; Grantham, 2020; Lundin, Leroux, & Stirling, 2010). Recent studies with the *Arabidopsis* demonstrated that CCT-deficient cells exhibited problems with cortical microtubule structure and tubulin

accumulation (Ahn et al., 2019), indicating the necessity of these CCT subunits for plant growth.

In our study, it was discovered that the reduction level of one peptide with one redox-modified Cys site, which corresponds to a member of CCT chaperone, CCT7 subunit, greatly increased upon germination suppression by ABA treatment in the presence of DPI compared to the water control in FH embryos. In contrast to the other peptides found to be both redox-regulated and changed in abundance in FH embryos, this peptide of the CCT7 subunit was found to be highly up-regulated in the reduction level (approximately a 3-fold increase). A different peptide with one Cys site corresponding to the same protein, the CCT7 subunit, was found to be up-regulated in abundance under the same conditions in FH embryos. Additionally, one peptide with one Cys site corresponding to the subunit alpha (CCT1) and two peptides with one Cys site in each corresponding to two isomers of subunit gamma (CCT3) of CCT chaperone was discovered to be elevated in abundance during germination inhibition in response to ABA in FH embryos. Among the isomers of the CCT3 subunit identified in FH embryos, one isomer was found to be only thiol-redox regulated (up-regulated in the reduction level) during the germination inhibition by ABA in the presence of DPI in FH aleurone. It was revealed that the same peptide, which had one Cys site and belonged to the CCT1 subunit, changed in abundance in AR embryos in response to ABA-mediated germination inhibition. It is intriguing to note that the peptide was decreased in abundance in AR embryos, indicating changes in functional involvement of the CCT1 subunit upon the after-ripening process.

Proteins/ Enzymes Associated with Biotic and Abiotic Stress Response Underwent Thiol-Redox Regulation and Exhibited Changes in Abundance during the Suppression of Germination by ABA in the Presence of DPI in FH and AR Embryos and Aleurones

In our study, thiol-responsive peptides belonging to proteins involved in abiotic and biotic stress responses were found to be redox-regulated and changing in abundance in response to the germination inhibition by DPI alone and ABA in the presence of DPI treatments in FH embryo, FH aleurone and AR aleurone. External stimuli response FG was the second-most prevalent FG found in FH embryos and aleurones, accounting for 11.1% and 15.3% of the RMPs identified after the ABA in the presence of DPI treatment, respectively. In FH embryos, one peptide with one redox-modified Cys site corresponding to the DIR protein was up-regulated in both the reduction level and abundance in response to germination inhibition by ABA in the presence of DPI. DIR proteins have been discovered to confer salt stress tolerance in a range of plants, including wheat (Guo et al., 2012; Peng et al., 2009), *Arabidopsis* (Jiang, Yang, Harris, & Deyholos, 2007), rice (Chitteti & Peng, 2007), and maize (Burlat, Kwon, Davin, & Lewis, 2001; Gang et al., 1999; Wang et al., 2022). Paniagua et al. (2017) discovered that the expression level of specific *Arabidopsis* DIR genes altered due to the ABA and oxidative stress.

Additionally, a large number of PR proteins were revealed to be thiol-redox regulated in common to both treatments with the high concentration of DPI and ABA in the presence of DPI in FH embryos (Supplementary Table S9, Figure 16B). Among those, one peptide with one redox-modified Cys site corresponding to the PR protein, Thionin, was highly up-

regulated in the reduction level during the germination inhibition by ABA treatment in the presence of DPI (approximately 8-fold increase) in comparison to the treatment with the high concentration of DPI (approximately 5-fold increase). The same peptide corresponding to the Thionin PR protein increased in abundance in both treatment categories in FH embryos (Supplementary Table 21).

Proteins belonging to miscellaneous FG were found to be thiol-redox regulated in FH embryos and FH aleurones as well as AR embryos and AR aleurones following the germination inhibition by the high concentration of DPI and ABA in the presence of DPI. The majority of proteins found in this FG were plant protease inhibitors (PPIs). PPIs are a broad set of tiny proteins found in storage tissues such as tubers and seeds, as well as aerial plant parts, that serve a variety of purposes in plants (De Leo et al., 2002). PPIs have gained considerable interest because of their potential role in defending plants against herbivorous insects, where the proteins serve as anti-metabolites, interfering with the digestive process of the insects (Hartl et al., 2011; Lawrence & Koundal, 2002). These PPIs are classified into four primary categories based on the unique reactive site present in the sequences: Cys protease inhibitors, metalloid protease inhibitors, serine protease inhibitors, and aspartic protease inhibitors (Laskowski & Qasim, 2000). Furthermore, PPIs are categorized into families, namely Bowman-Birk, Kunitz, Potato I, Potato II, Cereal, Serpine, Mustard, Squash, and Rapeseed (De Leo et al., 2002), according to their function and structural and biochemical characteristics.

In our study, wheat α -amylase/trypsin-inhibitors (ATIs) were the most prevalent redox-modified PPIs. ATIs are classified under serine protease inhibitor/ cereal families in the

PPIs classification system (De Leo et al., 2002; Laskowski & Qasim, 2000). ATIs are grouped into different categories based on their inhibitory action (amylase and/or trypsin inhibition) or solubility in chloroform/methanol (CM-types). At the protein level, wheat contains a total of 15 amylase inhibitors [UniProtKB: 0.19, 0.28, 0.53, CM1, CM2, CM3, CM16, CM17, CMX1/3, CMX2, wheat chymotrypsin inhibitor, wheat amylase subtilisin inhibitor (WASI), wheat dimeric amylase inhibitor (WDAI), xylanase inhibitor, and allergen C-C] (Geisslitz et al., 2020). ATIs, 0.19 and CM3 have been identified as the two most bioactive ATIs and the most abundant ATIs in wheat (Zevallos et al., 2017). During the seed germination in cereals, α -amylase in the aleurone layer plays a key role in endosperm starch degradation by hydrolyzing the starch into metabolizable sugars that supply energy for the growth of roots and shoots (Akazawa & Hara-Nishimura, 1985; Beck & Ziegler, 1989). Expression of α -amylase inhibitors suppresses starch degradation, which may facilitate germination inhibition through oxidative stress and ABA-mediated signal transduction mechanisms in the seeds from ND lines of white-seeded spring wheat.

As compared to embryos, a large number of ATIs in aleurones appeared to respond to the ABA treatment in the presence of DPI, resulting in germination inhibition. In FH aleurones and AR aleurones, miscellaneous FG comprised the highest number of RMPs, representing 21.6% (Figure 14A) and 66.7% (Figure 15) of the total RMPs identified after the treatment with ABA under DPI-induced oxidative stress conditions as compared to the water control. A substantial number of thiol-redox-regulated ATIs were found among these RMPs. Among the ATIs identified in FH aleurones, two peptides with four redox-modified Cys sites corresponding to the two isoforms of WDAI proteins were found to be both redox-responding as well as changing in abundance during the germination inhibition due to the

ABA treatment in the presence of DPI. Both of these thiol-responsive peptides were up-regulated in the reduction level. However, one thiol-responsive peptide was discovered to be down-regulated in abundance, while the other was up-regulated in abundance during ABA-mediated germination inhibition in FH aleurones.

Interestingly, all ATIs identified in AR aleurones as ABA-responsive upon oxidative stress RMPs and CysDAPs were down-regulated in both the reduction level and abundance (more prone to degradation). Altogether, four peptides with 12 redox-modified Cys sites corresponding to four ATIs were found to be down-regulated in both the reduction level and abundance in response to the ABA-mediated germination suppression in the presence of DPI in AR aleurones. Degradation of these ATIs can be related to the aging of seeds with the concomitant loss of stress-protective capacity, and it could be the result of changes in protein stability due to desensitization of ABA-signaling (Ali, Pardo, & Yun, 2020) in AR seeds compared to FH seeds.

In FH embryos, a large number of ATIs were discovered to be thiol-redox-regulated as common proteins responding to both DPI alone and DPI with ABA treatments. Among those, six peptides with 11 redox-modified Cys sites, corresponding to six ATI proteins, demonstrated a significant increase in the reduction level (with FC over 4). In contrast to the treatment with the high concentration of DPI, those ATIs appeared to respond effectively to the germination inhibition by ABA treatment in the presence of DPI. Only one PPI, trypsin inhibitor protein, was found to be redox-regulated only in response to the hormonal treatment in the presence of DPI in FH embryos. In AR embryos, only one ATI

was thiol-redox regulated following germination inhibition in response to ABA treatment in the presence of DPI.

Endogenous WASI was another ATI protein that responded to ABA treatment in the presence of DPI, resulting in germination suppression. Two distinct peptides, each with one Cys site corresponding to the WASI protein, were detected to be up-regulated in the reduction level and increased in abundance upon ABA-mediated germination inhibition in FH embryos. WASI proteins inhibit endogenous alpha-amylases and can inhibit subtilisin due to their bifunctional nature. Thus, this protein was annotated into the external stimuli response FG in our study. According to the protein structure, this family has been referred to as Kunitz-type inhibitors (Svensson, Fukuda, Nielsen, & Bønsager, 2004). The WASI proteins contain only four Cys residues, as opposed to the ten Cys residues found in exogenous alpha-amylase and protease inhibitors (Altenbach, Vensel, & Dupont, 2011). The inhibitor was produced in barley grains during the maturation stage, and its action was regulated by the ABA hormone (Robertson & Hill, 1989). Montrichard et al. (2009) revealed that the inhibitor was thiol-based redox-regulated under oxidative stress in wheat.

The Induction of Oxidative Stress by DPI in the Presence of ABA Led to Thiol-Based Redox Regulation and Changes in the Abundance of a High Number of Storage Proteins in FH Aleurones

All the identified storage proteins were annotated into the development FG in our study. Wheat storage proteins are known as gluten. Gluten is a complex mixture of two major forms of proteins: gliadin and glutenin. Gliadins and glutenins account for roughly 30% and 50% of the total protein in wheat grain, respectively (Urade, Sato, & Sugiyama, 2017).

Gliadins and glutenins were found to be reduced *in vivo* during the germination of wheat (Kobrehel et al., 1992). In our study, we discovered a large number of gliadins and glutenins that were redox-regulated and/or changed in abundance during germination inhibition by the treatments with the high concentration of DPI and ABA in the presence of DPI.

Gliadins are highly polymorphic seed storage proteins that are divided into four subfamilies based on changes in molecular mobility: α -, β -, γ -, and ω -gliadins (Jones, Taylor, & Senti, 1959). In this study, we discovered that the α - and γ -gliadins were thiol-redox regulated and changed in abundance during the germination suppression by the treatments with either the high concentration of DPI or ABA in the presence of DPI. Low Molecular Weight Glutenin Subunits (LMW-GS) and High Molecular Weight Glutenin Subunits (HMW-GS) are two subfamilies of the macro polymers that compose glutenin. Disulfide linkages crosslink these subunits to form the glutenin macropolymer, which then randomly combines with gliadins by non-covalent interactions to form the aggregate (Lindsay & Skerritt, 2000). These proteins play a crucial role in the composition and properties of gluten in wheat grains, which is significant for various food products.

In FH embryos, upon germination inhibition by ABA in the presence of DPI, three storage proteins, two isoforms of Gamma-gliadin and one HMW-GS protein were found to be thiol-redox regulated. Among these redox-modified storage proteins, one peptide with one redox-modified Cys site corresponding to an isoform of gamma-gliadin was highly up-regulated in the reduction level (approximately 3.0-fold increase) in FH embryos as compared to the water control. Among the ABA-responsive CysDAPs, one peptide with

three Cys sites corresponding to the isomer of LMW-GS storage protein was found to be highly up-regulated in abundance (approximately 4.0-fold increase) in FH embryos as compared to the water control. In AR embryos, storage proteins were identified to be only thiol-redox regulated (up-regulated in the reduction level), but they were not changing in abundance significantly in response to the ABA treatment in the presence of DPI.

In FH aleurones, HMW-GS, LMW-GS, Alpha-gliadin, and Gamma-gliadin were the most commonly detected reversibly thiol-redox modified storage proteins found during the germination inhibition by ABA treatment in the presence of DPI. Development FG exhibited the highest number of CysDAPs, representing 36.4% identified all ABA-responsive CysDAPs in FH aleurones, including Gamma-gliadin, Gliadin-like avenin, Alpha/beta-gliadin (Prolamin), and LMW-GS. In comparison to the water control, all of these storage proteins were up-regulated in the reduction level and abundance during the germination suppression by phytohormonal treatment in the presence of DPI. Among those, two peptides with two redox-modified Cys sites corresponding to the two isomers of gamma-gliadin storage protein were found to be both up-regulated in the reduction level and abundance in response to the germination inhibition in FH aleurones. However, during the suppression of germination by ABA treatment in the presence of DPI, the storage proteins found in the AR aleurones were down-regulated in both the reduction level and abundance. This could be attributed to the rapid germination processes accompanied by the utilization of storage reserves and the lack of sensitivity to the external ABA combined with DPI in the AR seeds as compared to FH seeds.

5 Conclusion

Pharmacological targeting of cellular ROS production sources and changing the ROS balance by DPI, a potent inhibitor of NADPH oxidases and other flavoenzymes, resulted in the suppression of germination in FH seeds from non-dormant DH lines. The concentration-dependent effect of DPI on germination arrest was demonstrated in FH but not in AR intact seeds with non-dormant genotypes. Treatment with DPI at a high concentration (higher than 1 mM) blocked the germination of FH seeds irreversibly and affected seed viability. The sensitivity of FH seeds to ABA-mediated germination suppression was evoked by external DPI added at a lower concentration, and the effect was comparable to the germination suppression level at a 4-fold higher concentration of DPI. High sensitivity to both DPI and ABA in the presence of DPI was lost upon seed after-ripening process.

The non-dormant FH wheat seeds were more sensitive to the ABA hormonal treatment and DPI-induced oxidative stress than non-dormant AR seeds. This study provided experimental evidence that by inhibiting ROS production with low, non-toxic concentrations of DPI and hence influencing ROS-sensitive pathways, the sensitivity to ABA-mediated response was induced in genetically non-dormant freshly harvested but not in after-ripened seeds. The quantitative redox proteomic analysis revealed that the germination suppression by ABA treatment in the presence of DPI was accompanied by changes in thiol-redox PTMs and/or abundance of peptides corresponding to the proteins associated with diverse FGs in FH embryos and FH aleurones (Figure 30). Prominent changes in the redoxome and total Cys-proteome in response to both oxidative stress and

external ABA combined with oxidative stress were revealed in FH but not in AR embryos and aleurones (Tables 5 and 6). This finding corresponds to the physiological GR response of FH and AR seeds to the pharmacological treatments, where FH seeds exhibited high sensitivity to both oxidative stress and external ABA combined with oxidative stress. This sensitivity was lost upon after-ripening of non-dormant seeds, and the reflection of it was evident from the lack of changes in the embryo redoxome and total Cys-proteome. In FH embryos, the majority of RMPs sensitive to DPI (both common and unique) showed changes in the redox level only (82% of the total DPI response, Table 7). The response to external ABA combined with oxidative stress resulted in significant changes in protein abundance levels (80% of total changes in RMPs and CysDAPs in response to the ABA with oxidative stress treatment). In FH aleurone, a total of 88% of responding proteins showed changes at the redox levels only upon exposure to external ABA combined with oxidative stress (Table 7). This indicates the high involvement of the existing redoxome in the suppression of germination by ABA and the lower involvement of protein biosynthesis and turnover processes within the aleurone layer cells.

In FH embryos, the majority of changes in RMPs and CysDAPs were detected for the proteins related to cellular respiration, protein biosynthesis, biotic and abiotic stress responses. A higher number of α -amylase inhibitors and storage proteins changed in abundance and/ or were thiol-redox regulated in FH aleurones. All redox-modified peptides that corresponded to the identified proteins were discovered to be up-regulated in the reduction level, and the majority of peptides and corresponding proteins increased in abundance in FH embryos as well as FH aleurones in response to the ABA-mediated germination inhibition in the presence of DPI.

In contrast to the FH embryos and aleurones, the AR embryos and aleurones had the minimum number of peptides corresponding to proteins that were significantly thiol-redox modified and altered in abundance in response to the ABA treatment in the presence of DPI. Interestingly, the majority of the peptides identified in the AR embryos and aleurones decreased in the reduction level and in abundance upon the ABA treatment in the presence of DPI.

The findings of the study revealed that the NADPH oxidases and other flavoenzymes constitute a significant source of ROS production in non-dormant FH wheat seeds, and their role changes upon seed after-ripening. The inhibition of ROS generation and the level of ABA phytohormone in wheat seeds are intricately linked to the successful ABA-mediated suppression of germination in the non-dormant white-seeded spring wheat DH lines. Furthermore, this study provides evidence for the possibility to suppress germination and induce dormancy-like response, even in non-dormant seeds, through the modulation of ROS generation, redox balance, and phytohormonal signaling. The synergistic developmental and metabolic reprogramming during germination suppression is demonstrated in this original experimental work. Understanding the molecular responses underlying germination suppression in wheat seeds is crucial for deciphering the mechanisms that regulate seed germination and dormancy. This study aimed to reveal redox-dependent sources of PHS resistance, proteins and corresponding genes involved in the control of germination suppression. The insights gained on the target genes can be employed genetically to create PHS resistant varieties or develop treatments that effectively prolong dormancy at the seed level. Leveraging these approaches has the potential to mitigate challenges faced by farmers, contributing to improved crop yield and

overall quality. In future research directions, quantitative analysis of the total proteome will be critical to comprehend the redox-dependent molecular mechanisms responsible for germination suppression by ABA in the presence of DPI and to identify specific gene targets for functional studies using gene editing approaches.

6 References

- Abdallah, C., Dumas-Gaudot, E., Renaut, J., & Sergeant, K. (2012). Gel-based and gel-free quantitative proteomics approaches at a glance. *International Journal of Plant Genomics*, 2012, 1-17. doi:10.1155/2012/494572
- Adams, D.R., Ron, D., & Kiely, P.A. (2011). RACK1, a multifaceted scaffolding protein: Structure and function. *Cell Communication and Signaling*, 9(1). doi:10.1186/1478-811x-9-22
- Ahn, H., Yoon, J., Choi, I., Kim, S., Lee, H., & Pai, H. (2019). Functional characterization of Chaperonin containing T-complex polypeptide-1 and its conserved and novel substrates in Arabidopsis. *Journal of Experimental Botany*, 70(10), 2741-2757. doi:10.1093/jxb/erz099
- Akazawa, T. & Hara-Nishimura, I. (1985). Topographic aspects of biosynthesis, extracellular secretion, and intracellular storage of proteins in plant cells. *Annual Review of Plant Physiology*, 36(1), 441-472. doi:10.1146/annurev.pp.36.060185.002301
- Alazem, M., He, M., Moffett, P., & Lin, N. (2017). Abscisic acid induces resistance against *bamboo mosaic virus* through *argonaute2* and *3*. *Plant Physiology*, 174(1), 339-355. doi:10.1104/pp.16.00015
- Albanèse, V., Yam, A. Y., Baughman, J., Parnot, C., & Frydman, J. (2006). Systems analyses reveal two chaperone networks with distinct functions in eukaryotic cells. *Cell*, 124(1), 75-88. doi:10.1016/j.cell.2005.11.039
- Albertos, P., Romero-Puertas, M.C., Tatematsu, K., Mateos, I., Sánchez-Vicente, I., Nambara, E., & Lorenzo, O. (2015). S-nitrosylation triggers ABI5 degradation to promote seed germination and seedling growth. *Nature Communications*, 6(1). doi:10.1038/ncomms9669
- Ali, A., Pardo, J.M., & Yun, D.-J. (2020). Desensitization of ABA-signaling: The swing from activation to degradation. *Frontiers in Plant Science*, 11. doi:10.3389/fpls.2020.00379
- Ali, S.S., Kumar, G.B., Khan, M., & Doohan, F.M. (2013). Brassinosteroid enhances resistance to Fusarium diseases of Barley. *Phytopathology*®, 103(12), 1260-1267. doi:10.1094/phyto-05-13-0111-r

- Alkhalfioui, F., Renard, M., Vensel, W.H., Wong, J., Tanaka, C.K., Hurkman, W.J., Buchanan, B.B., & Montrichard, F. (2007). Thioredoxin-linked proteins are reduced during germination of *Medicago truncatula* seeds. *Plant Physiology*, *144*(3), 1559-1579. doi:10.1104/pp.107.098103
- Altenbach, S.B., Vensel, W.H., & Dupont, F.M. (2011). The spectrum of low molecular weight alpha-amylase/protease inhibitor genes expressed in the US bread wheat cultivar Butte 86. *BMC Research Notes*, *4*(1). doi:10.1186/1756-0500-4-242
- Alvarez, S., Valdez, L.B., Zaobornyj, T., & Boveris, A. (2003). Oxygen dependence of mitochondrial nitric oxide synthase activity. *Biochemical and Biophysical Research Communications*, *305*(3), 771-775. doi:10.1016/s0006-291x(03)00818-0
- Amicucci, E., Gaschler, K., & Ward, J.M. (1999). NADPH oxidase genes from tomato (*Lycopersicon esculentum*) and curly-leaf pondweed (*Potamogeton Crispus*). *Plant Biology*, *1*(5), 524-528. doi:10.1111/j.1438-8677.1999.tb00778.x
- Anaya, F., Fghire, R., Wahbi, S., & Loutfi, K. (2018). Influence of salicylic acid on seed germination of *Vicia faba* L. under salt stress. *Journal of the Saudi Society of Agricultural Sciences*, *17*(1), 1-8. doi:10.1016/j.jssas.2015.10.002
- Araki, K., Kusano, H., Sasaki, N., Tanaka, R., Hatta, T., Fukui, K., & Natsume, T. (2016). Redox sensitivities of global cellular cysteine residues under reductive and oxidative stress. *Journal of Proteome Research*, *15*(8), 2548-2559. doi:10.1021/acs.jproteome.6b00087
- Arnao, M.B., & Hernández-Ruiz, J. (2019). Melatonin and reactive oxygen and nitrogen species: A model for the plant redox network. *Melatonin Research*, *2*(3), 152-168. doi:10.32794/11250036
- Asada, K. (1999). The water-water cycle in chloroplasts: Scavenging of active oxygens and dissipation of excess photons. *Annual Review of Plant Physiology and Plant Molecular Biology*, *50*(1), 601-639. doi:10.1146/annurev.arplant.50.1.601
- Asada, K. (2006). Production and scavenging of reactive oxygen species in chloroplasts and their functions. *Plant Physiology*, *141*(2), 391-396. doi:10.1104/pp.106.082040

- Astier, J., Rasul, S., Koen, E., Manzoor, H., Besson-Bard, A., Lamotte, O., Jeandroz, S., Durner, J., Lindermayr, C., & Wendehenne, D. (2011) S-nitrosylation: An emerging post-translational protein modification in plants. *Plant Sci* 181: 527–533
- Bagola, K., & Sommer, T. (2008). Protein quality control: On ipods and other junq. *Current Biology*, 18(21). doi:10.1016/j.cub.2008.09.036
- Bahin, E., Bailly, C., Sotta, B., Kranner, I., Corbineau, F., & Leymarie, J. (2011). Crosstalk between reactive oxygen species and hormonal signaling pathways regulates grain dormancy in Barley. *Plant, Cell & Environment*, 34(6), 980-993. doi:10.1111/j.1365-3040.2011.02298.x
- Bailey, P. C., McKibbin, R. S., Lenton, J. R., Holdsworth, M. J., Flintham, J. E., & Gale, M. D. (1999). Genetic map locations for orthologous VP1 genes in wheat and rice. *Theoretical and Applied Genetics*, 98(2), 281–284. doi:10.1007/s001220051069
- Bailly, C. (2004). Active oxygen species and antioxidants in seed biology. *Seed Science Research*, 14(2), 93-107. doi:10.1079/ssr2004159
- Bailly, C., El-Maarouf-Bouteau, H., & Corbineau, F. (2008). From intracellular signaling networks to cell death: The dual role of reactive oxygen species in seed physiology. *Comptes Rendus Biologies*, 331(10), 806-814. doi:10.1016/j.crv.2008.07.022
- Balzan, S., Johal, G.S., & Carraro, N. (2014). The role of Auxin transporters in monocots development. *Frontiers in Plant Science*, 5. doi:10.3389/fpls.2014.00393
- Barrero, J.M., Talbot, M.J., White, R.G., Jacobsen, J.V., & Gubler, F. (2009). Anatomical and transcriptomic studies of the Coleorhiza reveal the importance of this tissue in regulating dormancy in Barley . *Plant Physiology*, 150(2), 1006-1021. doi:10.1104/pp.109.137901
- Baulcombe, D.C., Huttly, A.K., Martienssen, R.A., Barker, R.F., & Jarvis, M.G. (1987). A novel wheat α -amylase gene (α -amy3). *Molecular and General Genetics MGG*, 209(1), 33-40. doi:10.1007/bf00329833

- Beck, E., & Ziegler, P. (1989). Biosynthesis and degradation of starch in higher plants. *Annual Review of Plant Physiology and Plant Molecular Biology*, 40(1), 95-117. doi:10.1146/annurev.pp.40.060189.000523
- Bedard, K., & Krause, K. (2007). The NOX family of ROS-generating NADPH oxidases: Physiology and pathophysiology. *Physiological Reviews*, 87(1), 245-313. doi:10.1152/physrev.00044.2005
- Bednarek, P., Piślewska-Bednarek, M., Svatoš, A., Schneider, B., Doubský, J., Mansurova, M., Humphry, M., Consonni, C., Panstruga, R., Sanchez-Vallet, A., Molina, A., & Schulze-Lefert, P. (2009). A glucosinolate metabolism pathway in living plant cells mediates broad-spectrum antifungal defense. *Science*, 323(5910), 101-106. doi:10.1126/science.1163732
- Beers, E. P., Woffenden, B.J., & Zhao, C. (2000). Plant proteolytic enzymes: Possible roles during programmed cell death. *Plant Molecular Biology*, 44(3), 399-415. doi:10.1023/a:1026556928624
- Beffa, R., & Meins, F. (1996). Pathogenesis-related functions of plant β -1,3-glucanases investigated by antisense transformation — a review. *Gene*, 179(1), 97-103. doi:10.1016/s0378-1119(96)00421-0
- Beligni, M.V., & Lamattina, L. (2000). Nitric oxide stimulates seed germination and de-etiolation, and inhibits hypocotyl elongation, three light-inducible responses in plants. *Planta*, 210(2), 215-221. doi:10.1007/pl00008128
- Belin, C., Megies, C., Hauserová, E., & Lopez-Molina, L. (2009). Abscisic acid represses growth of the *Arabidopsis* embryonic axis after germination by enhancing auxin signaling. *The Plant Cell*, 21(8), 2253-2268. doi:10.1105/tpc.109.067702
- Bernhardt, R. (2006). Cytochromes P450 as versatile biocatalysts. *Journal of Biotechnology*, 124(1), 128-145. doi:10.1016/j.jbiotec.2006.01.026
- Bethke, P.C., Libourel, I.G., & Jones, R.L. (2005). Nitric oxide reduces seed dormancy in *Arabidopsis*. *Journal of Experimental Botany*, 57(3), 517-526. doi:10.1093/jxb/erj060

- Bethke, P.C., Libourel, I.G., Aoyama, N., Chung, Y., Still, D.W., & Jones, R.L. (2007). The Arabidopsis aleurone layer responds to nitric oxide, gibberellin, and Abscisic acid and is sufficient and necessary for seed dormancy. *Plant Physiology*, 143(3), 1173-1188. doi:10.1104/pp.106.093435
- Bethke, P., Gubler, F., Jacobsen, J., & Jones, R. (2004). Dormancy of Arabidopsis seeds and barley grains can be broken by nitric oxide. *Planta*, 219(5), 847-855. doi:10.1007/s00425-004-1282-x
- Bewley, J.D. (1997). Seed germination and dormancy. *The Plant Cell*, 1055-1066. doi:10.1105/tpc.9.7.1055
- Bewley, J.D., & Black, M. (1994). *Seeds: Physiology of development and germination*. New York: Plenum Press.
- Bewley, J.D., Black, M., & Halmer, P. (2006). *The encyclopedia of seeds: science, technology and uses*: CABI.
- Bewley, J., & Nonogaki, H. (2017). Seed maturation and germination. *Reference Module in Life Sciences*, 623-626. doi:10.1016/b978-0-12-809633-8.05092-5
- Bhattacharjee, S. (2005). Reactive oxygen species and oxidative burst: Roles in stress, senescence and signal transduction in plants. *Current Science*, 89(7), 1113–1121. doi:http://www.jstor.org/stable/24110963
- Bhattacharjee, S., Chakrabarty, A., Kora, D., & Roy, U.K. (2022). Hydrogen peroxide induced antioxidant-coupled redox regulation of germination in Rice: Redox metabolic, transcriptomic and Proteomic evidences. *Journal of Plant Growth Regulation*, 42(2), 1084-1106. doi:10.1007/s00344-022-10615-3
- Bhogaraju, S., & Dikic, I. (2016). Ubiquitination without E1 and E2 enzymes. *Nature*, 533(7601), 43-44. doi:10.1038/nature17888

- Biddulph T.B., Plummer J.A., Setter T.L., & Mares D.J. (2007) Influence of high temperature and terminal moisture stress on dormancy in wheat (*Triticum aestivum* L.) *Field Crops Research*, 103(2), 139-153.
- Biddulph, T.B., Mares, D.J., Plummer, J.A., & Setter, T.L. (2005). Drought and high temperature increases pre-harvest sprouting tolerance in a genotype without grain dormancy. *Euphytica*, 143(3), 277-283. doi:10.1007/s10681-005-7882-0
- Biswas, S., Chida, A.S., & Rahman, I. (2006). Redox modifications of protein–Thiols: Emerging roles in Cell Signaling. *Biochemical Pharmacology*, 71(5), 551-564. doi:10.1016/j.bcp.2005.10.044
- Biteau, B., Labarre, J., & Toledano, M.B. (2003). ATP-dependent reduction of cysteine–sulphinic acid by *S. cerevisiae* sulphiredoxin. *Nature*, 425(6961), 980-984. doi:10.1038/nature02075
- Bondarenko, P.V., Chelius, D., & Shaler, T.A. (2002). Identification and relative quantitation of protein mixtures by enzymatic digestion followed by capillary reversed-phase liquid chromatography–tandem mass spectrometry. *Analytical Chemistry*, 74(18), 4741-4749. doi:10.1021/ac0256991
- Borner, G.H., Lilley, K.S., Stevens, T.J., & Dupree, P. (2003). Identification of glycosylphosphatidylinositol-anchored proteins in Arabidopsis. A proteomic and genomic analysis. *Plant Physiology*, 132(2), 568-577. doi:10.1104/pp.103.021170
- Botha, C.E., & Cross, R.M. (2000). Towards reconciliation of structure with function in plasmodesmata—who is the gatekeeper? *Micron*, 31(6), 713-721. doi:10.1016/s0968-4328(99)00108-0
- Bradford, M.M. (1975). A rapid and sensitive method for the quantitation of microgram quantities of protein utilizing the principle of protein-dye binding. *Analytical Biochemistry*, 72(1-2), 248-254. doi:10.1016/0003-2697(76)90527-3
- Buijs, G., Kodde, J., Groot, S.P., & Bentsink, L. (2018). Seed dormancy release accelerated by elevated partial pressure of oxygen is associated with dog loci. *Journal of Experimental Botany*, 69(15), 3601-3608. doi:10.1093/jxb/ery156

- Burlat, V., Kwon, M., Davin, L.B., & Lewis, N.G. (2001). Dirigent proteins and dirigent sites in lignifying tissues. *Phytochemistry*, *57*(6), 883-897. doi:10.1016/s0031-9422(01)00117-0
- Bykova, N.V., & Møller, I.M. (2001). Involvement of matrix NADP turnover in the oxidation of NAD⁺-linked substrates by pea leaf mitochondria. *Physiologia Plantarum*, *111*(4), 448–456. doi:10.1034/j.1399-3054.2001.1110404.x
- Bykova, N.V., & Rampitsch, C. (2013). Modulating protein function through reversible oxidation: Redox-mediated processes in plants revealed through proteomics. *PROTEOMICS*, *13*(3–4), 579–596. doi:10.1002/pmic.201200270
- Bykova, N.V., Hoehn, B., Rampitsch, C., Banks, T., Stebbing, J., Fan, T., & Knox, R. (2011a). Redox-sensitive proteome and antioxidant strategies in wheat seed dormancy control. *PROTEOMICS*, *11*(5), 865-882. doi:10.1002/pmic.200900810
- Bykova, N.V., Hoehn, B., Rampitsch, C., Hu, J., Stebbing, J., & Knox, R. (2011b). Thiol redox-sensitive seed proteome in dormant and non-dormant hybrid genotypes of wheat. *Phytochemistry*, *72*(10), 1162-1172. doi:10.1016/j.phytochem.2010.12.021
- Bykova, N.V., Rasmusson, A.G., Igamberdiev, A.U., Gardeström, P., & Møller, I.M. (1999). Two separate transhydrogenase activities are present in plant mitochondria. *Biochemical and Biophysical Research Communications*, *265*(1), 106–111. doi:10.1006/bbrc.1999.1627
- Bykova, N.V., Hu, J., Ma, Z., Igamberdiev, A.U. (2015). The Role of Reactive Oxygen and Nitrogen Species in Bioenergetics, Metabolism, and Signaling During Seed Germination. In: Gupta, K., Igamberdiev, A. (Eds) *Reactive Oxygen and Nitrogen Species Signaling and Communication in Plants*. Signaling and Communication in Plants. 23, (pp 177–195) :Springer, Cham. https://doi.org/10.1007/978-3-319-10079-1_9
- Calderini, D.F., & Reynolds, M.P. (2000). Changes in grain weight as a consequence of de-graining treatments at pre- and post-anthesis in synthetic hexaploid lines of wheat (*Triticum durum* x *T. tauschii*). *Functional Plant Biology*, *27*(3), 183. doi:10.1071/pp99066

- Caro, A., & Puntarulo, S. (1999). Nitric oxide generation by soybean embryonic axes. possible effect on mitochondrial function. *Free Radical Research*, 31(Sup1), 205-212. doi:10.1080/10715769900301521
- Carrera, E., Holman, T., Medhurst, A., Dietrich, D., Footitt, S., Theodoulou, F.L., & Holdsworth, M.J. (2008). Seed after-ripening is a discrete developmental pathway associated with specific gene networks in Arabidopsis. *The Plant Journal*, 53(2), 214-224. doi:10.1111/j.1365-313x.2007.03331.x
- Carvalho, M.E., Labate, C.A., Barboza da Silva, C., De Camargo e Castro, P.R., & Azevedo, R.A. (2022). Seed photorespiration: A perspective review. *Plant Growth Regulation*, 97(3), 477-484. doi:10.1007/s10725-022-00824-x
- Carvalho, T., Krzyzanowski, F., Ohlson, O. & Panobianco, M. (2013). Tetrazolium test adjustment for wheat seeds. *Journal of Seed Science*, 35(3), 361-367. doi.org/10.1590/S2317-15372013000300013.
- Cascales-Minana, B., Munoz-Bertomeu, J., Flores-Tornero, M., Anoman, A.D., Pertusa, J., Alaiz, M., Osorio, S., Fernie, A.R., Segura, J., & Ros, R. (2013). The phosphorylated pathway of serine biosynthesis is essential both for male gametophyte and embryo development and for root growth in Arabidopsis. *The Plant Cell*, 25(6), 2084-2101. doi:10.1105/tpc.113.112359
- Chang, C., Zhang, H.P., Feng, J.M., Yin, B., Si, H.Q., & Ma, C.X. (2009). Identifying alleles of viviparous-1b associated with pre-harvest sprouting in micro-core collections of Chinese wheat germplasm. *Molecular Breeding*, 25(3), 481-490. doi:10.1007/s11032-009-9346-z
- Chang, C., Zhang, H., Zhao, Q., Feng, J., Si, H., Lu, J., & Ma, C. (2011). Rich allelic variations of viviparous-1a and their associations with seed dormancy/pre-harvest sprouting of common wheat. *Euphytica*, 179(2), 343-353. doi:10.1007/s10681-011-0348-7
- Chen, B., Retzlaff, M., Roos, T., & Frydman, J. (2011). Cellular strategies of Protein Quality Control. *Cold Spring Harbor Perspectives in Biology*, 3(8). doi:10.1101/cshperspect.a004374

- Chen, J. (2006). RACK1 mediates multiple hormone responsiveness and developmental processes in Arabidopsis. *Journal of Experimental Botany*, 57(11), 2697-2708. doi:10.1093/jxb/erl035
- Chen, S., & Harmon, A.C. (2006). Advances in plant proteomics. *PROTEOMICS*, 6(20), 5504-5516. doi:10.1002/pmic.200600143
- Cheng, C., Che, Q., Su, S., Liu, Y., Wang, Y., & Xu, X. (2020). Genome-wide identification and characterization of respiratory burst oxidase homolog genes in six Rosaceae species and an analysis of their effects on adventitious rooting in Apple. *PLOS ONE*, 15(9). doi:10.1371/journal.pone.0239705
- Chitnis, V.R., Gao, F., Yao, Z., Jordan, M.C., Park, S., & Ayele, B.T. (2014). After-ripening induced transcriptional changes of hormonal genes in wheat seeds: The cases of brassinosteroids, ethylene, cytokinin and salicylic acid. *PLoS ONE*, 9(1). doi:10.1371/journal.pone.0087543
- Chitteti, B.R., & Peng, Z. (2007). Proteome and phosphoproteome differential expression under salinity stress in rice (*Oryza sativa*) roots. *Journal of Proteome Research*, 6(5), 1718-1727. doi:10.1021/pr060678z
- Chono, M., Matsunaka, H., Seki, M., Fujita, M., Kiribuchi-Otobe, C., Oda, S., Kojima, H., Kobayashi, D., & Kawakami, N. (2013). Isolation of a wheat (*Triticum aestivum* L.) mutant in ABA 8'-hydroxylase gene: Effect of reduced ABA catabolism on germination inhibition under field condition. *Breeding Science*, 63(1), 104-115. doi:10.1270/jsbbs.63.104
- Chopra, S., Athma, P., & Peterson, T. (1996). Alleles of the maize P gene with distinct tissue specificities encode Myb-homologous proteins with C-terminal replacements. *Plant Cell*, 8, 1149-1158.
- Chwacke, R., Ponce-Soto, G.Y., Krause, K., Bolger, A.M., Arsova, B., Hallab, A., Gruden, K., Stitt, M., Bolger, M.E., Usadel, B. (2019). MapMan4: a refined protein classification and annotation framework applicable to multi-omics data analysis. *Mol Plant. Jun 3;12(6)*, 879-892. doi: 10.1016/j.molp.2019.01.003

- Ciechanover, A. (1998). The Ubiquitin-proteasome pathway: On protein death and cell life. *The EMBO Journal*, 17(24), 7151-7160. doi:10.1093/emboj/17.24.7151
- Claiborne, A., Miller, H., Parsonage, D., & Ross, R.P. (1993). Protein-sulfenic acid stabilization and function in enzyme catalysis and gene regulation. *The FASEB Journal*, 7(15), 1483-1490. doi:10.1096/fasebj.7.15.8262333
- Coan, C., Ji, J., Hideg, K., & Mehlhorn, R.J. (1992). Protein sulfhydryls are protected from irreversible oxidation by conversion to mixed disulfides. *Archives of Biochemistry and Biophysics*, 295(2), 369-378. doi:10.1016/0003-9861(92)90530-a
- Correa-Aragunde, N., Graziano, M., & Lamattina, L. (2004). Nitric oxide plays a central role in determining lateral root development in tomato. *Planta*, 218(6), 900-905. doi:10.1007/s00425-003-1172-7
- Courtin C, & Delcour J. (2001). Relative activity of endoxylanases towards water-extractable and water-unextractable arabinoxylan. *Journal of cereal science* 33, 301-312.
- Creelman, R.A., & Mullet, J.E. (1997). Biosynthesis and action of Jasmonates in plants. *Annual Review of Plant Physiology and Plant Molecular Biology*, 48(1), 355-381. doi:10.1146/annurev.arplant.48.1.355
- Creissen, G.P., Broadbent, P., Kular, B., Reynolds, H., Wellburn, A.R., & Mullineaux, P.M. (1994). Manipulation of glutathione reductase in transgenic plants: Implications for plants' responses to environmental stress. *Proceedings of the Royal Society of Edinburgh. Section B. Biological Sciences*, 102, 167-175. doi:10.1017/s0269727000014081
- Cross, A.R., & Segal, A.W. (2004). The NADPH oxidase of professional phagocytes—prototype of the NOX Electron Transport Chain Systems. *Biochimica Et Biophysica Acta (BBA) - Bioenergetics*, 1657(1), 1-22. doi:10.1016/j.bbabi.2004.03.008
- Cuevasanta, E., Lange, M., Bonanata, J., Coitiño, E.L., Ferrer-Sueta, G., Filipovic, M.R., & Alvarez, B. (2015). Reaction of hydrogen sulfide with disulfide and sulfenic acid to form the strongly nucleophilic persulfide. *Journal of Biological Chemistry*, 290(45), 26866-26880. doi:10.1074/jbc.m115.672816

- Cutler, A.J. & Krochko, J.E. (1999). Formation and breakdown of ABA. *Trends Plant Sci.*, 4, 472–478.
- Dahm, C.C., Moore, K., & Murphy, M.P. (2006). Persistent S-nitrosation of complex I and other mitochondrial membrane proteins by S-Nitrosothiols but not nitric oxide or peroxynitrite. *Journal of Biological Chemistry*, 281(15), 10056-10065. doi:10.1074/jbc.m512203200
- Damania, D., Subramanian, H., Tiwari, A.K., Stypula, Y., Kunte, D., Pradhan, P., Roy, H., & Backman, V. (2010). Role of cytoskeleton in controlling the disorder strength of cellular nanoscale architecture. *Biophysical Journal*, 99(3), 989-996. doi:10.1016/j.bpj.2010.05.023
- Das, K., & Roychoudhury, A. (2014). Reactive oxygen species (ROS) and response of antioxidants as ROS-scavengers during environmental stress in plants. *Frontiers in Environmental Science*, 2. doi:10.3389/fenvs.2014.00053
- Davies, M.J. (2005). The oxidative environment and protein damage. *Biochimica Et Biophysica Acta (BBA) - Proteins and Proteomics*, 1703(2), 93-109. doi:10.1016/j.bbapap.2004.08.007
- Davies, P.J. (1995). The Plant Hormones: Their Nature, Occurrence, and Functions. In 2290176124 1565517446 P. J. Davies (Ed.), *Plant Hormones: Physiology, Biochemistry, and Molecular Biology* (pp. 1-5). Dordrecht, Netherlands: Springer. doi:https://doi.org/10.1007/978-94-011-0473-9_1
- De Laethauwer, S., De Riek, J., Stals, I., Reheul, D., & Haesaert, G. (2013). A-amylase gene expression during kernel development in relation to pre-harvest sprouting in wheat and triticale. *Acta Physiologiae Plantarum*, 35(10), 2927-2938. doi:10.1007/s11738-013-1323-9
- De Leo, F. (2002). Plant-PIS: A database for plant protease inhibitors and their genes. *Nucleic Acids Research*, 30(1), 347-348. doi:10.1093/nar/30.1.347
- De St. Groth, S., Webster, R., & Datyner, A. (1963). Two new staining procedures for quantitative estimation of proteins on electrophoretic strips. *Biochimica Et Biophysica Acta*, 71, 377-391. doi:10.1016/0006-3002(63)91092-8

- Debeaujon, I., Pourcel, L., & Routaboul, J.M. (2007). Seed coat development and dormancy. In L. Lepiniec (Ed.), *Seed Development, Dormancy and Germination* (Vol. 27, pp. 25-49). Oxford: Blackwell. doi:10.1002/9780470988848.ch2
- Del Río, L.A., Sandalio, L.M., Corpas, F.J., Palma, J.M., & Barroso, J.B. (2006). Reactive oxygen species and reactive nitrogen species in peroxisomes. production, scavenging, and role in cell signaling. *Plant Physiology*, *141*(2), 330-335. doi:10.1104/pp.106.078204
- DePauw, R.M., Knox, R.E., Singh, A.K., Fox, S.L., Humphreys, D.G., & Hucl, P. (2012). Developing standardized methods for breeding pre-harvest sprouting resistant wheat, challenges and successes in Canadian wheat. *Euphytica*, *188*(1), 7-14. doi:10.1007/s10681-011-0611-y
- Deracinois, B., Flahaut, C., Duban-Deweer, S., & Karamanos, Y. (2013). Comparative and quantitative global proteomics approaches: An overview. *Proteomes*, *1*(3), 180-218. doi:10.3390/proteomes1030180
- Derera, N.F., Bhatt, G.M., & McMaster, G.J. (1977). On the problem of pre-harvest sprouting of wheat. *Euphytica*, *26*(2), 299-308. doi:10.1007/bf00026991
- Dietz K.J., Jacob S., Oelze M.L., Laxa M., Tognetti V., De Miranda S.M., Baier, M., & Finkemeier, I. (2006). The function of peroxiredoxins in plant organelle redox metabolism. *J. Exp. Bot.* *57* 1697–1709. doi:10.1093/jxb/erj160
- Dobson, C.M. (2003). Protein folding and misfolding. *Nature*, *426*(6968), 884-890. doi:10.1038/nature02261
- Dolatabadian, A., Modarres Sanavy, S.A., & Sharifi, M. (2009). Effect of salicylic acid and salt on wheat seed germination. *Acta Agriculturae Scandinavica, Section B - Plant Soil Science*, *59*(5), 456-464. doi:10.1080/09064710802342350
- Domingos, P., Prado, A., Wong, A., Gehring, C., & Feijo, J. (2015). Nitric oxide: A multitasked signaling gas in plants. *Molecular Plant*, *8*(4), 506-520. doi:10.1016/j.molp.2014.12.010

- Dominguez-Solis, J.R., He, Z., Lima, A., Ting, J., Buchanan, B.B., & Luan, S. (2008). A cyclophilin links redox and light signals to cysteine biosynthesis and stress responses in chloroplasts. *Proceedings of the National Academy of Sciences*, *105*(42), 16386-16391. doi:10.1073/pnas.0808204105
- Donnelly, B.J. (1980). Effect of sprout damage on durum wheat quality. *Macaroni J*, *62*(8).
- Duan, Y., Zhang, W., Li, B., Wang, Y., Li, K., Sodmergen, Han, C., Zhang, Y., & Li, X. (2010). An endoplasmic reticulum response pathway mediates programmed cell death of root tip induced by water stress in Arabidopsis. *New Phytologist*, *186*(3), 681-695. doi:10.1111/j.1469-8137.2010.03207.x
- Durzan, D.G. & Pedroso, M.C. (2002). Nitric oxide and reactive nitrogen oxide species in plants, *Biotechnology and Genetic Engineering Reviews*, *19*, 293-337
- Eastwood, D., Tavener, R.J., & Laidman, D.L. (1969). Sequential action of cytokinin and gibberellic acid in wheat aleurone tissue. *Nature*, *221*(5187), 1267-1267. doi:10.1038/2211267a0
- Edwards, E., Rawsthorne, S., & Mullineaux, P. (1990). Subcellular distribution of multiple forms of glutathione reductase in leaves of PEA (*Pisum sativum* L.). *Planta*, *180*(2). doi:10.1007/bf00194008
- Ellis, C., & Turner, J. (2002). A conditionally fertile coi1 allele indicates cross-talk between plant hormone signalling pathways in Arabidopsis thaliana seeds and young seedlings. *Planta*, *215*(4), 549-556. doi:10.1007/s00425-002-0787-4
- Ellis, R.H. (2007). The encyclopaedia of seeds: Science, technology and uses. *Annals of Botany*, *100*(6), 1379-1379. doi:10.1093/aob/mcm225
- El-Maarouf-Bouteau, H., & Bailly, C. (2008). Oxidative signaling in seed germination and dormancy. *Plant Signaling & Behavior*, *3*(3), 175-182. doi:10.4161/psb.3.3.5539

- El-Maarouf-Bouteau, H., Meimoun, P., Job, C., Job, D., & Bailly, C. (2013). Role of protein and mrna oxidation in seed dormancy and germination. *Frontiers in Plant Science*, 4. doi:10.3389/fpls.2013.00077
- El-Maarouf-Bouteau, H., Sajjad, Y., Bazin, J., Langlade, N., Cristescu, S.M., Balzergue, S., Baudouin, E., & Bailly, C. (2014). Reactive oxygen species, Abscisic acid and ethylene interact to regulate sunflower seed germination. *Plant, Cell & Environment*, 38(2), 364-374. doi:10.1111/pce.12371
- Eltayeb, A.E., Kawano, N., Badawi, G.H., Kaminaka, H., Sanekata, T., Shibahara, T., Inanaga, S., & Tanaka, K. (2006). Overexpression of monodehydroascorbate reductase in transgenic tobacco confers enhanced tolerance to ozone, salt and Polyethylene Glycol stresses. *Planta*, 225(5), 1255-1264. doi:10.1007/s00425-006-0417-7
- Erb, M., & Kliebenstein, D.J. (2020). Plant secondary metabolites as defenses, regulators, and primary metabolites: The blurred functional trichotomy. *Plant Physiology*, 184(1), 39–52. doi:10.1104/pp.20.00433
- Esashi, Y., Ogasawara, M., Górecki, R., & Leopold, A.C. (1993). Possible mechanisms of after-ripening in Xanthium seeds. *Physiologia Plantarum*, 87(3), 359-364. doi:10.1111/j.1399-3054.1993.tb01742.x
- Evers, T., & Millar, S. (2002). Cereal Grain Structure and development: Some implications for quality. *Journal of Cereal Science*, 36(3), 261-284. doi:10.1006/jcrs.2002.0435
- Fang, Z., He, Y., Liu, Y., Jiang, W., Song, J., Wang, S., Ma, D-F., & Yin, J. (2020). Bioinformatic identification and analyses of the non-specific lipid transfer proteins in wheat. *Journal of Integrative Agriculture*, 19(5), 1170-1185. doi:10.1016/s2095-3119(19)62776-0
- Fanghänel, J., & Fischer, G (2004). Insights into the catalytic mechanism of peptidyl prolyl cis/trans isomerases. *Frontiers in Bioscience*, 9(1-3), 3453. doi:10.2741/1494
- Feeney, M.B. & Schoneich C. (2012). Tyrosine modifications in aging. *Antioxid Redox Signal*, 17, 1571–1579.

- Fettke, J., Hejazi, M., Smirnova, J., Höchel, E., Stage, M., & Steup, M. (2009). Eukaryotic starch degradation: Integration of plastidial and cytosolic pathways. *Journal of Experimental Botany*, *60*(10), 2907-2922. doi:10.1093/jxb/erp054
- Fincher, G.B. (1989). Molecular and Cellular Biology Associated with Endosperm Mobilization in Germinating Cereal Grains. *Annual Review of Plant Physiology and Plant Molecular Biology*, *40*(1), 305-346
- Finch-Savage, B. (2013). Seeds: Physiology of development, germination and dormancy (3rd edition) - J.D. Bewley, K.J. Bradford, H.W.M. Hilhorst, H. Nonogaki. 392 pp. Springer, New York – Heidelberg – Dordrecht – London 2013978-1-4614-4692-7. *Seed Science Research*, *23*(4), 289-289. doi:10.1017/S0960258513000287
- Finch-Savage, W.E., & Leubner-Metzger, G. (2006). Seed dormancy and the control of germination. *New Phytologist*, *171*(3), 501-523. doi:10.1111/j.1469-8137.2006.01787.x
- Finkel, T. (2012). From sulfenylation to sulfhydration: What a thiolate needs to tolerate. *Science Signaling*, *5*(215), 10. doi:10.1126/scisignal.2002943
- Finkelstein, R., Reeves, W., Ariizumi, T., & Steber, C. (2008). Molecular aspects of seed dormancy. *Annual Review of Plant Biology*, *59*(1), 387-415. doi:10.1146/annurev.arplant.59.032607.092740
- Finnie, C., Melchior, S., Roepstorff, P., & Svensson, B. (2002). Proteome Analysis of grain filling and seed maturation in Barley. *Plant Physiology*, *129*(3), 1308-1319. doi:10.1104/pp.003681
- Flintham, J.E. & Gale, M.D. (1982). The Tom Thumb dwarfing gene, Rht3 in wheat, I. Reduced pre-harvest damage to breadmaking quality. *Theor Appl Genet*, *62*, 121-126
- Fofana, B., Humphreys, D.G., Rasul, G., Cloutier, S., Brûlé-Babel, A., Woods, S., Lukow, O.M., & Somers, D.J. (2008). Mapping quantitative trait loci controlling pre-harvest sprouting resistance in a red × white seeded Spring Wheat Cross. *Euphytica*, *165*(3), 509-521. doi:10.1007/s10681-008-9766-6

- Fonslow, B., & Yates, J. (2012). Proteolytic digestion methods for shotgun proteomics. *Comprehensive Sampling and Sample Preparation*, 3, 261-276. doi:10.1016/b978-0-12-381373-2.00082-x
- Foster, M.W., McMahon, T.J. & Stamler, J.S. (2003). S-nitrosylation in health and disease. *Trends Mol Med*, 9, 160–168.
- Foyer, C.H., & Noctor, G. (2005). Redox homeostasis and antioxidant signaling: A metabolic interface between stress perception and physiological responses. *The Plant Cell*, 17(7), 1866-1875. doi:10.1105/tpc.105.033589
- Foyer, C.H., & Noctor, G. (2009). Redox regulation in photosynthetic organisms: Signaling, acclimation, and practical implications. *Antioxidants & Redox Signaling*, 11(4), 861-905. doi:10.1089/ars.2008.2177
- Foyer, C.H., Bloom, A.J., Queval, G., & Noctor, G. (2009). Photorespiratory metabolism: Genes, mutants, Energetics, and Redox Signaling. *Annual Review of Plant Biology*, 60(1), 455-484. doi:10.1146/annurev.arplant.043008.091948
- Foyer, C.H., Ruban, A.V., & Noctor, G. (2017). Viewing oxidative stress through the lens of oxidative signaling rather than damage. *Biochemical Journal*, 474(6), 877-883. doi:10.1042/bcj20160814
- Friso, G., & Van Wijk, K.J. (2015). Post-translational protein modifications in plant metabolism. *Plant Physiology*, 169(3), 1469-87. doi:10.1104/pp.15.01378
- Frova, C. (2003). The plant glutathione transferase Gene Family: Genomic structure, functions, expression and evolution. *Physiologia Plantarum*, 119(4), 469-479. doi:10.1046/j.1399-3054.2003.00183.x
- Frydman, J. (2001). Folding of newly translated proteins in vivo: The role of molecular chaperones. *Annual Review of Biochemistry*, 70(1), 603-647. doi:10.1146/annurev.biochem.70.1.603

- Fu, B.X., Hatcher, D.W., & Schlichting, L. (2014). Effects of sprout damage on durum wheat milling and pasta processing quality. *Canadian Journal of Plant Science*, 94(3), 545-553. doi:10.4141/cjps2013-094
- Fu, Q., Wang, B., Jin, X., Li, H., Han, P., Wei, K., Zhang, X., & Zhu, Y. (2005). Proteomic analysis and extensive protein identification from dry, germinating Arabidopsis seeds and young seedlings. *BMB Reports*, 38(6), 650-660. doi:10.5483/bmbrep.2005.38.6.650
- Gallardo, K., Job, C., Groot, S. P., Puype, M., Demol, H., Vandekerckhove, J., & Job, D. (2001). Proteomic analysis of Arabidopsis seed germination and priming. *Plant Physiology*, 126(2), 835-848. doi:10.1104/pp.126.2.835
- Gallardo, K., Job, C., Groot, S. P., Puype, M., Demol, H., Vandekerckhove, J., & Job, D. (2002). Proteomics of Arabidopsis seed germination. A comparative study of wild-type and gibberellin-deficient seeds. *Plant Physiology*, 129(2), 823-837. doi:10.1104/pp.002816
- Gang, D.R., Costa, M.A., Fujita, M., Dinkova-Kostova, A.T., Wang, H., Burlat, V., Martin, W., Sarkanen, S., Davin, L., & Lewis, N.G. (1999). Regiochemical control of Monolignol Radical Coupling: A new paradigm for lignin and Lignan biosynthesis. *Chemistry & Biology*, 6(3), 143-151. doi:10.1016/s1074-5521(99)89006-1
- Gao, X., Hu, C.H., Li, H.Z., Yao, Y.J., Meng, M., Dong, J., Zhao, W.C., Chen, Q.J., & Li, X.Y. (2013). Factors affecting pre-harvest sprouting resistance in wheat (*Triticum aestivum* L.): A review. *Journal of Animal and Plant Sciences*, 23. 556-565.
- Gara, L., Pinto, M.C., & Arrigoni, O. (1997). Ascorbate synthesis and ascorbate peroxidase activity during the early stage of wheat germination. *Physiologia Plantarum*, 100(4), 894-900. doi:10.1111/j.1399-3054.1997.tb00015.x
- Garciarrubio, A., Legaria, J.P., & Covarrubias, A.A. (1997). Abscisic acid inhibits germination of mature arabidopsis seeds by limiting the availability of energy and nutrients. *Planta*, 203(2), 182-187. doi:10.1007/s004250050180

- Geisslitz, S., Longin, C.F., Koehler, P., & Scherf, K.A. (2020). Comparative quantitative LC–MS/MS analysis of 13 amylase/trypsin inhibitors in ancient and modern triticum species. *Scientific Reports*, *10*(1). doi:10.1038/s41598-020-71413-z
- Ghafourifar, P., & Richter, C. (1997). Nitric oxide synthase activity in mitochondria. *FEBS Letters*, *418*(3), 291-296. doi:10.1016/s0014-5793(97)01397-5
- Ghezzi, P. (2005). Reviewregulation of protein function by glutathionylation. *Free Radical Research*, *39*(6), 573-580. doi:10.1080/10715760500072172
- Ghosh, S., & Pal, A. (2012). Identification of differential proteins of mungbean cotyledons during seed germination: A proteomic approach. *Acta Physiologiae Plantarum*, *34*(6), 2379-2391. doi:10.1007/s11738-012-1042-7
- Gietl, C. (1992). Malate dehydrogenase isoenzymes: Cellular locations and role in the flow of metabolites between the cytoplasm and cell organelles. *Biochimica Et Biophysica Acta (BBA) - Bioenergetics*, *1100*(3), 217-234. doi:10.1016/0167-4838(92)90476-t
- Gill, S.S., & Tuteja, N. (2010). Reactive oxygen species and antioxidant machinery in abiotic stress tolerance in crop plants. *Plant Physiology and Biochemistry*, *48*(12), 909-930. doi:10.1016/j.plaphy.2010.08.016
- Giulivi, C., Poderoso, J.J., & Boveris, A. (1998). Production of nitric oxide by mitochondria. *Journal of Biological Chemistry*, *273*(18), 11038-11043. doi:10.1074/jbc.273.18.11038
- Glazer, A.N., Delange, R.J., & Sigman, D.S. (1975). Chemical Modification of proteins: Selected methods and analytical procedures. *Elsevier Biomedical Press; Amsterdam*.
- Go, Y.M., Duong, D.M., Peng, J., & Jones, D.P. (2011). Protein Cysteines Map to Functional Networks According to Steady-state Level of Oxidation. *J Proteomics Bio inform* *4*(10), 196-209. doi:10.4172/jpb.1000190
- Gonai, T. (2003). Abscisic acid in the thermos inhibition of lettuce seed germination and enhancement of its catabolism by Gibberellin. *Journal of Experimental Botany*, *55*(394), 111-118. doi:10.1093/jxb/erh023

- Gordon, A.G. (1971). The germination resistance test — a new test for measuring germination quality of cereals. *Canadian Journal of Plant Science*, 51(2), 181-183. doi:10.4141/cjps71-036
- Goswami, A.K., Jain, M.K., & Paul, B. (1977). α - and β -amylases in seed germination. *Biologia Plantarum*, 19(6), 469-471. doi:10.1007/bf02922990
- Grantham, J. (2020). The Molecular Chaperone CCT/TRIC: An essential component of proteostasis and a potential modulator of protein aggregation. *Frontiers in Genetics*, 11. doi:10.3389/fgene.2020.00172
- Grantham, J., Brackley, K.I., & Willison, K.R. (2006). Substantial CCT activity is required for cell cycle progression and cytoskeletal organization in mammalian cells. *Experimental Cell Research*, 312(12), 2309-2324. doi:10.1016/j.yexcr.2006.03.028
- Grimsrud, P.A., Swaney, D.L., Wenger, C.D., Beauchene, N.A., & Coon, J.J. (2010). Phosphoproteomics for the masses. *Chem Biol*, 5, 105–119,
- Gronow, M., & Griffiths, G. (1971). Rapid isolation and separation of the non-histone proteins of rat liver nuclei. *FEBS Letters*, 15(5), 340-344. doi:10.1016/0014-5793(71)80329-0
- Groom, Q.J., Torres, M.A., Fordham-Skelton, A.P., Hammond-Kosack, K.E., Robinson, N.J., & Jones, J.D. (1996). RbohA, a rice homologue of the mammalian gp91phox respiratory burst oxidase gene. *The Plant Journal*, 10(3), 515-522. doi:10.1046/j.1365-313x.1996.10030515.x
- Groos, C., Gay, G., Perretant, M., Gervais, L., Bernard, M., Dedryver, F., & Charmet, G. (2002). Study of the relationship between pre-harvest sprouting and grain color by quantitative trait loci analysis in a white×red grain bread-wheat cross. *Theoretical and Applied Genetics*, 104(1), 39-47. doi:10.1007/s001220200004
- Gubler, F., Millar, A.A., & Jacobsen, J.V. (2005). Dormancy release, ABA and pre-harvest sprouting. *Current Opinion in Plant Biology*, 8(2), 183-187. doi:10.1016/j.pbi.2005.01.011

- Guo, G., Ge, P., Ma, C., Li, X., Lv, D., Wang, S., Ma, W., & Yan, Y. (2012). Comparative proteomic analysis of salt response proteins in seedling roots of two wheat varieties. *Journal of Proteomics*, 75(6), 1867-1885. doi:10.1016/j.jprot.2011.12.032
- Gupta, K.J., & Kaiser, W.M. (2010). Production and scavenging of nitric oxide by barley root mitochondria. *Plant and Cell Physiology*, 51(4), 576-584. doi:10.1093/pcp/pcq022
- Gupta, K.J., Stoimenova, M., & Kaiser, W.M. (2005). In higher plants, only root mitochondria, but not leaf mitochondria reduce nitrite to NO, in vitro and in situ. *Journal of Experimental Botany*, 56(420), 2601-2609. doi:10.1093/jxb/eri252
- Gutierrez, L., Van Wuytswinkel, O., Castelain, M., & Bellini, C. (2007). Combined networks regulating seed maturation. *Trends in Plant Science*, 12(7), 294-300. doi:10.1016/j.tplants.2007.06.003
- Halliwell, B. (2006). Reactive species and antioxidants. redox biology is a fundamental theme of aerobic life. *Plant Physiology*, 141(2), 312-322. doi:10.1104/pp.106.077073
- Halliwell, B., & Gutteridge, J.M.C. (2000) *Free Radicals in Biology and Medicine*. Oxford: Oxford University Press.
- Han, C., Ren, C., Zhi, T., Zhou, Z., Liu, Y., Chen, F., Peng, W., & Xie, D. (2013). Disruption of fumarylacetoacetate hydrolase causes spontaneous cell death under short-day conditions in Arabidopsis. *Plant Physiology*, 162(4), 1956-1964. doi:10.1104/pp.113.216804
- Han, X., & Kim, J. (2016). Integrating hormone- and micromolecule-mediated signaling with Plasmodesmal Communication. *Molecular Plant*, 9(1), 46-56. doi:10.1016/j.molp.2015.08.015
- Harlan, J.R., De Wet, J.M., & Price, E.G. (1973). Comparative evolution of cereals. *Evolution*, 27(2), 311. doi:10.2307/2406971
- Harris, T.K., & Turner, G.J. (2002). Structural basis of perturbed pK_a values of catalytic groups in enzyme active sites. *IUBMB Life (International Union of Biochemistry and Molecular Biology: Life)*, 53(2), 85-98. doi:10.1080/15216540211468

- Hartl, F.U., & Hayer-Hartl, M. (2002). Molecular chaperones in the cytosol: From nascent chain to folded protein. *Science*, *295*(5561), 1852-1858. doi:10.1126/science.1068408
- Hartl, F.U., & Hayer-Hartl, M. (2009). Converging concepts of protein folding in vitro and in vivo. *Nature Structural & Molecular Biology*, *16*(6), 574-581. doi:10.1038/nsmb.1591
- Hartl, M., Giri, A.P., Kaur, H., & Baldwin, I.T. (2011). The multiple functions of plant serine protease inhibitors. *Plant Signaling & Behavior*, *6*(7), 1009-1011. doi:10.4161/psb.6.7.15504
- Hashiguchi, A., & Komatsu, S. (2017). Posttranslational Modifications and Plant–Environment Interaction. In: Shukla, A. K. (Eds) *Proteomics in biology*. Vol. 586, (pp. 97-113): Cambridge (Mass.): Elsevier. Retrieved from <https://doi.org/10.1016/bs.mie.2016.09.030>.
- Hatcher, D.W., & Symons, S.J. (2000). Influence of sprout damage on oriental noodle appearance as assessed by image analysis. *Cereal Chemistry Journal*, *77*(3), 380-387. doi:10.1094/cchem.2000.77.3.380
- Hatz, S., Lambert, J.D., & Ogilby, P.R. (2007). Measuring the lifetime of singlet oxygen in a single cell: Addressing the issue of cell viability. *Photochemical & Photobiological Sciences*, *6*(10), 1106-1116. doi:10.1039/b707313e
- Hauvermale, A.L., Ariizumi, T., & Steber, C.M. (2012). Gibberellin signaling: A theme and variations on Della Repression. *Plant Physiology*, *160*(1), 83-92. doi:10.1104/pp.112.200956
- Havaux, M., Strasser, R.J., & Greppin, H. (1991). A theoretical and experimental analysis of the QP and QN coefficients of chlorophyll fluorescence quenching and their relation to photochemical and nonphotochemical events. *Photosynthesis Research*, *27*(1), 41-55. doi:10.1007/bf00029975
- He, M., Zhu, C., Dong, K., Zhang, T., Cheng, Z., Li, J., & Yan, Y. (2015). Comparative proteome analysis of embryo and endosperm reveals central differential expression proteins involved in wheat seed germination. *BMC Plant Biology*, *15*(1). doi:10.1186/s12870-015-0471-z

- He, Z. (2015). Protein inference in shotgun proteomics. *Data Mining for Bioinformatics Applications*, 39–49. doi:10.1016/b978-0-08-100100-4.00005-3
- Hedden, P., & Thomas, S. (2012). Gibberellin biosynthesis and its regulation. *Biochemical Journal*, 444(1), 11-25. doi:10.1042/bj20120245
- Henry, R.J., Battershell, V.G., Brennan, P.S., & Oono, K. (1992). Control of wheat α -amylase using inhibitors from cereals. *Journal of the Science of Food and Agriculture*, 58(2), 281-284. doi:10.1002/jsfa.2740580218
- Hess D. T., Matsumotom A., Kim, S.O., Marshall, H.E., & Stamler, J.S. (2005). Protein S-nitrosylation: Purview and parameters. *Nat Rev Mol Cell Biol*, 6, 150–166
- Higuchi, T. (2006). Look back over the studies of Lignin Biochemistry. *Journal of Wood Science*, 52(1), 2-8. doi:10.1007/s10086-005-0790-z
- Hilhorst H.W.M. (2007) Definitions and hypotheses of seed dormancy, In: K. J. Bradford and H. Nonogaki (Eds.), *Seed development, dormancy and germination*. Annual Plant Reviews. 27, (pp. 50-71), Oxford: Blackwell Publishing Ltd
- Himi, E. (2002). Effect of grain colour gene (R) on grain dormancy and sensitivity of the embryo to abscisic acid (ABA) in wheat. *Journal of Experimental Botany*, 53(374), 1569-1574. doi:10.1093/jxb/erf005
- Himi, E., & Noda, K. (2005). Red Grain Colour Gene (R) of wheat is a MYB-type transcription factor. *Euphytica*, 143(3), 239-242. doi:10.1007/s10681-005-7854-4
- Hite, D., Auh, C., & Scandalios, J. (1999). Catalase activity and hydrogen peroxide levels are inversely correlated in maize scutella during seed germination. *Redox Report*, 4(1-2), 29-34. doi:10.1179/135100099101534710
- Hu, X., Zhang, A., Zhang, J., & Jiang, M. (2006). Abscisic acid is a key inducer of hydrogen peroxide production in leaves of maize plants exposed to water stress. *Plant and Cell Physiology*, 47(11), 1484-1495. doi:10.1093/pcp/pcl014

- Huang, K., Lee, T., Kao, H., Ma, C., Lee, C., Lin, T., Chang, W., & Huang, H. (2018). DbPTM in 2019: Exploring disease association and cross-talk of post-translational modifications. *Nucleic Acids Research*, *47*(D1), D298-D308. doi:10.1093/nar/gky1074
- Huang, L., Hu, C., Cai, W., Zhu, Q., Gao, B., Zhang, X., & Ren, C. (2018). Fumarylacetoacetate hydrolase is involved in salt stress response in Arabidopsis. *Planta*, *248*(2), 499-511. doi:10.1007/s00425-018-2907-9
- Huttly, A.K., Martienssen, R.A., & Baulcombe, D.C. (1988). Sequence heterogeneity and differential expression of the α -amy2 gene family in wheat. *Molecular and General Genetics MGG*, *214*(2), 232-240. doi:10.1007/bf00337716
- Igamberdiev, A.U., & Hill, R.D. (2004). Nitrate, no and haemoglobin in plant adaptation to hypoxia: An alternative to classic fermentation pathways. *Journal of Experimental Botany*, *55*(408), 2473-2482. doi:10.1093/jxb/erh272
- Ikekawa, N., & Takatsuto, S. (1984). Microanalysis of brassinosteroids in plants by gas chromatography/mass spectrometry. *Journal of the Mass Spectrometry Society of Japan*, *32*(1), 55-70. doi:10.5702/massspec.32.55
- Intiaz, M., Ogonnaya, F.C., Oman, J., & Van Ginkel, M. (2008). Characterization of quantitative trait loci controlling genetic variation for preharvest sprouting in synthetic backcross-derived wheat lines. *Genetics*, *178*(3), 1725-1736. doi:10.1534/genetics.107.084939
- Iriti, M., & Faoro, F. (2008). Abscisic acid is involved in chitosan-induced resistance to tobacco necrosis virus (TNV). *Plant Physiology and Biochemistry*, *46*(12), 1106-1111. doi:10.1016/j.plaphy.2008.08.002
- Ishibashi, Y., Aoki, N., Kasa, S., Sakamoto, M., Kai, K., Tomokiyo, R., Watabe, G., Yuasa, T., & Iwaya-Inoue, M. (2017). The interrelationship between abscisic acid and reactive oxygen species plays a key role in barley seed dormancy and germination. *Frontiers in Plant Science*, *8*. doi:10.3389/fpls.2017.00275
- Ishibashi, Y., Kasa, S., Sakamoto, M., Aoki, N., Kai, K., Yuasa, T., Hanada, A., Yamaguchi, S., & Iwaya-Inoue, M. (2015). A role for reactive oxygen species produced by NADPH oxidases

- in the embryo and aleurone cells in barley seed germination. *PLOS ONE*, *10*(11). doi:10.1371/journal.pone.0143173
- Ishibashi, Y., Koda, Y., Zheng, S., Yuasa, T., & Iwaya-Inoue, M. (2012). Regulation of soybean seed germination through ethylene production in response to reactive oxygen species. *Annals of Botany*, *111*(1), 95-102. doi:10.1093/aob/mcs240
- Ishibashi, Y., Tawaratsumida, T., Zheng, S., Yuasa, T., & Iwaya-Inoue, M. (2010). NADPH oxidases act as key enzyme on germination and seedling growth in barley (*hordeum vulgare*L.). *Plant Production Science*, *13*(1), 45-52. doi:10.1626/pp.s.13.45
- Jacob, C., Holme, A.L., & Fry, F.H. (2004). The sulfinic acid switch in proteins. *Org. Biomol. Chem.*, *2*(14), 1953-1956. doi:10.1039/b406180b
- Jacobsen, J.V., Barrero, J.M., Hughes, T., Julkowska, M., Taylor, J.M., Xu, Q., & Gubler, F. (2013). Roles for blue light, jasmonate and nitric oxide in the regulation of dormancy and germination in wheat grain (*triticum aestivum* L.). *Planta*, *238*(1), 121-138. doi:10.1007/s00425-013-1878-0
- Jeevan Kumar, S.P., Rajendra Prasad, S., Banerjee, R., & Thammineni, C. (2015). Seed birth to death: Dual functions of reactive oxygen species in seed physiology. *Annals of Botany*, *116*(4), 663-668. doi:10.1093/aob/mcv098
- Jiang, Y., Yang, B., Harris, N.S., & Deyholos, M.K. (2007). Comparative proteomic analysis of NaCl stress-responsive proteins in Arabidopsis roots. *Journal of Experimental Botany*, *58*(13), 3591-3607. doi:10.1093/jxb/erm207
- Joachimiak, L., Walzthoeni, T., Liu, C.W., Aebersold, R., & Frydman, J. (2014). The structural basis of substrate recognition by the eukaryotic Chaperonin Tric/CCT. *Cell*, *159*(5), 1042-1055. doi:10.1016/j.cell.2014.10.042
- Johansson, E., Olsson, O., & Nyström, T. (2004). Progression and specificity of protein oxidation in the life cycle of Arabidopsis thaliana. *Journal of Biological Chemistry*, *279*(21), 22204-22208. doi:10.1074/jbc.m402652200

- Jones, R., Taylor, N., & Senti, F. (1959). Electrophoresis and fractionation of wheat gluten. *Archives of Biochemistry and Biophysics*, 84(2), 363-376. doi:10.1016/0003-9861(59)90599-5
- Kadariya, M., Glover, K.D., Wu, J., & Gonzalez, J.L. (2011). Multi-parental mating design analysis: Model Evaluation and application in spring wheat. *Conference on Applied Statistics in Agriculture*. doi:10.4148/2475-7772.1050
- Kader, J. (1996). Lipid-transfer proteins in plants. *Annual Review of Plant Physiology and Plant Molecular Biology*, 47(1), 627-654. doi:10.1146/annurev.arplant.47.1.627
- Kaganovich, D., Kopito, R., & Frydman, J. (2008). Misfolded proteins partition between two distinct quality control compartments. *Nature*, 454(7208), 1088-1095. doi:10.1038/nature07195
- Kamal, A.H.M., Kim, K.-H., Shin, D.-H., Seo, H.-S., Shin, K.-H., Park, C.-S., Heo, H.-Y., & Woo, S.-H. (2009). Proteomics profile of pre-harvest sprouting wheat by using MALDI-TOF mass spectrometry. *Plant Omics* 2(3), 110-119.
- Kampinga, H.H., & Craig, E.A. (2010). The hsp70 chaperone machinery: J proteins as drivers of functional specificity. *Nature Reviews Molecular Cell Biology*, 11(8), 579-592. doi:10.1038/nrm2941
- Kartal, G., Temel, A., Arican, E., & Gozukirmizi, N. (2009). Effects of brassinosteroids on barley root growth, antioxidant system and cell division. *Plant Growth Regulation*, 58(3), 261-267. doi:10.1007/s10725-009-9374-z
- Karuna Sree, B., Rajendrakumar, C.S., & Reddy, A.R. (2000). Aldose reductase in rice (*Oryza sativa* L.): Stress response and developmental specificity. *Plant Science*, 160(1), 149-157. doi:10.1016/s0168-9452(00)00376-9
- Keller, T., Damude, H.G., Werner, D., Doerner, P., Dixon, R.A., & Lamb, C. (1998). A plant homolog of the neutrophil NADPH oxidase GP91 phox subunit gene encodes a plasma membrane protein with Ca²⁺ binding motifs. *The Plant Cell*, 10(2), 255. doi:10.2307/3870703

- Kepczynski, J., Rudnicki, R.M., & Khan, A.A. (1977). Ethylene requirement for germination of partly after-ripened Apple embryo. *Physiologia Plantarum*, 40(4), 292-295. doi:10.1111/j.1399-3054.1977.tb04075.x
- Kermode, A.R. (1990). Regulatory mechanisms involved in the transition from seed development to germination. *Critical Reviews in Plant Sciences*, 9(2), 155-195. doi:10.1080/07352689009382286
- Kermode, A.R. (1995). Regulatory mechanisms in the transition from seed development to germination: interactions between the embryo and the seed environment. In: Kigel J., Galili G. (eds.), *Seed development and germination*, (pp. 273–332) New York, NY, USA: Marcel Dekker Inc.
- Kermode, A.R. (2005). Role of Absciscic acid in seed dormancy. *Journal of Plant Growth Regulation*, 24(4), 319-344. doi:10.1007/s00344-005-0110-2
- Khan, A.A. (1968). Inhibition of gibberellic acid-induced germination by abscisic acid and reversal by cytokinins. *Plant Physiology*, 43(9), 1463-1465. doi:10.1104/pp.43.9.1463
- Khan, A.A., & Downing, R.D. (1968). Cytokinin reversal of abscisic acid inhibition of growth and alpha-amylase synthesis in barley seed. *Physiologia Plantarum*, 21(6), 1301-1307. doi:10.1111/j.1399-3054.1968.tb07362.x
- Khorobrykh, S., Havurinne, V., Mattila, H., & Tyystjärvi, E. (2020). Oxygen and Ros in photosynthesis. *Plants*, 9(1), 91. doi:10.3390/plants9010091
- Khoury, G.A., Baliban, R.C., & Floudas, C.A. (2011). Proteome-wide post-translational modification statistics: Frequency Analysis and curation of the Swiss-prot database. *Scientific Reports*, 1(1), 90. doi:10.1038/srep00090
- Kibinza, S., Bazin, J., Bailly, C., Farrant, J.M., Corbineau, F., & El-Maarouf-Bouteau, H. (2011). Catalase is a key enzyme in seed recovery from ageing during priming. *Plant Sci.*; 181:309–315. doi: 10.1016/j.plantsci.2011.06.003.

- Kim, S.T., Wang, Y., Kang, S.Y., Kim, S.G., Rakwal, R., Kim, Y.C., & Kang, K.Y. (2009). Developing rice embryo proteomics reveals essential role for embryonic proteins in regulation of seed germination. *Journal of Proteome Research*, 8(7), 3598-3605. doi:10.1021/pr900358s
- Knox, R.E., Clarke, F.R., Clarke, J.M., Fox, S.L., DePauw, R.M., & Singh, A.K. (2011). Enhancing the identification of genetic loci and transgressive segregants for preharvest sprouting resistance in a durum wheat population. *Euphytica*, 186(1), 193-206. doi:10.1007/s10681-011-0557-0
- Kobayashi, M., Ohura, I., Kawakita, K., Yokota, N., Fujiwara, M., Shimamoto, K., Doke, N., & Yoshioka, H. (2007). Calcium-dependent protein kinases regulate the production of reactive oxygen species by potato NADPH oxidase. *The Plant Cell*, 19(3), 1065-1080. doi:10.1105/tpc.106.048884
- Kobrehel, K., Wong, J.H., Balogh, A., Kiss, F., Yee, B.C., & Buchanan, B.B. (1992). Specific reduction of wheat storage proteins by thioredoxin H. *Plant Physiology*, 99(3), 919-924. doi:10.1104/pp.99.3.919
- Kohyama, N., Chono, M., Nakagawa, H., Matsuo, Y., Ono, H., & Matsunaka, H. (2017). Flavonoid compounds related to seed coat color of wheat. *Bioscience, Biotechnology, and Biochemistry*, 81(11), 2112-2118. doi:10.1080/09168451.2017.1373589
- Koning, R.E. (1994). Seeds and Seed Germination. Retrieved March 30, 2021, from <https://www1.biologie.uni-hamburg.de/b-online/ibc99/koning/seedgerm.html>
- Koornneef, M., Bentsink, L., & Hilhorst, H. (2002). Seed dormancy and germination. *Curr Opin Plant Biol* 5: 33–36.
- Kraic, F., & Herdu, J. (2009). Chemometric analysis of nutritional and bread-making quality attributes of wheat cultivars. *Acta Chimica Slovaca* 2:139-146.
- Kramer, E.M., & Bennett, M.J. (2006). Auxin transport: A field in Flux. *Trends in Plant Science*, 11(8), 382-386. doi:10.1016/j.tplants.2006.06.002

- Kranner, I., Minibayeva, F.V., Beckett, R.P., & Seal, C.E. (2010). What is stress? concepts, definitions and applications in seed science. *New Phytologist*, 188(3), 655-673. doi:10.1111/j.1469-8137.2010.03461.x
- Krieger-Liszkay, A., Fufezan, C., & Trebst, A. (2008). Singlet oxygen production in photosystem II and related protection mechanism. *Photosynthesis Research*, 98(1-3), 551-564. doi:10.1007/s11120-008-9349-3
- Kucera, B., Cohn, M.A., & Leubner-Metzger, G. (2005). Plant hormone interactions during seed dormancy release and germination. *Seed Science Research*, 15(4), 281-307. doi:10.1079/ssr2005218
- Kushiro, T., Okamoto, M., Nakabayashi, K., Yamagishi, K., Kitamura, S., Asami, T., Hirai, N., Koshiba, T., Kamiya, Y., & Nambara, E. (2004). The *Arabidopsis* cytochrome P450 CYP707A encodes ABA 80-hydroxylases: Key enzymes in ABA catabolism. *EMBO J.* 23, 1647–1656.
- Laemmli, U.K. (1970). Cleavage of structural proteins during the Assembly of the head of bacteriophage T4. *Nature*, 227(5259), 680-685. doi:10.1038/227680a0
- Lansbury, P.T., & Lashuel, H.A. (2006). A century-old debate on protein aggregation and neurodegeneration enters the clinic. *Nature*, 443(7113), 774-779. doi:10.1038/nature05290
- Laskowski, M., & Qasim, M. (2000). What can the structures of enzyme-inhibitor complexes tell us about the structures of enzyme substrate complexes? *Biochimica Et Biophysica Acta (BBA) - Protein Structure and Molecular Enzymology*, 1477(1-2), 324-337. doi:10.1016/s0167-4838(99)00284-8
- Lassalle, L., Engilberge, S., Madern, D., Vauclare, P., Franzetti, B., & Girard, E. (2016). New insights into the mechanism of substrates trafficking in glyoxylate/hydroxypyruvate reductases. *Scientific Reports*, 6(1). doi:10.1038/srep20629
- Lawrence, P.K., & Koundal, K.R. (2002). Plant protease inhibitors in control of phytophagous insects. *Electronic Journal of Biotechnology*, 5(1). doi:10.2225/vol5-issue1-fulltext-3

- Lee, S., Kim, S., & Park, C. (2010). Salicylic acid promotes seed germination under high salinity by modulating antioxidant activity in Arabidopsis. *New Phytologist*, *188*(2), 626-637. doi:10.1111/j.1469-8137.2010.03378.x
- Leubner-Metzger, G. (2004). B-1,3-glucanase gene expression in low-hydrated seeds as a mechanism for dormancy release during tobacco after-ripening. *The Plant Journal*, *41*(1), 133-145. doi:10.1111/j.1365-313x.2004.02284.x
- Leubner-Metzger, G., Fründt, C., & Meins, F. (1996). Effects of gibberellins, darkness and osmotica on endosperm rupture and class I β -1,3-glucanase induction in tobacco seed germination. *Planta*, *199*(2), 282-288. doi:10.1007/bf00196570
- Levine, A., Pennell, R.I., Alvarez, M.E., Palmer, R., & Lamb, C. (1996). Calcium-mediated apoptosis in a plant hypersensitive disease resistance response. *Current Biology*, *6*(4), 427-437. doi:10.1016/s0960-9822(02)00510-9
- Levine, R.L., Williams, J.A., Stadtman, E.R., & Shacter, E. (1994). Carbonyl assays for determination of oxidatively modified proteins, *Methods in Enzymology*, *233*, 346-357
- Leymarie, J., Vitkauskaitė, G., Hoang, H.H., Gendreau, E., Chazoule, V., Meimoun, P., Corbineau, F., El-Maarouf-Bouteau, H., & Bailly, C. (2011). Role of reactive oxygen species in the regulation of Arabidopsis Seed Dormancy. *Plant and Cell Physiology*, *53*(1), 96-106. doi:10.1093/pcp/pcr129
- Li, K., Zhang, W., & Li, H. (2005). Effect of natural brassinolide on germination of *Ailanthus altissima* seeds. *Forestry Studies in China*, *7*(2), 12-14. doi:10.1007/s11632-005-0014-z
- Li, W., Chen, B., Chen, Z., Gao, Y., Chen, Z., & Liu, J. (2017). Reactive oxygen species generated by NADPH oxidases promote radicle protrusion and root elongation during rice seed germination. *International Journal of Molecular Sciences*, *18*(1), 110. doi:10.3390/ijms18010110
- Lin, L., Tai, S.S., Peng, C., & Tzen, J.T. (2002). Steroleosin, a sterol-binding dehydrogenase in seed oil bodies. *Plant Physiology*, *128*(4), 1200-1211. doi:10.1104/pp.010982

- Lindsay, M.P., & Skerritt, J.H. (2000). Immunocytochemical localization of gluten proteins uncovers structural organization of glutenin Macropolymer. *Cereal Chemistry Journal*, 77(3), 360-369. doi:10.1094/cchem.2000.77.3.360
- Liochev, S., & Fridovich, I. (1999). Superoxide and iron: Partners in crime. *IUBMB Life*, 48(2), 157-161. doi:10.1080/713803492
- Liu, A., Gao, F., Kanno, Y., Jordan, M.C., Kamiya, Y., Seo, M., & Ayele, B.T. (2013). Regulation of Wheat Seed Dormancy by After-Ripening Is Mediated by Specific Transcriptional Switches That Induce Changes in Seed Hormone Metabolism and Signaling. *PLoS ONE*, 8, e56570.
- Liu, F., Zhang, X., Lu, C., Zeng, X., Li, Y., Fu, D., & Wu, G. (2015). Non-specific lipid transfer proteins in plants: Presenting new advances and an integrated functional analysis. *Journal of Experimental Botany*, 66(19), 5663–5681. doi:10.1093/jxb/erv313
- Liu, H., Sadygov, R.G., & Yates, J.R. (2004). A model for random sampling and estimation of relative protein abundance in shotgun proteomics. *Analytical Chemistry*, 76(14), 4193-4201. doi:10.1021/ac0498563
- Liu, J., Du, H., Ding, X., Zhou, Y., Xie, P., & Wu, J. (2017). Mechanisms of callose deposition in rice regulated by exogenous abscisic acid and its involvement in rice resistance to *nilaparvata lugens* stål (Hemiptera: Delphacidae). *Pest Management Science*, 73(12), 2559-2568. doi:10.1002/ps.4655
- Liu, X., Shi, W., Zhang, S., & Lou, C. (2005). Nitric oxide involved in signal transduction of jasmonic acid-induced stomatal closure OFVICIA FABIA L. *Chinese Science Bulletin*, 50(6), 520-525. doi:10.1007/bf02897475
- Liu, Y., Shi, L., Ye, N., Liu, R., Jia, W., & Zhang, J. (2009). Nitric oxide-induced rapid decrease of abscisic acid concentration is required in breaking seed dormancy in Arabidopsis. *New Phytologist*, 183(4), 1030-1042. doi:10.1111/j.1469-8137.2009.02899.x

- Liu, Y., Ye, N., Liu, R., Chen, M., & Zhang, J. (2010). H₂O₂ mediates the regulation of ABA catabolism and GA biosynthesis in Arabidopsis seed dormancy and germination. *Journal of Experimental Botany*, *61*(11), 2979-2990. doi:10.1093/jxb/erq125
- Lohse, M., Nagel, A., Herter, T., May, P., Schroda, M., Zrenner, R., Tohge, T., Fernie, A.R., Stitt, M., Usadel, B. (2014). Mercator: A fast and simple web server for genome scale functional annotation of Plant Sequence Data. *Plant, Cell & Environment*, *37*(5), 1250-1258. doi:10.1111/pce.12231
- López-Huertas, E., Corpas, F.J., Sandalio, L.M., & Del Río, L.A. (1999). Characterization of membrane polypeptides from pea leaf peroxisomes involved in superoxide radical generation. *Biochemical Journal*, *337*(3), 531-536. doi:10.1042/bj3370531
- Lundin, V.F., Leroux, M.R., & Stirling, P.C. (2010). Quality control of cytoskeletal proteins and human disease. *Trends in Biochemical Sciences*, *35*(5), 288-297. doi:10.1016/j.tibs.2009.12.007
- Lüthje, S., & Martinez-Cortes, T. (2018). Membrane-bound class III peroxidases: Unexpected enzymes with exciting functions. *International Journal of Molecular Sciences*, *19*(10), 2876. doi:10.3390/ijms19102876
- Mak, Y., Willows, R.D., Roberts, T.H., Wrigley, C.W., Sharp, P.J., & Copeland, L. (2009). Germination of wheat: A functional proteomics analysis of the embryo. *Cereal Chemistry Journal*, *86*(3), 281-289. doi:10.1094/cchem-86-3-0281
- Mansour, K. (1993) Sprout damage in wheat and its effect on wheat flour products. In: M. K. Walker-Simmons (Author), J. L. Ried (Ed.) *Pre-harvest Sprouting in Cereals* (pp. 8-9). St. Paul, USA :Amer Assoc Cer Chem Press.
- Marchylo, B.A., Kruger, J.E., & MacGregor, A.W. (1984). Production of Multiple Forms of Alpha-Amylase in Germinated, Incubated, Whole, De-embryonated Wheat Kernels. *Cereal Chem*, *61*(4), 305-310.

- Mares, D. (1993). Pre-harvest sprouting in wheat. I. Influence of cultivar, rainfall and temperature during grain ripening. *Australian Journal of Agricultural Research*, 44(6), 1259. doi:10.1071/ar9931259
- Marino, D., Dunand, C., Puppo, A., & Pauly, N. (2012). A burst of plant NADPH oxidases. *Trends in Plant Science*, 17(1), 9–15. doi:10.1016/j.tplants.2011.10.001
- Matilla, A.J. (2000). Ethylene in seed formation and germination. *Seed Science Research*, 10(2), 111-126. doi:10.1017/s096025850000012x
- Matilla, A., & Matilla-Vázquez, M. (2008). Involvement of ethylene in seed physiology. *Plant Science*, 175(1-2), 87-97. doi:10.1016/j.plantsci.2008.01.014
- McCarty, D.R., Hattori, T., Carson, C.B., Vasil, V., Lazar, M., & Vasil, I.K. (1991). The viviparous-1 developmental gene of maize encodes a novel transcriptional activator. *Cell*, 66(5), 895-905. doi:10.1016/0092-8674(91)90436-3
- McClellan, A.J., Scott, M.D., & Frydman, J. (2005). Folding and quality control of the VHL tumor suppressor proceed through distinct chaperone pathways. *Cell*, 121(5), 739-748. doi:10.1016/j.cell.2005.03.024
- McClellan, A.J., Tam, S., Kaganovich, D., & Frydman, J. (2005). Protein quality control: Chaperones culling corrupt conformations. *Nature Cell Biology*, 7(8), 736-741. doi:10.1038/ncb0805-736
- McDonagh, B. (2012). Diagonal electrophoresis for the detection of protein disulfides. *Methods in Molecular Biology*, 869, 309-315. doi:10.1007/978-1-61779-821-4_26
- Mehler, A.H. (1951). Studies on reactions of illuminated chloroplasts. *Archives of Biochemistry and Biophysics*, 33(1), 65-77. doi:10.1016/0003-9861(51)90082-3
- Meier, K., Ehbrecht, M.D., & Wittstock, U. (2019). Glucosinolate content in dormant and germinating *Arabidopsis thaliana* seeds is affected by non-functional alleles of classical myrosinase and nitrile-specifier protein genes. *Frontiers in Plant Science*, 10. doi:10.3389/fpls.2019.01549

- Metzger, R. J., & Silbaugh, B. A. (1970). Location of genes for seed coat color in hexaploid wheat. *Crop Science*, 10(5), 495-496. doi:10.2135/cropsci1970.0011183x001000050012x
- Meza-Zepeda, L.A., Baudo, M.M., Palva, E.T., & Heino, P. (1998). Isolation and characterization of a cDNA corresponding to a stress-activated cyclophilin gene in *Solanum commersonii*. *Journal of Experimental Botany*, 49(325), 1451-1452. doi:10.1093/jxb/49.325.1451
- Mhamdi, A., Queval, G., Chaouch, S., Vanderauwera, S., Van Breusegem, F., & Noctor, G. (2010). Catalase function in plants: A focus on Arabidopsis mutants as stress-mimic models. *Journal of Experimental Botany*, 61(15), 4197-4220. doi:10.1093/jxb/erq282
- Minibaeva, F.V., & Gordon, L.K. (2003). Superoxide Production and the Activity of Extracellular Peroxidase in Plant Tissues under Stress Conditions. *Russian Journal of Plant Physiology*, 50(3), 411-416. doi:10.1023/a:1023842808624
- Minitab, LLC. (2021). Minitab. Pennsylvania State University, Pennsylvania, USA. Retrieved from <https://www.minitab.com>
- Mittler, R. (2002). Oxidative stress, antioxidants and stress tolerance. *Trends in Plant Science*, 7(9), 405-410. doi:10.1016/s1360-1385(02)02312-9
- Mittler, R., Vanderauwera, S., Gollery, M., & Van Breusegem, F. (2004). Reactive oxygen gene network of plants. *Trends in Plant Science*, 9(10), 490-498. doi:10.1016/j.tplants.2004.08.009
- Møller, I.M., Jensen, P.E., & Hansson, A. (2007). Oxidative modifications to cellular components in plants. *Annual Review of Plant Biology*, 58(1), 459-481. doi:10.1146/annurev.arplant.58.032806.103946
- Montrichard, F., Alkhalifioui, F., Yano, H., Vensel, W.H., Hurkman, W.J., & Buchanan, B.B. (2009). Thioredoxin targets in plants: The first 30 years. *Journal of Proteomics*, 72(3), 452-474. doi:10.1016/j.jprot.2008.12.002

- Moot, D.J., & Every, D. (1990). A comparison of bread baking, falling number, α -amylase assay and visual method for the assessment of pre-harvest sprouting in wheat. *Journal of Cereal Science*, *11*(3), 225-234. doi:10.1016/s0733-5210(09)80166-5
- Moothoo-Padayachie, A., Varghese, B., Pammenter, N.W., Govender, P., & Sershen. (2016). Germination associated ROS production and glutathione redox capacity in two recalcitrant-seeded species differing in seed longevity. *Botany*, *94*(12), 1103-1114. doi:10.1139/cjb-2016-0130
- Mori, M., Uchino, N., Chono, M., Kato, K., & Miura, H (2005). Mapping QTLs for grain dormancy on wheat chromosome 3A and the group 4 chromosomes, and their combined effect. *Theor Appl Genet*, *110*(7), 1315-23.
- Morohashi, Y. (2002). Peroxidase activity develops in the micropylar endosperm of tomato seeds prior to radicle protrusion. *Journal of Experimental Botany*, *53*(374), 1643-1650. doi:10.1093/jxb/erf012
- Morris, C.F., Moffatt, J.M., Sears, R.G., & Paulsen, G.M. (1989). Seed dormancy and responses of caryopses, embryos, and calli to abscisic acid in wheat. *Plant Physiology*, *90*(2), 643-647. doi:10.1104/pp.90.2.643
- Morris, R., Blevins, D., Dietrich, J., Durley, R., Gelvin, S., Gray, J., Hommes, N.G., Kaminek, M., Mathews, L.J., Meilan, R., Reinbott, T.M., & Sayavedra-Soto, L. (1993). Cytokinins in plant pathogenic bacteria and developing cereal grains. *Functional Plant Biology*, *20*(5), 621. doi:10.1071/pp9930621
- Müller, K., Carstens, A.C., Linkies, A., Torres, M.A., & Leubner-Metzger, G. (2009). The NADPH-oxidase *atrbohB* plays a role in Arabidopsis seed after-ripening. *New Phytologist*, *184*(4), 885–897. doi:10.1111/j.1469-8137.2009.03005.x
- Müller, K., Linkies, A., Vreeburg, R.A., Fry, S. C., Krieger-Liszkay, A., & Leubner-Metzger, G. (2009). In vivo cell wall loosening by hydroxyl radicals during cress seed germination and elongation growth. *Plant Physiology*, *150*(4), 1855-1865. doi:10.1104/pp.109.139204

- Mundy, J., Hejgaard, J., & Svendsen, I. (1984). Characterization of a bifunctional wheat inhibitor of endogenous α -amylase and subtilisin. *FEBS Letters*, *167*(2), 210-214. doi:10.1016/0014-5793(84)80128-3
- Mur, L.A., Mandon, J., Persijn, S., Cristescu, S.M., Moshkov, I.E., Novikova, G.V., Hall, A., Harren, J., Hebelstrup, H., & Gupta, K.J. (2012). Nitric oxide in plants: An assessment of the current state of knowledge. *AoB Plants*, *5*(0). doi:10.1093/aobpla/pls052
- Murthy, U.M.N., & Sun, W.Q. (2000). Protein modification by Amadori and Maillard reactions during seed storage: Roles of sugar hydrolysis and lipid peroxidation. *Journal of Experimental Botany*, *51*(348), 1221-1228. doi:10.1093/jexbot/51.348.1221
- Naguleswaran, S., Li, J., Vasanthan, T., Bressler, D., & Hoover, R. (2012). Amylolysis of large and small granules of native triticale, wheat and corn starches using a mixture of α -amylase and glucoamylase. *Carbohydrate Polymers*, *88*(3), 864-874. doi:10.1016/j.carbpol.2012.01.027
- Nakamura, S., Abe, F., Kawahigashi, H., Nakazono, K., Tagiri, A., Matsumoto, T., Utsugi, S., Ogawa, T., Handa, H., Ishida, H., Mori, M., Kawaura, K., Ogihara, Y., & Miura, H. (2011). A wheat homolog of mother of FT and TFL1 acts in the regulation of germination. *The Plant Cell*, *23*(9), 3215-3229. doi:10.1105/tpc.111.088492
- Nakashima, A., Chen, L., Thao, N.P., Fujiwara, M., Wong, H.L., Kuwano, M., Umemura, K., Shirasu, K., Kawasaki, T., & Shimamoto, K. (2008). RACK1 functions in rice innate immunity by interacting with the Rac1 immune complex. *The Plant Cell*, *20*(8), 2265-2279. doi:10.1105/tpc.107.054395
- Nambara, E., Okamoto, M., Tatematsu, K., Yano, R., Seo, M., & Kamiya, Y. (2010). Abscisic acid and the control of seed dormancy and germination. *Seed Science Research*, *20*(2), 55-67. doi:10.1017/S0960258510000012
- Navrot, N., Finnie, C., Svensson, B., & Häggglund, P. (2011). Plant redox proteomics. *Journal of Proteomics*, *74*(8), 1450-1462. doi:10.1016/j.jprot.2011.03.008

- Navrot, N., Rouhier, N., Gelhaye, E., & Jacquot, J. (2007). Reactive oxygen species generation and antioxidant systems in plant mitochondria. *Physiologia Plantarum*, *129*(1), 185-195. doi:10.1111/j.1399-3054.2006.00777.x
- Nesvizhskii, A.I., & Aebersold, R. (2005). Interpretation of shotgun proteomic data. *Molecular & Cellular Proteomics*, *4*(10), 1419-1440. doi:10.1074/mcp.r500012-mcp200
- Nishizuka, Y. (1984). The role of protein kinase C in cell surface signal transduction and tumour promotion. *Nature*, *308*(5961), 693-698. doi:10.1038/308693a0
- Noctor, G., & Foyer, C.H. (1998). A re-evaluation of the ATP :NADPH budget during C3 photosynthesis: A contribution from nitrate assimilation and its associated respiratory activity? *Journal of Experimental Botany*, *49*(329), 1895-1908. doi:10.1093/jxb/49.329.1895
- Noctor, G., & Foyer, C.H. (1998). Ascorbate and glutathione: Keeping active oxygen under control. *Annual Review of Plant Physiology and Plant Molecular Biology*, *49*(1), 249-279. doi:10.1146/annurev.arplant.49.1.249
- Noctor, G., De Paepe, R., & Foyer, C.H. (2007). Mitochondrial redox biology and homeostasis in plants. *Trends in Plant Science*, *12*(3), 125-134. doi:10.1016/j.tplants.2007.01.005
- Noctor, G., Gomez, L., Vanacker, H., & Foyer, C.H. (2002). Interactions between biosynthesis, compartmentation and transport in the control of glutathione homeostasis and signaling. *Journal of Experimental Botany*, *53*(372), 1283-1304. doi:10.1093/jexbot/53.372.1283
- Nyachiro, J., Clarke, F., DePauw, R., Knox, R., & Armstrong, K. (2002). Temperature effects on seed germination and expression of seed dormancy in wheat. *Euphytica*, *126*(1), 123-127. doi:10.1023/a:1019694800066
- O'Farrell P.H. (1975). High resolution two-dimensional electrophoresis of proteins. *The Journal of biological chemistry*, *250*(10), 4007-4021.
- Ogasawara, Y., Kaya, H., Hiraoka, G., Yumoto, F., Kimura, S., Kadota, Y., Hishinuma, H., Senzaki, E., Yamagoe, S., Nagata, K., Nara, M., Suzuki, K., Tanokura, M., & Kuchitsu, K.

- (2008). Synergistic activation of the Arabidopsis NADPH oxidase AtrbohD by Ca²⁺ and phosphorylation. *Journal of Biological Chemistry*, 283(14), 8885-8892. doi:10.1074/jbc.m708106200
- Ogawa, M., Hanada, A., Yamauchi, Y., Kuwahara, A., Kamiya, Y., & Yamaguchi, S. (2003). Gibberellin biosynthesis and response during Arabidopsis seed germination[w]. *The Plant Cell*, 15(7), 1591-1604. doi:10.1105/tpc.011650
- Ogbonnaya, F.C., Imtiaz, M., Ye, G., Hearnden, P.R., Hernandez, E., Eastwood, R.F., Ginkel, M. V., Shorter, S.C., Winchester, J.M. (2008). Genetic and QTL analyses of seed dormancy and preharvest sprouting resistance in the wheat germplasm CN10955. *Theoretical and Applied Genetics*, 116(7), 891-902. doi:10.1007/s00122-008-0712-8
- Ohkama-Ohtsu, N., Oikawa, A., Zhao, P., Xiang, C., Saito, K., & Oliver, D.J. (2008). A γ -Glutamyl transpeptidase-independent pathway of glutathione catabolism to glutamate via 5-oxoproline in Arabidopsis. *Plant Physiology*, 148(3), 1603-1613. doi:10.1104/pp.108.125716
- Oide, S., Bejai, S., Staal, J., Guan, N., Kaliff, M., & Dixelius, C. (2013). A novel role of pr 2 in abscisic acid (ABA) mediated, pathogen-induced callose deposition in *Arabidopsis thaliana*. *New Phytologist*, 200(4), 1187-1199. doi:10.1111/nph.12436
- Okamoto, M., Kuwahara, A., Seo, M., Kushiro, T., Asami, T., Hirai, N., Kamiya, Y., Koshiba, T., & Nambara, E. (2006). CYP707A1 and CYP707A2, which encode Abscisic acid 8'-hydroxylases, are indispensable for proper control of seed dormancy and germination in Arabidopsis. *Plant Physiology*, 141(1), 97-107. doi:10.1104/pp.106.079475
- Olsen, J.G., Pedersen, L., Christensen, C.L., Olsen, O., & Henriksen, A. (2008). Barley aldose reductase: Structure, cofactor binding, and substrate recognition in the Aldo/keto reductase 4C family. *Proteins: Structure, Function, and Bioinformatics*, 71(3), 1572-1581. doi:10.1002/prot.21996
- Op den Camp, R.G., Przybyla, D., Ochsenbein, C., Laloi, C., Kim, C., Danon, A., Wagner, D., Hideg, É., Göbel, C., Feussner, I., Nater, M., & Apel, K. (2003). Rapid induction of distinct stress responses after the release of singlet oxygen in Arabidopsis. *The Plant Cell*, 15(10), 2320-2332. doi:10.1105/tpc.014662

- Oracz, K., Bouteau, H.E., Farrant, J.M., Cooper, K., Belghazi, M., Job, C., Corbineau, F., & Bailly, C. (2007). ROS production and protein oxidation as a novel mechanism for seed dormancy alleviation. *The Plant Journal*, *50*(3), 452-465. doi:10.1111/j.1365-3113x.2007.03063.x
- O'Reilly, E., Köhler, V., Flitsch, S.L., & Turner, N.J. (2011). Cytochromes P450 as useful biocatalysts: Addressing the limitations. *Chemical Communications*, *47*(9), 2490. doi:10.1039/c0cc03165h
- Osa, M., Kato, K., Mori, M., Shindo, C., Torada, A., & Miura, H. (2003). Mapping QTLs for seed dormancy and the VP1 homologue on chromosome 3a in wheat. *Theoretical and Applied Genetics*, *106*(8), 1491-1496. doi:10.1007/s00122-003-1208-1
- Palma, J.M., Corpas, F.J., & Del Río, L.A. (2009). Proteome of plant peroxisomes: New Perspectives on the role of these organelles in Cell Biology. *PROTEOMICS*, *9*(9), 2301-2312. doi:10.1002/pmic.200700732
- Pan, K., Chen, Y., Pu, T., Chao, Y., Yang, C., Bomgardner, R.D., Rogers, J.C., Meng, T.-C., & Khoo, K. (2014). Mass spectrometry-based quantitative proteomics for dissecting multiplexed redox cysteine modifications in nitric oxide-protected cardiomyocyte under hypoxia. *Antioxidants & Redox Signaling*, *20*(9), 1365-1381. doi:10.1089/ars.2013.5326
- Pandey, A., & Mann, M. (2000). Proteomics to study genes and genomes. *Nature*, *405*(6788), 837-846. doi:10.1038/35015709
- Paniagua, C., Bilkova, A., Jackson, P., Dabravolski, S., Riber, W., Didi, V., Houser, J., Gigli-Bisceglia, N., Wimmerova, M., Budínská, E., Hamann, T., & Hejatko, J. (2017). Dirigent proteins in plants: Modulating cell wall metabolism during abiotic and biotic stress exposure. *Journal of Experimental Botany*, *68*(13), 3287-3301. doi:10.1093/jxb/erx141
- Panni, S. (2019). Phospho-peptide binding domains in *Saccharomyces cerevisiae* model organism. *Biochimie*, *163*, 117-127. doi:10.1016/j.biochi.2019.06.005
- Paulsen, G.M., & Auld, A.S. (2004). Preharvest sprouting of cereals. In R. L. Benech-Arnold & R. A. Sánchez (Authors), *Handbook of Seed Physiology: Applications to agriculture* (pp. 199-205). New York, USA: Food Products Press.

- Peng, Z., Wang, M., Li, F., Lv, H., Li, C., & Xia, G. (2009). A proteomic study of the response to salinity and drought stress in an introgression strain of bread wheat. *Molecular & Cellular Proteomics*, 8(12), 2676-2686. doi:10.1074/mcp.m900052-mcp200
- Pinto, E., Sigaud-kutner, T. C., Leitao, M. A., Okamoto, O. K., Morse, D., & Colepicolo, P. (2003). Heavy metal-induced oxidative stress in ALGAE1. *Journal of Phycology*, 39(6), 1008-1018. doi:10.1111/j.0022-3646.2003.02-193.x
- Pirbalouti, A.G., Sajjadi, S.E., & Parang, K. (2014). A review (Research and patents) on Jasmonic acid and its derivatives. *Archiv Der Pharmazie*, 347(4), 229-239. doi:10.1002/ardp.201300287
- Pisipati S.R. (2008). Pre-harvest sprouting tolerance in hard white winter wheat. [Kansas State University].
- Planchet, E., Jagadis Gupta, K., Sonoda, M., & Kaiser, W.M. (2005). Nitric oxide emission from tobacco leaves and cell suspensions: Rate limiting factors and evidence for the involvement of mitochondrial electron transport. *The Plant Journal*, 41(5), 732-743. doi:10.1111/j.1365-313x.2005.02335.x
- Podgórska, A., Burian, M., & Szal, B. (2017). Extra-cellular but extra-ordinarily important for cells: Apoplastic reactive oxygen species metabolism. *Frontiers in Plant Science*, 8. doi:10.3389/fpls.2017.01353
- Poole, L.B. (2015). The basics of Thiols and Cysteines in redox biology and Chemistry. *Free Radical Biology and Medicine*, 80, 148-157. doi:10.1016/j.freeradbiomed.2014.11.013
- Poole, L.B., & Nelson, K.J. (2008). Discovering mechanisms of signaling-mediated cysteine oxidation. *Current Opinion in Chemical Biology*, 12(1), 18-24. doi:10.1016/j.cbpa.2008.01.021
- Poole, L.B., Karplus, P.A., & Claiborne, A. (2004). Protein sulfenic acids in redox signaling. *Annual Review of Pharmacology and Toxicology*, 44(1), 325-347. doi:10.1146/annurev.pharmtox.44.101802.121735

- Pospíšil, P. (2016). Production of reactive oxygen species by Photosystem II as a response to light and temperature stress. *Frontiers in Plant Science*, 7. doi:10.3389/fpls.2016.01950
- Powers, E.T., Morimoto, R.I., Dillin, A., Kelly, J.W., & Balch, W.E. (2009). Biological and chemical approaches to diseases of proteostasis deficiency. *Annual Review of Biochemistry*, 78(1), 959-991. doi:10.1146/annurev.biochem.052308.114844
- Proteins - NCBI (2004). National Center for Biotechnology Information. National Library of Medicine, Bethesda, Maryland, USA. Retrieved March 03, 2021 from <https://www.ncbi.nlm.nih.gov/guide/proteins/>
- Puntarulo, S., Galleano, M., Sanchez, R., & Boveris, A. (1991). Superoxide anion and hydrogen peroxide metabolism in soybean embryonic axes during germination. *Biochimica Et Biophysica Acta (BBA) - General Subjects*, 1074(2), 277-283. doi:10.1016/0304-4165(91)90164-c
- Purvis, A.C. (1997). Role of the alternative oxidase in limiting superoxide production by plant mitochondria. *Physiologia Plantarum*, 100(1), 165-170. doi:10.1111/j.1399-3054.1997.tb03468.x
- Quan, L., Zhang, B., Shi, W., & Li, H. (2008). Hydrogen peroxide in plants: A versatile molecule of the reactive oxygen species network. *Journal of Integrative Plant Biology*, 50(1), 2-18. doi:10.1111/j.1744-7909.2007.00599.x
- Rabilloud, T. (1990). Mechanisms of protein silver staining in polyacrylamide gels: A 10-year synthesis. *Electrophoresis*, 11(10), 785-794. doi:10.1002/elps.1150111003
- Rabilloud, T., & Lelong, C. (2011). Two-dimensional gel electrophoresis in Proteomics: A tutorial. *Journal of Proteomics*, 74(10), 1829-1841. doi:10.1016/j.jprot.2011.05.040
- Radford, J.E., Vesik, M., & Overall, R.L. (1998). Callose deposition at plasmodesmata. *Protoplasma*, 201(1-2), 30-37. doi:10.1007/bf01280708
- Rajjou, L., Belghazi, M., Huguët, R., Robin, C., Moreau, A., Job, C., & Job, D. (2006). Proteomic investigation of the effect of salicylic acid on Arabidopsis seed germination and

- establishment of early defense mechanisms. *Plant Physiology*, 141(3), 910-923. doi:10.1104/pp.106.082057
- Ramaih, S., Guedira, M., & Paulsen, G.M. (2003). Relationship of indoleacetic acid and tryptophan to dormancy and preharvest sprouting of wheat. *Functional Plant Biology*, 30(9), 939. doi:10.1071/fp03113
- Ramana, K.V. (2011). Aldose reductase: New insights for an old enzyme. *BioMolecular Concepts*, 2(1-2), 103-114. doi:10.1515/bmc.2011.002
- Ramazi, S., & Zahiri, J. (2021). Post-translational modifications in proteins: Resources, tools and prediction methods. *Database*, 2021. doi:10.1093/database/baab012
- Rani, K., Rana, R., & Datt, S. (2015). Review on characteristics and applications of amylases. *International Journal of Microbiology and Bioinformatics*, 5(1), 1-5. <http://www.bretj.com>
- Rao, J.Y., Bonner, R.B., Hurst, R.F., Liang, Y.Y., Reznikoff, C.A., & Hemstreet, G.P. (1997). Quantitative changes in cytoskeletal and nuclear actins during cellular transformation. *International Journal of Cancer*, 70(4), 423-429. doi:10.1002/(sici)1097-0215(19970207)70:4<423::aid-ijc9>3.0.co;2-y
- Rasul, G., Humphreys, D.G., Brûlé-Babel, A., McCartney, C.A., Knox, R.E., DePauw, R.M., & Somers, D.J. (2009). Mapping QTLs for pre-harvest sprouting traits in the spring wheat cross 'RL4452/ac domain'. *Euphytica*, 168(3), 363-378. doi:10.1007/s10681-009-9934-3
- Rauniyar, N., & Yates, J.R. (2014). Isobaric labeling-based relative quantification in shotgun proteomics. *Journal of Proteome Research*, 13(12), 5293-5309. doi:10.1021/pr500880b
- Reisner, A., Nemes, P., & Bucholtz, C. (1975). The use of Coomassie Brilliant Blue G250 perchloric acid solution for staining in electrophoresis and isoelectric focusing on polyacrylamide gels. *Analytical Biochemistry*, 64(2), 509-516. doi:10.1016/0003-2697(75)90461-3

- Rhazi, L., Cazalis, R., & Aussenac, T. (2003). Sulfhydryl-disulfide changes in storage proteins of developing wheat grain: Influence on the SDS-UNEXTRACTABLE glutenin polymer formation. *Journal of Cereal Science*, *38*(1), 3-13. doi:10.1016/s0733-5210(03)00019-5
- Riganti, C., Gazzano, E., Polimeni, M., Costamagna, C., Bosia, A., & Ghigo, D. (2004). Diphenyleneiodonium inhibits the cell redox metabolism and induces oxidative stress. *Journal of Biological Chemistry*, *279*(46), 47726–47731. doi:10.1074/jbc.m406314200
- Rinalducci, S., Murgiano, L., & Zolla, L. (2008). Redox Proteomics: Basic principles and future perspectives for the detection of protein oxidation in plants. *Journal of Experimental Botany*, *59*(14), 3781-3801. doi:10.1093/jxb/ern252
- Ritchie, S., Swanson, S., & Gilroy, S. (2000). Physiology of the aleurone layer and starchy endosperm during grain development and early seedling growth: New insights from cell and molecular biology. *Seed Science Research*, *10*(3), 193-212. doi:10.1017/S0960258500000234
- Robertson, M., & Hill, R. (1989). Accumulation of an endogenous alpha-amylase inhibitor in barley during grain development. *Journal of Cereal Science*, *9*(3), 237-246. doi:10.1016/s0733-5210(89)80006-2
- Romano, P.G., Horton, P., & Gray, J.E. (2004). The Arabidopsis cyclophilin gene family. *Plant Physiology*, *134*(4), 1268-1282. doi:10.1104/pp.103.022160
- Roos, G., & Messens, J. (2011). Protein sulfenic acid formation: From cellular damage to Redox Regulation. *Free Radical Biology and Medicine*, *51*(2), 314-326. doi:10.1016/j.freeradbiomed.2011.04.031
- Ross, A.S., & Bettge, A.D. (2009). Passing the test on wheat end-use quality. In: B. F. Carver (Ed.). *Wheat science and trade* (pp. 455–493). Ames, IA, USA: Wiley-Blackwell. doi:10.1002/9780813818832.ch20
- Salchert, K., Bhalerao, R., Koncz-Kálmán, Z., & Koncz, C. (1998). Control of cell elongation and stress responses by steroid hormones and carbon catabolic repression in plants. *Philosophical*

- Transactions of the Royal Society of London. Series B: Biological Sciences*, 353(1374), 1517-1520. doi:10.1098/rstb.1998.0307
- Sarath, G., Hou, G., Baird, L. M., & Mitchell, R.B. (2007). Reactive oxygen species, ABA and nitric oxide interactions on the germination of warm-season C4-grasses. *Planta*, 226(3), 697-708. doi:10.1007/s00425-007-0517-z
- Sargeant, J.G. (1980). α -Amylase Isoenzymes and Starch. *Degradation Cereal Research Communications*, 8(1),77-86.
- Satoh, S., Takeda, Y., & Esashi, Y. (1984). Dormancy and impotency of cocklebur seeds. ix. changes in ACC-ethylene conversion activity and ACC content of dormant and non-dormant seeds during soaking. *Journal of Experimental Botany*, 35(10), 1515-1524. doi:10.1093/jxb/35.10.1515
- Savitsky, P.A., & Finkel, T. (2002). Redox regulation of CDC25C. *Journal of Biological Chemistry*, 277(23), 20535-20540. doi:10.1074/jbc.m201589200
- Schaller, A. (2004). A cut above the rest: The regulatory function of plant proteases. *Planta*, 220(2), 183-197. doi:10.1007/s00425-004-1407-2
- Schlaeppli, K., Bodenhausen, N., Buchala, A., Mauch, F., & Reymond, P. (2008). The glutathione-deficient mutant *pad2-1* accumulates lower amounts of glucosinolates and is more susceptible to the insect herbivore *Spodoptera littoralis*. *The Plant Journal*, 55(5), 774-786. doi:10.1111/j.1365-3113x.2008.03545.x
- Schulze, W.X., & Usadel, B. (2010). Quantitation in mass-spectrometry-based proteomics. *Annual Review of Plant Biology*, 61(1), 491-516. doi:10.1146/annurev-arplant-042809-112132
- Seo, M., Nambara, E., Choi, G., & Yamaguchi, S. (2009). Interaction of light and hormone signals in germinating seeds. *Plant Molecular Biology*, 69(4), 463-472. doi:10.1007/s11103-008-9429-y
- Sew, Y.S., Ströher, E., Fenske, R., & Millar, A.H. (2016). Loss of Mitochondrial Malate Dehydrogenase Activity Alters Seed Metabolism Impairing Seed Maturation and Post-

- Germination Growth in Arabidopsis. *Plant physiology*, 171(2), 849–863. doi.org/10.1104/pp.16.01654
- Shafqat, S. (2013). *Effect of different sprouting conditions on alpha amylase activity, functional properties of wheat flour and on shelf-life of bread supplemented with sprouted wheat* (Master's thesis, University of Guelph, 2013) (pp. 10-25). Guelph: University of Guelph. doi:http://hdl.handle.net/10214/6672
- Shao, R., Wang, K., & Shangguan, Z. (2010). Cytokinin-induced photosynthetic adaptability of *Zea mays* l. to drought stress associated with nitric oxide signal: Probed by ESR spectroscopy and fast OJIP fluorescence rise. *Journal of Plant Physiology*, 167(6), 472-479. doi:10.1016/j.jplph.2009.10.020
- Sharma, P., & Dubey, R. (2004). Ascorbate peroxidase from rice seedlings: Properties of enzyme isoforms, effects of stresses and protective roles of osmolytes. *Plant Science*, 167(3), 541-550. doi:10.1016/j.plantsci.2004.04.028
- Shewry, P.R., Halford, N.G., Belton, P.S., & Tatham, A.S. (2002). The structure and properties of gluten: An elastic protein from Wheat Grain. *Philosophical Transactions of the Royal Society of London. Series B: Biological Sciences*, 357(1418), 133-142. doi:10.1098/rstb.2001.1024
- Shu, K., Liu, X., Xie, Q., & He, Z. (2016). Two faces of one seed: Hormonal regulation of dormancy and germination. *Molecular Plant*, 9(1), 34-45. doi:10.1016/j.molp.2015.08.010
- Shu, K., Zhang, H., Wang, S., Chen, M., Wu, Y., Tang, S., Liu, C., Feng, Y., Cao, X., & Xie, Q. (2013). *Abi4* regulates primary seed dormancy by regulating the biogenesis of Abscisic acid and gibberellins in Arabidopsis. *PLoS Genetics*, 9(6). doi:10.1371/journal.pgen.1003577
- Silverstone, A.L. (2001). Repressing a repressor: Gibberellin-induced rapid reduction of the RGA protein in Arabidopsis. *The Plant Cell Online*, 13(7), 1555-1566. doi:10.1105/tpc.13.7.1555
- Simpson, C., Thomas, C., Findlay, K., Bayer, E., & Maule, A.J. (2009). An Arabidopsis GPI-anchor plasmodesmal neck protein with callose binding activity and potential to regulate cell-to-cell trafficking. *The Plant Cell*, 21(2), 581-594. doi:10.1105/tpc.108.060145

- Simsek, S., Ohm, J., Lu, H., Rugg, M., Berzonsky, W., Alamri, M.S., & Mergoum, M. (2013). Effect of pre-harvest sprouting on physicochemical changes of proteins in wheat. *Journal of the Science of Food and Agriculture*, 94(2), 205-212. doi:10.1002/jsfa.6229
- Simsek, S., Ohm, J., Lu, H., Rugg, M., Berzonsky, W., Alamri, M., & Mergoum, M. (2014). Effect of pre-harvest sprouting on physicochemical properties of starch in wheat. *Foods*, 3(2), 194-207. doi:10.3390/foods3020194
- Singh, A.K., Knox, R.E., Clarke, J.M., Clarke, F.R., Singh, A., DePauw, R.M., & Cuthbert, R.D. (2014). Genetics of pre-harvest sprouting resistance in a cross of Canadian adapted durum wheat genotypes. *Molecular Breeding*, 33(4), 919-929. doi:10.1007/s11032-013-0006-y
- Sivaguru, M., Fujiwara, T., Šamaj, J., Baluška, F., Yang, Z., Osawa, H., Maeda, T., Mori, T., Volkmann, D., & Matsumoto, H. (2000). Aluminum-induced 1 \rightarrow 3- β -d-glucan inhibits cell-to-cell trafficking of molecules through plasmodesmata. A new mechanism of aluminum toxicity in plants. *Plant Physiology*, 124(3), 991-1006. doi:10.1104/pp.124.3.991
- Skamnaki, V.T., Owen, D.J., Noble, M.E., Lowe, E.D., Lowe, G., Oikonomakos, N.G., & Johnson, L.N. (1999). Catalytic mechanism of Phosphorylase Kinase probed by mutational studies. *Biochemistry*, 38(44), 14718-14730. doi:10.1021/bi991454f
- Smithies, O. (2012). How it all began: A personal history of gel electrophoresis. *Methods in Molecular Biology*, 869, 1-21. doi:10.1007/978-1-61779-821-4_1
- Sponsel, V.M., Hedden, P. (2010). Gibberellin Biosynthesis and Inactivation. In: Davies, P. J. (eds), *Plant Hormones: Biosynthesis, Signal transduction and Action* (pp. 63-94). Dordrecht, Netherlands: Springer. doi.org/10.1007/978-1-4020-2686-7_4
- Stadtman, E.R. (1992). Protein oxidation and aging. *Science*, 257(5074), 1220-1224. doi:10.1126/science.1355616
- Stadtman, E.R., & Levine, R.L. (2003). Free radical-mediated oxidation of free amino acids and amino acid residues in proteins. *Amino Acids*, 25(3-4), 207-218. doi:10.1007/s00726-003-0011-2

- Steber, C.M., & McCourt, P. (2001). A role for Brassinosteroids in germination in Arabidopsis. *Plant Physiology*, 125(2), 763-769. doi:10.1104/pp.125.2.763
- Stitt, M., & Zeeman, S.C. (2012). Starch turnover: Pathways, regulation and role in growth. *Current Opinion in Plant Biology*, 15(3), 282-292. doi:10.1016/j.pbi.2012.03.016
- Stone, S.L. (2019). Role of the ubiquitin proteasome system in plant response to abiotic stress. *International Review of Cell and Molecular Biology*, 343, 65-110. doi:10.1016/bs.ircmb.2018.05.012
- Stonebloom, S., Brunkard, J.O., Cheung, A.C., Jiang, K., Feldman, L., & Zambryski, P. (2012). Redox states of plastids and mitochondria differentially regulate intercellular transport via plasmodesmata. *Plant Physiology*, 158(1), 190-199. doi:10.1104/pp.111.186130
- Sun, M., Tuan, P.A., Izydorczyk, M.S., & Ayele, B.T. (2019). Ethylene regulates post-germination seedling growth in wheat through spatial and temporal modulation of Aba/Ga Balance. *Journal of Experimental Botany*, 71(6), 1985-2004. doi:10.1093/jxb/erz566
- Sun, W.Q., & Leopold, A.C. (1995). The Maillard reaction and oxidative stress during aging of soybean seeds. *Physiologia Plantarum*, 94(1), 94-104. doi:10.1111/j.1399-3054.1995.tb00789.x
- Sun, Z., & Henson, C.A. (1991). A quantitative assessment of the importance of barley seed α -amylase, β -amylase, debranching enzyme, and α -glucosidase in starch degradation. *Archives of Biochemistry and Biophysics*, 284(2), 298-305. doi:10.1016/0003-9861(91)90299-x
- Suzuki, N., Miller, G., Morales, J., Shulaev, V., Torres, M.A., & Mittler, R. (2011). Respiratory burst oxidases: The engines of Ros Signaling. *Current Opinion in Plant Biology*, 14(6), 691-699. doi:10.1016/j.pbi.2011.07.014
- Suzuki, T., Matsuura, T., Kawakami, N., & Noda, K. (2000). Accumulation and leakage of abscisic acid during embryo development and seed dormancy in wheat. *Plant Growth Regulation*, 30(3), 253-260. doi:10.1023/a:1006320614530

- Svensson, B., Fukuda, K., Nielsen, P.K., & Bønsager, B.C. (2004). Proteinaceous α -amylase inhibitors. *Biochimica Et Biophysica Acta (BBA) - Proteins and Proteomics*, 1696(2), 145-156. doi:10.1016/j.bbapap.2003.07.004
- Thannickal, V.J., & Fanburg, B.L. (2000). Reactive oxygen species in cell signaling. *American Journal of Physiology-Lung Cellular and Molecular Physiology*, 279(6). doi:10.1152/ajplung.2000.279.6.11005
- Thomason, W.E., Hughes, J.R., Griffey, C.A., Parrish, D.J., & Barbeau, W.E., (2019). Understanding Pre-harvest Sprouting of Wheat. *Virginia Cooperative extension*, 424, 060.
- Tola, A.J., Jaballi, A., & Missihoun, T.D. (2021). Protein carbonylation: Emerging roles in plant redox biology and future prospects. *Plants*, 10(7), 1451. doi:10.3390/plants10071451
- Tommasi, F., Paciolla, C., De Pinto, M.C., & Gara, L.D. (2001). A comparative study of glutathione and ascorbate metabolism during germination of *Pinus pinea* L. seeds. *Journal of Experimental Botany*, 52(361), 1647-1654. doi:10.1093/jxb/52.361.1647
- Torres, M.A., & Dangl, J.L. (2005). Functions of the respiratory burst oxidase in biotic interactions, abiotic stress and development. *Current Opinion in Plant Biology*, 8(4), 397-403. doi:10.1016/j.pbi.2005.05.014
- Toujani, W., Muñoz-Bertomeu, J., Flores-Tornero, M., Rosa-Téllez, S., Anoman, A.D., Alseekh, S., Fernie, A.R., & Ros, R. (2013). Functional characterization of the plastidial 3-phosphoglycerate dehydrogenase family in Arabidopsis. *Plant Physiology*, 163(3), 1164-1178. doi:10.1104/pp.113.226720
- Triantaphylidès, C., & Havaux, M. (2009). Singlet oxygen in plants: Production, detoxification and signaling. *Trends in Plant Science*, 14(4), 219-228. doi:10.1016/j.tplants.2009.01.008
- Triantaphylidès, C., Krischke, M., Hoerberichts, F.A., Ksas, B., Gresser, G., Havaux, M., Van Breusegem, F., & Mueller, M.J. (2008). Singlet oxygen is the major reactive oxygen species involved in photooxidative damage to plants. *Plant Physiology*, 148(2), 960-968. doi:10.1104/pp.108.125690

- Turrens, J.F. (2003). Mitochondrial formation of reactive oxygen species. *The Journal of Physiology*, 552(2), 335-344. doi:10.1113/jphysiol.2003.049478
- Tuszynski, G.P., Buck, C.A., & Warren, L. (1979). A two-dimensional polyacrylamide gel electrophoresis (page) system using sodium dodecyl sulfate—page in the first dimension. *Analytical Biochemistry*, 93, 329-338. doi:10.1016/s0003-2697(79)80159-1
- Tyedmers, J., Mogk, A., & Bukau, B. (2010). Cellular strategies for controlling protein aggregation. *Nature Reviews Molecular Cell Biology*, 11(11), 777-788. doi:10.1038/nrm2993
- Ueki, S., & Citovsky, V. (2005). Identification of an interactor of cadmium ion-induced glycine-rich protein involved in regulation of callose levels in plant vasculature. *Proceedings of the National Academy of Sciences*, 102(34), 12089-12094. doi:10.1073/pnas.0505927102
- Ullah, H., Scappini, E.L., Moon, A.F., Williams, L.V., Armstrong, D.L., & Pedersen, L.C. (2008). Structure of a signal transduction regulator, RACK1, from *Arabidopsis thaliana*. *Protein Science*, 17(10), 1771-1780. doi:10.1110/ps.035121.108
- Umate, P. (2012). Comparative genomics of the lipid-body-membrane proteins Oleosin, Caleosin and steroleosin in magnoliophyte, Lycophyte and Bryophyte. *Genomics, Proteomics & Bioinformatics*, 10(6), 345-353. doi:10.1016/j.gpb.2012.08.006
- Urade, R., Sato, N., & Sugiyama, M. (2017). Gliadins from Wheat Grain: An overview, from primary structure to nanostructures of aggregates. *Biophysical Reviews*, 10(2), 435-443. doi:10.1007/s12551-017-0367-2
- Usadel, B., Poree, F., Nagel, A., Lohse, M., Czedik-Eysenberg, A., & Stitt, M. (2009). A guide to using MapMan to visualize and compare omics data in plants: A case study in the crop species, maize. *Plant, Cell & Environment*, 32(9), 1211-1229. doi:10.1111/j.1365-3040.2009.01978.x
- Van der Hoorn, R.A. (2008). Plant proteases: From phenotypes to molecular mechanisms. *Annual Review of Plant Biology*, 59(1), 191-223. doi:10.1146/annurev.arplant.59.032607.092835

- Van der Schoot, C., Paul, L.K., Paul, S.B., & Rinne, P.L. (2011). Plant lipid bodies and cell-cell signaling: A new role for an old organelle? *Plant Signaling & Behavior*, 6(11), 1732-1738. doi:10.4161/psb.6.11.17639
- van Vliet, E. (2014). Omics and related recent technologies. *Encyclopedia of Toxicology*, 689-693. doi:10.1016/b978-0-12-386454-3.01056-3
- Vardhini, V.B., & Rao, S.R. (2003). Amelioration of osmotic stress by brassinosteroids on seed germination and seedling growth of three varieties of sorghum. *Plant Growth Regulation*, 41(1), 25-31. doi:10.1023/a:1027303518467
- Veraverbeke, W.S., & Delcour, J.A. (2002). Wheat protein composition and properties of wheat glutenin in relation to breadmaking functionality. *Critical Reviews in Food Science and Nutrition*, 42(3), 179-208. doi:10.1080/10408690290825510
- Vranová, E., Atichartpongkul, S., Villarroel, R., Van Montagu, M., Inzé, D., & Van Camp, W. (2002). Comprehensive analysis of gene expression in *Nicotiana tabacum* leaves acclimated to oxidative stress. *Proceedings of the National Academy of Sciences*, 99(16), 10870-10875. doi:10.1073/pnas.152337999
- Wagner, D., Przybyla, D., Op den Camp, R., Kim, C., Landgraf, F., Lee, K.P., Würsch, M., Laloi, C., Nater, M., Hideg, E., & Apel, K. (2004). The genetic basis of singlet oxygen-induced stress responses of *Arabidopsis thaliana*. *Science*, 306(5699), 1183-1185. doi:10.1126/science.1103178
- Walker-Simmons, M. (1987). ABA levels and sensitivity in developing wheat embryos of sprouting resistant and susceptible cultivars. *Plant Physiology*, 84(1), 61-66. doi:10.1104/pp.84.1.61
- Wang, W. (2011). Eppendorf Tube Clip Art [Digital image]. Retrieved December 27, 2022, from <http://www.clker.com/cliparts/g/u/N/o/v/G/eppendorf-tube-md.png>
- Wang, Y., Cao, Y., Liang, X., Zhuang, J., Wang, X., Qin, F., & Jiang, C. (2022). A dirigent family protein confers variation of Casparian strip thickness and salt tolerance in maize. *Nature Communications*, 13(1). doi:10.1038/s41467-022-29809-0

- Wang, Y., Li, L., Ye, T., Zhao, S., Liu, Z., Feng, Y., & Wu, Y. (2011). Cytokinin antagonizes ABA suppression to seed germination of Arabidopsis by downregulating ABI5 expression. *The Plant Journal*, 68(2), 249-261. doi:10.1111/j.1365-313x.2011.04683.x
- Wang, Z. (2011). Brassinosteroids modulate plant immunity at multiple levels. *Proceedings of the National Academy of Sciences*, 109(1), 7-8. doi:10.1073/pnas.1118600109
- Wardman, P., & Von Sonntag, C. (1995). [3] kinetic factors that control the fate of thiyl radicals in cells. *Methods in Enzymology*, 71(5), 31-45. doi:10.1016/0076-6879(95)51108-3
- Waszczak, C., Akter, S., Jacques, S., Huang, J., Messens, J., & Van Breusegem, F. (2015). Oxidative post-translational modifications of cysteine residues in plant signal transduction. *Journal of Experimental Botany*, 66(10), 2923-2934. doi:10.1093/jxb/erv084
- Wei, W., Min, X., Shan, S., Jiang, H., Cao, J., Li, L., Si, H., Xia, X., Ma, C., Zhang, H., & Chang, C. (2019). Isolation and characterization of TAQSD1 genes for period of dormancy in common wheat (*Triticum aestivum* L.). *Molecular Breeding*, 39(10-11). doi:10.1007/s11032-019-1060-x
- Weidinger, A., & Kozlov, A. (2015). Biological activities of reactive oxygen and nitrogen species: Oxidative stress versus signal transduction. *Biomolecules*, 5(2), 472-484. doi:10.3390/biom5020472
- Willems, P., Van Breusegem, F., & Huang, J. (2020). Contemporary proteomic strategies for cysteine redoxome profiling. *Plant Physiology*, 186(1), 110-124. doi:10.1093/plphys/kiaa074
- Wilson, D.O., & McDonald, M.B. (1986) The lipid peroxidation model of seed aging. *Seed Sci. Technol.*14, 269-300.
- Winterbourn, C.C. (1993). Superoxide as an intracellular radical sink. *Free Radical Biology and Medicine*, 14(1), 85-90. doi:10.1016/0891-5849(93)90512-s

- Winterbourn, C.C., & Hampton, M.B. (2008). Thiol chemistry and specificity in redox signaling. *Free Radical Biology and Medicine*, 45(5), 549-561. doi:10.1016/j.freeradbiomed.2008.05.004
- Wittstock, U., & Halkier, B.A. (2000). Cytochrome P450 CYP79A2 from *Arabidopsis thaliana* L. catalyzes the conversion of L-phenylalanine to phenylacetaldoxime in the biosynthesis of benzylglucosinolate. *Journal of Biological Chemistry*, 275(19), 14659-14666. doi:10.1074/jbc.275.19.14659
- Wong, L.H., Gatta, A.T., & Levine, T.P. (2018). Lipid transfer proteins: The lipid commute via shuttles, bridges and tubes. *Nature Reviews Molecular Cell Biology*, 20(2), 85-101. doi:10.1038/s41580-018-0071-5
- Xi, W., Liu, C., Hou, X., & Yu, H. (2010). *Mother of FT and TFL1* regulates seed germination through a negative feedback loop modulating ABA signaling in *Arabidopsis*. *The Plant Cell*, 22(6), 1733-1748. doi:10.1105/tpc.109.073072
- Xie, Z., Zhang, Z., Hanzlik, S., Cook, E., & Shen, Q.J. (2007). Salicylic acid inhibits gibberellin-induced alpha-amylase expression and seed germination via a pathway involving an abscisic-acid-inducible WRKY gene. *Plant Molecular Biology*, 64(3), 293-303. doi:10.1007/s11103-007-9152-0
- Xiong, Y., Uys, J.D., Tew, K.D., & Townsend, D.M. (2011). S-glutathionylation: From molecular mechanisms to health outcomes. *Antioxidants & Redox Signaling*, 15(1), 233-270. doi:10.1089/ars.2010.3540
- Yamaguchi, S. (2008). Gibberellin metabolism and its regulation. *Annual Review of Plant Biology*, 59(1), 225-251. doi:10.1146/annurev.arplant.59.032607.092804
- Yamaguchi, S., & Kamiya, Y. (2000). Gibberellin biosynthesis: Its regulation by endogenous and environmental signals. *Plant and Cell Physiology*, 41(3), 251-257. doi:10.1093/pcp/41.3.251
- Yan, L. (2009). Analysis of oxidative modification of proteins. *Current Protocols in Protein Science*, 56(1), 18-30. doi:10.1002/0471140864.ps1404s56

- Yang, P., Li, X., Wang, X., Chen, H., Chen, F., & Shen, S. (2007). Proteomic analysis of rice (*Oryza sativa*) seeds during germination. *PROTEOMICS*, 7(18), 3358-3368. doi:10.1002/pmic.200700207
- Yano, H., Wong, J.H., Cho, M., & Buchanan, B.B. (2001). Redox changes accompanying the degradation of seed storage proteins in germinating rice. *Plant and Cell Physiology*, 42(8), 879-883. doi:10.1093/pcp/pce119
- Ye, W., Hossain, M.A., Munemasa, S., Nakamura, Y., Mori, I.C., & Murata, Y. (2013). Endogenous Abscisic acid is involved in methyl Jasmonate-induced reactive oxygen species and nitric oxide production but not in cytosolic alkalization in Arabidopsis Guard cells. *Journal of Plant Physiology*, 170(13), 1212-1215. doi:10.1016/j.jplph.2013.03.011
- Yin, J., Fang, Z., Sun, C., Zhang, P., Zhang, X., Lu, C., Wang, S-P., Ma, D-F., & Zhu, Y. (2018). Rapid identification of a stripe rust resistant gene in a space-induced wheat mutant using specific locus amplified fragment (SLAF) sequencing. *Scientific Reports*, 8(1). doi:10.1038/s41598-018-21489-5
- Yoshida, K., Ohtaka, K., Hirai, M.Y., & Hisabori, T. (2020). Biochemical insight into redox regulation of plastidial 3-phosphoglycerate dehydrogenase from Arabidopsis thaliana. *Journal of Biological Chemistry*, 295(44), 14906-14915. doi:10.1074/jbc.ra120.014263
- Yoshioka, H., Numata, N., Nakajima, K., Katou, S., Kawakita, K., Rowland, O., Jones, D., & Doke, N. (2003). *Nicotiana benthamiana* GP91phox homologs nbrboha and nbrboh b participate in H₂O₂ accumulation and resistance to *Phytophthora infestans*. *The Plant Cell*, 15(3), 706-718. doi:10.1105/tpc.008680
- Yoshioka, H., Sugie, K., Park, H., Maeda, H., Tsuda, N., Kawakita, K., & Doke, N. (2001). Induction of plant GP91 phox homolog by fungal cell wall, arachidonic acid, and salicylic acid in potato. *Molecular Plant-Microbe Interactions*®, 14(6), 725-736. doi:10.1094/mpmi.2001.14.6.725
- Yuan, Y.P., Chen, X., Xiao, S.H., & Zhang, W. (2005). Extraction and identification of barley α -amylase/subtilisin inhibitor. *J Triticeae Crops*, 25, 40-43.

- Zanardo, D.I.L., Zanardo, F.M.L., Ferrarese, M.D.L.L., Magalhaes, J., & Ferrarese-Filho, O. (2005). Nitric oxide affecting seed germination and peroxidase activity in canola (*Brassica napus* L.). *Physiology and Molecular Biology of Plants*, *11*, 81-86.
- Zeeshan, H., Lee, G., Kim, H., & Chae, H. (2016). Endoplasmic Reticulum stress and associated Ros. *International Journal of Molecular Sciences*, *17*(3), 327. doi:10.3390/ijms17030327
- Zeng, J., Dong, Z., Wu, H., Tian, Z., & Zhao, Z. (2017). Redox regulation of Plant Stem Cell Fate. *The EMBO Journal*, *36*(19), 2844-2855. doi:10.15252/embj.201695955
- Zevallos, V.F., Raker, V., Tenzer, S., Jimenez-Calvente, C., Ashfaq-Khan, M., Rüssel, N., Pickert, G., Schild, H., Steinbrink, K., & Schuppan, D. (2017). Nutritional wheat amylase-trypsin inhibitors promote intestinal inflammation via activation of myeloid cells. *Gastroenterology*, *152*(5). doi:10.1053/j.gastro.2016.12.006
- Zhang, X., Yu, X., & Yue, D. (2015). Phytotoxicity of dimethyl sulfoxide (DMSO) to Rice Seedlings. *International Journal of Environmental Science and Technology*, *13*(2), 607-614. doi:10.1007/s13762-015-0899-6
- Zhang, Y., Fonslow, B.R., Shan, B., Baek, M., & Yates, J.R. (2013). Protein analysis by Shotgun/bottom-up proteomics. *Chemical Reviews*, *113*(4), 2343-2394. doi:10.1021/cr3003533
- Zhao, Y. (2010). Auxin biosynthesis and its role in plant development. *Annual Review of Plant Biology*, *61*(1), 49-64. doi:10.1146/annurev-arplant-042809-112308
- Zhao, Y., Yu, H., Zhou, J., Smith, S.M., & Li, J. (2020). Malate circulation: Linking chloroplast metabolism to mitochondrial Ros. *Trends in Plant Science*, *25*(5), 446-454. doi:10.1016/j.tplants.2020.01.010
- Zheng Y.X., & Oegema K. (2008). Cell structure and dynamics. *Curr. Opin. Cell Biol.* *20*(1-3).
- Ziegler, P. (1999). Cereal beta-amylases. *Journal of Cereal Science*, *29*(3), 195-204. doi:10.1006/jcrs.1998.0238

Zweier, J.L., Chen, C., & Druhan, L.J. (2011). S-glutathionylation reshapes our understanding of endothelial nitric oxide synthase uncoupling and nitric oxide/reactive oxygen species-mediated signaling. *Antioxidants & Redox Signaling*, 14(10), 1769-1775. doi:10.1089/ars.2011.3904

7 Appendices

Supplementary Table S1: Unique significant RMPs found in freshly harvested embryo tissues of DPI-treated seeds after the differential blocking of redox-active protein thiols with IAA (DPI-IAA category) [Excel]

Supplementary Table S2: Unique significant RMPs found in after-ripened embryo tissues of DPI-treated seeds after the differential blocking of redox-active protein thiols with IAA (DPI-IAA category) [Excel]

Supplementary Table S3: Unique significant RMPs found in freshly harvested aleurone tissues of DPI-treated seeds after the differential blocking of redox-active protein thiols with IAA (DPI-IAA category) [Excel]

Supplementary Table S4: Unique significant RMPs found in after-ripened aleurone tissues of DPI-treated seeds after the differential blocking of redox-active protein thiols with IAA (DPI-IAA category) [Excel]

Supplementary Table S5: Unique significant RMPs found in freshly harvested embryo tissues of seeds treated with DPI in the presence of ABA after the differential blocking of redox-active protein thiols with IAA (DPI+ABA)-IAA category [Excel]

Supplementary Table S6: Unique significant RMPs found in after-ripened embryo tissues of seeds treated with DPI in the presence of ABA after the differential blocking of redox-active protein thiols with IAA (DPI+ABA)-IAA category [Excel]

Supplementary Table S7: Unique significant RMPs found in freshly harvested aleurone tissues of seeds treated with DPI in the presence of ABA after the differential blocking of redox-active protein thiols with IAA (DPI+ABA)-IAA category [Excel]

Supplementary Table S8: Unique significant RMPs found in after-ripened aleurone tissues of seeds treated with DPI in the presence of ABA after the differential blocking of redox-active protein thiols with IAA (DPI+ABA)-IAA category [Excel]

Supplementary Table S9: Common RMPs found in freshly harvested embryo tissues of seeds treated with DPI and DPI in the presence of ABA after the differential blocking of redox-active protein thiols with IAA in both DPI-IAA and (DPI+ABA)-IAA categories (Common-IAA) [Excel]

Supplementary Table S10: Common RMPs found in after-ripened embryo tissues of seeds treated with DPI and DPI in the presence of ABA after the differential blocking of redox-active protein thiols with IAA in both DPI-IAA and (DPI+ABA)-IAA categories (Common-IAA) [Excel]

Supplementary Table S11: Common RMPs found in freshly harvested aleurone tissues of seeds treated with DPI and DPI in the presence of ABA after the differential blocking of redox-active protein thiols with IAA in both DPI-IAA and (DPI+ABA)-IAA categories (Common-IAA) [Excel]

Supplementary Table S12: Common RMPs found in after-ripened aleurone tissues of seeds treated with DPI and DPI in the presence of ABA after the differential blocking of redox-active protein thiols with IAA in both DPI-IAA and (DPI+ABA)-IAA categories (Common-IAA) [Excel]

Supplementary Table S13: Unique significant CysDAPs found in freshly harvested embryo tissues of seeds treated with DPI after the reduction of all redox-active protein thiols with DTT, (DPI- DTT) category [Excel]

Supplementary Table S14: Unique significant CysDAPs found in after-ripened embryo tissues of seeds treated with DPI after the reduction of all redox-active protein thiols with DTT, (DPI- DTT) category [Excel]

Supplementary Table S15: Unique significant CysDAPs found in freshly harvested aleurone tissues of seeds treated with DPI after the reduction of all redox-active protein thiols with DTT, (DPI- DTT) category [Excel]

Supplementary Table S16: Unique significant CysDAPs found in after-ripened aleurone tissues of seeds treated with DPI after the reduction of all redox-active protein thiols with DTT, (DPI- DTT) category [Excel]

Supplementary Table S17: Unique significant CysDAPs found in freshly harvested embryo tissues of seeds treated with DPI in the presence of ABA after the reduction of all redox-active protein thiols with DTT, (DPI+ABA)-DTT category [Excel]

Supplementary Table S18: Unique significant CysDAPs found in after-ripened embryo tissues of seeds treated with DPI in the presence of ABA after the reduction of all redox-active protein thiols with DTT, (DPI+ABA)-DTT category [Excel]

Supplementary Table S19: Unique significant CysDAPs found in freshly harvested aleurone tissues of seeds treated with DPI in the presence of ABA after the reduction of all redox-active protein thiols with DTT, (DPI+ABA)-DTT category [Excel]

Supplementary Table S20: Unique significant CysDAPs found in after-ripened aleurone tissues of seeds treated with DPI in the presence of ABA after the reduction of all redox-active protein thiols with DTT, (DPI+ABA)-DTT category [Excel]

Supplementary Table S21: Common CysDAPs found in freshly harvested embryo tissues of seeds treated with DPI or DPI in the presence of ABA after the reduction of all redox-active protein thiols with DTT, both DPI-DTT and (DPI+ABA)-DTT categories (Common-DTT) [Excel]

Supplementary Table S22: Common CysDAPs found in after-ripened embryo tissues of seeds treated with DPI or DPI in the presence of ABA after the reduction of all redox-active protein thiols with DTT, both DPI-DTT and (DPI+ABA)-DTT categories (Common-DTT) [Excel]

Supplementary Table S23: Common CysDAPs found in freshly harvested aleurone tissues of seeds treated with DPI or DPI in the presence of ABA after the reduction of all redox-active protein thiols with DTT, both DPI-DTT and (DPI+ABA)-DTT categories (Common-DTT) [Excel]

Supplementary Table S24: Common CysDAPs found in after-ripened aleurone tissues of seeds treated with DPI or DPI in the presence of ABA after the reduction of all redox-active protein thiols with DTT, both DPI-DTT and (DPI+ABA)-DTT categories (Common-DTT) [Excel]

Supplementary Table S25: Comparison of the RMPs in freshly harvested and after-ripened aleurone tissues of seeds treated with DPI in the presence of ABA after the differential blocking of redox-active protein thiols with IAA (DPI+ABA)-IAA category [Excel]

Supplementary Table S26: Comparison of the CysDAPs in freshly harvested and after-ripened embryo tissues of seeds treated with DPI in the presence of ABA after the reduction of all redox-active protein thiols with DTT, (DPI+ABA)-DTT category [Excel]

Supplementary Table S27: Comparison of the thiol-containing proteins identified from approach I of the DPI-IAA category and approach II of the DPI-DTT category in freshly harvested embryo tissues [Excel]

Supplementary Table S28: Comparison of the thiol-containing proteins identified from approach I of the DPI+ABA-IAA category and approach II of the DPI+ABA-DTT category in freshly harvested aleurone tissues [Excel]